



**HAL**  
open science

# Multi-scale characterization of flax stems and fibers : structure and mechanical performances

Camille Goudenhoft

► **To cite this version:**

Camille Goudenhoft. Multi-scale characterization of flax stems and fibers : structure and mechanical performances. Materials. Université de Bretagne Sud, 2018. English. NNT : 2018LORIS500 . tel-02301223

**HAL Id: tel-02301223**

**<https://theses.hal.science/tel-02301223>**

Submitted on 30 Sep 2019

**HAL** is a multi-disciplinary open access archive for the deposit and dissemination of scientific research documents, whether they are published or not. The documents may come from teaching and research institutions in France or abroad, or from public or private research centers.

L'archive ouverte pluridisciplinaire **HAL**, est destinée au dépôt et à la diffusion de documents scientifiques de niveau recherche, publiés ou non, émanant des établissements d'enseignement et de recherche français ou étrangers, des laboratoires publics ou privés.

# THÈSE DE DOCTORAT DE

L'UNIVERSITÉ BRETAGNE SUD  
COMUE UNIVERSITÉ BRETAGNE LOIRE

ÉCOLE DOCTORALE N° 602  
*Sciences pour l'Ingénieur*  
Spécialité : *Génie des Matériaux*

Par

**Camille GOUDENHOFT**

**Multi-scale characterization of flax stems and fibers: structure and mechanical performances**

Caractérisation multi-échelle des tiges et fibres de lin: structure et performances mécaniques

Thèse présentée et soutenue à Lorient, le 19 septembre 2018

Unité de recherche: IRDL

Thèse N° 500

## Rapporteurs avant soutenance :

Vincent PLACET      Ingénieur de Recherche, HDR, Université de Franche-Comté, Institut FEMTO-ST  
Damien SOULAT      Professeur, ENSAIT Roubaix

## Composition du Jury :

Président : **Joël BRÉARD**      Professeur, Université du Havre Normandie  
Examineurs : **Tancrède ALMÉRAS**      Chargé de Recherche, CNRS Montpellier  
                  **Fabienne GUILLON**      Directrice de Recherche, INRA Nantes  
                  **Bruno MOULIA**      Directeur de Recherche, INRA Clermont-Ferrand  
Dir. de thèse : **Christophe BALEY**      Professeur, Université de Bretagne Sud  
Co-dir. de thèse : **Alain BOURMAUD**      Ingénieur de Recherche, HDR, Université de Bretagne Sud



« La plante est un modèle d'existence à prendre en considération.  
Elle est discrète, d'une incontestable utilité, elle est d'une très grande beauté et  
d'une complète non-violence.

J'ai l'impression que l'être humain devrait s'en inspirer. »

Francis Hallé

**Un grand merci à vous pour cette belle rencontre (Groix, 2017) !**

## REMERCIEMENTS

---

Avant tout, je tiens à remercier Alain et Christophe, pour avoir encadré et suivi ces travaux d'un bout à l'autre. Merci pour vos nombreux conseils, vos encouragements, votre bonne humeur, votre enthousiasme, votre disponibilité et pour tout ce que nous avons pu partager durant ces trois années de thèse. J'ai eu la chance de passer de très bons moments et de faire de belles rencontres avec vous et grâce à vous, à travers votre réseau et au fil de nos déplacements. Merci pour votre confiance et votre soutien ! Et un très grand merci pour cette belle aventure !

J'exprime ma reconnaissance à Vincent Placet et Damien Soulat, pour avoir accepté de rapporter ce travail de thèse. Merci également à Tancrede Alméras, Joël Bréard, Fabienne Guillon et Bruno Moulia, pour avoir accepté d'être membres de mon jury en tant qu'examineurs.

Je souhaite aussi remercier toutes les personnes ayant pris part à ces travaux de thèse, pour leurs conseils, pour le partage de leurs connaissances, de leurs savoir-faire techniques, mais aussi pour leur investissement concernant les manipulations ou la rédaction de publications. C'est grâce à l'apport de chacun de vous que ce travail a pu s'enrichir et se concrétiser ; la confrontation de vos connaissances, de vos réflexions et de vos points de vue a fait de cette aventure une expérience formatrice, riche et si captivante. Je vous exprime ma gratitude, et si votre nom n'apparaît pas dans ces lignes, je suis certaine que vous vous reconnaitrez malgré tout !

Je remercie chaleureusement tous les membres de l'IRDL pour avoir toujours été disponibles, et plus particulièrement Antoine Kervoelen, Antoine Le Duigou, Samuel Réquillé, Chloé Joly, David Siniscalco, Justin Mérotte, Clément Gourier, Morgane Tanguy, Mickaël Castro, Bastien Seantier, Françoise Péresse, Marianne Gibaud, Anthony Magueresse, Véronique Le Tilly et Olivier Sire pour vos conseils et vos apports de toute sorte au cours de ma thèse.

Un grand merci également à Johnny Beaugrand, Sylvie Durand, Marie-Françoise Devaux, Camille Alvarado, Fabienne Guillon, Angeline Paturel, Xavier Falourd, Loïc Foucat, David Legland, et Bruno Pontoire de l'INRA (Nantes) pour votre investissement, votre aide, vos conseils et pour votre accueil durant mes séjours au sein de votre équipe.

De même, je remercie Patrick Perré, Floran Pierre et Pin Lu (Centrale Supélec) pour votre contribution à ces travaux.

Je remercie également Tancrede Alméras et Olivier Arnould du LMGC (Montpellier) pour nos collaborations scientifiques, vos conseils et pour nos nombreux échanges.

Merci aussi à l'équipe PIAF de l'INRA (Clermont-Ferrand), et plus particulièrement à Nicole Brunel pour ton accueil et le partage de ton savoir-faire, et à Bruno Moulia, Mélanie Ducourteix et Nathalie Leblanc-Fournier pour nos échanges à Clermont.

Un grand merci à Jean-Paul Trouvé, Géraldine Dambry et Christelle Leroux (Terre De Lin) pour votre disponibilité et votre coopération, si essentielles à de nombreux travaux réalisés au cours de cette thèse.

I also thank very warmly Tatyana Gorshkova and her team from KIBB (Kazan), for welcoming me twice in their institute, for our fruitful discussions, for your many tips and for answering my (so numerous !) questions. Thank you very much to Polina Mikshina, Natalia Mokshina and Liudmila Kozlova for our great times in Kazan !

Merci aux organisateurs de la "Journée franco-russe du jeune chercheur" et à l'ambassade de France en Russie, pour leur soutien financier qui m'a permis de me rendre une première fois à Kazan et de faire partager mes premiers travaux à l'étranger.

Un travail est réalisé plus efficacement dans un contexte de bonne humeur et d'enthousiasme au quotidien. Merci donc à tous mes petits camarades de bureau(x) et de labo, qui ont su faire briller mes journées, et ce tout au long de ces trois années !

Enfin, encore un grand et gros merci à toute ma petite famille (et aux copains aussi, mais c'est presque pareil !), pour vos encouragements, votre soutien, vos visites à Lorient et en Bretagne ou encore toutes vos petites attentions. Même si vous ne comprenez pas tout le temps ce que je vous raconte (je crois bien que c'est le propre d'une thèse !), vous êtes toujours là et partants pour m'écouter et m'encourager, et c'est bien ça le plus important. Merci à vous !!!



## TABLE OF CONTENTS

---

<b>GENERAL INTRODUCTION .....</b>	<b>11</b>
<b>CHAPTER I – LITERATURE REVIEW.....</b>	<b>15</b>
<b>1. INTRODUCTION.....</b>	<b>17</b>
<b>2. GROWTH OF THE FLAX PLANT AND DEVELOPMENT OF ITS FIBERS.....</b>	<b>19</b>
2.1. Growth of the plant.....	19
2.2. Internal organization of flax biological tissues .....	21
2.3. Cell growth of flax fibers.....	24
2.4. Cell wall thickening .....	26
2.5. Cell wall composition and organization.....	28
2.6. The slenderness of the flax stem: an incredibly slender structure in the plant kingdom .....	30
<b>3. EVOLUTION OF INDUSTRIAL CROPS AND VARIETAL SELECTION.....</b>	<b>32</b>
3.1. New varieties of major industrial crops and selection criteria .....	33
3.2. Focus on new flax varieties and related selection criteria.....	35
3.3. Lodging of flax: investigations toward a better lodging resistance .....	39
<b>4. INFLUENCE OF CULTURAL CONDITIONS AND OF THE ENVIRONMENT ON THE     PROPERTIES OF FLAX STEMS AND FIBERS.....</b>	<b>44</b>
4.1. Sowing rate and crop canopy .....	45
4.2. Wind-induced movements of crop canopies.....	47
4.3. Tropisms and plant responses .....	49
4.3.1. <i>Thigmotropism and seismotropism</i> .....	50
4.3.2. <i>Gravitropism</i> .....	53
<b>5. CONCLUSIONS.....</b>	<b>57</b>
<b>6. REFERENCES .....</b>	<b>58</b>
<b>CHAPTER II – FLAX – FROM THE STEM TO THE FIBER.....</b>	<b>71</b>
<b>1. INTRODUCTION.....</b>	<b>73</b>
1.1. History of the varietal selection of flax .....	73
1.2. Flax: from the plants to composites reinforced by flax fibers .....	74
1.3. A plant as an interesting structure and source of bioinspiration.....	76
<b>2. MATERIALS AND METHODS .....</b>	<b>78</b>
2.1. Plant materials .....	78

2.2.	Architectural analysis of the stems.....	79
2.3.	Measurement of single fiber length and diameter.....	80
2.4.	3D reconstruction of a fiber bundle.....	80
2.5.	Scanning electron microscopy.....	80
2.6.	Atomic Force Microscopy.....	80
2.7.	Tensile tests on elementary fibers.....	81
2.8.	Statistical analysis.....	81
2.9.	Carbon/epoxy sample.....	82
<b>3.</b>	<b>RESULTS AND DISCUSSION – IMPACT OF THE VARIETAL SELECTION ON PLANT ARCHITECTURE AND FIBER MECHANICAL PROPERTIES.....</b>	<b>82</b>
3.1.	Morphological study of the stems of different varieties.....	82
3.1.1.	<i>Stem height</i> .....	82
3.1.2.	<i>Stem diameter</i> .....	83
3.2.	Anatomy of the stems of different varieties.....	84
3.3.	Mechanical properties of the fibers of different varieties.....	87
<b>4.</b>	<b>RESULTS – ARCHITECTURE OF PLANTS FROM A SINGLE FLAX VARIETY.....</b>	<b>89</b>
4.1.	Overall morphological study of a stem.....	89
4.2.	Geometrical and mechanical properties of flax fibers depending on the sampling height along the stem.....	91
4.3.	Evolution of fiber diameter along length.....	93
4.4.	Tensile behavior in transverse direction and middle lamellae.....	94
<b>5.</b>	<b>DISCUSSION – REINFORCEMENT MECHANISMS IN A FLAX STEM.....</b>	<b>95</b>
5.1.	Anatomical analysis of a stem.....	95
5.2.	Analysis of elementary fibers and bundle characteristics.....	96
5.2.1.	<i>Fiber aspect ratio and mechanical properties</i> .....	96
5.2.2.	<i>Cohesion within a fiber bundle and middle lamellae</i> .....	97
5.3.	Analogy between specific properties of flax fibers and glass ones.....	98
5.4.	Analogy between flax stems and composites reinforced by thin plies	100
<b>6.</b>	<b>CONCLUSIONS.....</b>	<b>101</b>
<b>7.</b>	<b>REFERENCES.....</b>	<b>103</b>
 <b>CHAPTER III – EVOLUTION OF FLAX FIBER PROPERTIES DURING PLANT DEVELOPMENT AND RETTING.....</b>		 <b>107</b>
<b>1.</b>	<b>INTRODUCTION.....</b>	<b>109</b>
1.1.	The flax fiber: several uncommon features.....	109
1.2.	From plant development to fiber thickening.....	110

1.3. The retting step.....	110
<b>2. MATERIALS AND METHODS .....</b>	<b>112</b>
2.1. Plant material, culture conditions and retted fibers.....	112
2.2. Sample preparation prior AFM PF-QNM measurements .....	112
2.3. AFM PF-QNM Measurements.....	113
2.4. Tensile tests on elementary fibers from non-retted stems.....	114
2.5. Raman spectroscopy.....	114
2.6. Statistical analysis.....	114
2.7. X-Ray Diffraction .....	114
2.8. NMR investigations .....	115
<b>3. RESULTS AND DISCUSSION – FIBER PROPERTIES DURING PLANT</b>	
<b>DEVELOPMENT.....</b>	<b>116</b>
3.1. Indentation modulus and morphology of fiber cell walls analyzed by AFM Peak Force QNM measurements.....	116
3.2. Tensile tests performed on elementary fibers .....	119
3.3. Composition of the cell wall approached by Raman spectroscopy .....	120
<b>4. RESULTS AND DISCUSSION – FIBER PROPERTIES DURING RETTING.....</b>	<b>122</b>
4.1. Indentation modulus and morphology of fiber cell walls analyzed by AFM Peak Force QNM measurements.....	122
4.2. Monitoring of crystallinity degree during retting using X-ray diffraction and NMR analysis.....	125
4.3. Investigation of cell wall biochemical structure using NMR .....	129
<b>5. CONCLUSIONS.....</b>	<b>132</b>
<b>6. REFERENCES .....</b>	<b>134</b>

## **CHAPTER IV – BENDING PROPERTIES OF FLAX PLANTS – ROLE OF THE FIBERS WITHIN THE STEMS .....**

<b>1. INTRODUCTION.....</b>	<b>139</b>
1.1. Description of a flax stem .....	140
1.1.1. <i>General features and organization.....</i>	<i>140</i>
1.1.2. <i>Two main mechanical tissues – Flax fiber crown and xylem....</i>	<i>140</i>
1.2. Bending properties of stems .....	141
1.3. Compressive strength of flax-based composites .....	141
<b>2. MATERIALS AND METHODS .....</b>	<b>142</b>
2.1. Plant materials – Stems and fibers .....	142
2.2. Anatomical analysis of the stems .....	143
2.3. Specific gravity measurements.....	143

2.4.	Three-point bending test .....	144
2.5.	Tensile test on elementary fibers .....	146
2.6.	Nanotomography .....	147
2.7.	Unidirectional composites .....	147
2.8.	Scanning electron microscopy (SEM) .....	147
<b>3.</b>	<b>RESULTS AND DISCUSSION – LINK BETWEEN BENDING BEHAVIOR OF FLAX STEMS AND FIBER STIFFNESS .....</b>	<b>147</b>
3.1.	Architecture and morphology of stems.....	147
3.2.	Analysis of bending characterization conditions .....	149
3.3.	Characterization of the bending stiffness of flax stems.....	150
3.3.1.	<i>Stress-strain behavior of stems and xylem cores.....</i>	<i>150</i>
3.3.2.	<i>Bending stiffness of stems and xylem cores.....</i>	<i>151</i>
3.3.3.	<i>Apparent bending moduli of stems and xylem cores.....</i>	<i>152</i>
3.4.	Longitudinal modulus of flax fibers estimated by bending tests.....	153
<b>4.</b>	<b>RESULTS – COMPRESSIVE STRENGTH OF FLAX FIBERS WITHIN STEMS ....</b>	<b>155</b>
4.1.	Mechanical properties of elementary flax fibers.....	155
4.2.	Failure mechanisms of flax stems during bending tests .....	156
4.3.	Compressive properties of Bolchoï stems through bending tests .....	157
4.4.	Compressive properties of flax stems of different varieties.....	158
4.5.	Compressive properties of xylem cores through bending tests .....	160
<b>5.</b>	<b>DISCUSSION – CORRELATION BETWEEN COMPRESSIVE PROPERTIES OF UD (FLAX/EPOXY) AND FIBER BUNDLES WITHIN A STEM .....</b>	<b>162</b>
5.1.	Compressive properties of unidirectional flax/epoxy composites .....	162
5.2.	First approach to estimate the fiber compressive strength.....	164
5.3.	Second Approach to estimate the fiber compressive strength.....	164
5.4.	Is the modest compression strength of flax fibers a problem for living plants?.....	166
<b>6.</b>	<b>CONCLUSIONS .....</b>	<b>167</b>
<b>7.</b>	<b>REFERENCES .....</b>	<b>168</b>

## **CHAPTER V – INFLUENCE OF CULTURAL CONDITIONS AND STIMULI ON FLAX STEMS AND FIBERS .....**

<b>1.</b>	<b>INTRODUCTION.....</b>	<b>173</b>
1.1.	Slenderness of plants and mechanical stability.....	174
1.2.	Plant response to a mechanical stress: case of wind .....	175
1.3.	Lodging and plant gravitropic response.....	176

<b>2. MATERIALS AND METHODS .....</b>	<b>177</b>
2.1. Plant materials and measurements .....	177
2.1.1. <i>Plant materials for the study of the mechanical stability</i> .....	177
2.1.2. <i>Plant materials for the study of the influence of wind</i> .....	177
2.1.3. <i>Plant materials for the study of gravitropic reaction</i> .....	178
2.2. Anatomical analysis .....	180
2.2.1. <i>Samples from living materials</i> .....	180
2.2.2. <i>Samples from dried materials</i> .....	181
2.3. Three-point bending tests .....	181
2.4. Greenhill's model .....	182
2.5. Effect of a gradient in elastic modulus .....	183
2.6. Measurements of elementary fiber length .....	184
2.7. Tensile tests on elementary fibers .....	185
2.8. Statistical analysis .....	185
<b>3. RESULTS – SLENDERNESS AND STABILITY OF FLAX PLANTS .....</b>	<b>186</b>
3.1. Stem properties and anatomy obtained from living plants .....	186
3.2. Bending properties along the stem .....	188
3.3. Safety against buckling of a living stem .....	189
3.4. Effect of elastic modulus gradient on the stability of a flax stem .....	190
<b>4. DISCUSSION – SLENDERNESS AND STABILITY OF FLAX PLANTS .....</b>	<b>190</b>
<b>5. RESULTS – CONVENTIONAL VERSUS GREENHOUSE CULTIVATION .....</b>	<b>193</b>
5.1. Architectural study of the stems grown outdoor or in greenhouse .....	193
5.2. Anatomy of the stems grown outdoor and in greenhouse .....	194
5.3. Impact of the type of cultivation on the length of elementary fibers ..	196
5.4. Bending properties of the stems .....	197
5.5. Influence of the type of cultivation on fiber mechanical properties ...	199
<b>6. DISCUSSION – CONVENTIONAL VERSUS GREENHOUSE CULTIVATION .....</b>	<b>200</b>
<b>7. RESULTS AND DISCUSSION – PLANT GRAVITROPIC RESPONSE .....</b>	<b>201</b>
<b>8. CONCLUSIONS .....</b>	<b>204</b>
<b>9. REFERENCES .....</b>	<b>205</b>
<b>GENERAL CONCLUSION .....</b>	<b>209</b>
<b>CONCLUSIONS .....</b>	<b>209</b>
<b>ON-GOING WORKS AND PERSPECTIVES .....</b>	<b>211</b>



## GENERAL INTRODUCTION

---

Due to the combination of high specific mechanical performances and plant-based origin, flax (*Linum usitatissimum* L.) fibers are interesting reinforcement for environmentally friendly composite materials. Over the past few years, an increasing number of research articles and reviews has focused on the processing and properties of flax-based products, without taking into account the original key role of flax fibers in the stem. Indeed, these latter are supporting tissues of the living flax stem, a primary function that explains the outstanding flax fiber characteristics as well as the mechanical stability of slender flax plants. Nevertheless, the ontogeny of the plant, scattering of fiber properties along the stem or the plant growth conditions are rarely considered. Conversely, exploring the development of flax fibers and parameters influencing the plant mechanical properties (from the whole plant to the fiber scale) is an interesting way to understand and control the reproducibility of fiber performances, and to a greater extent, to optimize flax fiber-based products.

This thesis presents, through its five chapters, a multi-scale mechanical study of flax stems and of its fibers. A description of the behavior of flax at both scales is given, with the objective of the improving fiber performances and their reproducibility, and optimizing those of the associated composites.

*Chapter I* consists of a literature review. It synthesizes a relevant background for the work exposed in this thesis. This chapter includes a survey on the growth stages of flax plants and the internal organization of the stem biological tissues. Additionally, key findings regarding the development of its fibers are reviewed and a state of the art of the varietal selection of several main industrial crops is given. The third section reviews the influence of the cultural conditions as well as the impact of main tropisms on the stem and fiber characteristics.

In *Chapter II*, a general approach of flax architecture analysis, from the stem to the fibers, is performed. Attention is given to the impact of varietal selection on the properties of plants and resulting fibers, based on varieties registered at different times. Moreover, the overall reinforcement mechanisms of stems, considered as a natural composite structure, are investigated in order to provide a model for bioinspired composite materials.

*Chapter III* details the changes in fiber performances taking place over two main processes of industrial interest, namely plant development and retting, which are both fiber quality-related steps. The results of *Chapter III* are based on investigations at the fiber and cell wall scales, combining mechanical analysis and biochemical composition study.

*Chapter IV* presents the fiber contribution to the stiffness of flax stems subjected to bending. This chapter also allows to propose a new method of estimating the apparent modulus of elementary flax fibers based on three-point bending tests performed on stems. Additionally, the compressive behavior of flax fiber bundles within the stem, as well as of the xylem core, is highlighted. It illustrates the buckling mechanisms of flax fibers within a stem subjected to compressive loads, linking the function and behavior of the fibers within the plant in order to reduce compressive failure of flax-based composites.

Finally, *Chapter V* investigates the influence of cultural conditions on flax characteristics, at the stem level as well as at the fiber scale. Namely, the mechanical stability of flax under conventional cultural conditions is explored and related to the specific architecture and bending modulus of the plant. Then, greenhouse cultivation of flax is considered regarding modifications of plant architecture and anatomy, as well as changes of the flax fiber yield and mechanical performances. As a final section, the gravitropic response of flax is studied to provide knowledge about possible lodging recovery and its impact on fiber quality.

Several articles have arisen from the works presented in this thesis, in the form of international peer-reviewed journal papers. First, a review derives from the literature survey presented in *Chapter I* [1]; this former is currently under examination. Secondly, original research articles, based on *Chapter II*, have been published [2,3]. *Chapter III* led to two articles, one being already published [4] and the second one being under review [5]. Similarly, two articles result from *Chapter IV* with one accepted at present [6] and a second recently submitted [7]. Finally, three potential articles derive from *Chapter V* [8–10], including one accepted very recently [9].

**Publications (accepted or under review) and corresponding chapters:****Chapter I:**

1. **Goudenhooff, C.**; Bourmaud, A.; Baley, C. Flax (*Linum usitatissimum* L.) fibers for composite reinforcement: exploring the link between plant growth, cell walls development and fiber performances. *Front. Plant Sci.*, under review.

**Chapter II:**

2. **Goudenhooff, C.**; Bourmaud, A.; Baley, C. Varietal selection of flax over time: Evolution of plant architecture related to influence on the mechanical properties of fibers. *Ind. Crops Prod.* **2017**, *97*, 56–64, doi:10.1016/j.indcrop.2016.11.062.
3. Baley, C.; **Goudenhooff, C.**; Gibaud, M.; Bourmaud, A. Flax stems: from a specific architecture to an instructive model for bioinspired composite structures. *Bioinspir. Biomim.* **2018**, *13*, 26007, doi:10.1088/1748-3190/aaa6b7.

**Chapter III:**

4. **Goudenhooff, C.**; Siniscalco, D.; Arnould, O.; Bourmaud, A.; Sire, O.; Gorshkova, T.; Baley, C. Investigation of the Mechanical Properties of Flax Cell Walls during Plant Development: The Relation between Performance and Cell Wall Structure. *Fibers* **2018**, *6*, 6, doi:10.3390/fib6010006.
5. Bourmaud, A.; Siniscalco, D.; Falourd, X.; **Goudenhooff, C.**; Foucat, L.; Pontoire, B.; Arnould, A.; Beaugrand, J.; Baley, C. Evolution of the parietal structure and mechanical properties of flax cell walls during the retting step. *Carbohydrate Polymers*, under review.

**Chapter IV:**

6. Réquilé, S.; **Goudenhooff, C.**; Bourmaud, A.; Duigou, A. Le; Baley, C.; Le Duigou, A.; Baley, C. Exploring the link between flexural behaviour of hemp and flax stems and fibre stiffness. *Ind. Crops Prod.* **2018**, *113*, 179–186, doi:10.1016/j.indcrop.2018.01.035.
7. Baley, C.; **Goudenhooff, C.**; Perré, P.; Liu, P.; Pierre, F.; Bourmaud, A. Compressive strength of flax fibre bundles within the stem and comparison with unidirectional flax/epoxy composites. *Ind. Crops Prod.*, under review.

**Chapter V:**

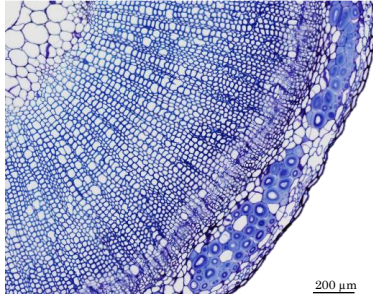
8. **Goudenhooff, C.**; Alméras, T.; Bourmaud, A.; Baley, C. The remarkable slenderness of flax plant and pertinent factors affecting its mechanical stability. *Biosyst. Eng.*, under review.
9. **Goudenhooff, C.**; Bourmaud, A.; Baley, C. Conventional or greenhouse cultivation of flax: What influence on the number and quality of flax fibers? *Ind. Crops Prod.* **2018**, *123*, 111–117, doi:10.1016/j.indcrop.2018.06.066.
10. **Goudenhooff, C.**; Bourmaud, A.; Baley, C. Study of plant gravitropic response: exploring the influence of lodging and recovery on the mechanical performances of flax fibers. *Ind. Crops Prod.*, under review.



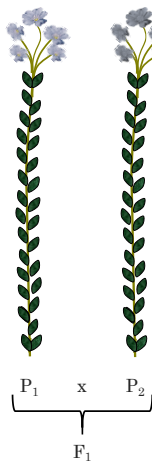
**CHAPTER I –  
LITERATURE REVIEW**

## Graphical abstract

---



- ❖ What are the main stages of stem and fiber development?



- ❖ What could be the influence of the varietal selection on flax plant characteristics?



- ❖ How could cultural conditions or external stimuli influence the properties of flax stems and fibers?

**Goudenhooff, C.;** Bourmaud, A.; Baley, C. Flax (*Linum usitatissimum* L.) fibers for composite reinforcement: exploring the link between plant growth, cell walls development and fiber performances. *Front. Plant Sci.*, under review.

## CHAPTER I – LITERATURE REVIEW

---

### 1. Introduction

Flax (*Linum usitatissimum* L.) is an industrial plant of growing interest. Since its domestication started from Neolithic times about 10,000 years ago [1], this plant has been cultivated for its fibers, leading to its designation of “fiber crop” or “fiber plant”. Flax fibers have been used as textile raw material, composing cords and weaving yarn and later on more fashionable garments or high-quality fabric upholstery. More recently, starting around the 1930s [2], and supported by both mechanical performances and impressive length-to-diameter ratio of flax fibers (average diameter of 20  $\mu\text{m}$  for a length of 25 mm)[3], their applications have been extended to more technical uses, namely as reinforcements for composite materials for the development of more sustainable materials [4]. In recent years, the popularity of plant fiber-based composites has been greatly increasing to substitute glass fibers; the advantages of plant fibers compared with glass ones are their biological origin from photosynthesis and their renewable aspect, low density, low hazard manufacturing process for human health, low abrasion of processing tools, *etc.* [5]. Although, flax fibers have a similar range of specific mechanical properties than glass fibers, with average elastic modulus of 52.4 GPa, strength at break of 976 MPa and strain at break of 2.15% for a fiber density of 1.53 [6]. In the case of flax-based composite materials, the fibrous part or reinforcement consists of either technical flax fibers or short fibers, impregnated with a polymer matrix. The technical fibers are composed of fiber bundles (being more or less individualized)[7] in a random aligned nonwoven form [8], unidirectional plies [9] or as more complex fabrics [10]. Short fibers of a few millimeters in length and well individualized can be used to process biocomposites too, through extrusion or injection routes [11]. The polymer matrix holds the reinforcement; it can be a thermoplastic polymer [12–14] but also a thermoset resin [15–17]. Finally, the development of flax-based composites is a continuously expanding research area, whether at the reinforcement scale, at the matrix scale or regarding the optimization of the reinforcement/matrix interface, and is the subject of an increasing number of papers including reviews [4,5,18,19].

Thus, even though flax is the earliest domesticated plant [20], its fibers are used in the constitution of a large range of materials, from everyday clothing to technical

composites. These numerous existing applications and the constant development towards more innovative materials make flax a plant of growing industrial interest. In other words, flax is the subject of intensive works of research in the field of material science, with the aim of improving different criteria depending on whether fibers are intended for textiles or composite materials. For instance, loads transfers by friction is investigated for textiles, whereas matrix adhesion is of interest for composite materials; in both cases, fiber individualization is a subject of improvement research. However, much less studies focus on flax as a living plant to investigate the relationships between the properties of flax fibers and the development of the plants from which they are obtained. Among the different plants cultivated by man for fiber production, flax has many particularities that make it a unique model of development and architecture [21]. The control of its growth allows its fibers to reach an optimized maturity and exceptional characteristics in terms of mechanical morphology and performances [22,23]. Moreover, for nearly one hundred years, it has been the subject of a varietal selection that has made it a plant with a strong technical potential but also a great source of remuneration for farmers [24]. The varietal selection is most probably the origin of the uncommon slenderness of flax, which allows one to consider flax plant as a model of stability. Like any plant, it reacts to external stresses and its development and stem architecture can be influenced by thigmomorphogenesis, gravitropism as well as environmental or cultivation conditions [25].

The present chapter proposes a review of the literature to highlight possible links between the characteristics of flax plants and their possible impact on the fibers performances. In the first section, the main growth stages of flax plants and the internal organization of the stem biological tissues are investigated. In addition, the development of flax fibers, from their elongation to their thickening, is reviewed. The slenderness of flax is then highlighted through a comparison with herbaceous plants and trees. Secondly, the selection of new flax varieties and related selection criteria are explored. This second section includes an overview of the influence of the varietal selection on plant characteristics, together with a more extensive review of the changes inducing an improved lodging resistance. Finally, the last section explores the influence of the cultural conditions, more particularly of the seedling, on the stem and fiber characteristics. The impact of environmental conditions, such as the wind flow in a plant canopy and main tropisms, is reviewed.

## 2. Growth of the flax plant and development of its fibers

### 2.1. Growth of the plant

The ideal climate for flax cultivation is in temperate and humid regions where the daily temperature does not exceed 30°C and providing about 700 mm of annual rainfall; for instance, the temperate and maritime areas of Belgium, the Netherlands or France in coastal Western Europe are highly suitable locations for the flax cultivation [26]. The cultivation of flax starts with sowing, usually when the upper layer of soil reaches about 7-9°C, *i.e.* for example between 15th of March and 15th of April in France [27]. Afterwards, the growth stages of flax are divided into four main steps, like most crops: germination (or emergence of the plant), vegetative stage, flowering and seed formation, and finally senescence [28,29]. Germination usually starts around 5 to 10 days after sowing [22,30], and is characterized by the apparition of two fully developed cotyledons [31] which justify its classification as a dicotyledonous plant [32]. The vegetative stage starts quite slowly, the flax plant reaching 15 cm after about 15 to 20 days after germination [30,33]. This slow development is followed by a period of fast growth that takes place during about 15-20 days [30,33]. The flax plant is able to elongate several centimeters per day during fast growth [22,34], reaching 80-90 cm over this 2-week period of fast development [22,30]. Then, plant growth slows down and finalizes during flowering, and the plant reaches a final length of about 1 meter [33]. Flowering starts about 50 days after germination; it lasts about 15 days for a whole field, even though a single flower lasts only one day [35]. Seeds, contained inside capsules, are formed from 15 days after flowering; their full maturity is reached “late ripening”, happening after 5 to 6 weeks after flowering [36]. Finally, like for all plants, senescence takes place [29]. However, in the case of industrial flax plants, neither seed maturity nor the senescence are reached. In fact, plants are pulled out at fiber maturity, *i.e.* about 40 days after flowering or “yellow ripening”, phase that succeeds the “green ripening” (or “early-ripening”)[22]. Finally, the cultivation of flax, from sowing to fiber maturity, takes about 100 to 120 days.

In addition to farmers' experience, the different stages of intervention during the flax growing cycle are also determined taking into account the cumulative temperature received by the plant after sowing, also called cumulative growing degree-day [37]. The growing degree-day (GDD) is usually calculated as Equation I-1.

$$GDD = \frac{T_{max} + T_{min}}{2} - T_{base}$$

**Equation I-1. Growing degree-day (GDD) formula with  $T_{max}$  being the maximal daily temperature,  $T_{min}$  being the minimal daily temperature and  $T_{base}$  being the base temperature.**

For flax, the base temperature is equal to 5°C, as it is considered to be the zero vegetation for this plant (*i.e.* the temperature below which no growth occurs)[30,38], whereas it is usually 10°C for most crops. In the case of an average daily temperature being lower than the base temperature, GDD is considered equal to 0.

Finally, the cumulative temperature on day n is calculated as Equation I-2.

$$GDD_n = \sum_{i=1}^n \frac{T_{max,i} + T_{min,i}}{2} - T_{base}$$

**Equation I-2. Cumulative growing degree-day formula ( $GDD_n$ ) with  $T_{max,i}$  being the maximal daily temperature and  $T_{min,i}$  being the minimal daily temperature on the day  $i$  (with  $i$  equals to 1 on the day of sowing) and  $T_{base}$  being the base temperature (5°C for flax).**

The scheme visible on Figure I-1 illustrates the path of flax growth according to the cumulative GDD.

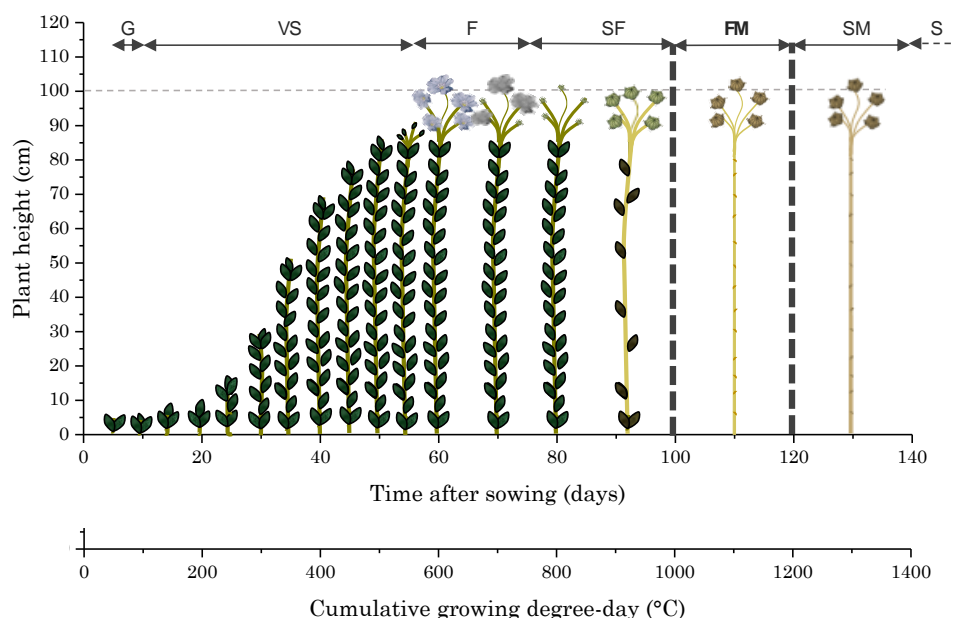


**Figure I-1. Scheme illustrating the growth of flax starting from the sowing day, according to the time after sowing and corresponding cumulative growing degree-day (GDD).  $G$ : germination;  $VS$ : vegetative stage;  $F$ : flowering;  $SF$ : seed formation;  $FM$ : fiber maturity;  $SM$ : seed maturity and  $S$ : senescence.**

By taking into account this method of calculation, the germination of flax happens when the cumulative GDD reaches about 50°C. Flowering takes place for a cumulative GDD of 550°C whereas the capsules are formed when a higher cumulative GDD is reached, namely around 650-700°C. Finally, fibers are considered mature when the cumulative GDD reaches from 950°C to 1100°C. The seeds would be mature around 1150°C but plants are actually pulled out at fiber maturity [30,38].

It is important to notice that, under different growth conditions (such as temperature or amount of rainfall) [6,39] or different cultivation methods (such as sowing density)[40], the growth pattern of flax is modified. In summary, Figure I-1 only gives a general indication of the flax growth stages. Finally, once fibers are mature and plants are pulled out, stems are laid on the field to undergo dew-retting. During this natural process, fiber bundles become gradually separated from adjoining tissues through the action of hydrolytic enzymes provided by microorganisms [41]. This delicate process (that will not be explained in depth in this review) intends to facilitate the fiber extraction; this stage is realized by further industrial processes being required steps for textiles and composite manufacturing [42].

## **2.2. Internal organization of flax biological tissues**

Flax is, like every plant, composed of different body parts known as plant organs; the vegetative organs can be reduced to the stem, the leaf and the root, each having particular functions [43]. The plant organs form a continuous structure because they have a common origin. The present section as well as the whole paper will focus only on the stem, which is the key organ of the flax fiber ontogeny.

The stem has two main functions: conduction and support [44]. To perform its vital functions, the stem is itself composed of different elements, *i.e.* several types of tissues made of grouping of different cell types distinguishable in position, structure, origin or developmental phase [45]. The tissues composing the stem can be separated in three basic tissue systems: epidermal, vascular or ground [45]. Each of them is initiated by differentiating meristems, *i.e.* by regions where non-differentiated cells have the ability to divide, in order to produce additional cells that will differentiate [46], such as fibers. Meristems involved in the longitudinal growth of the stem are called primary meristems and are located at the top of the shoot (and roots)[47]; they are responsible of the primary growth that leads to primary tissues [48]. For example, the protoderm is formed by meristematic cells that generate the epidermis, a primary tissue; the

procambium is also a primary meristem that is responsible for the primary vascular system [49]. On the other hand, the secondary growth, leading to secondary tissues, originates from lateral meristems. For instance, the vascular cambium is a lateral meristem responsible for the secondary vascular tissues. This secondary growth is responsible for the thickening of the stem, rather limited and essentially attributed to the secondary xylem in the case of flax [48]. Thus, flax is an herbaceous plant, a category which refers to plants expressing either a lack of or a poor organ secondary growth. The arrangement of the tissues within the stem defines and enables the functionality of this organ [50]. However, it is difficult to separate cells and tissues into clear categories, as the whole stem system comes from the interaction of each of them. Table I-1 presents a general classification based on literature about plant structures, that slightly differs between authors [3,44–46,48,50]; this present classification focuses on main cell types found in flax stems so is not exhaustive.

**Table I-1. Main tissues and cell types composing flax stems.**

Basic tissue system	Tissue	Cell type	Location	Main functions
Dermal	Epidermis		Outermost layer	Protection
Ground	Parenchyma	Parenchyma	Through the stem body	Metabolism
	Sclerenchyma	Fiber	Bundles in phloem	Mechanical support
Vascular	Phloem	Sieve-tube element	Phloem	Food/elaborated sap conduction
		Companion cell	Phloem	Delivery of substances to the sieve-tube element
	Xylem	Vessel element	Xylem	Water and raw sap conduction Mechanical support
		Tracheid	Xylem	Water and raw sap conduction Mechanical support

As a complement to Table I-1, the main tissues or cells visible on a transverse cross-section are identified in Figure I-2, with fibers gathered in bundles (up to 40 cells per bundle [51]) present at the periphery of the section. Figure I-2 also shows

imperfections, such as a heterogeneous fiber thickening within the same bundle for a given cross-section, which is part of this natural composite structure.

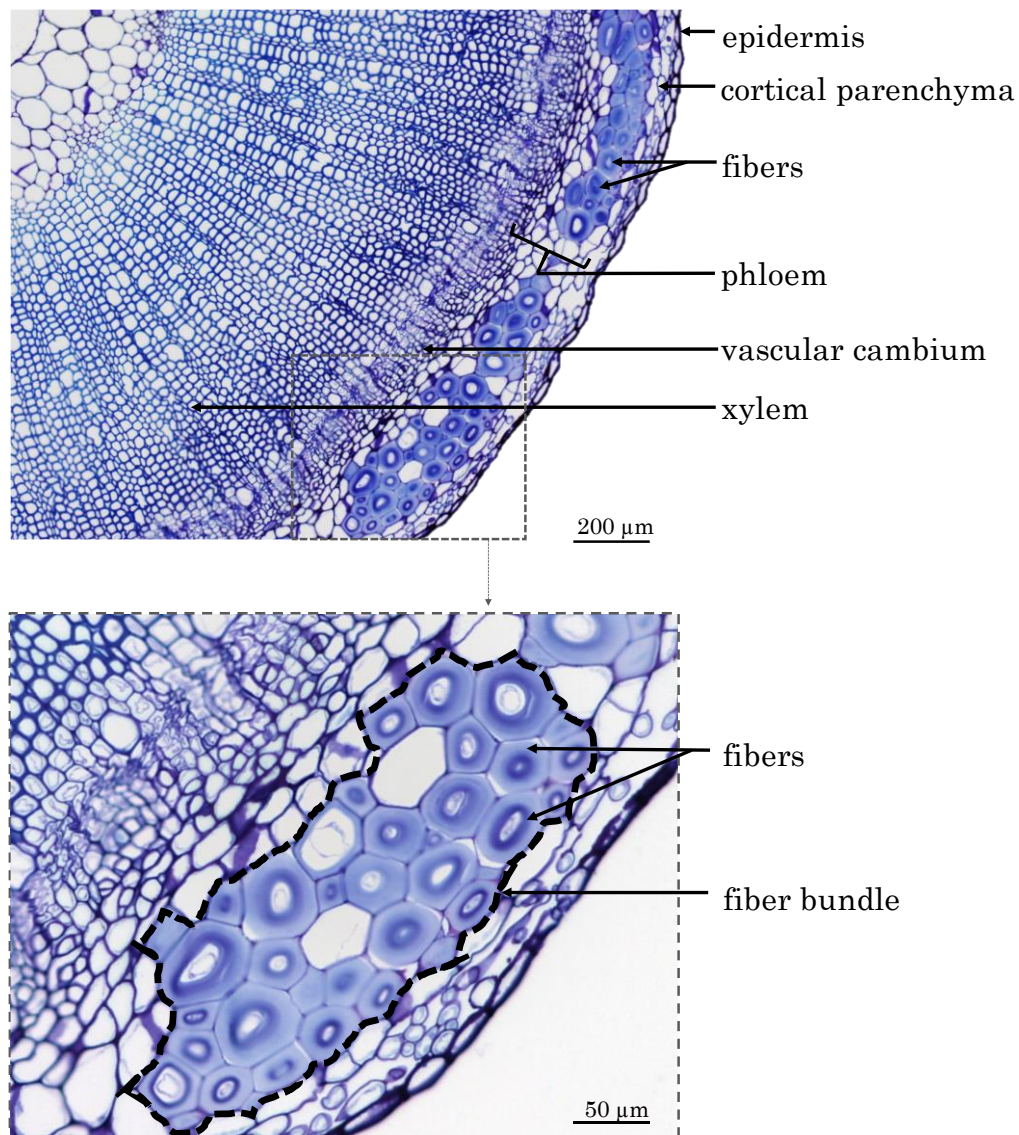


**Figure I-2. Description of identifiable tissues and cells on the transverse cross-section in the bottom part of a growing flax stem (adapted from literature [50,52,53]) stained with toluidine blue.**

Finally, flax fibers, occurring in bundles, are elements of the sclerenchymatous tissue located in the primary phloem [52], which has led to the terms ‘bast fibers’ [52,54,55], ‘primary phloem fibers’ [50,56,57] or ‘pericyclic fibers’ [58,59] sometimes found in literature. Contrary to some other fiber plants, flax generates only primary fibers *i.e.* fibers originate exclusively from primary growth [3]. For example, hemp has both primary and secondary fibers, whose latter are subjected to specific studies [60–62]. However, the formation of secondary fibers will not be detailed in the present work for the reasons mentioned above.

### 2.3. Cell growth of flax fibers

In terms of plant biology, a fiber is an individual sclerenchyma cell that provides mechanical support to the plant. In addition, a fiber is characterized by an extreme length along with a length-to-diameter ratio higher than 1000 [3]. Besides, this type of cell exhibits an impressively thick cell wall, as this latter can reach a ten micrometers in thickness, *i.e.* around ten times thicker than most other cell types [21]. Additional characteristics of a fiber are tapered ends and spindle-like shape [63]. Those remarkable properties, and more interestingly the intensified elongation and cell wall thickening, are verified by flax fibers, making them an appropriate model of plant cell growth.

In the case of flax fibers (referred to here as ‘fibers’), the cells are initiated by primary growth, from the apical meristem [64,65]. The fiber initiation is then followed by two main stages: elongation and cell wall thickening [66]. The stage of elongation is particularly outstanding in the case of flax fibers, as their final length can reach up to 65 mm with average values of 25 mm [67]. These extreme values could be explained by the two-step process of elongation: coordinated growth then intrusive growth [51]. Actually, the elongation process of flax fibers starts with coordinated growth, *i.e.* fibers elongate synchronously with neighboring cells [65]. Coordinated growth starts the fiber elongation from cell formation up to first millimeters from the apex, and it occurs for all types of cells of the upper region of the stem [3]. However, diverse sizes between cell types can result from coordinated growth, due to different cell division frequency and timing of division cessation [68]. The coordinated growth of a fiber leads to multinucleate cells and lasts only for several hours, at the end of which the cell reaches averages of 100  $\mu\text{m}$  in length for about 5  $\mu\text{m}$  in diameter [65,68]. Fiber elongation continues with intrusive growth, when the rate of fiber longitudinal growth exceeds that of neighboring cells still growing by symplastic growth; in this case, the fiber cell forces its way in between other cells and both of its ends form a “knee” being the characteristic of the beginning of the intrusive growth (Figure I-3) [51,65]. The shapes of knee disappear with the advance of the intrusion, and the apparition of the spindle-like shape with tapered ends happens as the fiber elongates [65]. In addition, the intrusive growth is realized by diffuse growth, *i.e.* the whole surface of the fiber is elongating [33] even though the diffuse elongation can have different rates over the fiber length which explains the formation of knees and tapered ends [65].

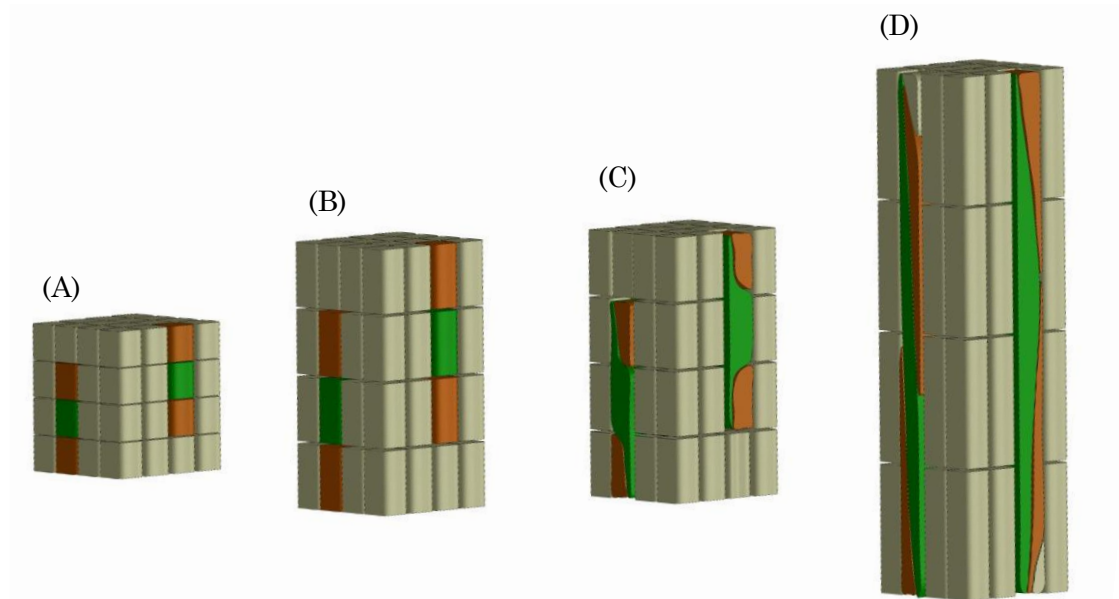


**Figure I-3.** Scheme illustrating the fiber elongation, with the fiber represented in orange. (A) first phase of the coordinated growth; (B) more advanced step of the coordinated growth; (C) beginning of the intrusive growth with a fiber having “knees” on both ends; (D) more advanced phase of the intrusive growth, with the fiber becoming a much longer structure than the neighboring cells and showing tapered end. Scheme inspired from [68,69].

The intrusive growth lasts longer than coordinated growth of the fibers, namely several days during which the elongation ranges about 1-2 cm per day [33]. Thus, intrusive growth happens starting below the first millimeters to the snap point region, and leads to fibers reaching several centimeters in length (average of 25 mm previously mentioned) for an average diameter of 20  $\mu\text{m}$  [3]. The so-called ‘snap point’ is defined as the crucial point past which no fiber elongation occurs, *i.e.* the length of a fiber reaches its maximum at the level of the snap point [22,33](Figure I-4).

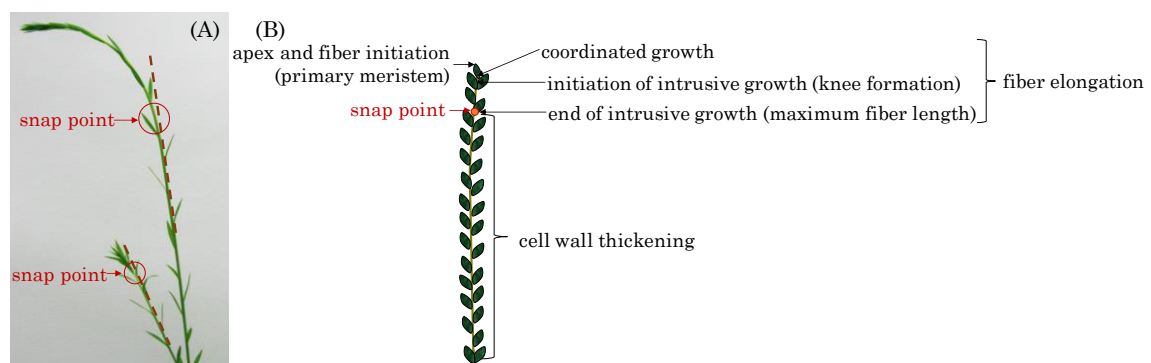


**Figure I-4.** (A) Pictures of two flax stems of different height having a different snap point location. (B) Scheme illustrating the different stages of the fiber formation along a flax stem according to the localization of the snap point. Scheme inspired from [33].

In addition, as intrusive growth no longer occurs below the snap point, the number of fibers on a transverse cross-section at a given stem height does not increase anymore at or below the snap point [33]. As the plant develops, the snap point moves along the stem; it is identifiable from the beginning of the fast growth until the plant ends its growth, and located up to 10 cm below the apex [33]. Furthermore, the snap point is simply identified as “the point where a difference in load is needed to break the stem in tensile” [33], due to a major change into fiber thickening and consequently stem bending stiffness, with much softer stem above the snap point. Impressively, the softer parts sometimes exhibit an almost vertical position of the top part of the plant with its own weight and wind (Figure I-4 (A)). This phenomenon of changes in stiffness is directly related to the second stage of fiber formation, namely cell wall thickening, happening essentially below the snap point [33]. Cell wall thickening is a much longer process than cell elongation, as it lasts weeks until plant maturity, *i.e.* it can take up to 60 days [33,65]. Thus, this stage is a long and complex process that is detailed in the dedicated following subsection.

#### **2.4. Cell wall thickening**

Due to the impressive thickness of the flax fiber cell wall compared to other plant species (flax fiber cell walls can reach more than 10  $\mu\text{m}$  whereas most cell walls are few microns thick)[21], the process of fiber thickening has been subjected to many studies. This process results in a uniform cell wall deposition along the fiber length but several cell wall layers, whose deposition is described hereafter [68].

At its formation, flax fiber cell, similarly as other plant cells, is constituted by a primary cell wall (PW) and stuck with other cell through the surrounding middle lamellae (ML) [22,70]. PW of flax fibers is a very thin and extensible structure able to withstand the impressive fiber elongation. In addition, it has the ability to withstand the deposition of the newest cell wall layers [71]. This foremost additional layer to be deposited inside the cell on PW is the so-called S1 layer, the first and very thin layer of the secondary cell wall (SW)[72,73]. The further deposited layers responsible of the extreme fiber thickening, and more specifically their denomination, are the subject of debates between authors. Based on a recent article focusing on mature fibers [72], it is possible to describe the next additional layer as the major thick layer denominated as S2 secondary cell wall layer or preferentially G-layer because of its specific properties. Namely, the G-layer is fiber-specific and has a pronounced content of cellulose (up to 90%) with a high crystallinity, a low angle of cellulose microfibrils

being almost parallel to the fiber longitudinal axis (with a microfibrillar angle reaching 8-10°), and is also characterized by the absence of both lignin and xylan, its high water content, its impressive porosity as well as contractile properties (that will be detailed further)[21]. This remarkable cell wall layer that is the G-layer has led to the term ‘G-fiber’ sometimes used to name the fibers having such a layer [74–76]. Lastly, the innermost thin deposited layer is defined as S3 or Gn-layer [72,77]. The organization of the different cell wall layers and the main stages of the fiber thickening are illustrated in Figure I-5.

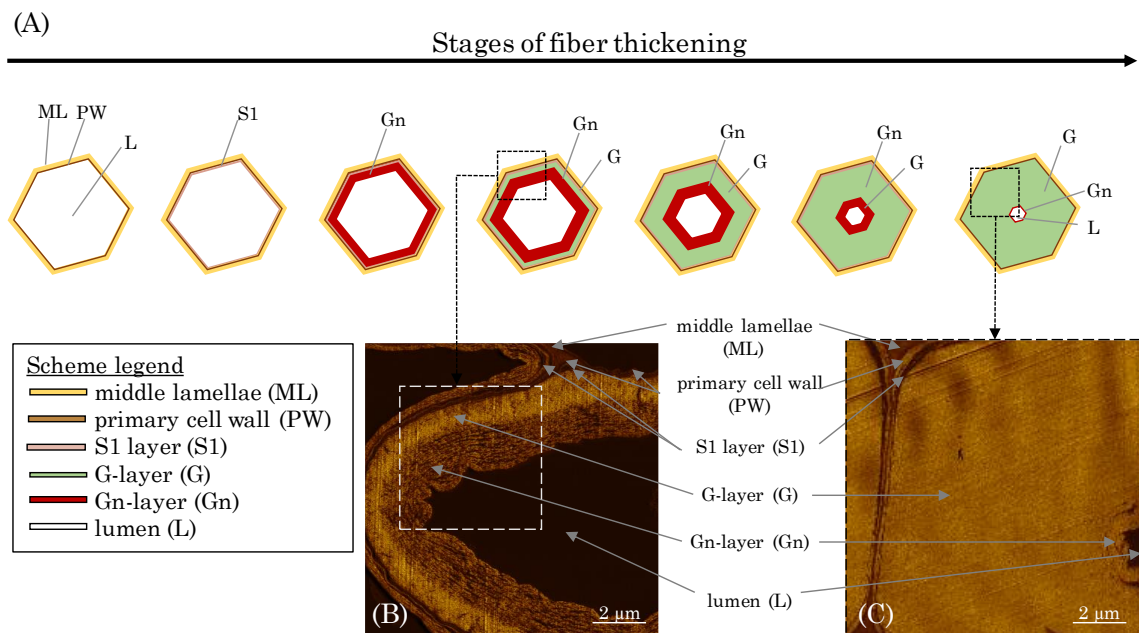


**Figure I-5.** (A) Scheme illustrating the different stages of the fiber thickening, starting from a cell having only a primary cell wall (PW) and ending with a fiber having a thick G-layer, a small lumen and a possibly remaining thin Gn-layer. (B) AFM image of an intermediate stage of cell wall thickening showing the G-layer and the innermost newest Gn-layer. (C) AFM image of a final stage of cell wall thickening showing the thick G-layer and the innermost residual Gn-layer. Scheme inspired from [21,78] and AFM image performed as detailed in [79].

In addition, the Gn-layer is usually hardly visible at the end of the thickening reached fiber maturity (Figure I-5); nevertheless, this Gn-layer can remain in cases of exogenous accidents such as drought or lodging during plant growth [80]. Thus, this latter layer is defined as a transient layer. In fact, the newest Gn-layer progressively transforms into the mature G-layer over cell wall thickening, gradually increasing the thickness of the G-layer [71]. Gn- and G-layers differ in appearance, namely the Gn-layer exhibits a loosen structure whereas the G-layer shows a much more compact

and homogenous configuration [81]. The differences that can be extended to other cell wall layers are explained by their composition as well as the microfibrils arrangement within layers.

## 2.5. Cell wall composition and organization

The composition and organization of flax cell wall constituents are the subject of numerous debates as they are different between authors [80,82,83].

**Table I-2. Characteristics and approximate composition of the different cell wall layers of flax fibers.**

Cell wall layer	Average thickness	Microfibrils orientation	Approximate composition
PW	0.2 $\mu\text{m}$ [87]	disperse orientation, preferentially $0^\circ$ [70,72]	~25-40% cellulose ~30% hemicelluloses (mainly xyloglucan and lesser amounts of arabinoxylan) ~30% pectins (mainly homogalacturonan; possibly rhamnogalacturonan (RG) I; RG II and arabinogalactan) [53,70,83,88–90]
S1	0.5 $\mu\text{m}$ [73,91]	60-80° [92]	~30-50% cellulose ~30% hemicelluloses (xylan, xyloglucan) ~5% pectins (homogalacturonan and RG I) ~10-20% lignin [70,72,78,89]
G	up to 15 $\mu\text{m}$ or 90% of the total cell wall area at maturity [71,83]	8-10° [91,93]	~75-90% cellulose ~15-20% hemicelluloses (glucomanan) ~5-10% pectins (RG I) [53,71,72,83,89]
Gn	0.5-1 $\mu\text{m}$ through thickening [79,91]	loosely packed as an heterogeneous structure [94]	cellulose hemicelluloses (glucomanan) pectins (nascent RG I (i.e. long galactan chains)) [71,72,78,94]

These characteristics are of great interest as they can be correlated to the mechanical performances of flax fibers [84]. Table I-2 attempts to give a general overview of the cell wall architecture, considering that this latter is influenced by several parameters (such as the flax selected variety, growth conditions, cultural practices, *etc.*) [85,86] and the disagreements between sources. In addition, the term ‘hemicelluloses’ used in Table I-2 is sometimes replaced by ‘neutral polysaccharides’ in literature, to echo back the ‘pectic’ polysaccharides that are pectins [72]. One can notice that the approximate composition of the Gn-layer is not well detailed in literature. However, the composition of the Gn-layer is expected to be quite similar to the G-layer one, as this latter is supposed to be a remodeling of the Gn-layer [71]. G- and Gn-layers, due to their high cellulose content, have a great affinity with toluidine blue (Figure I-2), which facilitates the fiber microscopic identification. The mentioned remodeling consists of the modification or trimming of the nascent rhamnogalacturonan RG I having long galactan chains by specific  $\beta$ -(1;4)-galactosidase [94]. The shortening of the RG I galactan chains enables stronger lateral interaction of cellulose microfibrils; thus, it leads to transform the heterogeneous loosen Gn-layer enriched in long chains of galactan into the homogeneous and mature G-layer composed of shortened and entrapped galactan chains (Figure I-6) [71].

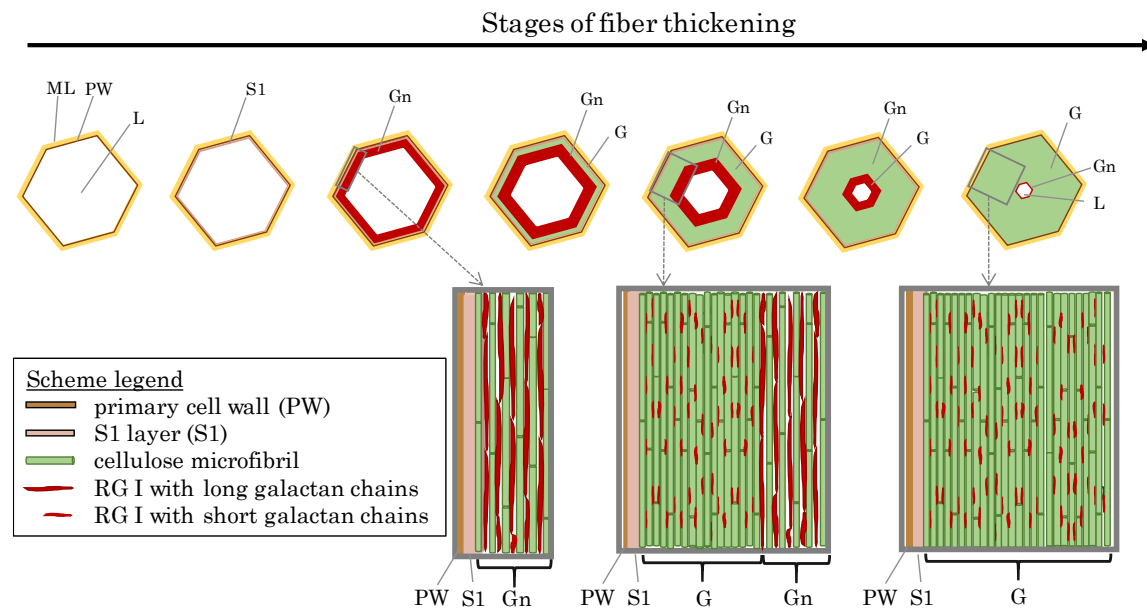


**Figure I-6.** Scheme illustrating the cell wall thickening in relation with the remodeling of the Gn-layer. Cellulose microfibrils are originally separated by long galactan chains present in nascent RG I [5]. The long galactan chains are then trimmed off which leads to the G-layer with compact cellulose microfibrils. Scheme inspired from [21,78].

## 2.6. The slenderness of the flax stem: an incredibly slender structure in the plant kingdom

‘Slenderness’ is defined as the ratio between the height of a column to its least radius of gyration [95], a definition that can be applied to engineered structures but to plants as well. More commonly for plants, slenderness is defined as the ratio between the maximal height and the basal diameter of the stem [96,97]. Based on literature, flax stems have no identified challenger in terms of slenderness, compared with plants exhibiting the same range of diameter (namely herbaceous plants, also called non-woody plants).



**Figure I-7. At the finalization stage of plant growth, flax can reach more than 1 m high for a basal diameter usually lower than 0.003 m for a conventional sowing rate of 1500-1800 plants per square meter [3,98]; these dimensions make flax a very slender structure.**

In fact, taking an average total height of 1 m (Figure I-7) and a slightly overestimated average basal diameter of 0.003 m [3,98], flax possesses a greater slenderness than herbaceous stems, for example in comparison with 190 other non-woody species studied by Niklas in 1993 [99](Figure I-8).

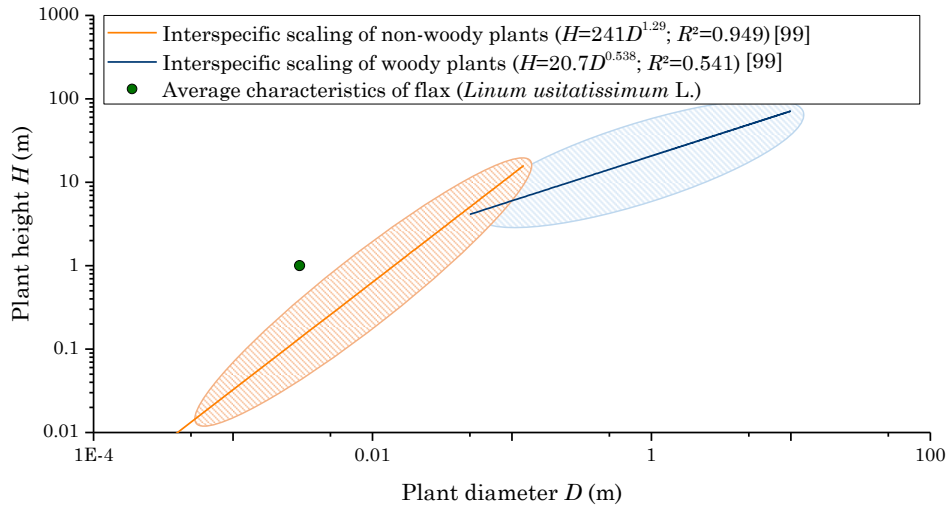


**Figure I-8. Interspecific scaling of plant height ( $H$ ) as a function of the plant basal diameter ( $D$ ) of flax in comparison with scaling formulas and maximal dispersion of non-woody plants (190 species) and woody plants (420 species) proposed by Niklas [99].**

The comparison has to be interpreted carefully, as flax is a plant cultivated under an optimal context, whereas most other plants are wild ones. Moreover, despite being an herbaceous plant, flax remarkably appears to present a scaling relationship closely resembling woody plants (including trees) rather than non-woody ones (Figure I-8). Thus, the slenderness factor highlights geometric aspects of the plant (namely its length and diameter), making flax an incredibly slender structure among the biological world. This interesting characteristic of flax can be attributed to the internal organization and properties of its composing tissues previously detailed, but the varietal selection work is most likely the main cause that has led to incredibly slender flax plants. In fact, although the varietal selection of food crops has been focusing on breeding dwarf cultivars to decrease their lodging vulnerability [100,101], the flax varietal selection has never intended to reduce the plant height, for profitable reasons. Indeed, on the contrary, reasonably high plants are desired to provide higher yield, as fibers are extracted from the stem.

The following section is mainly dedicated to review the literature about the work of varietal selection of industrial crops and more particularly for the case of flax. Moreover, examination of the growth of flax plant and development of its fibers detailed above is proposed as a reference for the rest of the present work. Based on the presented vocabulary and development stages of flax stems and fibers, the following paragraphs aim at explaining the link between exhaustive parameters modifying the

conventional plant growth, its slenderness and the resulting plant mechanical properties.

### 3. Evolution of industrial crops and varietal selection

The selection of crops, in the present paper also called ‘varietal selection’, is a work of great importance to achieve plant cultivation for industrial purposes. The varietal selection is the process or work through which breeders intent to change the regular characteristics of a domesticated plant in order to promote it with one or several desirable properties [46]. In few words, it consists of breeding existing varieties having wanted properties to provide a new selected variety (also called ‘cultivar’) that will exhibit the advantages of both parents (Figure I-9).

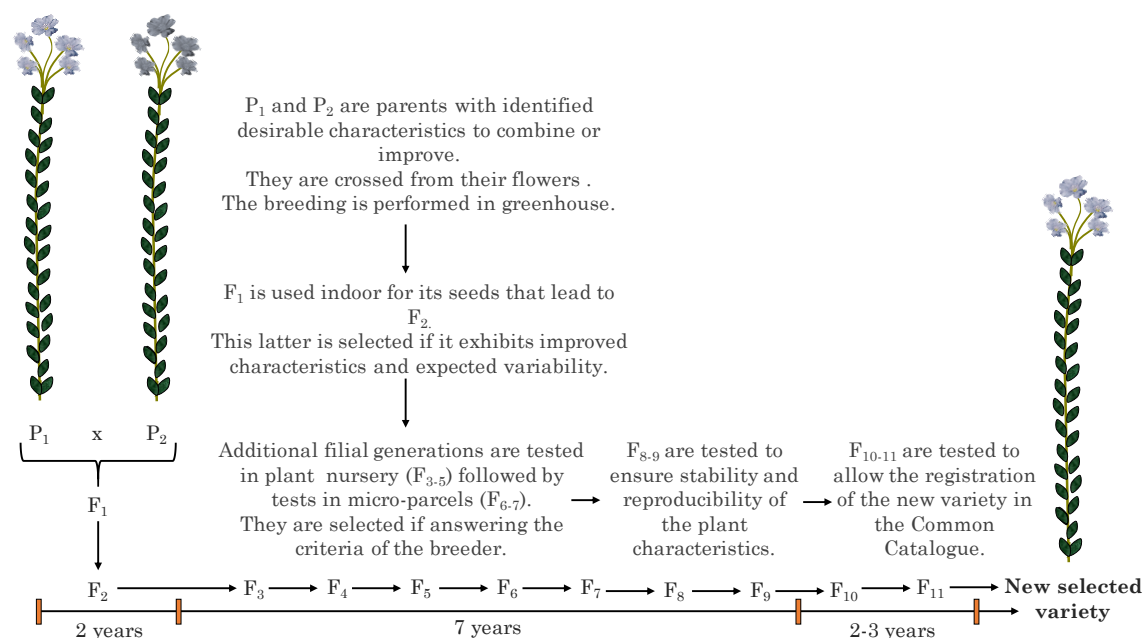


**Figure I-9. Scheme illustrating the main steps of the varietal selection in the case of flax, from the parents P<sub>1</sub> and P<sub>2</sub> to the numerous filial generations F<sub>i</sub> to achieve the obtainment of a new selected variety. Scheme inspired from [35,46].**

Thus, this selection is an artificial process that would not occur naturally. For flax, being a self-pollinating plant, crossing is performed manually from the flowers by breeders. More than 10 years are required to provide a genetically fixed variety and for its proper multiplication [35]. The detailed principle of the varietal selection and how it affects the plant genetics will not be discussed in the present review, that rather aims at explaining the criteria of selection and their influence on the plant characteristics.

### 3.1. New varieties of major industrial crops and selection criteria

Among industrial plants, cereals such as rice (*Oryza sativa*), wheat (*Triticum aestivum*), rye (*Secale cereale*), barley (*Hordeum vulgare*) or maize (*Zea mays*), have been domesticated then selected over the years. The major goals of their selection are for instance higher grain yields, larger grains, thicker straws or seeds that separate easier from the chaff.

As a first example, rice has been greatly studied regarding the process of selection; it is considered to be the major model system for crop plant research [102]. Indeed, rice, cultivated for over 6,000 years, is currently one of the most cultivated cereals over the world, especially in Asia, and a major source of nutrition for billion people [102,103]. In addition, it has the smallest genome among major food crops, thus provides an easier obtained knowledge that could be extended to wheat, barley or maize [46]. There are over 40,000 varieties of rice, but not many are grown industrially for their high grain yields [46]. Efficiently started in the 1950s, the selection of new rice varieties, especially through semi-dwarf varieties, has enabled an increase of 30% of the rice yield potential [104]. The plant height has been reduced over selection as shorter rice plants exhibit a higher stability to lodging [100,105]. Lodging is defined as the process through which the plant is displaced from its vertical position; it is as critical as when the plant lies on the ground, sometimes permanently [106]. Thus, lodging can diminish grain yields up to 80% and can have other side effects such as including reducing the grain quality or slowing the harvest [106]. Moreover, during the past years, the demand for high-quality rice has also augmented, requiring a varietal selection focusing on another rice characteristic; however, new varieties exhibiting high quality grain do not give high yields and are challenging the rice breeders [104]. Finally, breeders intend to develop varieties having a compromise of high yield, high quality but short enough to prevent lodging. In the case of rice, drought-resistant varieties were also developed [107] to face the more frequent droughts associated with global warming [108]. As the rice losses imputed to diseases are enormous [109], another aim for breeders is to provide selected varieties with an efficient resistance to diseases and insects pests [110].

Such as rice, wheat is also the subject of a deep varietal selection, and is currently one of the most commonly cultivated cereals, principally in North America and Europe [46]. Its cultivation started about 10,000 years ago, most probably in Europe, and since many varieties have been selected [111]. Like for rice, an efficient varietal selection

leading to large increases in wheat yields started in the 1950s-1960s [46]; these increases are due to the development of grain-richer varieties, but also to the dwarfing properties allowing shorter plants to be richer grain and poorer in straw while decreasing the risk of lodging [101,112]. Another major criterion of selection is the resistance of the wheat variety towards diseases, such as toward the black stem rust (*Puccinia graminis*) responsible for impressive yield losses [113].

Fiber crops are also subjects of the varietal selection. One major example of a fiber crop selected for its fibers is hemp (*Cannabis sativa* L.) [114]. In the case of hemp, the use of this fiber crop used as a raw material goes back to 6,000 years ago, and for thousands years, its fibers have been used for the manufacture of rope, fabric or paper [115]. The varietal selection of hemp started about 200 years ago, and nowadays less than 50 European fiber cultivars are registered [114,116]. In the same way as for food crops, one of the major goals of the varietal selection of hemp is to increase the plant yields, mainly in terms of fiber content of the plant but also in seeds or woody core [117]. The yields of hemp were proven to depend on the features of the flowering system, a reason why the varietal selection intends to develop late-flowering cultivars that lead to higher fiber yields [118]. In addition, the sexual dimorphism of hemp, and particularly the monoecious cultivars, also affects the fiber and seed productions, while facilitating the harvest and reducing the crop heterogeneity [119]. Indeed, hemp plants are naturally dioecious, leading to high heterogeneity between plants as the male ones have finer fibers, flower sooner and dry in the fields while female ones start the seed ripening [120]. However, monoecious plants exhibit unstable sexual phenotype, challenging the breeders [119]. Additionally, hemp has the ability to produce secondary fibers [60]. Nevertheless, the number of secondary fibers should be limited, even though the secondary fiber bundles are often easily taken as primary once [121], as these short and highly lignified fibers bring scattering in performances and are not desirable for most applications [122]. Thus, cultivars with low secondary fiber content should be privileged by breeders. Another parameter challenging the varietal selection is the property of the cultivar to provide high yields in a restrictive range of environmental conditions. It is notably in the case of multipurpose crops, *i.e.* providing both high fiber yield and high seed yield [123] Thus, a better adaptation under contrasting environmental conditions would provide more flexibility to the farmers, and can be a desirable selection criterion. Last but not least, an additional parameter specific to hemp has to be considered regarding the varietal selection, namely the delta-9-tetrahydrocannabinol (THC) content of the plant. This

psychoactive substance has to be monitored in order to represent lower than the legal limit (EU Regulation No. 796/2004 requires less than 0.2% THC) [124,125]. This latter parameter challenged and is still challenging breeders, as well-known cultivars exceeding the legal THC restrictions had to be excluded from the European Common Catalogue of recognized cultivars, despite exhibiting much lower THC content than the psychoactive cultivars (ranging typically 5-10% THC)[125]. The difficulties encountered by hemp breeders towards decreasing the THC content as well as increasing yields or favoring plant adaptation are hoped to be faced with the help of plant biotechnology; genetic improvement of hemp is expected to assist the process of varietal selection and to be an interesting tool for breeders [126,127].

In conclusion, since the beginning of agriculture, crops have been domesticated by humans, mainly to produce food (such as cereals) but also raw materials. Over the years, farmers have saved seeds of plants with advantageous characteristics to domesticate plants exhibiting the naturally most attractive properties. More recently, started about 200 years ago, breeders have been crossing plants and have been selecting new varieties to provide improved plants; this process is called varietal selection and could be referred to as ‘selective breeding’ [46]. The selection criteria are slightly the same from an industrial crop to another, so the examples of rice and wheat detailed above could be considered as generalities for other types of industrial food crops. Some other crops have additional required selection criteria, such as hemp which also have legal restrictions. However, a more recent type of breeding is currently expected to go beyond selective breeding and overcome the plateau beyond which selective breeding is not able to increase yields anymore [46,104]; it is referred to as ‘plant biotechnology’ and involves genetic engineering such as recombinant DNA technology [46,128]. This additional type of breeding is considered beyond the scope of this work, and will not be presently discussed.

### **3.2. Focus on new flax varieties and related selection criteria**

In the category of industrial crops, flax is also a major plant whose current cultivars are the result of the varietal selection. Selected for two main purposes, namely its seeds and its fibers, a different approach was adopted by breeders according to the expected applications, leading to two distinct groups of cultivars [34]. In addition, it is also known that some cultivars were selected to provide a balance between seed and fiber yields [129]. The present review of the flax selection focuses on the development of fiber varieties exclusively.

From the time when agriculture was developed, *i.e.* about 10,000 years ago, humans have domesticated and intuitively selected the strains of flax that gave the best-looking plants providing fibers of good quality [1,46]. The seeds of these plants with attractive properties were kept and sowed the following year, expecting desirable traits to come again.

More recently, like other industrial crops, humans have purposely been crossing and selecting flax plants to produce improved varieties. Literature suggests that current varieties of fiber flax originated from older varieties developed in Eastern Europe [20,130]. More precisely, it is possible that flax breeding started in Lithuania in 1922, after more than 4,000 years of cultivation in this country [131]. An example of the current fiber flax varieties registered in 2018 in the Common Catalogue of France is given in Table I-3, showing that after a century of varietal selection, this work is performed by only a few breeders and fewer than 50 varieties, excluding any GMO one, are currently registered and commercially used. In 2017, seven new varieties were registered, which demonstrates the dynamism regarding the work of flax varietal selection. Moreover, older varieties are still registered in 2018, such as Marilyn or Alizée, even though more recent ones were registered and deleted in the meantime [134]; the numerous deletions confirm the challenge and investment of flax breeders to select varieties with actual improved qualities. For economic reasons, since the beginning of flax breeding and even more in today's world facing the development of flax-based composites [4], the principal aim of textile flax breeders is to select high fiber yielding flax varieties to meet the industrial demand [24]. A numerical example of the incredible increase of the fiber yield could be the following one: in France in 1930-1935, the average fiber yield was about 0.30-0.65 t/ha [135] whereas in 2015, an average fiber yield of 2.02 t/ha was obtained with an highest value of 3.92 t/ha for the recent cultivar Aramis in experimental fields [136].

**Table I-3. List of registered fiber flax varieties in the Common Catalogue for multiplication and commercialization in France in 2018 [132–134].**

Variety	Registered since	Breeding company name (country)
Marylin	1998	Landbouwbureau Wiersum B.V. (NL)
Alizée	2003	Terre de Lin Sca (FR)
Drakkar	2003	Terre de Lin Sca (FR)
Loréa	2003	Lin 2000 Sca (FR)
Mélina	2003	Cebeco Seeds B.V. (NL)
Suzanne	2004	Landbouwbureau Wiersum B.V. (NL)
Boréal	2006	Terre de Lin Sca (FR)
Vesta	2007	Cebeco Seeds B.V. (NL)
Andréa	2008	GIE Linea (FR)
Arétha	2008	Cebeco Seeds B.V. (NL)
Calista	2009	Limagrain Nederland B.V. (NL)
Eden	2009	Terre de Lin Sca (FR)
Violin	2009	GIE Linea (FR)
Altéa	2010	GIE Linea (FR)
Chantal	2010	Landbouwbureau Wiersum B.V. (NL)
Evéa	2010	GIE Linea (FR)
Aramis	2011	Terre de Lin Sca (FR)
Damara	2011	Limagrain Nederland B.V. (NL)
Noémie	2011	Van De Bilt Zaden (NL)
Filéa	2012	GIE Linea (FR)
Lisette	2012	Landbouwbureau Wiersum B.V. (NL)
Podium	2012	Terre de Lin Sca (FR)
Télios	2012	Terre de Lin Sca (FR)
Toundra	2012	Terre de Lin Sca (FR)
Avian	2013	Wiersum Plantbreeding B.V. (NL)
Christine	2013	Wiersum Plantbreeding B.V. (NL)
Magéa	2013	GIE Linea (FR)
Nathalie	2013	Van De Bilt Zaden (NL)
Axelle	2014	Wiersum Plantbreeding B.V. (NL)
Bolchoï	2014	Terre de Lin Sca (FR)
Novéa	2014	GIE Linea (FR)
Vivéa	2014	GIE Linea (FR)
Arkéa	2015	GIE Linea (FR)
Jade	2015	GIE Linea (FR)
Cirrus	2016	Terre de Lin Sca (FR)
Olga	2016	Terre de Lin Sca (FR)
WPB Anette	2016	Wiersum Plantbreeding B.V. (NL)
Dauréa	2017	GIE Linea (FR)
Elixir	2017	Terre de Lin Sca (FR)
Evasion	2017	Terre de Lin Sca (FR)
Malika	2017	Limagrain Nederland B.V. (NL)
Stelléa	2017	GIE Linea (FR)
Végéa	2017	GIE Linea (FR)
WPB Felice	2017	Wiersum Plantbreeding B.V. (NL)

The average values and tendencies regarding changes in yields are visible on Figure I-10; this figure illustrates the general increase of yields since the beginning of the varietal selection, in the case of France.

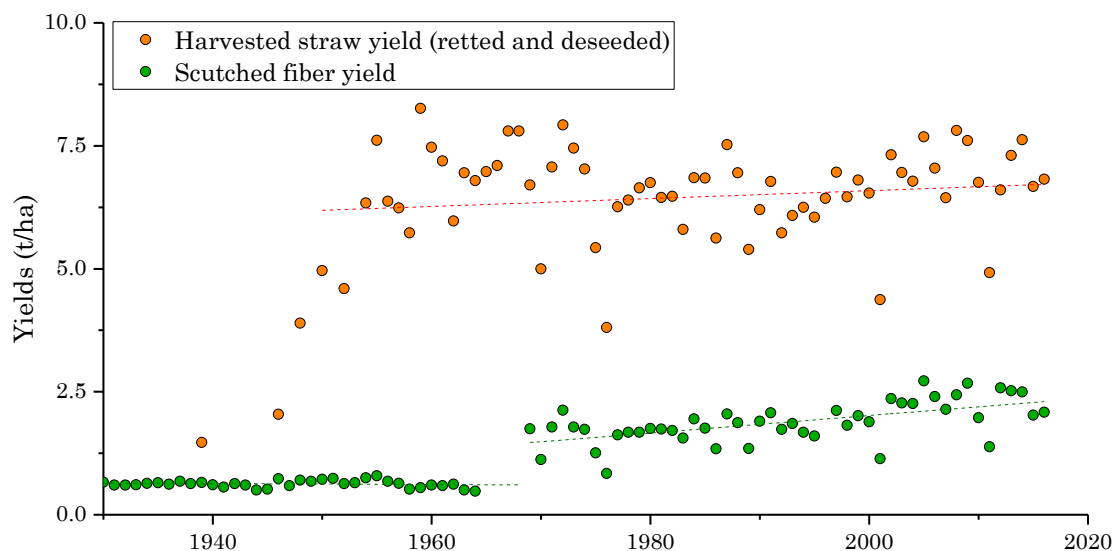


**Figure I-10. Average yields of flax straw and scutched fibers (production per area under cultivation) in France since the beginning of the varietal selection. Dash lines illustrate the average tendency over the year. Data provided in literature [135–139] and from personal communication.**

In few words, an increase of about 35 kg/ha of fibers was obtained each year between 2003 and 2013, corresponding to about +2.3% in fiber yield each year [35]. Of course, the increase of fiber yield is attributed to the work of varietal selection, but is also due to the mechanization that appeared in parallel starting from the 1960s, as well as higher germination rate (about 92% [40]) and a rise of scientific studies focusing on flax providing a more precise knowledge of the plant growth [26,140,141]. In addition, the harvested straw yield only slightly increases over the years despite mechanization, which confirms the key role of the varietal selection in the increase of fiber yield.

Furthermore, the resistance to diseases is also a selection criterion for flax breeders, as diseases can be devastating for cultures and are thus limiting factors in flax production. For instance, the resistance to the fungal pathogen fusarium wilt (*Fusarium oxysporum*) is a priority of the varietal selection of flax [142]. Moreover, the powdery mildew (*Oidium lini*) is also a major flax disease [143], as well as the different races of flax rust [144] or flax scorch (*Phytium megalacanthum*) [145], and the resistance against them is a desired characteristic for new cultivars and challenges for breeders.

Finally, another criterion is the priority for flax breeders, namely the lodging resistance. The phenomenon of flax lodging is illustrated in Figure I-11.



**Figure I-11. (A) Lodged flax plants at the end of the flowering stage. (B) Lodging in the flax field persists during the seed formation.**

This undesired event has been previously defined in 3.1, as the lodging resistance is also a major selection criterion for rice or wheat [100,101]. Lodging phenomenon generally happens after rainfalls and wind [146]. For the food crops, the main solution proposed to prevent lodging is the selection of dwarf varieties, *i.e.* shorter stems [147,148]. This is indeed a suitable solution for those crops whose grains are located in the ears, the stem having only a supporting role. For flax, conversely, the interesting fibers are situated within the stem, making the reduction of its length much less wise for economic reasons; thus, more suitable solutions are required to avoid lodging without penalization of the fiber yield. The understanding of this phenomenon, challenging the biomechanics of flax plants, is the subject of the next section.

### **3.3. Lodging of flax: investigations toward a better lodging resistance**

The lodging phenomenon is of crucial importance, as it can greatly impact the process of flax harvesting together with fiber yields [146]. Because plants are intertwined and close to the ground (Figure I-11), the use of agricultural machines is much more complicated and the harvesting process slowed down. In addition, lodging constrains the plants to high moisture conditions when laid on the soil; this impacts the harvesting process by increasing the mass of the plants covered with mud but also promotes the development of fungal diseases, such as Pasm caused by *Septoria linicola* [149]. However, only a few studies focus on the understanding of the lodging of flax, which makes this phenomenon quite complicated to restrain. Thus, a literature

review on industrial food crops (mostly studied for their commercial significance) is of importance, as many of them are susceptible to lodging, to provide leads to investigation for the particular case of flax.

For food crops, two main types of lodging are mentioned in literature, namely stem lodging and root lodging, and occur through interactions between wind, rain, soil and the plant [101,150,151]. Thus, the occurrence of lodging, for both types, is mostly influenced by meteorological parameters, for example with wind acting as a force which can bend the plant and rain increasing the load tolerated by the plants; however, some structural elements of the plants are also thought to be involved [151]. Root lodging is due to the failure of the root anchorage and it is preferentially undergone over stem lodging for example by rice [100]. However, within the same field, root lodging can also be accompanied by stem lodging [106]. Regarding the empirical knowledge of flax farmers, root lodging is rare and, therefore, the given review of lodging mechanisms focuses essentially on stem lodging and structural elements relevant to the lodging vulnerability. In these cases, lodging results in stem buckling [152], when the strength of the stem in the lodged part is not high enough to withstand the bending moment provoked by the stem leverage (induced by the action of the wind, combined or not with rain)[106]. For barley, the lodging can occur at any point along the stem, but preferentially at mid-high [148]. This is explained by the high flexibility of barley associated with a rapid reduction of the strength along the stem toward higher positions [148]. On the other hand, in the example of wheat, lodging takes place close to the soil surface, in the very basal part of the stem [151]; this type of lodging is also happening for flax according to flax farmers. To prevent lodging of wheat, shorter varieties are favorable, as well as strong stemmed plants in the basal part. In order to increase the stem strength, the quantity of matter located in the first internode is a crucial factor; in this way, the seedling rate, date of sowing, residual soil nitrogen with reduced inputs of it and use of PGR is beneficial for the stems [153–155]. These parameters were also previously mentioned being advantageous for flax, emphasizing the appropriate parallel between these two crops.

If assimilated to an ideal column, the global buckling of a plant can be approached by considering the Euler column formula [95]. Even though plants are in fact never ideal columns, the Euler column formula provides insights into the relations between variables (being much more complex in actual biological perspectives); it is a

reasonable approximation for plant stems, which are free at their top and are anchored at their base by roots, and can be expressed by Equation I-3.

$$P_{crit} = \frac{\pi^2 EI}{4H^2}$$

**Equation I-3. Euler column formula for an ideal column anchored at its base and free at its top.**  $P_{crit}$  is the critical buckling load,  $E$  is the apparent elastic modulus,  $I$  the second moment of inertia (being  $I = \frac{\pi D^4}{64}$  for a circular section) and  $H$  the height of the column [95].

This equation shows that an increase in stem length or decrease in stem diameter ( $I$  is proportional to  $D^4$ ), *i.e.* an increase of the slenderness ratio, result in reducing the critical buckling load and therefore increase the risk of buckling. The influence of the material properties is also represented (distinctly) by the apparent elastic modulus  $E$ . Finally, a stout structure is able to support greater load than a slender one composed of the same material, *i.e.* a high slenderness ratio would imply an enlarged risk of buckling, setting a potential limit of standing plant structures [156].

A complementary critical parameter to consider in order to evaluate the influence of flax stem slenderness is the critical buckling height. This latter parameter, derived from the Euler column formula, is defined as the maximal height that the plant can reach while remaining stable, given its diameter and material properties [157]. It is given by the Greenhill equation (also found as Euler-Greenhill formula)[157,158], expressed by Equation I-4.

$$H_{crit} = K \left( \frac{ED^2}{\rho} \right)^{1/3}$$

**Equation I-4. Greenhill equation for a vertical column such as a stem.**  $H_{crit}$  is the critical buckling height,  $K$  is a proportionality constant,  $E$  is the apparent elastic modulus of the stem,  $D$  is the diameter at the base and  $\rho$  is the bulk density of the material [157].

The Greenhill formula highlights that, for given material properties, the decrease of the stem diameter reduces the maximum height that a stem can attain before failure. In addition, the critical buckling height depends on other parameters defining the proportionally constant  $K$ ; these parameters are the distribution of diameters (*i.e.* the tapering) and the distribution of mass along the stem, as well as the gradients in mechanical properties along the stem [159,160]. Finally, the safety factor can be

defined; it is the ratio between the critical buckling height and the actual height of the plant [97,99].

The exposed formulas confirm the key importance of the flax slenderness as a factor to understand plant instabilities, such as lodging. It also explains the solution of stem length shortening adopted for food crops having increased grain yields. Additionally, these formulas also highlight the significance of the material properties. For instance, light-weight materials (*i.e.* having low bulk density  $\rho$ ) are preferable over heavyweight ones. In addition, the apparent elastic modulus  $E$  is confirmed to have a great role toward the resistance to buckling, as slender plants must develop stiffer stems to prevent instabilities. In conclusion, higher density-specific stiffness ( $E/\rho$ ) are required to decrease the plant vulnerability to buckling [161]. Nevertheless, the density-specific stiffness precise values, as well as the proportionality constant, are difficult to predict; of course, they differ between plant species [158], but they also vary as a function of stem development and growth too like it is demonstrated for trees [160].

As complements to mechanical characterization of the stems, anatomical analyses are of interest to understand lodging. Ford et al. [162] suggested that solid stems of some wheat cultivars, *i.e.* filled with pith, have a greater apparent stiffness thus an increased resistance to lodging than cultivars having the hollow stems. This result was demonstrated later as well by Leblicq et al. [163] through a mechanical analysis of the bending behavior of wheat stems; these authors demonstrated that the bending resistance of crop stems is significantly increased by the presence of a cellular core of lower density than the outer part of the stem. For rice as well, low density tissues comparable with a foam visible in the inner part of the stem are favorable to the stem lodging resistance [164]. In the study performed in 1982, Menoux et al. [165] investigated the morphological characteristics of flax stems as well as cultural conditions influencing the lodging resistance based on the comparison of several varieties. The authors showed that flax plants are sensible to lodging (Figure I-11) during the fast growth stage, from 15-cm high to flowering, but with the most critical time at flowering [165]. Menoux et al. [165] also demonstrated that the lodging resistance is linked with the elongation rate during the early growth stage. Indeed, the resistance to lodging is increased for plants having a slow elongation *i.e.* exhibiting a short internode length in the basal 18 cm and a low fiber length-to-diameter ratio. A hypothesis could be that the thickening of cell walls is better performed for slower elongation rates, *i.e.* there is a compromise between the elongation rate and the tissue

quality, like wood is denser in trees with slower growth [166]. Thus, according to the mentioned study, all parameters inducing a slow elongation rate at the beginning of the plant growth is in favor of the lodging resistance. In this way, as nitrogen is known to advantage plant growth and to increase the yield [26,167], a rather low nitrogen content in soil, as long as providing a good compromise with the fiber yield, is appropriate to decrease the risk of lodging [168]. The use of plant growth regulators (PGR) is also a widespread solution used by farmers to decrease the risk of lodging [169]; nevertheless this practice is not consistent with evolution toward a more environmentally friendly agriculture. In addition, a reasonably low sowing density is suitable to diminish the risk of lodging if not compromising the fiber yield [167], especially due to the linked stem diameter increase, ensuring a better stability of stems. Regarding the link between the stem properties, the fiber content and the lodging stability, authors' points of view have changed over time. Controversially, Sieben [170] showed in 1953 that, for selected varieties, a higher stiffness of the stem (induced by a lower fiber content) increases the lodging stability. However, to this study, Dorst [171] brings a shade of difference, affirming that breeders could find a favorable combination of lodging resistance (or high stem strength) and fiber content if the two parameters are seemed as independent ones; this author affirms that the breeders' aim is "to find genotype that will break through the correlation". In 2015, the study of Bourmaud et al. [172] goes further than Dorst's hypothesis, as the authors highlight the role of fibers in the support of the plant. The same year, a correlation between the stiffness of the stem and the stiffness of its fibers was found [98]. However, little is known about the mechanisms of flax lodging, but the development of strategies to avoid the phenomenon requires an understanding of the factors influencing plant vulnerability to lodging.

Finally, based on literature, the phenomenon of flax lodging is expected to be linked to the pattern of plant development itself, besides meteorological parameters that also affect this pattern. In fact, the lodging would be greatly related to both elongation and thickening of the cells (correlated with the elongation of the plant), more particularly fibers, and the secondary growth of the plant, namely the xylem part. The changes in fiber as well as the xylem core properties would be of interest, both anatomically and mechanically speaking; indeed, these processes would define the mechanical stiffness of the stems, by determining the length-to-diameter ratio of flax fibers, as well as their filling rate and stiffness, but also determining the density and thickness of the xylem

tissue. Therefore, beyond the fiber yield, the xylem content of new selected varieties would also be a plant property to take into consideration for a more accurate breeding work. Concurrently with the fiber content of the stem, the fiber mechanical properties could be a relevant parameter to take as perspectives for breeders to improve the lodging resistance; this parameter is all the more interesting as its optimization would be appropriate for the use of flax fibers in the composite field. Besides, the analysis of flax plants could be of great interest for structural engineering in reason for its incredible slenderness (Figure I-8). This analysis could be performed through the evolution of morphology and cell development, as well as material properties over plant growth. Moreover, studies on numerous plant species report an adaptive growth response to external stimuli [173–175]; these latter are a possible approach toward the understanding of flax slenderness, stability and overall biomechanics.

#### 4. Influence of cultural conditions and of the environment on the properties of flax stems and fibers

In the present section, the influence of both cultural and environmental conditions on plants are reviewed, with a focus on the case of flax. This implies several notions, which are cited with corresponding illustrations in Figure I-12 for a better understanding of resulting plant responses.

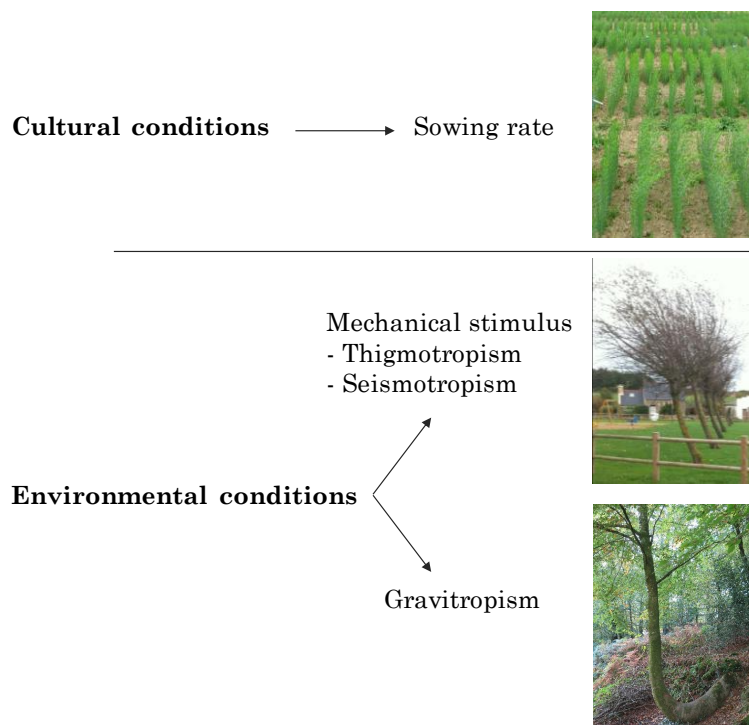


**Figure I-12. Main notions addressed in this section with corresponding examples of illustration.**

#### 4.1. Sowing rate and crop canopy

The number of neighboring trees and their proximity are important parameters for an individual tree growing in a forest; the competition explains changes in height and diameter growth of individual trees [176,177]. Similarly, the plant development is very dependent on the sowing rate, the main parameter determining the plant density within a field for industrial crops. Indeed, growing conditions such as light intensity, water and nutrient availability, as well as mechanical challenges, strongly vary on whether the plant is growing isolated or within a canopy [178]. For example, high flax crop density, most probably due to competition between plant species, can decrease the amount of unwanted weeds within the fields [179]; this is an interesting result toward the reduction in the use of herbicides. Reduced line intervals by inducing increased crop density would thus be beneficial in this way. Nowadays, for cereals and flax, the similar in-line seeding technique by means of the same types of crop seed drills is used, controlling the line intervals [18]. The line spacing commonly ranges from 10 to 15 cm, usually 12.5 cm for flax, with a distance between two consecutive seeds of about 0.5 cm (determined by the speed of the drilling machine), leading to about 0.3 cm between two consecutive stems [30,180,181] (Figure I-13).

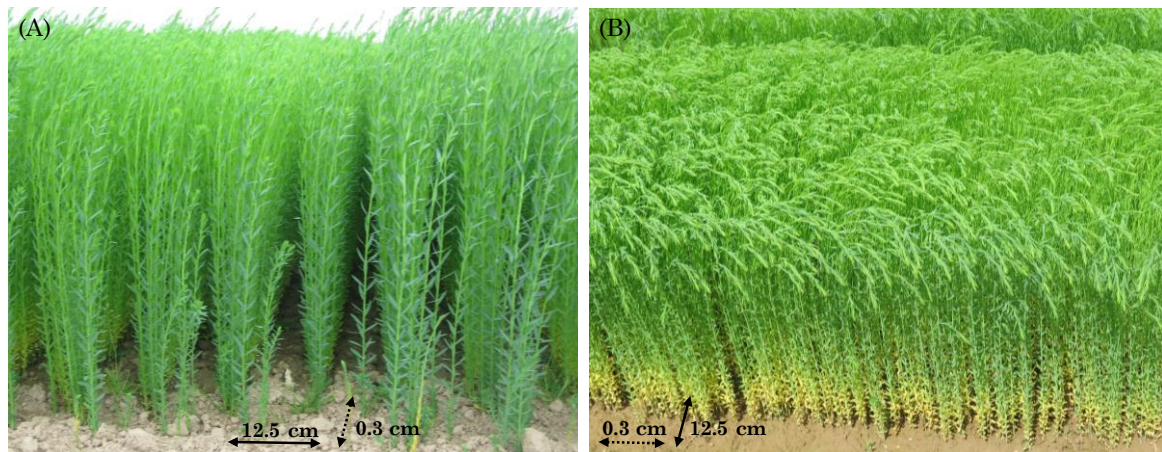


**Figure I-13. Pictures of a flax field illustrating the in-line seeding. (A) Lines spacing is about 12.5 cm. (B) Plants belonging to the same line are spaced 0.3 cm apart.**

First studies in the 80s investigated the influence of the sowing rate on the resulting flax plant growth [182,183]. Fowler [182] demonstrated that the sowing rate has a great influence on the plant height (namely, increasing the sowing density decreases the final stem height). Gubbels and Kenaschuk [183] confirmed this result, if reasonably high sowing rate is used (below 400 seeds/m<sup>2</sup>, the opposite phenomenon is obtained, but this sowing rate is anyway not appropriate for industrial cultivation).

The effect of the sowing rate, by influencing the stem height, logically impacts the final scutched fiber length too, *i.e.* these highest sowing density led to the shortest scutched fiber length [40]. In addition, increasing the sowing rate decreases the resulting stem diameter; nevertheless, the straw yield and fiber yield are improved, as the increase of the plants per meter square has more impact on the yields than the decrease of the plant height [40,167]. However, despite decreasing the plant height, high sowing rates negatively influence the lodging stability of the plant, as well as the mechanical properties of flax fibers for greatest sowing rates [40,167]. Moreover, increasing the sowing density decreases the number of capsules, and consequently seeds, per plant [184]. Thus, a sowing density providing a trade-off between yields (mainly fiber yield), fiber properties and lodging resistance is preferred for flax cultivation, namely a sowing rate of about 1800 seeds/m<sup>2</sup> is encouraged and commonly used, leading to about 1650-1750 plants/m<sup>2</sup> thank to high germination rates [40,167]. This results in a relatively homogeneous and dense canopy (Figure I-14).



**Figure I-14. Flax fields resulting from a conventional sowing rate of 1800 seeds/m<sup>2</sup>. (A) soft apical portions due to the snap point presence are still visible, leading the softer upper part of the stem to topple down all over the dense canopy. (B) capsules are well-formed and yellow ripening is advancing so the canopy exhibits yellowing shades.**

On the other hand, the competition experienced by the plant is more complex than only sowing density dependent. Sowing density, sowing spatial pattern and germination date are indeed interacting factors [182]. For a conventional sowing density, the time of the emergence of one individual plant related to neighboring ones has a considerable importance on the plant growth; the first emerged plants are greater competitors, and will be the highest all along their development. They will be even higher, whereas late-emerged plants will be even smaller, than in the case of plants emerged all on the same date [182]. Moreover, the special organization of the plants, such as the diverse line spacing, the different arrangement if along the drilling line or perpendicularly previously mentioned, or as illustrated by the different early-emerged versus lately emerged plants special patterns [182], will impact on the plant competition and so the plant development. For flax, the best way to regulate the homogeneity of plant emergence is to control the sowing depth of simultaneous stands; namely, a sowing depth of 2 cm is preconized for a homogeneous emergence [141,180]. To a lesser extent, the seedbed preparation, such as soil rolling especially for lighter soils [180] or the use of medium conservation tillage to prevent soil erosion [181,185] can be a complement to the use of conventional 2-cm sowing depth.

In the case of a relatively dense and homogeneous canopy, such as a forest or a flax crop field (Figure I-14), the interactions between wind and plants (more specifically the whole canopy) are of great interest, particularly as regards lodging induced by wind [106]. Given the conventional sowing rate used for flax and the sowing recommendations mentioned above, a flax field can hence be assimilated to a dense and uniform continuous canopy structure. The following section shortly reviews the interactions between wind and crop canopies (excluding sparse fields, *i.e.* the plant spacing is in the range of plant height or more [186], which is not the case for flax) in order to investigate the influence of wind-induced movements on flax lodging.

#### **4.2. Wind-induced movements of crop canopies**

At first sight, wind is visible as waves over the upper layer of a crop field (Figure I-15), as is the case for flax or wheat ones; this wavelike motion of plants was referred to as *honami* first by Inoue in a study of rice fields [187]. Even though the effects of wind on plants are the subject of many studies on a large range of plant species [101,148,155], little is known about the specific case of flax. Nevertheless, the interactions between wind and crop canopies are thought to be valid for a flax canopy as well.



**Figure I-15. Flax plants moving in the wind in a wave-like movement. The wave is visible as it bends over the plants as it passes.**

Based on literature, plant stems are very lightweight and flexible structures that are typically modeled as isolated elementary oscillating rods [188,189]. These plants assimilated as rods have a natural resonance frequency at which they oscillate [190]. Finally, the plant motion is defined by several plant parameters, namely its natural resonance frequency, its bending stiffness and modal mass, a reference damping and a modal displacement shape [191]. However, within a canopy, the plants are not individualized, but their properties and interactions can be seen as the canopy characteristics; hence, a canopy can be modeled as a discrete set of oscillating identical rods [190–192]. In short, the motion of the canopy is described by the oscillations of a set of stems along a vertical row. In a complementary manner, the average distance between plants is a parameter to consider when modeling the coupling between plants [193] so the effects of elastic contacts between neighboring crops along a row have been assessed; collisions were found to increase the resonant frequency of individual plants while providing additional support to the stems [192]. Crops motions in the canopy induced by wind are then described in literature in relation to wind characteristics. In the absence of plants, the horizontal distribution of wind mean velocity is logarithmic, increasing with the height, and exists as a so-called boundary layer flow [189,191]. Conversely, in a canopy, wind that bends over the plants as it passes, occurs as a flow within an inner boundary layer, also called canopy layer; it is then associated with the outer boundary layer flow above the canopy. However, the canopy layer shows great differences regarding turbulence characteristics when compared to the boundary

layer, due to the inflection in the wind mean velocity profile, with this inflection becoming even greater over gust events [189,191]. The differences between the two flows create a zone of turbulence near the top of a canopy; this zone is called the plane mixing layer and the turbulence is assimilated to Kelvin-Helmholtz instabilities [186]. Yet, the impact on flows of the presence of a snap point on plants composing such a canopy has to be investigated. Turbulence emerging in the mixing layer is, nevertheless, not random, with the major contribution of turbulent motions coming from coherent eddies of the scale of the canopy height [186]. Indeed, the plants oscillate at their common natural frequency, with a different small phase between adjacent plants when slightly sheltered from the gust, leading to the impression of *honami* waves moving through the field [188]. When the gust frequency reaches the natural frequency of the plants, a resonant interaction results in a more pronounced waving and stronger *honami* which may lead to crop damage such as lodging [188].

This bibliographic synthesis enables to highlight several elements of thought related to the development and stability of flax. The link between stem stiffness, induced movement and lodging resistance is demonstrated. Thus, measuring the stem stiffness can therefore be a good indicator of lodging resistance, because it directly influences the resonance frequency. In addition, due to the geometry of the seed drills, the distances between the stems are very different depending on the axis considered. In this way, the sowing course could be adapted according to the major wind direction, as is for example the case for seaside crops. By standardizing crop density, this would reduce the probability of reaching stem resonance frequency during severe weather events. Finally, interestingly, the presence of a flexible zone between the apex of the plant and the snap point during the growth of a flax stem could modify the turbulence induced by the wind at the top of the canopy and why not create a transitional regime more favorable to the plant stability. Therefore, the presence of the snap point on the natural frequency and the motion of the plants would be interesting parameters to investigate. Moreover, wind-induced motion does not necessarily have a negative impact on yields. It can indeed influence plant growth and biomass allocation as well, phenomena that will be discussed in the following section.

### 4.3. Tropisms and plant responses

Living plants have the ability to respond to a wide range of changes in their environments and they can regulate their patterns of growth in accordance with the stimuli. A growth response involving an active motion due to a stimulus is called a

tropism, coming from the Greek word *trepein* meaning ‘to change direction’ [194]; a tropism can be either positive (a response toward the stimulus) or negative (a response away from the stimulus)[46]. Major plant tropisms and their consequences on plant characteristics are detailed hereafter.

#### **4.3.1. Thigmotropism and seismotropism**

The motion of a plant caused by a mechanical stimulus is often defined by two different tropisms, namely thigmotropism (from the Greek word *thigma* meaning ‘touch’) and seismotropism (from the Greek word *seismos* meaning ‘shaking’) [195]. Indeed, a mechanically induced stress can result from either a direct contact such as through passing animals or artificial rubbing of the plant, or from a non-tactile stress such as wind action or artificial ventilation [175]. In the first case, the plant response is called thigmomorphogenesis [173] and in the latter, it is often called seismomorphogenesis [196]; nonetheless, the term thigmomorphogenesis can also be found to describe the plant response to wind [164,194]. However, this classical categorization according to the contact or non-tactile origin of the mechanical stress is rather confusing, as it can also intertwine both tropisms (for instance, a contact between oscillating neighboring plants can be induced by wind, as previously mentioned in 4.1); thus, the growth response induced by a mechanical stimulus would be termed as mechanosensing or mechanoperception [197–199]. Such responses are the subject of many works, but little is known about the special case of flax. Generally speaking, mechanical stimuli have great consequences on the size and shapes of the herbaceous plants and trees, as well as on the mechanical properties of their constitutive tissues. A first example is the widespread reduction in plant height, often accompanied by a greater radial growth of plants submitted to a mechanical stress in many canopies of both herbaceous and wood plants [175,196,200,201](Figure I-16). This reduction of the plant height is consistent with the reduction of the stem buckling risk and the effective canopy profile to wind, *i.e.* the plants develop a strategy to minimize the impact on safety [199,202]. However, the shortening induced by a mechanical perturbation is not necessarily the adopted strategy, as for example wheat plants do not exhibit significant changes in stem height under the influence of wind sway [203]. Similarly, the increase in plant diameter, even though very common, is not a fundamental rule; indeed, some herbaceous plants have no significant changes in stem diameter despite consistent mechanical stimuli [204–206], whereas a reduction in diameter of wind-exposed trees can sometimes be observed [207].



**Figure I-16. At the end of their development, flax plants growing in field are about 1 m high (A) whereas plants are much higher (up to 1.70 m) when grown in greenhouse under much gentle conditions (B).**

Thus, the plant response to a mechanical stimulus can result in changes in the developmental rate, depending on the species, crop density, type of mechanical load, growth stage, growth form (primary or secondary), plant life history, *etc.*, which illustrates the complexity of predicting the plant response [164,204,206]. Regarding plant anatomy, changes in constitutive tissue geometry and configuration can also be induced by mechanical stimuli. Changes in tissue geometry can include modification of cell shape and thickness, whereas changes in tissue configuration consist of a modification of the cellulose microfibrillar angle, arrangement of the cell wall layers as well as reallocation of biomass in a cross-section. As mentioned previously, at the whole plant morphological scale, there is no fundamental rule to describe a plant response to a mechanical perturbation at the cell scale neither. However, Gardiner et al. [164] registered the main plant changes induced by wind loading at different scales, for non-woody and wood plants respectively. Based on this latter review, Table I-4 lists the main changes that may be most possibly applicable to flax.

**Table I-4. Possible acclimation of flax plants as a result of a mechanical stress. Adapted from [164].**

Scale	Flax plants
Stem	Shorter stems
	Wider stems
	Changes in plant developmental rate
	Changes in stiffness
	Damping
Xylem cells	Increased lignification
	Increased in xylem tissue density and production
	Increase in cellulose microfibrillar angle
	Changes in longitudinal elastic modulus
Fibers	Changes in length, diameter and wall thickness
	Increase in cellulose microfibrillar angle
	Changes in longitudinal elastic modulus
	Increased strengthening
Phloem cells	Larger phloem vessels

In terms of changes in the mechanical properties of plants subjected to a mechanical perturbation, two types of reactions were recorded [208]: increase of the elastic resilience and intensification of the bending stiffness. These two opposite types of biomechanical responses allow the plants to reach a better resistance to mechanical failure; indeed, increasing the elastic resilience (like it is the case for bean plants *Phaseolus vulgaris* [209] or *Arabidopsis thaliana* [204]) enables the plants to remain within their elastic limits for greater loads than unstimulated ones, whereas increasing the bending stiffness (like tomato *Lycopersicon esculentum* stems [210] or *Pinus taeda* pine trees [211]) avoids exceeding the strain limit.

Morphological, anatomical and mechanical changes caused by mechanical perturbations are guided by a trade-off triangle, *i.e.* plants structure and functions are the natural compromise between the mechanical strength needed to withstand the perturbation, with the conductive efficiency and the resistance to embolism [202]. Thus, varietal selection, if aiming at optimizing the mechanical properties of flax, could lead to suboptimal performances in one of the two other points of the triangle [202,212]. Interestingly, when plants are subjected to a mechanical stimulus, they become stronger toward mechanical failure by subsequent mechanical perturbations

and exhibit an adaptive advantage by becoming less susceptible to injuries than controlled plants [213]. If the plants are able to adapt to a natural mechanical perturbation, they also do so toward artificial solicitations. If little is known about the impact of a mechanical stimulus on flax, it would be an interesting way to investigate whether it could influence the flax stability toward lodging as well as on mechanical properties of flax fibers in view of optimizing their applications in composite materials.

### 4.3.2. Gravitropism

Another tropism well reported in literature is gravitropism, the plant response to gravity. Actually, gravitropism and thigmomorphogenesis are challenging to disentangle; mechanosensing (better studied in gravitropic responses) is involved in both tropisms and their respective involvement, for example when organs experience bending, is difficultly determined [164,197].



**Figure I-17.** Example of a gravitropic response of *Linum usitatissimum* L. (A) Control flax plants at the very beginning of the fast growth stage (plants are about 20cm-high). (B) Flax stems immediately after inclination of about 85°. (C) Flax stems showing restored vertical positions (10 days after inclination) with a remaining curvature zone in the basal part. Protocol inspired from [76].

For stems, gravitropism is negative, *i.e.* the plant will move upward, whereas gravitropism is positive for shoots that are dictated to grow downward [197]. This plant reaction is very important for agriculture, as it ensures some crops to come back ascending after lodging [214]. For stem lodging inducing a gravitropic stimulus, the gravitropic response of plants is a stem curvature; at the end of the gravitropic reaction, the stem is generally straight [197](Figure I-17).

Gravitropism is attributed to the plant ability to perceive inclination in a first step [215]. This plant aptitude, called gravisensing hereafter, is particularly studied in the case of different herbaceous angiosperms [215] but also woody ones [216]. As gravisensing is a very complex mechanism studied in several highly detailed articles, for both herbaceous and woody angiosperms [216–219], but also claiming some aspects that still need to be discovered, only concise general explanations are given in the present work. In a few words, gravisensing occurs by inclination perception through the sedimentation in the direction of gravity of specialized starch-filled amyloplasts, called statoliths [220]. In stems, these latter occur in specialized gravisensing cells named statocytes [220] localized in the innermost layer of endodermis cells of the cortex [216,221,222], as well as in secondary phloem cells for stems exhibiting a more extensive secondary growth [216]. The sedimentation of statoliths induces a biochemical signal modifying the movements of calcium ions, which then triggers the polar auxin transport and distribution [197,221]. The auxin is the major hormone involved in plant tropism [223], but ethylene [224] and gibberellic acid [225] are most probably also involved in the gravisensing signal of woody angiosperms; however, the interactions between these hormones still require further understanding. Changes in the auxin transport and distribution finally result in stem curvature upward. Nevertheless, auxin-related changes differ if considering herbaceous or woody angiosperms, more specifically between stems undergoing primary growth or secondary growth. In fact, changes related to auxin distribution lead to two different types of gravitropic motors inciting stem bending.

In the first case, if the stem undergoes primary growth, the gravitropic motor is the differential elongation growth [226]. According to the “Cholodny-Went” hypothesis [227], auxin is transported laterally toward the lower side of the stem. It creates an auxin gradient between the upper and lower sides of the stem, inducing an increase elongation growth on the lower side. This gradient results in “pushing” the plant organ upward, *i.e.* curving of the stem toward a vertical position. In elongating stems, this

up-curving is a reaction along the entire growing organ; it starts at the apex, which then becomes straight first by decurving, and the straightening moved downward gradually along the elongating stem [217]. Finally, a remaining curvature is visible at the base of the elongating growth zone [217]. Actually, gravisensing is accompanied by sensing of local curvature, so-called proprioception, that enables the control of the straightening autotropic response and posture control [25].

In the second case, if the stem undergoes secondary growth, *i.e.* in stem regions where elongation is finalized but where radial growth happens due to the active cambium, the stem curvature occurs through the asymmetric generation of a specialized xylem tissue called reaction wood [228]. In woody angiosperms, the reaction wood is more particularly named tension wood whereas the xylem formed across from the reaction wood is called opposite wood. [219,229]. Once again, auxin is designated at the origin of the differential cambial growth in woody plants [230,231]. Indeed, auxin is distributed toward the cambium and the center of the stem on the upper side of the stem and triggers tension wood formation; conversely, auxin is transported away from the cambium, toward the periphery of the stem on the lower side of the stem and triggers opposite wood formation [216]. Even though it is confirmed that tension wood is capable of generating high tensional stress moving the plant upward [89,232,233], the mechanism linking the generation of stress with gravitropism is the subject of many disagreements between authors. In fact, the similarity between opposite wood and normal wood, as well as on the composition and organization of tension wood is clearly accepted. In addition, this latter type of wood, is characterized by a specific G-layer having a high cellulose content, with highly crystalline cellulose microfibrils exhibiting an MFA close to 0° in a free-lignin matrix composed of non-cellulosic polysaccharides and glycosylated proteins [89,234,235]. Moreover, it has been demonstrated that the tensile stress in tension wood results from tensions into the cellulose microfibrils of the G-layer [236]. The origin of tensions in cellulose microfibrils is nevertheless not known with certainty, and different hypotheses were reviewed and discussed by Alméras and Clair [237].

However, even if the generation of tension wood is essentially a characteristic of woody plants, recent studies highlighted its presence in herbaceous stems of *Arabidopsis thaliana* [238], alfalfa (*Medicago sativa* L.) [239] and flax [76]. These results interestingly confirm the ability of some herbaceous angiosperms to generate tension tissues, somehow analogous to tension wood of woody angiosperms. The study of flax

gravitropism is of great interest as this plant naturally exhibits fibers with a G-layer in a normal plant growth, namely the flax primary fibers whose development was detailed in 2.4. In addition, xylem of flax exhibiting G-layer can be produced as a gravitropic response on the upper side of the stem [76], which interrogates about the involvement of flax fibers in the response of the plant. The study of Ibragimova et al. [76] demonstrates that the remaining curvature occurs in a stem part that has already ceased fiber elongation (much below the snap point); however, the fiber thickening still processing at this level is impacted by the gravitropic response. As neither cell elongation nor cambium differentiation are involved in the fiber reaction, the authors [76] suggest that a part of this gravitropic reaction actually occurs within the fiber cell wall itself. Indeed, when comparing fibers of control plants and fibers from the opposite side of the stem, a significant increase of the fiber diameter is obtained on the pulling side (side where reaction wood occurs in the xylem part); in addition, the proportion of the lumen area from fiber area is significantly increased in fibers subjected to gravitropism, on both sides of the stem, with a much greater increase on the pulling side. Last but not least, the shape of the fibers along their length is highly modified, as fibers exhibit “sausage-like” shape with a deposition of callose, a polysaccharide generally present in injured cell walls [68], in the fiber thinner zones. Finally, the MFA is also impacted by the gravitropic reaction, namely increased from about 0° in control plants to 18° on the pulling side of inclined ones, impacting the characteristics of the G-layer [76]. Thus, even if little is known about the impact of gravitropism on the mechanical properties of flax fibers and stems, changes in fiber thickening and morphology would most probably decrease the fiber mechanical properties and their homogeneity. Even though flax plants are able to recover from lodging through a gravitropic response, stem lodging happening during the early thickening process would jeopardize the mechanical properties of the fibers by impacting this development process. This makes lodging an even more undesired phenomenon, both from the farmer point of view (by decreasing the fiber yield) and the composite manufacturer side (by impacting the fiber properties). If lodging appears closer to fiber maturity, fibers would be already well thickened; in this case, a negative direct impact on the fiber properties would be limited, but would still involve greater susceptibility toward diseases and harvesting problems. In this latter situation, the gravitropic response would probably rely essentially on xylem tension wood, demonstrating once more the essential role of this tissue in the flax plant characteristics.

## **5. Conclusions**

Flax is one of the oldest plants cultivated by mankind, essentially for the fibers contained in its stem. Flax fibers have always been intended for textile production, including clothing and upholstery. Moreover, a more contemporary application has been advanced over the past decades, namely the use of flax fibers for composite reinforcement. Growth stages of this plant are quite well described in literature, probably thank to the industrial potential of flax fibers. The processes of fiber development, from initiation to thickening, are the subject of several studies, essentially due to the uncommon properties of flax fibers, morphologically speaking but also due to the remarkable G-layer constituting most of the cell wall. Flax, by being an annual herbaceous plant, providing fibers exhibiting a thick G-layer similar to tension wood as well as a substantial xylem quantity, gathers very promising characteristics to understand the mechanisms of plant responses to a large range of cultural conditions and external stimuli.

Nevertheless, it remains difficult to find general average data regarding flax fiber composition, either during plant ontogeny or at fiber maturity. This is partially explained by the numerous existing flax varieties and irreproducible meteorological conditions between regions and years inducing a great composition variability, but also due to many protocols followed by authors. In addition, if the meteorological conditions are hardly controllable, the influence of the variety on fiber composition and performances is of greater interest, as it relies on the mastered expertise of varietal selection. This latter has successfully selected flax varieties exhibiting high fiber yields, good disease resistance and a worthy stability toward lodging, while ensuring plant characteristics (height and diameters) remains adapted to existing agricultural machinery and scutching machines. Thus, one can reasonably expect an efficient selection work toward the development of new flax varieties dedicated to technical applications. This innovative approach would come together with studies investigating flax plant adaptation and reinforcement mechanisms in natural or experimental environments, including a complementary interest in the xylem contribution to flax mechanisms. To a larger extent, such investigations would also provide food for thought about the adaptation of flax to current climate changes, including global warming, in order to preserve the cultivation of this outstanding industrial crop.

## 6. References

1. Quillien, L. Flax and Linen in the First Millennium Babylonia BC : the origins, craft industry and uses of a remarkable textile. In *Prehistoric, Ancient Near Eastern & Aegean Textiles and Dress*; Books, O., Ed.; 2014; pp. 271–296 ISBN 1782977198, 9781782977193.
2. de Bruyne, N. A. Plastic progress - Some further developments in the manufacture and use of synthetic materials for aircraft construction. *Flight Aircr. Eng.* 1939, 77–79.
3. van Dam, J. E. G.; Gorshkova, T. A. Cell walls and Fibers / Fiber formation. In *Encyclopedia of Applied Plant Sciences*; Elsevier Ltd, 2003; pp. 87–96.
4. Yan, L.; Chouw, N.; Jayaraman, K. Flax fibre and its composites – A review. *Compos. Part B Eng.* 2014, 56, 296–317, doi:10.1016/j.compositesb.2013.08.014.
5. Pickering, K. L.; Efendy, M. G. A.; Le, T. M. A review of recent developments in natural fibre composites and their mechanical performance. *Compos. Part A Appl. Sci. Manuf.* 2016, 83, 98–112, doi:10.1016/j.compositesa.2015.08.038.
6. Lefeuvre, A.; Bourmaud, A.; Morvan, C.; Baley, C. Tensile properties of elementary fibres of flax and glass: Analysis of reproducibility and scattering. *Mater. Lett.* 2014, 130, 289–291.
7. Bensadoun, F.; Verpoest, I.; Baets, J.; Müssig, J.; Graupner, N.; Davies, P.; Gomina, M.; Kervoelen, A.; Baley, C. Impregnated fibre bundle test for natural fibres used in composites. *J. Reinf. Plast. Compos.* 2017, 0731684417695461, doi:10.1177/0731684417695461.
8. Merotte, J.; Le Duigou, A.; Bourmaud, A.; Behloul, K.; Baley, C. Mechanical and acoustic behaviour of porosity controlled randomly dispersed flax/PP biocomposite. *Polym. Test.* 2016, 51, doi:10.1016/j.polymertesting.2016.03.002.
9. Lefeuvre, A.; Bourmaud, A.; Baley, C. Optimization of the mechanical performance of UD flax/epoxy composites by selection of fibres along the stem. *Compos. Part A Appl. Sci. Manuf.* 2015, 77, 204–208, doi:10.1016/j.compositesa.2015.07.009.
10. Robitaille, F.; Gauvin, R. Compaction of textile reinforcements for composites manufacturing. III: Reorganization of the fiber network. *Polym. Compos.* 1999, 20, 48–61, doi:10.1002/pc.10334.
11. Doumbia, A. S.; Castro, M.; Jouannet, D.; Kervoelen, A.; Falher, T.; Cauret, L.; Bourmaud, A. Flax/polypropylene composites for lightened structures: Multiscale analysis of process and fibre parameters. *Mater. Des.* 2015, 87, 331–341, doi:10.1016/j.matdes.2015.07.139.
12. Dickson, A. R.; Even, D.; Warnes, J. M.; Fernyhough, A. The effect of reprocessing on the mechanical properties of polypropylene reinforced with wood pulp, flax or glass fibre. *Compos. Part A Appl. Sci. Manuf.* 2014, 61, 258–267, doi:10.1016/j.compositesa.2014.03.010.
13. Le Duigou, A.; Pillin, I.; Bourmaud, A.; Davies, P.; Baley, C. Effect of recycling on mechanical behaviour of biocompostable flax/poly(L-lactide) composites. *Compos. Part A* 2008, 39, 1471–1478, doi:10.1016/j.compositesa.2008.05.008.
14. Le Duigou, A.; Bourmaud, A.; Gourier, C.; Baley, C. Multi-scale shear properties of flax fibre reinforced polyamide 11 biocomposites. *Compos. Part A Appl. Sci. Manuf.* 2016, 85, 123–129, doi:10.1016/j.compositesa.2016.03.014.
15. Mahboob, Z.; El Sawi, I.; Zdero, R.; Fawaz, Z.; Bougherara, H. Tensile and compressive damaged response in Flax fibre reinforced epoxy composites. *Compos. Part A Appl. Sci. Manuf.* 2017, 92, 118–133, doi:10.1016/j.compositesa.2016.11.007.
16. Joffe, R.; Andersons, J.; Wallström, L. Interfacial shear strength of flax fiber/thermoset polymers estimated by fiber fragmentation tests. *J. Mater. Sci.* 2005, 40, 2721–2722, doi:10.1007/s10853-005-2115-4.
17. Åkesson, D.; Skrifvars, M.; Seppälä, J.; Turunen, M. Thermoset lactic acid-based resin as a matrix for flax fibers. *J. Appl. Polym. Sci.* 2011, 119, 3004–3009, doi:10.1002/app.33030.

18. Summerscales, J Dissanayake, N. P.; Virk, A. S.; Hall, W. A review of bast fibres and their composites. Part 1–Fibres as reinforcements. *Compos. Part A Appl. Sci. Manuf.* 2010, 41, 1329–1335, doi:10.1016/j.compositesa.2010.06.001.
19. Ku, H.; Wang, H.; Pattarachaiyakoo, N.; Trada, M. A review on the tensile properties of natural fiber reinforced polymer composites. *Compos. Part B Eng.* 2011, 42, 856–873, doi:10.1016/j.compositesb.2011.01.010.
20. Allaby, R. G.; Peterson, G. W.; Merriwether, D. A.; Fu, Y. B. Evidence of the domestication history of flax (*Linum usitatissimum* L.) from genetic diversity of the sad2 locus. *Theor. Appl. Genet.* 2005, 112, 58–65, doi:10.1007/s00122-005-0103-3.
21. Mikshina, P.; Chernova, T.; Chemikosova, S.; Ibragimova, N.; Mokshina, N.; Gorshkova, T. Cellulosic fibers: Role of matrix polysaccharides in structure and function. In *Cellulose - Fundamental Aspects*; InTech, 2013; pp. 91–112 ISBN 978-953-51-1183-2.
22. Gorshkova, T. A.; Wyatt, S. E.; Salnikov, V. V.; Gibeaut, D. M.; Ibragimov, M. R.; Lozovaya, V. V.; Carpita, N. C. Cell-wall polysaccharides of developing flax plants. *Plant Physiol.* 1996, 110, 721–729, doi:10.1104/pp.110.3.721.
23. Baley, C.; Bourmaud, A. Average tensile properties of French elementary flax fibers. *Mater. Lett.* 2014, 122, 159–161, doi:10.1016/j.matlet.2014.02.030.
24. Jankauskiene, Z. Results of 90 years of flax breeding in Lithuania. *Proc. Latv. Acad. Sci. Sect. B Nat. Exact, Appl. Sci.* 2014, 68, 184–192, doi:10.2478/prolas-2014-0022.
25. Moulia, B.; Coutand, C.; Lenne, C. Posture control and skeletal mechanical acclimation in terrestrial plants: implications for mechanical modeling of plant architecture. *Am. J. Bot.* 2006, 93, 1477–1489, doi:10.3732/ajb.93.10.1477.
26. Sultana, C. Growing and harvesting of flax. In *The Biology and Processing of Flax*; Sharma, H. S. S. and V. S., Ed.; M Publications, Belfast, Northern Ireland, 1992; pp. 83–109.
27. Sultana, C. The cultivation of fibre flax. *Outlook Agric.* 1983, 12, 104–110, doi:10.1177/003072708301200301.
28. Mediavilla, V.; Jonquera, M.; Schmid-Slembrouck, I.; Soldati, A. Decimal code for growth stages of hemp (*Cannabis sativa* L.). *J. Int. Hemp Ass.* 1998, 5, 68–74.
29. Lancashire, P. D.; Bleiholder, H.; Boom, T. Van Den; Langelüddeke, P.; Stauss, R.; Weber, E.; Witzemberger, A. A uniform decimal code for growth stages of crops and weeds. *Ann. Appl. Biol.* 1991, 119, 561–601, doi:10.1111/j.1744-7348.1991.tb04895.x.
30. ARVALIS - Institut du végétal Choisir et décider lin fibre; Paris, 2014;
31. Paul-Victor, C.; Vacche, S. D.; Sordo, F.; Fink, S.; Speck, T.; Michaud, V.; Speck, O. Effect of mechanical damage and wound healing on the viscoelastic properties of stems of flax cultivars (*Linum usitatissimum* L. cv . Eden and cv . Drakkar ). *PLoS One* 2017, 1–23, doi:10.1371/journal.pone.0185958.
32. Edwards, H. G. M.; Farwell, D. W.; Webster, D. FT Raman microscopy of untreated natural plant fibres. *Spectrochim. Acta - Part A Mol. Biomol. Spectrosc.* 1997, 1425, 2383–2392, doi:10.1016/S1386-1425(97)00178-9.
33. Gorshkova, T. A.; Sal'nikov, V. V.; Chemikosova, S. B.; Ageeva, M. V.; Pavlencheva, N. V.; Van Dam, J. E. G. The snap point: A transition point in *Linum usitatissimum* bast fiber development. *Ind. Crops Prod.* 2003, 18, 213–221, doi:10.1016/S0926-6690(03)00043-8.
34. Heller, K.; Sheng, Q. C.; Guan, F.; Alexopoulou, E.; Hua, L. S.; Wu, G. W.; Jankauskienė, Z.; Fu, W. Y. A comparative study between Europe and China in crop management of two types of flax: linseed and fibre flax. *Ind. Crops Prod.* 2015, 68, 24–31, doi:10.1016/j.indcrop.2014.07.010.
35. Bert, F. *Lin fibre - Culture et transformation*; Arvalis, Ed.; 2013; ISBN 9782817901572.

36. Tiver, N. S.; Williams, R. P. Studies of the flax plant 2. The effect of artificial drought on growth and oil production in a inseed variety. *Aust. J. Exp. Biol. Med. Sci.* 1943, 21, 201–209.
37. Prentice, I. C.; Cramer, W.; Harrison, S. P.; Leemans, R.; Monserud, R. A.; Solomon, A. M. Special Paper: A global biome model based on plant physiology and dominance, soil properties and climate. *J. Biogeogr.* 1992, 19, 117–134, doi:10.2307/2845499.
38. Lefeuvre, A. Contribution à l'étude des propriétés mécaniques et morphologiques des fibres de lin, Université de Rouen et Normandie Université, 2014.
39. Du, G.-H.; Liu, F.-H.; Rowland, G. Fiber cell development and fiber yield of flax (*Linum usitatissimum* L.) affected by the seasonal temperature pattern. *Can. J. Plant Sci.* 2015, 95, 1215–1220, doi:10.4141/cjps-2014-185.
40. Bourmaud, A.; Gibaud, M.; Baley, C. Impact of the seeding rate on flax stem stability and the mechanical properties of elementary fibres. *Ind. Crops Prod.* 2016, 80, 17–25, doi:10.1016/j.indcrop.2015.10.053.
41. Djemiel, C.; Grec, S.; Hawkins, S. Characterization of bacterial and fungal community dynamics by high-throughput sequencing (HTS) metabarcoding during flax dew-retting. *Front. Microbiol.* 2017, 8, 1–16, doi:10.3389/fmicb.2017.02052.
42. Martin, N.; Mouret, N.; Davies, P.; Baley, C. Influence of the degree of retting of flax fibers on the tensile properties of single fibers and short fiber/polypropylene composites. *Ind. Crops Prod.* 2013, 49, 755–767, doi:10.1016/j.indcrop.2013.06.012.
43. Arber, A. *The natural philosophy of plant form*; Cambridge University Press, 2012;
44. Gartner, B. *Plant stems: physiology and functional morphology*; Academic Press, 1995; ISBN 0080539084.
45. Romberger, J. A.; Hejnowicz, Z.; Hill, J. F. *Plant structure: Function and development*; Springer Berlin Heidelberg: Berlin, Heidelberg, 1993; ISBN 978-3-662-01664-0.
46. Evert, R. F.; Eichorn, S. E. *Raven Biology of Plants*; 8th ed.; W.H. Freeman & Company, New York NY, 2013; ISBN 978-1-4292-1961-7.
47. Meicenheimer, R. D. Cellular basis for growth and tissue differentiation patterns in *Linum usitatissimum* (Linaceae) stems: The stem unit. *Am. J. Bot.* 1992, 79, 914–920, doi:10.2307/2445002.
48. Schweingruber, F. H.; Börner, A.; Schulze, E.-D. *Atlas of woody plants stems - Evolution, structure and environmental modifications*; Springer: Berlin, 2006; ISBN 9783540325239.
49. Esau, K. Vascular differentiation in the vegetative shoot of *Linum*. I. The procambium. *Am. J. Bot.* 1942, 29, 738–747, doi:10.2307/2437727.
50. Evert, R. F. *Esau's Plant Anatomy*; 3rd editio.; John Wiley & Sons, Inc., 2006; ISBN 9788578110796.
51. McDougall, G. J.; Morrison, I. M.; Stewart, D.; Weyers, J. D. B.; Hillman, J. R. Plant fibres: Botany, chemistry and processing for industrial use. *J. Sci. Food Agric.* 1993, 62, 1–20, doi:10.1002/jsfa.2740620102.
52. Esau, K. Vascular differentiation in the vegetative shoot of *Linum*. III. The origin of the bast fibers. *Am. J. Bot.* 1943, 30, 579–586, doi:10.2307/2437468.
53. His, I.; Andème-Onzighi, C.; Morvan, C.; Driouich, A. Microscopic studies on mature flax fibers embedded in LR white: immunogold localization of cell wall matrix polysaccharides. *J. Histochem. Cytochem.* 2001, 49, 1–11, doi:10.1177/002215540104901206.
54. Aldaba, V. C. The structure and development of the cell wall in plants I. Bast fibers of *Boehmeria* and *Linum*. *Am. J. Bot.* 1927, 14, 16, doi:10.2307/2435518.

55. Bergfjord, C.; Holst, B. A procedure for identifying textile bast fibres using microscopy: Flax, nettle/ramie, hemp and jute. *Ultramicroscopy* 2010, 110, 1192–1197, doi:10.1016/j.ultramic.2010.04.014.
56. Gorshkov, O.; Mokshina, N.; Ibragimova, N.; Ageeva, M.; Gogoleva, N.; Gorshkova, T. Phloem fibres as motors of gravitropic behaviour of flax plants : level of transcriptome. *Funct. Plant Biol.* 2017, doi:10.1071/FP16348.
57. Gorshkova, T.; Morvan, C. Secondary cell-wall assembly in flax phloem fibres: Role of galactans. *Planta* 2006, 223, 149–158, doi:10.1007/s00425-005-0118-7.
58. Tiver, N. S. Studies of the flax plant 1. Physiology of growth, stem anatomy and fibre development in fibre flax. *Aust. J. Exp. Biol. Med. Sci.* 1942, 20, 149–160.
59. Catling, D.; Grayson, J. Identification of vegetable fibres; Springer, Dordrecht, 1982; ISBN 978-94-011-8070-2.
60. Bourmaud, A.; Malvestio, J.; Lenoir, N.; Siniscalco, D.; Habrant, A.; King, A.; Legland, D.; Baley, C.; Beaugrand, J. Exploring the mechanical performance and in-planta architecture of secondary hemp fibres. *Ind. Crops Prod.* 2017, 108, 1–5, doi:10.1016/j.indcrop.2017.06.010.
61. Snegireva, A.; Chernova, T.; Ageeva, M.; Lev-Yadun, S.; Gorshkova, T. Intrusive growth of primary and secondary phloem fibres in hemp stem determines fibre-bundle formation and structure. *AoB Plants* 2015, 7, plv061, doi:10.1093/aobpla/plv061.
62. Fernandez-Tendero, E.; Day, A.; Legros, S.; Habrant, A.; Hawkins, S.; Chabbert, B. Changes in hemp secondary fiber production related to technical fiber variability revealed by light microscopy and attenuated total reflectance Fourier transform infrared spectroscopy. *PLoS One* 2017, 12, 1–14, doi:10.1371/journal.pone.0179794.
63. Gorshkova, T.; Brutch, N.; Chabbert, B.; Deyholos, M.; Hayashi, T.; Lev-Yadun, S.; Mellerowicz, E. J.; Morvan, C.; Neutelings, G.; Pilate, G. Plant fiber formation: State of the art, recent and expected progress, and open questions. *CRC. Crit. Rev. Plant Sci.* 2012, 31, 201–228.
64. Anderson, D. B. A microchemical study of the structure and development of flax fibers. *Am. J. Bot.* 1927, 14, 187–211.
65. Ageeva, M. V.; Petrovská, B.; Kieft, H.; Sal'nikov, V. V.; Snegireva, A. V.; Van Dam, J. E. G.; Van Veenendaal, W. L. H.; Emons, A. M. C.; Gorshkova, T. A.; Van Lammeren, A. A. M. Intrusive growth of flax phloem fibers is of intercalary type. *Planta* 2005, 222, 565–574, doi:10.1007/s00425-005-1536-2.
66. Roach, M. J.; Deyholos, M. K. Microarray analysis of flax (*Linum usitatissimum* L.) stems identifies transcripts enriched in fibre-bearing phloem tissues. *Mol. Genet. Genomics* 2007, 278, 149–165, doi:10.1007/s00438-007-0241-1.
67. Gorshkova, T. A.; Ageeva, M. V.; Salnikov, V. V.; Pavlencheva, N. V.; Snegireva, A. V.; Chernova, T. E.; Chemikosova, S. B. стадии формирования лубяных волокон *Linum usitatissimum* (Linaceae). *Bot. J.* 2003, 88, 1–11.
68. Snegireva, A. V.; Ageeva, M. V.; Amenitskii, S. I.; Chernova, T. E.; Ebskamp, M.; Gorshkova, T. A. Intrusive growth of sclerenchyma fibers. *Russ. J. Plant Physiol.* 2010, 57, 342–355, doi:10.1134/S1021443710030052.
69. Chernova, T. E.; Gorshkova, T. A. Biogenesis of plant fibers. *Russ. J. Dev. Biol.* 2007, 38, 221–232, doi:10.1134/S1062360407040054.
70. Cosgrove, D. J.; Jarvis, M. C. Comparative structure and biomechanics of plant primary and secondary cell walls. *Front. Plant Sci.* 2012, 3, 1–6, doi:10.3389/fpls.2012.00204.
71. Gorshkova, T.; Chernova, T.; Mokshina, N.; Ageeva, M.; Mikshina, P. Plant ‘muscles’: fibers with a tertiary cell wall. *New Phytol.* 2018, 218, 66–72, doi:10.1111/nph.14997.

72. Rihouey, C.; Paynel, F.; Gorshkova, T.; Morvan, C. Flax fibers: assessing the non-cellulosic polysaccharides and an approach to supramolecular design of the cell wall. *Cellulose* 2017, 24, 1985–2001, doi:10.1007/s10570-017-1246-5.
73. Domenges, B.; Charlet, K. Direct insights on flax fiber structure by focused ion beam microscopy. *Microsc. Microanal.* 2010, 16, 175–182, doi:10.1017/S1431927609991292.
74. Bowling, A. J.; Vaughn, K. C. Immunocytochemical characterization of tension wood: Gelatinous fibers contain more than just cellulose. *Am. J. Bot.* 2008, 95, 655–663, doi:10.3732/ajb.2007368.
75. Roussel, J. R.; Clair, B. Evidence of the late lignification of the G-layer in Simarouba tension wood, to assist understanding how non-G-layer species produce tensile stress. *Tree Physiol.* 2015, 35, 1366–1377, doi:10.1093/treephys/tpv082.
76. Ibragimova, N. N.; Ageeva, M. V.; Gorshkova, T. A. Development of gravitropic response: unusual behavior of flax phloem G-fibers. *Protoplasma* 2017, 254, 749–762, doi:10.1007/s00709-016-0985-8.
77. Hearle, J. W. S. The fine structure of fibers and crystalline polymers. III. Interpretation of the mechanical properties of fibers. *J. Appl. Polym. Sci.* 1963, 7, 1207–1223, doi:10.1002/app.1963.070070403.
78. Gorshkova, T. A.; Gurjanov, O. P.; Mikshina, P.; Ibragimova, N.; Mokshina, N.; Salnikov, V.; Ageeva, M.; Amenitskii, S.; Chernova, T.; Chemikosova, S. Specific type of secondary cell wall formed by plant fibers. *Russ. J. Plant Physiol.* 2010, 57, 328–341, doi:10.1134/s1021443710030040.
79. Arnould, O.; Siniscalco, D.; Bourmaud, A.; Le Duigou, A.; Baley, C. Better insight into the nano-mechanical properties of flax fibre cell walls. *Ind. Crops Prod.* 2017, 97, 224–228, doi:10.1016/j.indcrop.2016.12.020.
80. Gorshkova, T. A.; Mikshina, P. V.; Gurjanov, O. P.; Chemikosova, S. B. Formation of plant cell wall supramolecular structure. *Biochemistry* 2010, 75, 159–72, doi:10.1134/S0006297910020069.
81. Gorshkova, T. A.; Chemikosova, S. B.; Salnikov, V. V.; Pavlencheva, N. V.; Gurjanov, O. P.; Stolle-Smits, T.; Van Dam, J. E. G. Occurrence of cell-specific galactan is coinciding with bast fiber developmental transition in flax. *Ind. Crops Prod.* 2004, 19, 217–224, doi:10.1016/j.indcrop.2003.10.002.
82. McDougall, G. J. Isolation and partial characterisation of the non-cellulosic polysaccharides of flax fibre. *Carbohydr. Res.* 1993, 241, 227–236, doi:10.1016/0008-6215(93)80109-R.
83. Morvan, C.; Andème-Onzighi, C.; Girault, R.; Himmelsbach, D. S.; Driouich, A.; Akin, D. E. Building flax fibres: more than one brick in the walls. *Plant Physiol. Biochem.* 2003, 41, 935–944.
84. Lefeuvre, A.; Bourmaud, A.; Morvan, C.; Baley, C. Elementary flax fibre tensile properties: Correlation between stress–strain behaviour and fibre composition. *Ind. Crops Prod.* 2014, 52, 762–769, doi:10.1016/j.indcrop.2013.11.043.
85. Alix, S.; Goimard, J.; Morvan, C.; Baley, C.; Schols, H. A.; Visser, R. G. F.; Voragen, A. G. J. Influence of pectin structure on the mechanical properties of flax fibres: a comparison between linseed-winter variety (Oliver) and a fibre-spring variety of flax. In *Pectins and Pectinases*; 2009; pp. 85–96 ISBN 9789086861088.
86. Milthorpe, F. L. Fibre development of flax in relation to water supply and light intensity. *Ann. Bot.* 1945, 9, 31–53.
87. Bos, H. L.; Donald, A. M. In ESEM study of the deformation of elementary flax fibre. *J. Mater. Sci.* 1999, 34, 3029–3034, doi:10.1023/A:1004650126890.
88. Carpita, N. C.; Gibeaut, D. M. Structural models of primary cell walls in flowering plants: consistency of molecular structure with the physical properties of the walls during growth. *Plant J.* 1993, 3, 1–30, doi:10.1111/j.1365-313X.1993.tb00007.x.

89. Mellerowicz, E. J.; Gorshkova, T. A. Tensional stress generation in gelatinous fibres: a review and possible mechanism based on cell-wall structure and composition. *J. Exp. Bot.* 2012, 63, 551–565, doi:10.1093/jxb/err339.
90. Andème-Onzighi, C.; Girault, R.; His, I.; Morvan, C.; Driouich, A. Immunocytochemical characterization of early-developing flax fiber cell walls. *Protoplasma* 2000, 213, 235–245, doi:10.1007/BF01282161.
91. Bourmaud, A.; Morvan, C.; Bouali, A.; Placet, V.; Perré, P.; Baley, C. Relationships between microfibrillar angle, mechanical properties and biochemical composition of flax fibers. *Ind. Crops Prod.* 2013, 44, 343–351, doi:10.1016/j.indcrop.2012.11.031.
92. Barnett, J. R.; Bonham, V. A. Cellulose microfibril angle in the cell wall of wood fibres. *Biol. Rev.* 2004, 79, 461–472, doi:10.1017/S1464793103006377.
93. Bledzki, A. K.; Gassa, J. Composites reinforced with cellulose based fibers. *Prog. Polym. Sci.* 1999, 24, 221–274.
94. Roach, M. J.; Mokshina, N. Y.; Badhan, A.; Snegireva, A. V.; Hobson, N.; Deyholos, M. K.; Gorshkova, T. A. Development of cellulosic secondary walls in flax fibers requires b-galactosidase. *Plant Physiol.* 2011, 156, 1351–1363, doi:10.1104/pp.111.172676.
95. Niklas, K. J. *Plant biomechanics: an engineering approach to plant form and function*; University of Chicago press, 1992;
96. Romberger, J. A.; Hejnowicz, Z.; Hill, J. F. *Plant structure: Function and development. A treatise on anatomy and vegetative development, with special reference to woody plants*; Springer Berlin, 1993;
97. Niklas, K. J. Interspecific allometries of critical buckling height and actual plant height. *Am. J. Bot.* 1994, 81, 1275–1279, doi:10.2307/2445403.
98. Gibaud, M.; Bourmaud, A.; Baley, C. Understanding the lodging stability of green flax stems; The importance of morphology and fibre stiffness. *Biosyst. Eng.* 2015, 137, 9–21.
99. Niklas, K. J. The scaling of plant height: A comparison among major plant clades and anatomical grades. *Ann. Bot.* 1993, 72, 165–172, doi:10.1006/anbo.1993.1095.
100. Oladokun, M. A. O.; Ennos, A. R. Structural development and stability of rice *Oryza sativa* L. var. Nerica 1. *J. Exp. Bot.* 2006, 57, 3123–3130, doi:10.1093/jxb/erl074.
101. Crook, M. J.; Ennos, A. R. Stem and root characteristics associated with lodging resistance in four winter wheat cultivars. *J. Agric. Sci.* 1994, 123, 167–174, doi:10.1017/S0021859600068428.
102. Zhu, X. G.; Shan, L.; Wang, Y.; Quick, W. P. C4 Rice - an ideal arena for systems biology research. *J. Integr. Plant Biol.* 2010, 52, 762–770, doi:10.1111/j.1744-7909.2010.00983.x.
103. Fuller, D. Q.; Qin, L.; Zheng, Y.; Zhao, Z.; Chen, X.; Hosoya, L. A.; Sun, G.-P. The domestication process and domestication rate in rice: Spikelet bases from the lower Yangtze. *Science* (80-. ). 2009, 323, 1607–1610.
104. Peng, S.; Tang, Q.; Zou, Y. Current status and challenges of rice production in China. *Plant Prod. Sci.* 2009, 12, 3–8, doi:10.1626/pp.s.12.3.
105. Lang, Y.; Yang, X.; Wang, M.; Zhu, Q. Effects of lodging at different filling stages on rice yield and grain quality. *Rice Sci.* 2012, 19, 315–319, doi:10.1016/S1672-6308(12)60056-0.
106. Berry, P. M.; Sterling, M.; Spink, J. H.; Baker, C. J.; Sylvester-Bradley, R.; Mooney, S. J.; Tams, A. R.; Ennos, A. R. Understanding and reducing lodging in cereals. *Adv. Agron.* 2004, 84, 217–271, doi:10.1016/S0065-2113(04)84005-7.
107. Yue, B.; Xue, W.; Xiong, L.; Yu, X.; Luo, L.; Cui, K.; Jin, D.; Xing, Y.; Zhang, Q. Genetic basis of drought resistance at reproductive stage in rice: Separation of drought tolerance from drought avoidance. *Genetics* 2006, 172, 1213–1228, doi:10.1534/genetics.105.045062.

108. Xiong, W.; Lin, E.; Ju, H.; Xu, Y. Climate change and critical thresholds in China's food security. *Clim. Change* 2007, 81, 205–221, doi:10.1007/s10584-006-9123-5.
109. Savary, S.; Elazegui, F. A.; Teng, P. S. Special Report Assessing the Representativeness of Data on Yield Losses Due to Rice Diseases in Tropical Asia. *Plant Dis.* 1998, 82, 705–709.
110. Mew, T. W.; Leung, H.; Savary, S.; Vera Cruz, C. M.; Leach, J. E. Looking ahead in rice disease research and management. *CRC. Crit. Rev. Plant Sci.* 2004, 23, 103–127, doi:10.1080/07352680490433231.
111. Peleg, Z.; Fahima, T.; Korol, A. B.; Abbo, S.; Saranga, Y. Genetic analysis of wheat domestication and evolution under domestication. *J. Exp. Bot.* 2011, 62, 5051–5061, doi:10.1093/jxb/err206.
112. Piñera-Chavez, F. J.; Berry, P. M.; Foulkes, M. J.; Molero, G.; Reynolds, M. P. Avoiding lodging in irrigated spring wheat. II. Genetic variation of stem and root structural properties. *F. Crop. Res.* 2016, 196, 64–74, doi:10.1016/j.fcr.2016.06.007.
113. Wilcoxon, R. D.; Skovmand, B.; Atif, A. H. Evaluation of wheat cultivars for ability to retard development of stem rust. *Ann. Appl. Biol.* 1975, 80, 275–281.
114. Ranalli, P. Current status and future scenarios of hemp breeding. *Euphytica* 2004, 140, 121–131, doi:10.1007/s10681-004-4760-0.
115. Schultes, R. E. *Random thoughts and queries on the botany of cannabis.*; J. & A. Churchill.: London, UK, 1970;
116. De Meijer, E. P. M. Fibre hemp cultivars: A survey of origin, ancestry, availability and brief agronomic characteristics. *J. Int. Hemp Assoc.* 1995, 2, 66–73.
117. van der Werf, H.; Mathussen, E. W. J. M.; Haverkort, A. J. The potential of hemp (*Cannabis sativa* L.) for sustainable fibre production: a crop physiological appraisal. *Ann. Appl. Biol.* 1996, 129, 109–123, doi:10.1111/j.1744-7348.1996.tb05736.x.
118. de Meijer, E. P. M.; Keizer, L. C. P. Variation of *Cannabis* for phenological development and stem elongation in relation to stem production. *F. Crop. Res.* 1994, 38, 37–46, doi:10.1016/0378-4290(94)90030-2.
119. Faux, A. M.; Draye, X.; Lambert, R.; d'Andrimont, R.; Raulier, P.; Bertin, P. The relationship of stem and seed yields to flowering phenology and sex expression in monoecious hemp (*Cannabis sativa* L.). *Eur. J. Agron.* 2013, 47, 11–22, doi:10.1016/j.eja.2013.01.006.
120. Amaducci, S.; Colauzzi, M.; Zatta, A.; Venturi, G. Flowering dynamics in monoecious and dioecious hemp genotypes. *J. Ind. Hemp* 2008, 13, 5–19, doi:10.1080/15377880801898691.
121. Placet, V.; Méteau, J.; Froehly, L.; Salut, R.; Boubakar, M. L. Investigation of the internal structure of hemp fibres using optical coherence tomography and Focused Ion Beam transverse cutting. *J. Mater. Sci.* 2014, 49, 8317–8327, doi:10.1007/s10853-014-8540-5.
122. van der Werf, H. M. G.; Harsveld van der Veen, J. E.; Bouma, A. T. M.; ten Cate, M. Quality of hemp (*Cannabis sativa* L.) stems as a raw material for paper. *Ind. Crops Prod.* 1994, 2, 219–227, doi:10.1016/0926-6690(94)90039-6.
123. Tang, K.; Struik, P. C.; Yin, X.; Thouminot, C.; Bjelková, M.; Stramkale, V.; Amaducci, S. Comparing hemp (*Cannabis sativa* L.) cultivars for dual-purpose production under contrasting environments. *Ind. Crops Prod.* 2016, 87, 33–44, doi:10.1016/j.indcrop.2016.04.026.
124. Grassi, G.; Ranalli, P. Detecting and monitoring plant THC content: Innovative and conventional methods. In *Advances in Hemp Research*; Ranalli, P., Ed.; The Haworth Press, Binghamton, New York (USA), 1999; pp. 43–60.
125. Callaway, J. C. A more reliable evaluation of hemp THC levels is necessary and possible. *J. Ind. Hemp* 2008, 13, 117–144, doi:10.1080/15377880802391142.

126. Salentijn, E. M. J.; Zhang, Q.; Amaducci, S.; Yang, M.; Trindade, L. M. New developments in fiber hemp (*Cannabis sativa* L.) breeding. *Ind. Crops Prod.* 2015, 68, 32–41, doi:10.1016/j.indcrop.2014.08.011.
127. Mandolino, G.; Carboni, A. Potential of marker-assisted selection in hemp genetic improvement. *Euphytica* 2004, 140, 107–120, doi:10.1007/s10681-004-4759-6.
128. Wielgus, K.; Szalata, M.; Słomski, R. 17 - Genetic engineering and biotechnology of natural textile fiber plants. In *Handbook of Natural Fibres*; Kozłowski, R. M., Ed.; Woodhead Publishing Series in Textiles; Woodhead Publishing, 2012; Vol. 1, pp. 550–575 ISBN 978-1-84569-697-9.
129. Foster, R.; Pooni, H. S.; Mackay, I. J. Quantitative analysis of *Linum usitatissimum* crosses for dual-purpose traits. *J. Agric. Sci.* 1998, 131, 285–292, doi:10.1017/S0021859698005917.
130. Helbaek, H. Domestication of food plants in the old world. *Science* (80-. ). 1959, 130, 365–372.
131. Razukas, A.; Jankauskiene, Z.; Jundulas, J.; Asakaviciute, R. Research of technical crops (potato and flax) genetic resources in Lithuania. *Agron. Res.* 2009, 7, 59–72.
132. GNIS Available online: <http://www.gnis.fr/> (accessed on Feb 20, 2018).
133. GEVES Available online: <https://www.geves.fr/> (accessed on Feb 20, 2018).
134. Plant variety database - European Commission Available online: <http://ec.europa.eu> (accessed on Feb 20, 2018).
135. Chevalier, A. Histoire de deux plantes cultivées d'importance primordiale. Le Lin et le Chanvre. *Rev. Bot. appliquée d'agriculture Colon.* 1944, 24e année, 51–71, doi:10.3406/jatba.1944.6107.
136. ARVALIS - Institut du végétal Lin fibre - Résultats et préconisations; Paris, 2016;
137. Billaux, P. Le lin au service des hommes: sa vie, ses techniques, son histoire; Baillière.; J.-B. Baillière, 1969;
138. Plonka, F.; Anselme, C. Les variétés de lin et leurs principales maladies cryptogamiques; Institut National de la Recherche Agronomique, Paris, 1956;
139. Eurostat Eurostat - Your key to European statistics Available online: <http://ec.europa.eu/eurostat/fr/web/agriculture/data/database> (accessed on Feb 14, 2018).
140. Montaigne, J. M. Images du lin textile: 8000 ans +2000 ans; ASI Editions, 1997; ISBN 9782912461001.
141. O'connor, B. J.; Gusta, L. V Effect of low temperature and seeding depth on the germination and emergence of seven flax (*Linum usitatissimum* L.) cultivars. *Can. J. plant Sci.* 1994, 74, 247–253.
142. Spielmeier, W.; Lagudah, E. S.; Mendham, N.; Green, A. G. Inheritance of resistance to flax wilt (*Fusarium oxysporum* f.sp. lini Schlecht) in a doubled haploid population of *Linum usitatissimum* L. *Euphytica* 1998, 101, 287–291, doi:10.1023/A:1018353011562.
143. Rashid, K.; Duguid, S. Inheritance of resistance to powdery mildew in flax. *Can. J. Plant Pathol.* 2005, 27, 404–409, doi:10.1080/07060660509507239.
144. Rashid, K. Y. Evaluation of components of partial resistance to rust in flax. *Can. J. Plant Pathol.* 1991, 13, 212–217, doi:10.1080/07060669109500932.
145. Wiersema, H. T. Flax scorch. *Euphytica* 1955, 4, 197–205, doi:10.1007/BF00037287.
146. Vera, C. L.; Duguid, S. D.; Fox, S. L.; Rashid, K. Y.; Dribnenki, J. C. P.; Clarke, F. R. Short Communication: Comparative effect of lodging on seed yield of flax and wheat. *Can. J. Plant Sci.* 2012, 92, 39–43, doi:10.4141/cjps2011-031.
147. Berry, P. M.; Sylvester-Bradley, R.; Berry, S. Ideotype design for lodging-resistant wheat. *Euphytica* 2007, 154, 165–179, doi:10.1007/s10681-006-9284-3.

148. Berry, P. M.; Sterling, M.; Mooney, S. J. Development of a model of lodging for barley. *J. Agron. Crop Sci.* 2006, 192, 151–158, doi:10.1111/j.1439-037X.2006.00194.x.
149. Muir, A. D.; Westcott, N. D. *Flax: the genus Linum*; D., N., Ed.; CRC Press, 2003;
150. Neenan, M.; Spencer-Smith, J. L. An analysis of the problem of lodging with particular reference to wheat and barley. *J. Agric. Sci.* 1975, 85, 495–507, doi:10.1017/S0021859600062377.
151. Berry, P. M.; Griffin, J. M.; Sylvester-Bradley, R.; Scott, R. K.; Spink, J. H.; Baker, C. J.; Clare, R. W. Controlling plant form through husbandry to minimise lodging in wheat. *F. Crop. Res.* 2000, 67, 59–81, doi:10.1016/S0378-4290(00)00084-8.
152. Brazier, L. G. On the flexure of thin cylindrical shells and other “thin” sections. *Proc. R. Soc. London. Ser. A, Contain. Pap. a Math. Phys. Character* 1927, 116, 104–114, doi:10.1098/rspa.1927.0125.
153. Berry, P. M.; Spink, J. H.; Gay, A. P.; Craigon, J. A comparison of root and stem lodging risks among winter wheat cultivars. *J. Agric. Sci.* 2003, 141, 191–202, doi:10.1017/S002185960300354X.
154. Berry, P. M.; Spink, J.; Sterling, M.; Pickett, A. A. Methods for rapidly measuring the lodging resistance of wheat cultivars. *J. Agron. Crop Sci.* 2003, 189, 390–401, doi:10.1046/j.0931-2250.2003.00062.x.
155. Berry, P. M.; Sterling, M.; Baker, C. J.; Spink, J.; Sparkes, D. L. A calibrated model of wheat lodging compared with field measurements. *Agric. For. Meteorol.* 2003, 119, 167–180.
156. McMahon, T. Size and shape in biology. Elastic criteria impose limits on biological proportions, and consequently on metabolic rates. *Science* (80). 1973, 179, 1201–1204, doi:10.1017/CBO9781107415324.004.
157. Greenhill, A. G. Determination of the greatest height consistent with stability that a vertical pole or mast can be made, and the greatest height to which a tree of given proportions can grow. *Proc. Camb. Philol. Soc.* 1881, 4, 65–73.
158. Niklas, K. J. The influence of gravity and wind on land plant evolution. *Rev. Palaeobot. Palynol.* 1998, 102, 1–14, doi:10.1016/S0034-6667(98)00011-6.
159. Jaouen, G.; Alméras, T.; Coutand, C.; Fournier, M. How to determine sapling buckling risk with only few measurements. *Am. J. Bot.* 2007, 94, 1583–1593.
160. Holbrook, N. M.; Putz, F. E. Influence of neighbors on tree form: effects of lateral shade and prevention of sway on the allometry of *Liquidambar Styraciflua* (sweet gum). *Am. J. Bot.* 1989, 76, 1740–1749, doi:10.1002/j.1537-2197.1989.tb15164.x.
161. Niklas, K. J. Influence of tissue density-specific mechanical properties on the scaling of plant height. *Ann. Bot.* 1993, 72, 173–179, doi:10.1006/anbo.1993.1096.
162. Ford, M. A.; Blackwell, R. D.; Parker, M. L.; Austin, R. B. Associations between stem solidity, soluble carbohydrate accumulation and other characters in wheat. *Ann. Bot.* 1979, 44, 731–738.
163. Leblicq, T.; Vanmaercke, S.; Ramon, H.; Saeys, W. Mechanical analysis of the bending behaviour of plant stems. *Biosyst. Eng.* 2015, 129, 87–99, doi:10.1016/j.biosystemseng.2014.09.016.
164. Gardiner, B.; Berry, P.; Moulia, B. Review: Wind impacts on plant growth, mechanics and damage. *Plant Sci.* 2016, 245, 94–118, doi:10.1016/j.plantsci.2016.01.006.
165. Menoux, Y.; Katz, E.; Eyssautier, A.; Parcevaux, D.; Robinet, L.; Durand, B.; Gleo, M. Le; Menoux, Y.; Katz, E.; Eyssautier, A.; Parcevaux, D.; Sainte-beuve, D.; Katz, E. Résistance à la verse du lin textile: influence du milieu et critères de sélection proposés. *Agronomie* 1982, 2, 173–180.
166. Lawton, R. O. Ecological constraints on wood density in a tropical montane rain forest. *Am. J. Bot.* 1984, 71, 261, doi:10.2307/2443754.

167. Easson, D. L.; Long, F. N. J. The effect of time of sowing, seed rate and nitrogen level on the fibre yield and quality of flax (*Linum usitatissimum* L.). *Irish J. Agric. Food Res.* 1992, 31, 163–172.
168. Dimmock, J. P. R. E.; Bennet, S. J.; Wright, D.; Edwards-Jones, G.; Harris, I. M. Agronomic evaluation and performance of flax varieties for industrial fibre production. *J. Agric. Sci.* 2005, 143, 299–309, doi:10.1017/S0021859605005277.
169. Hoffmann, G. Use of plant growth regulators in arable crops: Survey and outlook. In *Progress in Plant Growth Regulation. Current Plant Science and Biotechnology in Agriculture*; Karssen, C. M., van Loon, L. C., Vreugdenhil, D., Eds.; Springer Netherlands: Dordrecht, 1992; Vol. 13, pp. 798–808 ISBN 978-94-011-2458-4.
170. Sieben, J. W. W. The correlation between resistance to lodging and fibre content in flax. *Euphytica* 1953, 2, 101–106, doi:10.1007/BF00038908.
171. Dorst, J. C. Does the present trend to select for resistance to lodging in flax involve dangers of a loss in quality? *Euphytica* 1953, 2, 96–100.
172. Bourmaud, A.; Gibaud, M.; Lefeuvre, A.; Morvan, C.; Baley, C. Influence of the morphology characters of the stem on the lodging resistance of Marilyn flax. *Ind. Crops Prod.* 2015, 66, 27–37, doi:10.1016/j.indcrop.2014.11.047.
173. Jaffe, M. J. Thigmomorphogenesis : The response of plant growth and development to mechanical stimulation. *Planta* 1973, 114, 143–157, doi:10.1007/BF00387472.
174. Grace, J.; Russell, G. The effect of wind on grasses. *J. Exp. Bot.* 1977, 28, 268–278, doi:http://dx.doi.org/10.1016/0378-7788(77)90014-7.
175. Biddington, N. L. The effects of mechanically-induced stress in plants - a review. *Plant Growth Regul.* 1986, 4, 103–123, doi:10.1007/BF00025193.
176. Biging, G. S.; Dobbertin, M. Evaluation of competition Indices in individual tree growth models. *For. Sci.* 1995, 41, 360–377, doi:10.1093/forestscience/41.2.360.
177. von Oheimb, G.; Lang, A. C.; Bruelheide, H.; Forrester, D. I.; Wäsche, I.; Yu, M.; Härdtle, W. Individual-tree radial growth in a subtropical broad-leaved forest: The role of local neighbourhood competition. *For. Ecol. Manage.* 2011, 261, 499–507, doi:10.1016/j.foreco.2010.10.035.
178. Moulia, B.; Der Loughian, C.; Bastien, R.; Martin, O.; Rodríguez, M.; Gourcilleau, D.; Barbacci, A.; Badel, E.; Franchel, G.; Lenne, C.; Roeckel-Drevet, P.; Allain, J. M.; Frachisse, J. M.; de Langre, E.; Coutand, C.; Fournier-Leblanc, N.; Julien, J. L. Integrative mechanobiology of growth and architectural development in changing mechanical environments. In *Mechanical Integration of Plant Cells and Plants*; Wojtaszek, P., Ed.; Springer Berlin Heidelberg: Berlin, Heidelberg, 2011; pp. 269–302 ISBN 978-3-642-19091-9.
179. Stevenson, F. C.; Wright, A. T. Seeding rate and row spacing affect flax yields and weed interference. *Can. J. Plant Sci.* 1996, 76, 537–544, doi:10.4141/cjps96-098.
180. Couture, S. J.; DiTommaso, A.; Asbil, W. L.; Watson, A. K. Influence of seeding depth and seedbed preparation on establishment, growth and yield of fibre flax (*Linum usitatissimum* L.) in Eastern Canada. *J. Agron. Crop Sci.* 2004, 190, 184–190, doi:10.1111/j.1439-037X.2004.00091.x.
181. Couture, S. J.; DiTommaso, A.; Asbil, W. L.; Watson, A. K. Evaluation of fibre flax (*Linum usitatissimum* L.) performance under minimal and zero tillage in Eastern Canada. *J. Agron. Crop Sci.* 2004, 190, 191–196, doi:10.1111/j.1439-037X.2004.00092.x.
182. Fowler, N. L. The role of germination date, spatial arrangement, and neighbourhood effects in competitive interactions in *Linum*. *J. Ecol.* 1984, 72, 307–318, doi:10.2307/2260023.
183. Gubbels, G. H.; Kenaschuk, E. O. Effect of seeding rate on plant and seed characteristics of new flax cultivars. *Can. J. Plant Sci.* 1989, 69, 791–795, doi:10.4141/cjps89-094.
184. Casa, R.; Russell, G.; Lo Cascio, B.; Rossini, F. Environmental effects on linseed (*Linum usitatissimum* L.) yield and growth of flax at different stand densities. *Eur. J. Agron.* 1999, 11, 267–278, doi:10.1016/S1161-0301(99)00037-4.

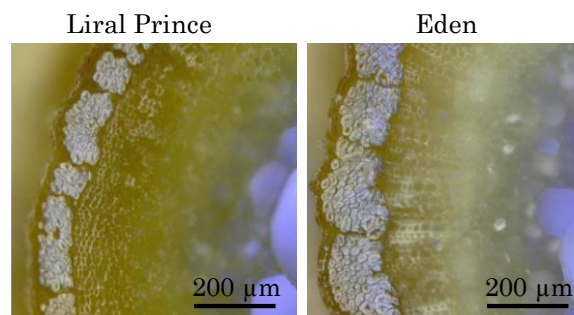
185. Lafond, G. P.; Boyetchko, S. M.; Brandt, S. A.; Clayton, G. W.; Entz, M. H. Influence of changing tillage practices on crop production. *Can. J. Plant Sci.* 1996, 76, 641–649, doi:10.4141/cjps96-114.
186. Raupach, M. R.; Finnigan, J. J.; Brunet, Y. Coherent eddies and turbulence in vegetation canopies: The mixing-layer analogy. In *Boundary-Layer Meteorology 25th Anniversary Volume, 1970–1995*; Springer Netherlands: Dordrecht, 1996; pp. 351–382.
187. Inoue, E. Studies of the phenomena of waving plants ('honami') caused by wind. *J. Agric. Meteorol.* 1955, 11, 87–90.
188. Finnigan, J. J. Turbulence in waving wheat: I. Mean statistics and honami. *Boundary-Layer Meteorol.* 1979, 16, 181–211, doi:10.1007/BF03335366.
189. Finnigan, J. Turbulence in plant canopies. *Annu. Rev. Fluid Mech.* 2000, 32, 519–571.
190. Farquhar, T.; Zhou, J.; Haslach, H. W. A possible mechanism for sensing crop canopy ventilation. In *Sensors and Sensing in Biology and Engineering*; Barth, F. G., Humphrey, J. A. C., Secomb, T. W., Eds.; Springer: Vienna, 2003; pp. 213–219 ISBN 978-3-7091-6025-1.
191. de Langre, E. Effects of wind on plants. *Annu. Rev. Fluid Mech.* 2008, 40, 141–168, doi:10.1146/annurev.fluid.40.111406.102135.
192. Doaré, O.; Moulia, B.; de Langre, E. Effect of plant interaction on wind-induced crop motion. *J. Biomech. Eng.* 2004, 126, 146–151, doi:10.1115/1.1688773.
193. Py, C.; De Langre, E.; Moulia, B. A frequency lock-in mechanism in the interaction between wind and crop canopies. *J. Fluid Mech.* 2006, 568, 425, doi:10.1017/S0022112006002667.
194. Moulia, B. Plant biomechanics and mechanobiology are convergent paths to flourishing interdisciplinary research. *J. Exp. Bot.* 2013, 64, 4617–4633, doi:10.1093/jxb/ert320.
195. Hart, J. W. *Plant tropisms and other growth movements*; Springer Science & Business Media, 1990;
196. Mitchell, C. Seismomorphogenic regulation of plant growth. *J. Am. Soc. Hortic. Sci.* 1975, 100, 161–165.
197. Coutand, C. Mechanosensing and thigmomorphogenesis, a physiological and biomechanical point of view. *Plant Sci.* 2010, 179, 168–182, doi:10.1016/j.plantsci.2010.05.001.
198. Moulia, B.; Coutand, C.; Julien, J.-L. Mechanosensitive control of plant growth : bearing the load, sensing, transducing, and responding. *Front. Plant Sci.* 2015, 6, 1–20.
199. Hamant, O. Widespread mechanosensing controls the structure behind the architecture in plants. *Curr. Opin. Plant Biol.* 2013, 16, 654–660, doi:10.1016/j.pbi.2013.06.006.
200. Niklas, K. J. Differences between *Acer saccharum* leaves from open and wind-protected sites. *Ann. Bot.* 1996, 78, 61–66, doi:0305-7364.
201. Moulia, B.; Combes, D. Thigmomorphogenetic acclimation of plants to moderate winds greatly affects height structure in field-grown alfalfa (*medicago sativa* l.), an indeterminate herb. *Comp. Biochem. Physiol. Part A Mol. Integr. Physiol.* 2004, 137, 8.
202. Badel, E.; Ewers, F. W.; Cochard, H.; Telewski, F. W. Acclimation of mechanical and hydraulic functions in trees: impact of the thigmomorphogenetic process. *Front. Plant Sci.* 2015, 6, 1–12, doi:10.3389/fpls.2015.00266.
203. Crook, M.; Ennos, R. Mechanical differences between free-standing and supported wheat plants, *Triticum aestivum* L. *Ann. Bot.* 1996, 77, 197–202, doi:10.1006/anbo.1996.0023.
204. Paul-Victor, C.; Rowe, N. Effect of mechanical perturbation on the biomechanics, primary growth and secondary tissue development of inflorescence stems of *Arabidopsis thaliana*. *Ann. Bot.* 2011, 107, 209–218, doi:10.1093/aob/mcq227.

205. Goodman, A. M.; Ennos, A. R. A comparative study of the response of the roots and shoots of sunflower and maize to mechanical stimulation. *J. Exp. Bot.* 1996, 47, 1499–1507.
206. Smith, V. C.; Ennos, A. R. The effects of air flow and stem flexure on the mechanical and hydraulic properties of the stems of sunflowers *Helianthus annuus* L. *J. Exp. Bot.* 2003, 54, 845–849.
207. Cordero, R. A. Ecophysiology of *Cecropia schreberiana* saplings in two wind regimes in an elfin cloud forest: Growth, gas exchange, architecture and stem biomechanics. *Tree Physiol.* 1999, 19, 153–163, doi:10.1093/treephys/19.3.153.
208. Jaffe, M. J.; Forbes, S. Thigmomorphogenesis: the effect of mechanical perturbation on plants. *Plant Growth Regul.* 1993, 12, 313–324, doi:10.1007/BF00027213.
209. Jaffe, M. J.; Telewski, F. W.; Cooke, P. W. Thigmomorphogenesis: On the mechanical properties of mechanically perturbed bean plants. *Physiol. Plant.* 1984, 62, 73–78.
210. Coutand, C.; Julien, J. L.; Moulia, B.; Mauget, J. C.; Guitard, D. Biomechanical study of the effect of a controlled bending on tomato stem elongation: global mechanical analysis. *J. Exp. Bot.* 2000, 51, 1813–24, doi:10.1093/jexbot/51.352.1813.
211. Telewski, F. W.; Jaffe, M. J. Thigmomorphogenesis: Anatomical, morphological and mechanical analysis of genetically different sibs of *Pinus taeda* in response to mechanical perturbation. *Physiol. Plant.* 1986, 66, 219–226, doi:10.1111/j.1399-3054.1986.tb02412.x.
212. Lachenbruch, B.; Mcculloh, K. A. Traits, properties, and performance: How woody plants combine hydraulic and mechanical functions in a cell, tissue, or whole plant. *New Phytol.* 2014, 204, 747–764, doi:10.1111/nph.13035.
213. Jaffe, M. J.; Telewski, F. W. Thigmomorphogenesis: callose and ethylene in the hardening of mechanically stressed plants. In *Phytochemical Adaptations to Stress*; Timmermann, B. N., Steelink, C., Loewus, F. A., Eds.; Springer US: Boston, MA, 1984; pp. 79–95 ISBN 978-1-4684-1206-2.
214. Chen, R.; Rosen, E.; Masson, P. H. Gravitropism in higher plants. *Plant Physiol.* 1999, 120, 343–350, doi:10.1104/pp.120.2.343.
215. Chauvet, H.; Pouliquen, O.; Forterre, Y.; Legué, V.; Moulia, B. Inclination not force is sensed by plants during shoot gravitropism. *Sci. Rep.* 2016, 6, 35431, doi:10.1038/srep35431.
216. Gerttula, S.; Zinkgraf, M.; Muday, G. K.; Lewis, D. R.; Ibatullin, F. M.; Brumer, H.; Hart, F.; Mansfield, S. D.; Filkov, V.; Groover, A. Transcriptional and hormonal regulation of gravitropism of woody stems in populus. *Plant Cell* 2015, 27, 2800–2813, doi:10.1105/tpc.15.00531.
217. Bastien, R.; Bohr, T.; Moulia, B.; Douady, S. Unifying model of shoot gravitropism reveals proprioception as a central feature of posture control in plants. *Proc. Natl. Acad. Sci.* 2013, 110, 755–760, doi:10.1073/pnas.1214301109.
218. Muday, G. K. Auxins and tropisms. *J. Plant Growth Regul.* 2001, 20, 226–243.
219. Coutand, C.; Fournier, M.; Moulia, B. The gravitropic response of poplar trunks: Key roles of prestressed wood regulation and the relative kinetics of cambial growth versus wood maturation. *Plant Physiol.* 2007, 144, 1166–1180, doi:10.1104/pp.106.088153.
220. Sack, F. D. Plastids and gravitropic sensing. *Planta* 1997, 203, S63–S68, doi:10.1007/PL00008116.
221. Hoson, T.; Saito, Y.; Soga, K.; Wakabayashi, K. Signal perception, transduction, and response in gravity resistance. Another graviresponse in plants. *Adv. Sp. Res.* 2005, 36, 1196–1202.
222. Fukaki, H.; Wysocka-Diller, J.; Kato, T.; Fujisawa, H.; Benfey, P. N.; Tasaka, M. Genetic evidence that the endodermis is essential for shoot gravitropism in *Arabidopsis thaliana*. *Plant J.* 1998, 14, 425–430, doi:10.1046/j.1365-313X.1998.00137.x.
223. Morita, M. T. Directional gravity sensing in gravitropism. *Annu. Rev. Plant Biol.* 2010, 61, 705–720, doi:10.1146/annurev.arplant.043008.092042.

224. Andersson-Gunnerås, S.; Hellgren, J. M.; Björklund, S.; Regan, S.; Moritz, T.; Sundberg, B. Asymmetric expression of a poplar ACC oxidase controls ethylene production during gravitational induction of tension wood. *Plant J.* 2003, 34, 339–349, doi:10.1046/j.1365-313X.2003.01727.x.
225. Mauriat, M.; Moritz, T. Analyses of GA20ox- and GID1-over-expressing aspen suggest that gibberellins play two distinct roles in wood formation. *Plant J.* 2009, 58, 989–1003.
226. Cosgrove, D. J. Cellular mechanisms underlying growth asymmetry during stem gravitropism. *Planta* 1997, 203, S130–S135, doi:10.1007/PL00008101.
227. Went, F. W. Reflections and speculations; Annual Reviews 4139 El Camino Way, PO Box 10139, Palo Alto, CA 94303-0139, USA, 1974; Vol. 25;.
228. Alméras, T.; Fournier, M. Biomechanical design and long-term stability of trees: Morphological and wood traits involved in the balance between weight increase and the gravitropic reaction. *J. Theor. Biol.* 2009, 256, 370–381, doi:10.1016/j.jtbi.2008.10.011.
229. Clair, B.; Gril, J.; Baba, K.; Thibaut, B.; Sugiyama, J. Precautions for the structural analysis of the gelatinous layer in tension wood. *IAWA J.* 2005, 26, 189–195.
230. Forest, L.; Padilla, F.; Martínez, S.; Demongeot, J.; San Martín, J. Modelling of auxin transport affected by gravity and differential radial growth. *J. Theor. Biol.* 2006, 241, 241–251.
231. Kennedy, R. W.; Farrar, J. L. Induction of tension wood with the antiauxin 2,3,5-tri-iodobenzoic acid. *Nature* 1965, 208, 406.
232. Fisher, J. B.; Stevenson, J. W. Occurrence of reaction wood in branches of dicotyledons and its role in tree architecture. *Bot. Gaz.* 1981, 142, 82–95, doi:10.1086/337199.
233. Fang, C. H.; Clair, B.; Gril, J.; Liu, S. Q. Growth stresses are highly controlled by the amount of G-layer in poplar tension wood. *IAWA J.* 2008, 29, 237–246, doi:10.1163/22941932-90000183.
234. Lafarguette, F.; Leplé, J. C.; Déjardin, A.; Laurans, F.; Costa, G.; Lesage-Descauses, M. C.; Pilate, G. Poplar genes encoding fasciclin-like arabinogalactan proteins are highly expressed in tension wood. *New Phytol.* 2004, 164, 107–121, doi:10.1111/j.1469-8137.2004.01175.x.
235. Chang, S. S.; Salmén, L.; Olsson, A. M.; Clair, B. Deposition and organisation of cell wall polymers during maturation of poplar tension wood by FTIR microspectroscopy. *Planta* 2014, 239, 243–254.
236. Clair, B.; Alméras, T.; Sugiyama, J. Compression stress in opposite wood of angiosperms: observations in chestnut, mani and poplar. *Ann. For. Sci.* 2006, 63, 507–510.
237. Alméras, T.; Clair, B. Critical review on the mechanisms of maturation stress generation in trees. *J. R. Soc. Interface* 2016, 13, 20160550, doi:10.1098/rsif.2016.0550.
238. Wyatt, S. E.; Sederoff, R.; Flaishman, M. A.; Lev-Yadun, S. *Arabidopsis thaliana* as a model for gelatinous fiber formation. *Russ. J. Plant Physiol.* 2010, 57, 363–367.
239. Patten, A. M.; Jourdes, M.; Brown, E. E.; Laborie, M.-P.; Davin, L. B.; Lewis, N. G. Reaction tissue formation and stem tensile modulus properties in wild-type and p-coumarate-3-hydroxylase downregulated lines of alfalfa, *Medicago sativa* (Fabaceae). *Am. J. Bot.* 2007, 94, 912–925.

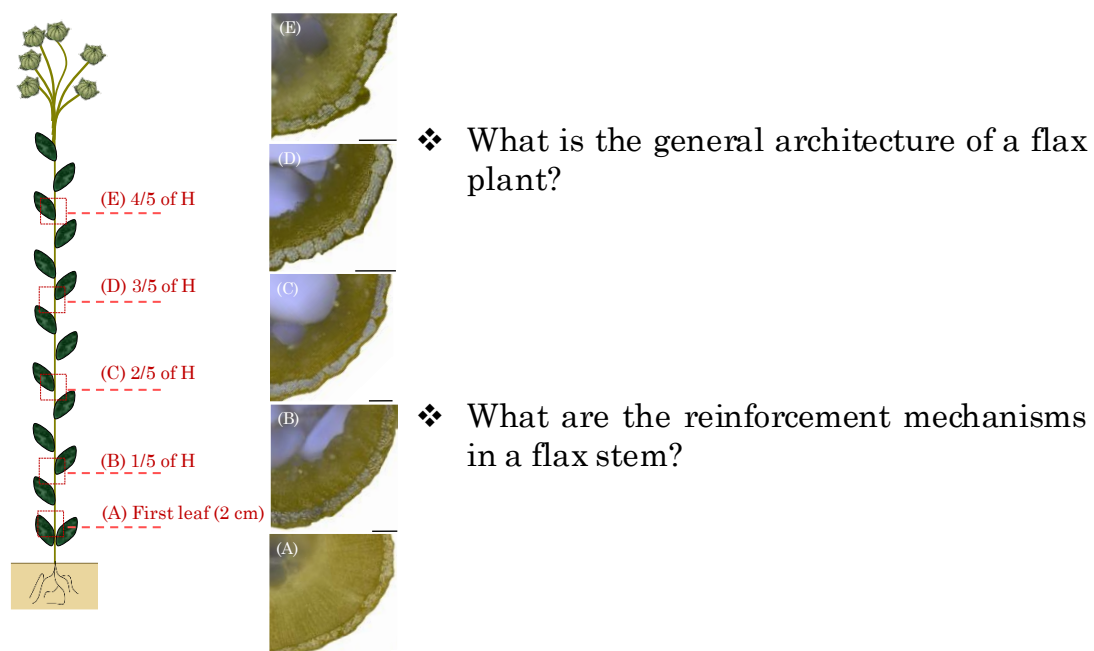
**CHAPTER II –  
FLAX – FROM THE STEM TO THE FIBER**

## Graphical abstract



- ❖ What is the impact of the varietal selection of flax on plant architecture and fiber mechanical properties?

**Goudenhooff, C.;** Bourmaud, A.; Baley, C. Varietal selection of flax over time: Evolution of plant architecture related to influence on the mechanical properties of fibers. *Ind. Crops Prod.* **2017**, *97*, 56–64, doi:10.1016/j.indcrop.2016.11.062.



Baley, C.; **Goudenhooff, C.;** Gibaud, M.; Bourmaud, A. Flax stems: from a specific architecture to an instructive model for bioinspired composite structures. *Bioinspir. Biomim.* **2018**, *13*, 26007, doi:10.1088/1748-3190/aaa6b7.

## CHAPTER II – FLAX – FROM THE STEM TO THE FIBER

---

The use of flax-based biocomposite materials is greatly increasing. However, it is necessary to study the properties of the fibers as well as the structure of the plants themselves, in view of optimizing composite performances and benefit at best of the great mechanical potential of flax fibers. The present chapter aims at providing a broad understanding of flax architecture, from its stem to its fibers. In a first step, an investigation of the impact of varietal selection on the properties of the resulting plants and fibers is proposed. Secondly, the structure and reinforcement mechanisms of individual flax stems, considered as a natural composite, are explored. Finally, the results are compared with manmade fibers as well as stacking reinforcements by synthetic fibers to highlight the potential of flax fibers for composite manufacturing and flax stems as a model for bioinspired materials.

### 1. Introduction

#### 1.1. History of the varietal selection of flax

Flax (*Linum usitatissimum* L.) has been cultivated for several centuries in line with two different orientations: oleaginous flax (yielding linseed oil) and fiber flax (also called textile flax). In the case of fiber flax, the plant was originally harvested to extract fibers used to produce clothing or domestic textiles. The particular interest in fiber flax (referred as ‘flax’ in the rest of the work) cultivation is also explained by the various advantages of its fibers. First, fiber flax is widely cultivated in Europe, and especially in France with 80% of the production being located in the coastal zone of this country. It is therefore possible to offer fibers locally, which could then provide future industrial products. Moreover, many actors are involved in this domain: varietal selection, farmers with a real know-how, specialists in fiber extraction and marketing, manufacturers of specific machinery (seeders, harvesters, turner binders, machines for scutching, combing and carding, etc.).

New varieties have been developed and selected by breeders during the last century. For instance, in Eastern Europe, fiber flax breeding started in 1922 in Lithuania with two varieties, namely ‘Dotnuvos pluotiniai’ and ‘Dotnuvos ilguneliai I’ [1]. Meanwhile, in Western Europe, the flax variety ‘Concurrent’ was selected in 1921 by one of the several Dutch agricultural experiment stations (Leeuwarden) [2]. ‘Concurrent’ was

used as a reference until the 1950s [3], when a new selected variety was shown to be superior [4]. The varietal selection, whatever its origin, has always been undertaken to increase the fiber production yield [1], the resistance against diseases [5] as well as the lodging stability [6]. In this way, cultivated flax varieties have evolved over time and have been selected, among other purposes, with the aim of increasing the biomass. Figure II-1 gives averages regarding fiber flax culture over the past decades in France based on several sets of data found in the literature and from personal communication.

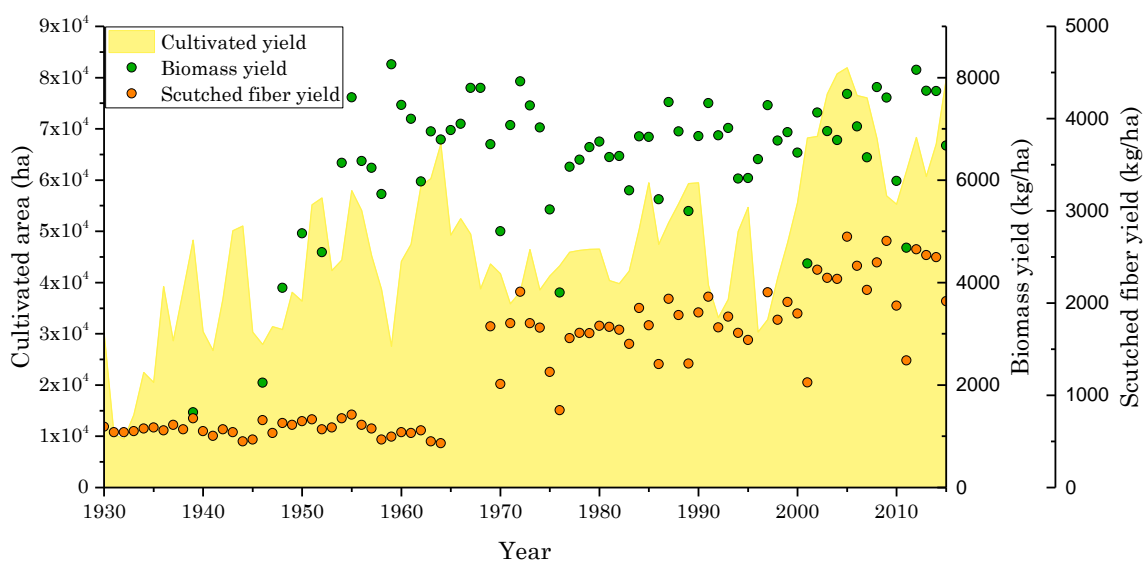


**Figure II-1. Evolution of cultivated area, biomass yield and scutched fiber yield of textile flax from 1935 to 2015 in France [2,4,7].**

From this figure, it appears that flax culture has been on the increase since the 1930s overall. This is combined with a pronounced rise of fiber yields, while straw yields remain generally stable. Although fluctuations can be seen over time (mostly attributed to severe weather conditions) and a great isolated increase of the scutched fiber yield in the 60s (attributed to the mechanization of cultural and fiber extraction methods), the tendency toward improved results is very encouraging in terms of quantities required for composite manufacturing.

## 1.2. Flax: from the plants to composites reinforced by flax fibers

‘Fiber’ is a term used by many researchers referring to natural fibers in composites. However, ‘fiber’ (or ‘fibre’ in British usage) has a strict botanical meaning, designating a single elongated thick-walled plant cell. In-vivo, the plant fiber function may be mechanical and/or conductive (conduction of crude sap or elaborated sap). Vincent [8] proposes a unified nomenclature for plant fibers for use in industry. In the case of flax,

the fibers used for textile and composite applications have a supporting function in the plant [9].

While many plants provide fibers, flax is particularly used as a reinforcement for composite materials, owing to its fibers high-performance mechanical properties, low density (about 1.5) and natural origin to reduce environmental impacts [10]. The good properties of adherence with polymer matrices [11] and recycling possibilities [12,13] make flax fibers even more interesting. In addition, elementary flax fibers can be considered as very long, reaching 25 mm in average [14]. They have an average fiber diameter ( $16.8 \pm 2.7 \mu\text{m}$ ), which is close to E glass fibers (conventionally used for polymer reinforcement), showing good mechanical properties under tension [15]. Indeed, it is currently possible to guarantee reproducible specific mechanical properties able to compete and substitute glass fibers in composite parts [15]. In Europe, the automotive industry is the main consumer of biocomposites (polymer reinforced by plant fibers). The main drivers for the use of natural-fiber-based composites in automotive applications are the demands for lightweight parts, which leads to a lowering of fuel consumption and good recycling possibilities, reducing the waste disposal problem [16]. In addition, biocomposites are used for structural applications in other fields such as sports and leisure, furniture manufacture and lute making [17].

The use of flax fibers as reinforcement is not a recent innovation. Indeed, in 1937, de Bruyne developed Gordon Aerolite, a composite made of flax roving impregnated with a phenolic resin matrix (Bakelite). This material was used for aircraft applications during the Second World War [18,19]. Based on an inverse method, a Young's modulus of about 60 GPa can be estimated for the flax fibers used in Bakelite, which already show good mechanical performances for the period in question.

However, these good average mechanical properties of flax fibers are favorable but not sufficient for industrial applications. Indeed, given their agricultural origin and structure, flax fibers exhibit disparate properties and complex behavior. The tensile behavior of elementary flax fibers should be borne in mind, since it greatly influences the behavior of the plies in composite materials. Plant fibers generally show a non-linear tensile behavior, contrary to ceramic, glass or carbon fibers. In fact, a single plant fiber is analogous to superposed plies reinforced by cellulose fibrils. The microfibrils are helically arranged and oriented at a determined angle. During a tensile test, the fiber behavior depends not only on its components, but is also

influenced by two mechanisms: the partial reorientation of cellulose fibrils toward the load axis and the sliding of these micro-fibrils along each other [20]. As a consequence, the tensile behavior is not perfectly linear-elastic, and the reorientation of the microfibrils toward the tensile axis leads to an increase in Young's modulus of the fiber during the test [20].

If the overall mechanical performances and behavior of flax fibers is well referenced, little attention has been focused on the selection of flax varieties producing fibers with high mechanical performances. Recent studies have demonstrated that the performances of final composites could be linked to the mechanical properties of the fibers [21,22]. Moreover, mechanical studies combined with biochemical analyses have shown that the performances of flax fibers could be related to their composition [23]. Additionally, since these same authors showed that varieties could lead to different fiber compositions, the flax variety could play a key role in affecting the performances of both flax fibers and their composites. From now on, breeders need to pay attention to the criteria of mechanical properties, especially if, as predicted, the use of scutched flax fibers continues to expand for the industrialization of composites.

### **1.3. A plant as an interesting structure and source of bioinspiration**

Using plant fibers in the field of materials science brings us toward a change of mind-set about plants. In fact, plants are natural high-performance structures. First, the plant properties are dictated by their growth, composition and structure, as well as environmental constraints/conditions and the limited availability of materials. Moreover, stems are organized at several different levels (from nano- to ultra-scale).

Secondly, living plants react to stress. They possess a self-healing capacity, as well as the ability to maintain a vertical position (*i.e.* gravitropism) and adapt to mechanical stimulation (*e.g.* thigmomorphogenesis)[24]. In nature, these growth patterns can develop as a response to wind, raindrops, and rubbing by passing animals. In addition, most industrial structures are designed to be rigid, especially to limit the risks of instability and displacement. However, the contrary is often found in natural structures, particularly in the case of plants subject to high abiotic stresses such as aerodynamic loads [25]. Plants are relatively flexible, minimizing the effects of aerodynamic loads through large-amplitude deformation. In the context of a flax field, the term “crop canopy” can be used to define a homogeneous group of plants whose crowns are closed or even touching, forming a dense plant layer. From a mechanical

point of view, a crop canopy can be modelled as a continuous vibratory porous medium [25], providing an example of fluid structure interactions. For instance, the behavior of a crop canopy under wind forcing has been explored in different modelling studies [25]. The plant density in the field (*i.e.* the number of plants per square meter) is an important agricultural parameter as it influences plant yield and height, as well as the mechanical properties and lodging resistance of the fibers [9]. For flax, the best compromise is obtained with 1500 to 1800 plants per square meter. Under these conditions, the plant yields a single stem with a moderate inflorescence and optimizes its shape to capture light while depending on a limited amount of resources [9].

Thus, the internal structure of plants is a bioinspiration for the design of new structures. As an illustration, we can cite two examples in nature. As a first example, a foam-like cellular core supports thin-walled cylindrical structures, as seen in the case of grass stems [26]. This architecture increases the buckling resistance of a cylindrical shell compared to a hollow cylinder of same weight [26]. This principle is transferable to engineering structures, such as space shuttle fuel tanks, aircraft fuselages and offshore oil platforms [26]. In the second example, horsetail (*Equisetum hyemale*) and giant reed (*Arundo donax*) are used as templates for the construction of ultra-lightweight technical structures with an interesting combination of mechanical properties (very high stiffness with excellent damping qualities and a benign fracture behavior) [27]. By mimicking the architecture of these stems, Millwich et al. [27] have made high-performing structures in composite materials (pultrusion and braiding technique).

This chapter investigates the impact of varietal selection on the properties of the resulting plants and fibers. In this way, an architectural analysis of plants derived from several varieties is first presented. The comparison of four varieties selected over time, between the 1940s and 2011, is performed. Secondly, the mechanical properties of elementary fibers are determined, using conventional tensile tests to evaluate eventual changes in performance between the four studied varieties. Then, an analysis of overall flax stem architecture, which can be view as a composite structure with an outer protection, a unidirectional ply on the periphery and a porous core, is performed.

## 2. Materials and methods

### 2.1. Plant materials

Regarding the study about the impact of varietal selection, samples were provided from Terre De Lin, an agricultural cooperative based in Normandy (France). Four flax varieties were studied: two old varieties that are no longer registered and two currently used varieties. The old varieties chosen here are Liral Prince and Ariane. Liral Prince derives from a selection by the Linen Industry Research Association (L.I.R.A, Ireland) in the 1940s (the exact year is unknown but is assumed to be 1944 [4]). Ariane was registered in 1978 by the Coopérative Linière de Fontaine Cany (France). These two old varieties were specifically studied as they were largely cultivated with high fiber yields during their respective times (Terre De Lin, personal communication). The recent varieties are Eden (registered since 2009) and Aramis (registered since 2011) selected by Terre De Lin. Eden and Aramis were chosen among others as they give a good compromise regarding productivity, lodging stability and disease resistance. Moreover, they are among the most cultivated varieties during the past few years [7]. Flax plants were all cultivated in France (Saint-Pierre le Viger, Normandy) in 2015. Similar conventional seeding densities were used (Bert, 2013) under identical sowing conditions (same soil and same fertilization treatments). These identical cultivation parameters allow us to draw comparisons in the present study. Moreover, in 2015, the weather conditions could be considered as normal [28]. The plants were pulled out at maturity, when the accumulated temperature received by the plants reaches between 950 and 1100°C (Bert, 2013). The accumulated temperature has been used for years by farmers to estimate the development and the harvesting time of flax. The formula used to calculate this parameter is given by Equation I-1.

Some of the plants (called green stems) were sampled at this step for architectural analyses. These stems were then stored in hermetic bags and placed in a freezer until the beginning of the tests. The rest of the stems were dew retted on cultivation soils for about six weeks. This natural process facilitates the fiber individualization thanks to the action of microorganisms, rain and light. After this step, a mechanical scutching was performed. Firstly, flax stems are crushed by fluted rollers and then occurs a beating step from the bottom to the top of the straw to completely separate the fibers

and the shives. Elementary fibers can finally be manually extracted from scutched technical fibers for mechanical tests.

Regarding the overall plant architecture, studied plant material consists of stems and fibers from a batch of Marylin, a currently commonly grown variety having an intermediate date of registration (registered in 1998 in Landbouwbureau Wiersum, a Dutch breeding company), grown in 2012. Only mature plants are studied here: they were pulled up after flowering and filling of the seed cap. The plant maturity is checked using the sum-of-temperatures criterion (Equation I-1). Non-retted flax stems from the same batch are also used for morphological studies. The CTLN Company (Le Neubourg, France) provided the fiber bundles, which were dew-retted and scutched.

## 2.2. Architectural analysis of the stems

The architectural analysis was performed by adapting the method described in a previous study [6]. First, morphological characteristics of stems were evaluated by determining heights of the stems (from the bottom of the stem to the first floral ramification, named “technical height”, and from the bottom of the stem to the top of stem, named “total height”), using a measuring tape and the diameter along the stems was measured using a caliper. Then, for the anatomical analysis of plants, stem samples were either taken at middle height of the technical height for the varietal selection study, or all along the technical stem for the overall architecture study. To facilitate the cut, the samples were immersed in a mixture of 50/50-water/ethanol for at least 12h, prior being embedded in elder marrow. Histological sections were cut transversally from embedded samples with a razor blade, using a hand microtome to clamp and guide the samples. The resulting sections were observed through a microscope (Olympus AX70) and pictures were taken with an Olympus DP25 camera. Although the pictures are locally blurred due to small variations in sample thickness, they are sufficiently clear to be used as a basis for the analysis as well as for identifying the main biological tissues described in Figure I-2. First, the outline of each fiber for each sample is manually drawn using Gimp®. Then, the number of fibers per section and their surface-area are automatically evaluated using ImageJ®. Average diameter of elementary fibers can be calculated by assuming circular fiber sections, even though this calculation is known to be approximate [29]. Other anatomical parameters can be based on the same approach. Namely, the parameters selected for the analysis are the tissue content, the fiber content and the number of fibers per section at a given stem height.

### 2.3. Measurement of single fiber length and diameter

This protocol is inspired from [30]. According to the literature, there are about 10,000 and 40,000 fibers in a flax stem [30]. In the present study, a description of the general structure is given rather than a precise statistical analysis. Taking into account the difficulty of manipulation, we tested from 26 to 50 fibers per extraction area. Firstly, a flax roving was extracted from a batch of scutched fibers, choosing a length of about 150 mm to be sure to include whole fibers. To facilitate separation, the fibers were placed in a mixture of 10% CrO<sub>3</sub> and 10% HNO<sub>3</sub> for about 4h under slow magnetic stirring to avoid damage [30]. Then, fibers were then manually separated using tweezers. Each fiber was observed under the microscope to check its integrity and the presence of pointed ends. Finally, the diameter was measured at regular intervals (about 100 μm between 2 measurements) along the fiber with a Leica optical microscope (x20 magnification); the fiber is assumed to be cylindrical.

### 2.4. 3D reconstruction of a fiber bundle

To analyze and reconstruct the architecture of a bundle in an area including the end of a single fiber, successive cuts were performed across the bundle. In a first step, an epoxy unidirectional composite was molded, reinforced by a few bundles. Then, the composite cross-section was machined and polished; one embedded bundle was selected and observed by optical microscopy, and the different fibers were outlined from the image. Then, the sample was polished again and the successive operations repeated several times on the same bundle to obtain a virtual scan of its cross-section including at least one fiber end. The distance between two cuts was measured precisely by measuring the length of the sample with the aim of obtaining 100 μm between each polishing step. From sections observed at different heights, the bundles were reconstructed in 3D using the software Solidwork®.

### 2.5. Scanning electron microscopy

The stem samples were coated with a thin layer of gold in an Edwards Sputter Coater, and then observed under a Jeol JSM 6460LV scanning electron microscope (SEM).

### 2.6. Atomic Force Microscopy

Mechanical characterization of the stiffness of bundle cross-sections was carried out using a Multimode Atomic Force Microscopy (AFM) instrument (Bruker Corporation, USA) with Peak-Force Quantitative Nano-Mechanical property mapping (PF-QNM)

imaging mode. Measurements were performed using a RTESPA-525 (Bruker) probe with a spring constant of 139 N/m. The probe was calibrated with the so-called Sader method using a Scanning Electron Microscope (Jeol JSM 6460LV) to determine cantilever length and width. The tip radius of 32 nm was tuned during measurements on a Highly Oriented Pyrolytic Graphite (HOPG) standard from Bruker to obtain an indentation modulus of around 18 GPa. The applied maximum load was set to 200 nN for all the measurements. The sample was cut using a diamond blade, and the whole preparation is described elsewhere [31].

## 2.7. Tensile tests on elementary fibers

Fiber mechanical properties (strain at break, strength at break and tangent modulus) were determined from tensile tests on elementary fibers in accordance with NF T 25-501-2. For each batch, elementary fibers were extracted manually from the middle part of technical flax fibers. The extracted fibers were bonded onto a paper frame to obtain a gauge length of 10 mm. Immediately after this step, they were conditioned at a temperature of  $23 \pm 2^\circ\text{C}$  and a relative humidity of  $50 \pm 4\%$  for at least 12h prior to further manipulations. The average fiber diameter was obtained from 6 measurements under the microscope. The paper frame was then clamped onto a universal MTS-type tensile-testing machine equipped with a 2 N capacity load cell under the standard alternative atmosphere described above. The crosshead displacement speed was fixed at 1 mm/min until rupture of the fiber. For each batch, at least 50 elementary fibers were tested. For comparison, four E-glass batches were studied as well. All batches followed the same fabrication process (melting, fiberization, coating, drying and weaving) leading to woven roving designed for composites. Elementary fibers were submitted to the same tensile test previously explained. Using glass as a material for tensile tests enables to control the machine and its compliance, the handling of the protocol and the experimenter.

## 2.8. Statistical analysis

The results were statistically tested using the RStudio® software. One way-analysis of variance (ANOVA) was performed on the results of the tensile tests. Each mean was compared with each of the others, and two results were considered as statistically different if a *P*-value of less than 0.05 was obtained for one of the mechanical properties.

## 2.9. Carbon/epoxy sample

The thin plies of carbon/epoxy laminates were carried out by Multiplast (Carboman Group, France), for comparison of the fiber distribution. The laminates [+45°/0°/-15°] are made of T700 carbon fibers in 40 w% of epoxy resin (prepreg cured at 80 °C for 12h).

## 3. Results and discussion – Impact of the varietal selection on plant architecture and fiber mechanical properties

### 3.1. Morphological study of the stems of different varieties

#### 3.1.1. Stem height

Firstly, an analysis of the morphology was performed on stems from each variety using the measurements of stem height and diameter. Figure II-2 shows the distribution of the stem height according to the variety.

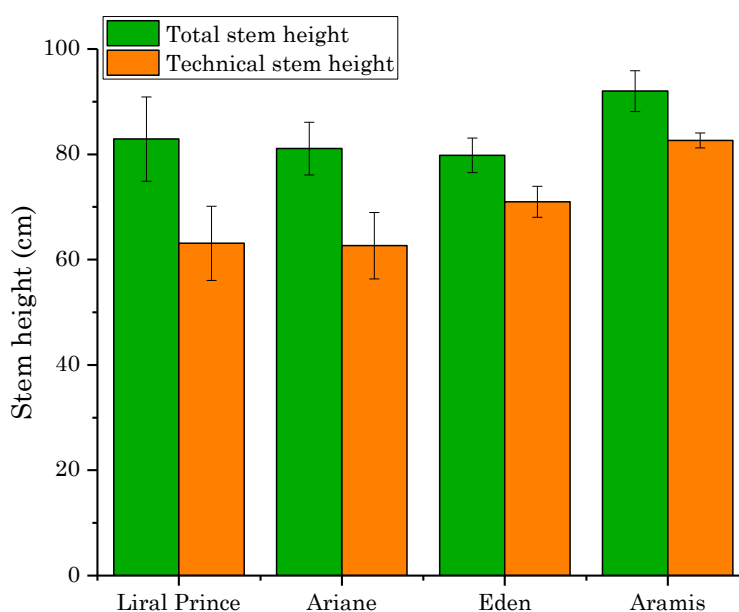


**Figure II-2. Measurements of the total height and technical height (height below the inflorescence) of stems belonging to different varieties.**

No correlation between the time of selection and the stem height were found. This characteristic has stayed broadly the same with selection even though Aramis appears to be slightly higher. Nevertheless, despite this general stability, an increase of the technical height for recent varieties was noted. Although the varietal selection does not focus on this point, the later commercialized varieties seem to exhibit a reduced height of floral ramifications.

### 3.1.2. Stem diameter

Furthermore, the distribution of the diameter along the stem was also examined. When ramifications were observed, the diameter was measured on the main apical ramification. The diameter distribution so obtained can be approximated by a third-order polynomial regression for each tested stem and for each variety. Figure II-3 gives the resulting regression curves calculated from ten stems for each variety.

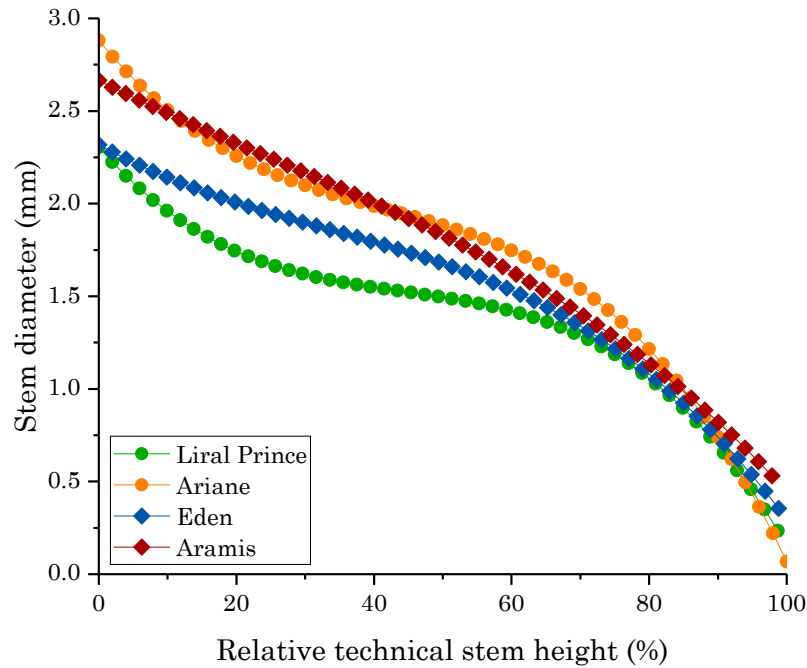


**Figure II-3. Distributions of the stem diameter along the technical height depending on the variety (curves obtained by third-order polynomial regressions of measurements on ten stems per variety).**

First of all, both recent varieties show a more gradual decrease of the stem diameter along the height than the older varieties. Moreover, the diameter all along the stem is not correlated with the height of the plant. Indeed, even though Aramis is higher than the other varieties, the average stem diameter at a given height (both in normal height and relative height) stays similar from one variety to another. Additionally, the height of ramifications does not influence the diameter of the stem, neither at the bottom nor at middle height. In fact, all the varieties have a similar range of diameters at the bottom part and at middle height of the total or technical stem even if recent varieties have shorter ramifications. These observations confirm the trend previously observed with the Marilyn variety [32]. Hence, the varietal selection was able to develop new varieties without impacting the general morphology of the stems.

### 3.2. Anatomy of the stems of different varieties

Figure II-4 presents optical images of transverse sections of the different varieties at middle height, along with analyses of their anatomical criteria. The middle part of the stem was chosen for the study since it is known to yield the greatest number of fibers and the most favorable mechanical properties [33,34]. First of all, a similar internal organization of the biological tissues is visible for all varieties, in accordance with the description given in Figure I-2. Then, from Figure II-4 (A), the observations regarding the differences of diameter are in accordance with previous results: there is no correlation between the time of selection and the diameter at middle height.

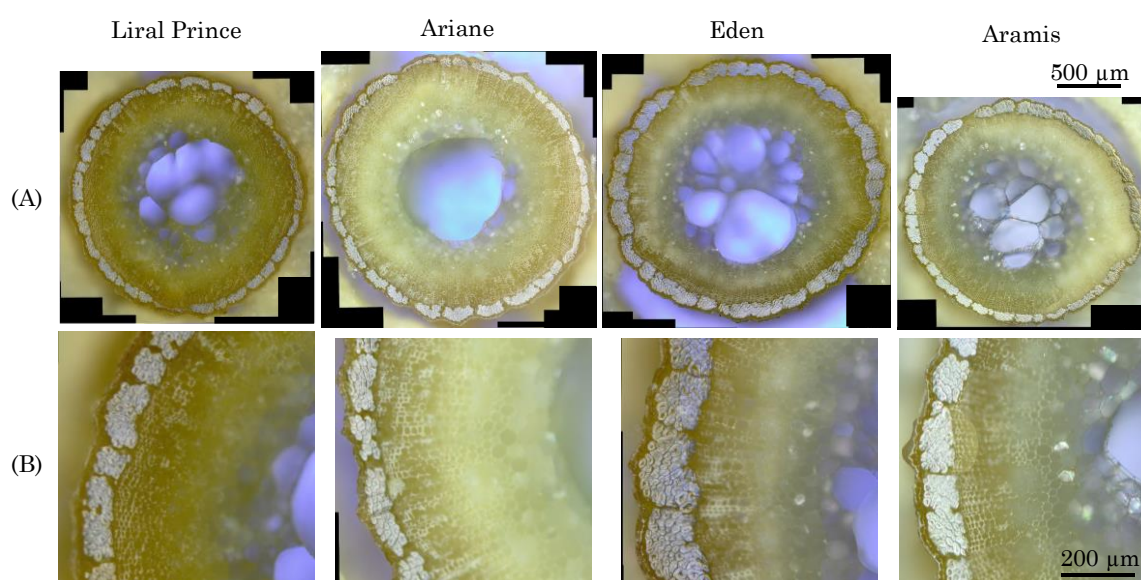


**Figure II-4. (A) Pictures of stem sections at middle height (same scale); (B) fiber bundles from the same sections at higher magnification (same scale).**

Moreover, differences regarding fiber bundles can be noticed from Figure II-4 (B). Indeed, recent varieties give thicker bundles and the separation between two successive bundles is less pronounced. The bundles almost form a continuous ring of fibers for Eden and Aramis.

Complementary, Table II-1 summarizes the average values of the main parameters obtained from the sections. The different steps of the analysis are illustrated in Figure II-5. The total proportion of the different tissues (Figure II-5 (A)) is evaluated from the total area of the stem section.

**Table II-1. Anatomical parameters of stem sections determined by image analysis.**

Variety	Total stem height (cm)	Stem diameter (middle height) (mm)	Tissue content (% of stem area)	Fiber content (% of tissue area)	Fibers per section	Fiber diameter ( $\mu\text{m}$ )
Liral Prince	82.9 $\pm$ 8.0	1.96 $\pm$ 0.12	75.5 $\pm$ 5.5	9.1 $\pm$ 0.5	828 $\pm$ 173	19.9 $\pm$ 6.2
Ariane	81.1 $\pm$ 5.0	2.03 $\pm$ 0.09	84.6 $\pm$ 0.2	7.8 $\pm$ 0.8	883 $\pm$ 56	19.3 $\pm$ 5.9
Eden	79.8 $\pm$ 3.3	2.02 $\pm$ 0.11	75.4 $\pm$ 6.0	10.1 $\pm$ 0.9	1259 $\pm$ 1	19.8 $\pm$ 6.2
Aramis	92.0 $\pm$ 3.9	1.82 $\pm$ 0.07	70.4 $\pm$ 1.9	13.4 $\pm$ 1.6	1361 $\pm$ 99	17.5 $\pm$ 5.4

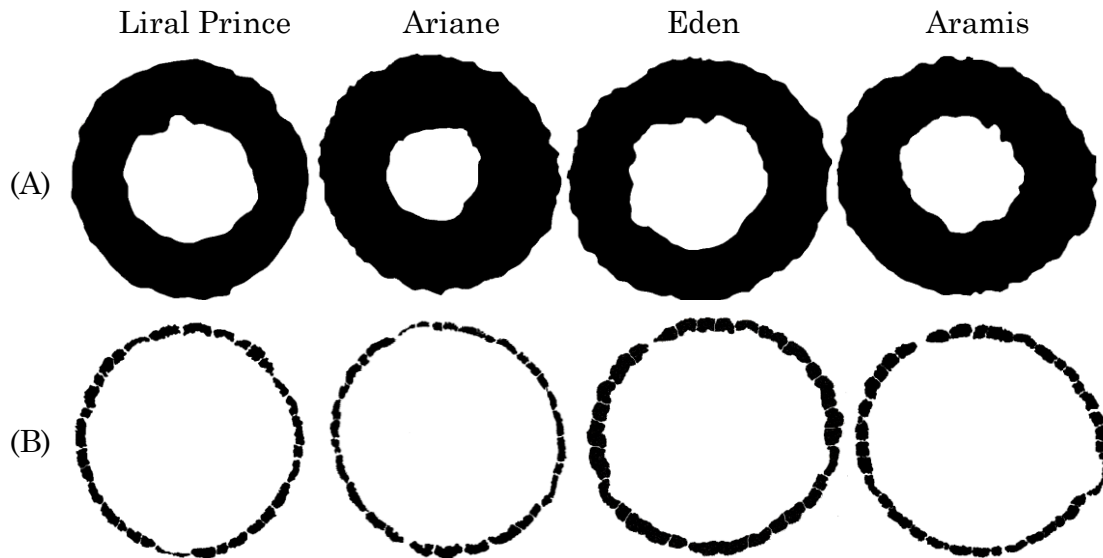


**Figure II-5. Images used for analyzing some criteria regarding the constitution of the plants with (A) the tissue area and (B) the fiber area (for comparison, images are given for an equivalent stem diameter).**

The varieties have different morphologies according to the tissue content, as this component can range from 70.4% for Aramis to 84.6% for Ariane. However, there is no correlation between the dimension of the central lacuna and the stem diameter. For example, Ariane and Eden have similar diameters but a large difference in terms of anatomy as a function of tissue content. Once more, there is no correlation between the time of selection and the observed anatomical differences.

In addition, by comparing the fibrous area contents (Figure II-5 (B)), this latter criterion allows us to identify two categories: varieties with a low proportion of fibers

(about 8% of the tissue area) and varieties with a greater proportion of fibers (above 10%). Regarding these categories, it is noteworthy that the proportion of tissue represented by the fibers appears to be correlated with the time of selection. Indeed, the older varieties have a lower fiber content than the recent varieties. This result is in line with the main aim of the varietal selection, namely increasing the fiber yield.

Moreover, it could be interesting to compare the varietal influence on the number of fiber bundles for given culture conditions [33]. However, this criterion is not used in the present study since it is problematic to assess the number of bundles in recent varieties. Indeed, for Eden and Aramis, the gap between two successive bundles is much narrower and their separation is difficult to define with any certainty. This criterion matches the increase in fiber yield. By comparing the number of fibers per section and their diameters, the results show that the varietal selection can be used to control the fiber content without impacting the fiber morphology: diameters of fibers belong to the same range despite an increasing number of fibers over time. Finally, a correlation between the technical stem height and the fiber content was made, highlighting the key role of the fibers in the stability of the plants (Figure II-6).

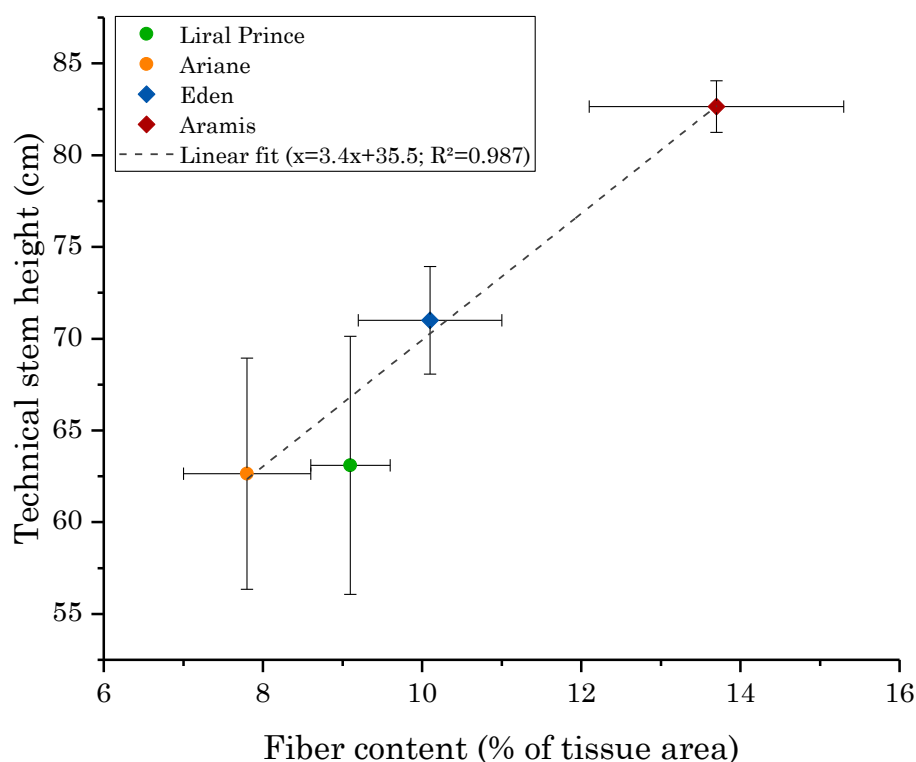


**Figure II-6. Correlation between the fiber content in cross-section at mid-height and the technical stem height of flax varieties selected at different times.**

Thus, it is possible to influence the fiber content, highlighted by a greater number of fibers per section and an increased technical stem height, without changing the overall architecture of the stems or the fiber diameter. The change is also visible through thicker bundles whose limits are harder to identify over the selection.

### 3.3. Mechanical properties of the fibers of different varieties

As the varietal selection has been shown to increase the fiber yield without changing the stem or the fiber diameters, it might be asked whether this increase could impact the mechanical performances. For this study, the culture conditions were similar from one variety to another. Therefore, the fiber development and properties can be considered as a parameter depending solely on the varietal architecture. Tensile tests were carried out to determine the mechanical properties of the fibers extracted from the four varieties. The results obtained are summarized in Table II-2 and compared with literature data sets for the same varieties [6,9,20,21].

**Table II-2. Results of tensile tests performed on four flax varieties. In a given column, values with the same superscript letters (a, b, c, etc.) are considered as statistically similar ( $P > 0.05$ ).**

Variety	Diameter ( $\mu\text{m}$ )	Tangent modulus (GPa)	Strength at break (MPa)	Strain at break (%)	Reference
Liral Prince	$21.4 \pm 2.5$	$41.2 \pm 10.3^{\text{d}}$	$878 \pm 284^{\text{g}}$	$2.40 \pm 0.60^{\text{k}}$	This study
Ariane	$17.5 \pm 2.8^{\text{a,b}}$	$44.3 \pm 9.7^{\text{d,e}}$	$1089 \pm 365^{\text{h,i}}$	$2.53 \pm 0.51^{\text{k}}$	This study
	$23.2 \pm 5.7$	$54.1 \pm 15.1^{\text{f}}$	$1339 \pm 486$	$3.27 \pm 0.84$	[20]
Eden	$16.2 \pm 3.0^{\text{c}}$	$55.5 \pm 9.6^{\text{f}}$	$1175 \pm 288^{\text{h}}$	$2.46 \pm 0.40^{\text{k}}$	This study
	$16.7 \pm 2.6^{\text{a,c}}$	$63.4 \pm 15.9$	$940 \pm 350^{\text{ij}}$	$1.81 \pm 0.71^{\text{l}}$	[21]
	$13.0 \pm 2.7$	$68.9 \pm 24.6$	$1164 \pm 464^{\text{h}}$	$2.51 \pm 0.97^{\text{k}}$	[6]
Aramis	$18.6 \pm 2.9^{\text{b}}$	$46.1 \pm 13.0^{\text{e}}$	$855 \pm 323^{\text{gj}}$	$1.96 \pm 0.52^{\text{l}}$	This study
	$14.4 \pm 3.4$	$47.9 \pm 14.2^{\text{e}}$	$1015 \pm 373^{\text{i}}$	$2.47 \pm 0.85$	[9]

To allow a suitable comparison, all the tests, whether carried out in this study or explained in the literature, were performed using the same equipment and method. To complete the comparison between the batches of a given variety and between

varieties as well, the data sets of each mechanical property were statistically tested using one way-analysis of variance (ANOVA). Due to the large number of  $P$ -values obtained from the statistical analysis, further details are not given here. Nevertheless, mechanical properties considered as statistically similar are marked with the same superscript letters (see Table II-2). Finally, all the different batches of the studied varieties are found to be statistically different for at least one of the mechanical properties, as shown on Table II-2. As a consequence, each batch has its own specific properties, even for the same variety.

To assess the significance of the differences mentioned above, the data sets given in Table II-2 are compared with numerous other batches. The related properties of the additional batches were investigated in a previous study [15]. The comparison with literature data sets is given Figure II-7, which also gives the average tensile strength at break of the varieties tested in this study as a function of the tangent modulus.

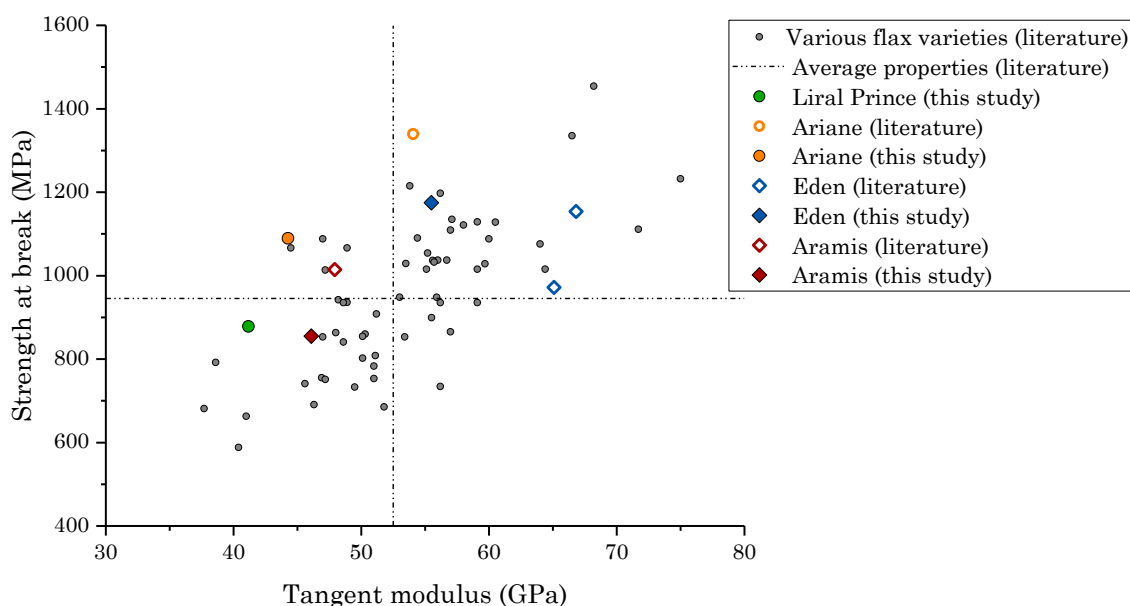


**Figure II-7. Average tensile strength at break vs. average tangent modulus for different flax varieties tested in this study and compared with literature values [6,9,15,20,21].**

As regards tangent modulus, the graph shows that the batches tested for the four varieties yield values slightly below the average. Exceptions for Eden and a single batch of Ariane are noted. This stiffness scattering between flax varieties can also be explained by biochemical structure and composition differences; previous works [23,35,36] highlighted an improvement of the single fiber Young's modulus with the

increase of structuring parietal polysaccharides. Moreover, the values for strength at break are slightly scattered without any correlation with the variety. Figure II-8 also shows a scattering of strain at break for the results.

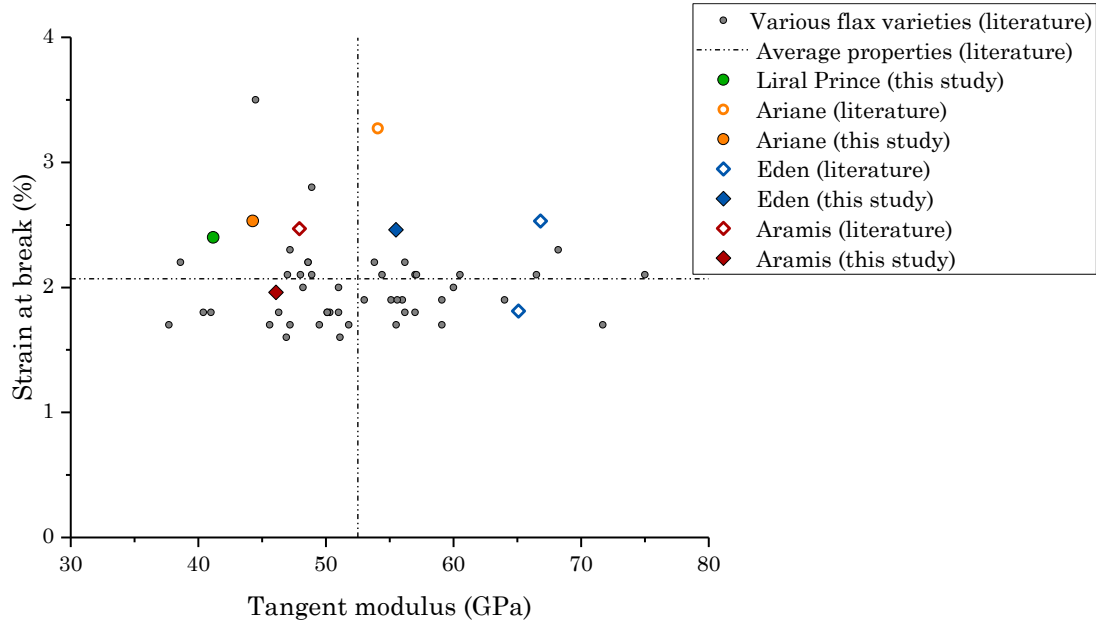


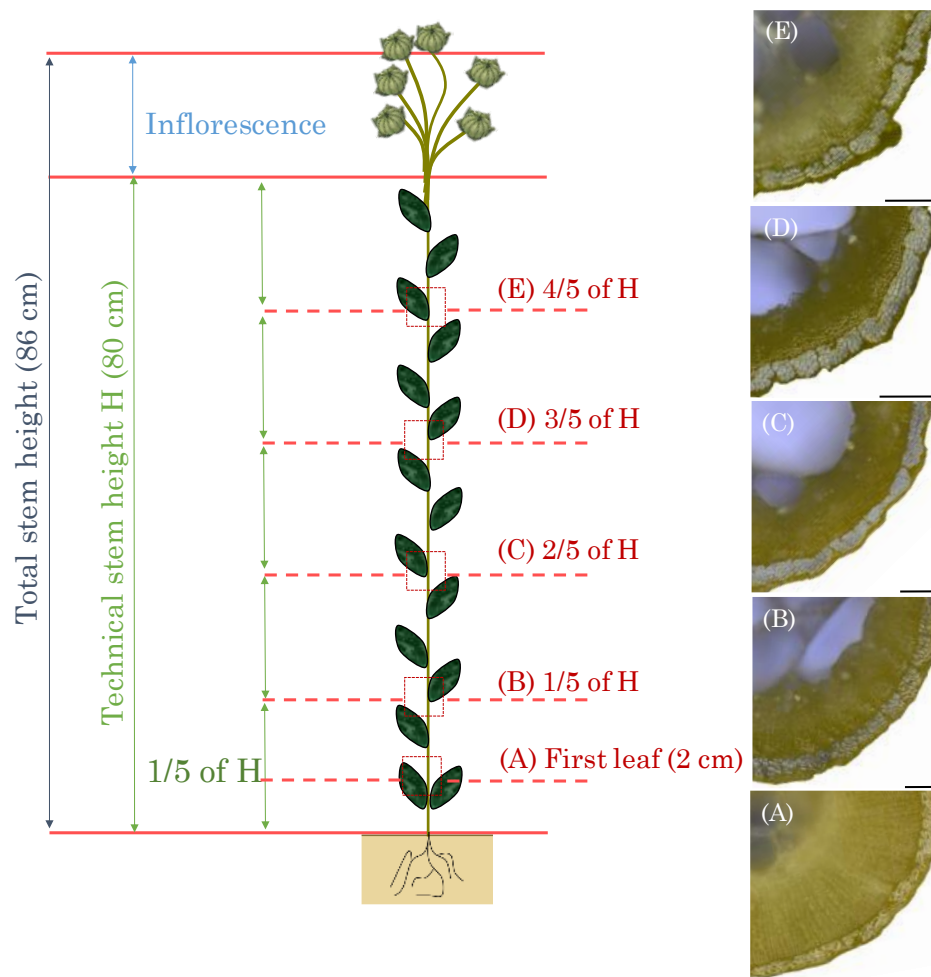
**Figure II-8. Average strain at break vs. average tangent modulus for different flax varieties tested in this study and compared with literature values [6,9,15,20,21].**

For this criterion as well, no tendency can be observed between varieties and strain properties. Whatever the case, despite the scattering for a given variety, the mechanical properties of the four studied varieties belong to the same range than the literature data sets. Moreover, the recent varieties are quite similar regarding the performances and the scattering. Thus, the mechanical properties of the fibers are not impacted by the varietal selection; increasing the fiber yield does not reduce the performance of this natural material.

## 4. Results – Architecture of plants from a single flax variety

### 4.1. Overall morphological study of a stem

Figure II-9 shows several stem transverse cross-sections at different heights of the stem; a similar stem architecture is observed whatever the position of the cross-section. Indeed, we can note the composite structure of the stem with two main constitutive areas: fiber bundles located at the periphery of the stem and the woody core of the plant (xylem) located between the fibers and the central cavity, all along the stem. Anatomical parameters were measured from each stem section.



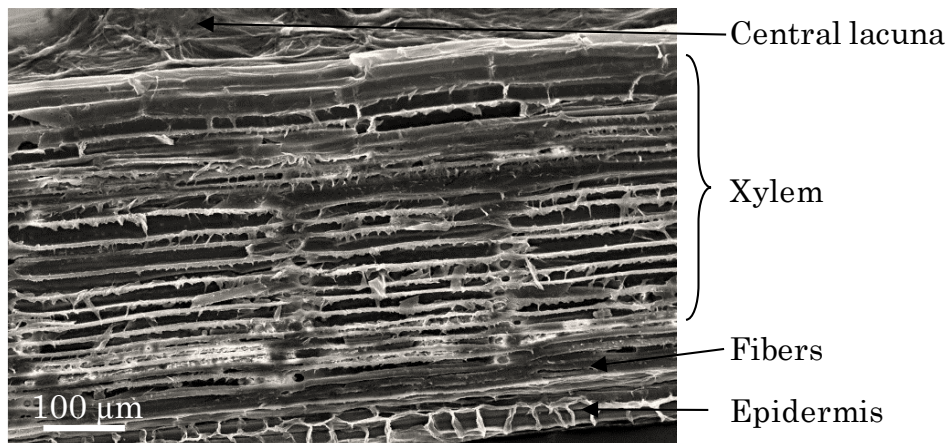
**Figure II-9. Images of transverse stem sections at different stem heights (scale bars = 200  $\mu\text{m}$ ).**

Table II-3 summarizes the results obtained along the stem based on image analysis.

**Table II-3. Anatomical parameters of transverse stem sections determined by image analysis.**

Image	Stem diameter (mm)	Tissue content (% of stem area)	Fiber content (% of tissue area)	Number of fibers (per section)	Fiber diameter ( $\mu\text{m}$ )
(A)	$1.65 \pm 0.06$	90.1	10.7	367	$25.2 \pm 10.0$
(B)	$1.78 \pm 0.02$	74.1	18.7	857	$21.6 \pm 7.5$
(C)	$1.52 \pm 0.03$	71.4	17.2	898	$17.1 \pm 5.4$
(D)	$1.30 \pm 0.04$	69.4	19.9	1045	$14.4 \pm 4.7$
(E)	$0.97 \pm 0.06$	72.1	13.4	668	$11.4 \pm 3.4$

While the overall architecture is similar whatever the position on the stem, some tendencies can be noted. Firstly, there is a slight increase of the diameter in the lower part of the stem, probably to ensure a better plant stability; this is followed by a regular decrease up to the top of the stem, confirming the tapered shape previously observed in different other flax varieties (Figure II-3). The overall architecture is also marked by an increase of the central stem cavity as far as the middle of the stem; a stabilization of the lacuna surface-area ratio is then noted between the middle and the top of the stem, with a mean value close to 30% of the total stem cross-sectional area. Regarding the properties of the supporting fiber, results indicate that the middle of the stem is the most fiber rich area, as compared to the bottom or top of the stem, in accordance with literature [21]. In addition, to visualize the different biological tissues, the stem was fissured along the longitudinal axis. Figure II-10 shows the corresponding longitudinal structure of a flax stem.



**Figure II-10. Longitudinal section exhibiting the inner porous structure of the stem.**

The woody core, composed essentially of xylem, give rise to the shives sometimes used in composites, is located in the inner part of the stem and has a porous structure. Moreover, the xylem cells are short cells (about 250 μm long), whereas the epidermis are even shorter (about 25 μm long).

#### **4.2. Geometrical and mechanical properties of flax fibers depending on the sampling height along the stem**

The influence of the height of the stem selected for fiber extraction is studied here in three sampling areas: bottom, middle and top. Table II-4 gives the mean length and tensile properties of elementary fibers extracted from each of the three studied parts of the plant.

**Table II-4. Average lengths and tensile mechanical properties of elementary flax fibers sampled at different height along the stem.**

Sampling zone along the stem	Bottom	Middle	Top
Mean length $L_f$ and standard deviation (mm)	15.9 ± 5.4	35.5 ± 16.3	17.2 ± 5.8
Minimum length (mm)	5.4	11	9.2
Maximum length (mm)	27.3	87	31.3
Average fiber diameter $D_f$ and standard deviation (μm)	19.2 ± 3.4	19.4 ± 3.1	15.3 ± 3.9
Average aspect ratio $L_f/D_f$	828	1830	1124
Tangent modulus (GPa)	47.2 ± 18.1	58.7 ± 21.3	50.1 ± 22.7
Tensile strength at break (MPa)	872 ± 437	911 ± 422	768 ± 363
Strain at break (%)	2.1 ± 0.8	1.8 ± 0.6	1.8 ± 0.8

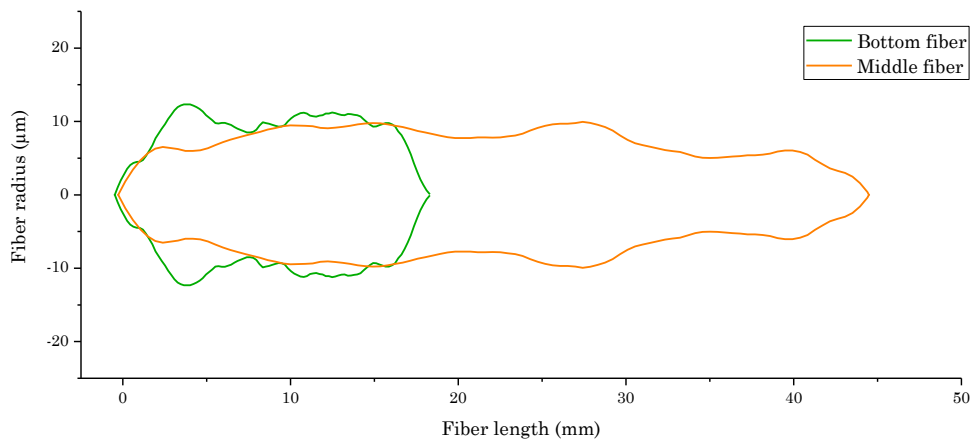
Despite a noticeable scattering of fiber length, the longest fibers originate from the central part of the stem. In fact, the length ranges from 11 to 87 mm with an average value of 35 mm. The maximum length of 87 mm is distinctly higher than the usual results in the literature [3,4,37–42], but close to the value of 90 mm indicated by Billaux [4]. Moreover, the central part of the plant provides the greatest amount of generated fibers, as previously shown (Figure II-9 and Table II-3). Although the mean length of an elementary fiber is an interesting parameter, it is not a sufficient to describe a composite material. In fact, the aspect ratio  $L_f/D_f$  is much more useful, being defined as the total length of the fiber divided by its average diameter. The ratio  $L_f/D_f$  is an important parameter to quantify the possibility of load transfer between fiber and matrix in the case of staple fibers. In fact, under a tensile load, the aspect ratio of a fiber must be higher than its critical aspect ratio to ensure maximum stress transfer, *i.e.* the fiber is able to break without debonding. In our study, the average aspect ratio is respectively 828 for bottom fibers, 1830 for the middle fibers and 1124 for fibers from the top. In addition, the longest elementary fibers also display the best aspect ratio and the highest tensile performances, in accordance with average values given in the literature, namely a tangent modulus of  $52.5 \pm 8.6$  GPa, tensile strength of  $945 \pm 200$  MPa and strain at break of  $2.07 \pm 0.45$  [15].

As a complement, for composites reinforced with short flax fibers, it is possible to estimate the fiber critical aspect ratio below which the fiber would break within the composite without debonding. The fiber critical aspect ratio is estimated by

$\left(\frac{L_f}{D_f}\right)_{critical} = \frac{\sigma_f}{2\tau_i}$  where  $\sigma_f$  is the average fiber tensile strength and  $\tau_i$  is the interfacial shear stress between the fiber and the matrix [43]. By taking an average tensile strength  $\sigma_f$  of 945 MPa and an average interfacial shear stress  $\tau_i$  of 22.3 MPa (in literature, it reaches 22.2 MPa for flax/PA11 composites [44] and 22.3 MPa for flax/epoxy ones [45]), the mean critical aspect ratio is about 21.2. Thus, the high aspect ratios naturally reached by flax fibers enable to benefit from fiber mechanical properties, even if cut for compounding applications.

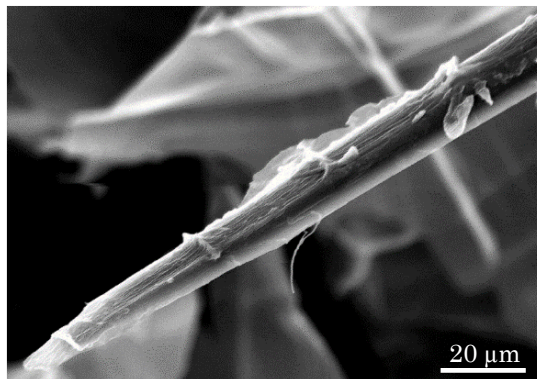
### 4.3. Evolution of fiber diameter along length

Figure II-11 shows the evolution of diameter along the fiber length, based on samples extracted from the middle and the bottom of the stem. Thus, individual flax fibers show tapered ends and have an irregular diameter along their length.



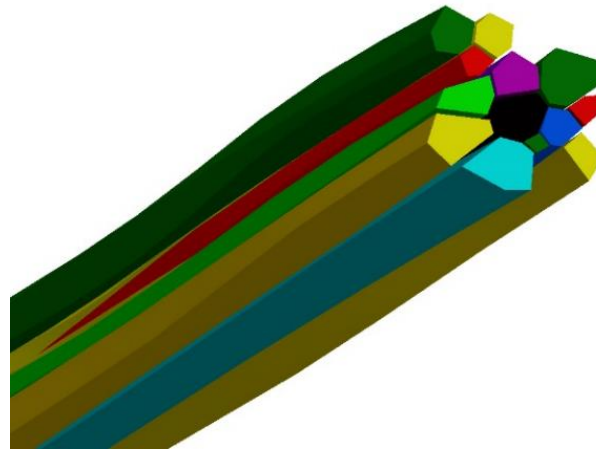
**Figure II-11. Geometry of an elementary fiber from the bottom (green) and middle (orange) of the stem.**

Figure II-12 shows a fiber extremity, illustrating the variation in diameter along the fiber, with tapered and pointed ends as schematized in Figure II-11.



**Figure II-12. Flax fiber extremity observed by SEM shows tapered ends.**

Finally, Figure II-13 gives a 3D reconstruction of a fiber bundle including the fiber ends.



**Figure II-13. 3D reconstruction of a bundle in an area, with a fiber extremity (red fiber).**

From this figure, we can see that the fibers ends are randomly distributed, which can be explained by the intrusive growth of fibers during plant development [30].

#### **4.4. Tensile behavior in transverse direction and middle lamellae**

A transverse section of a fiber bundle by AFM in PF-QNM mode highlights the polygonal cross-section of fibers, as well as the presence of the middle lamellae maintaining bundle cohesion (Figure II-14).

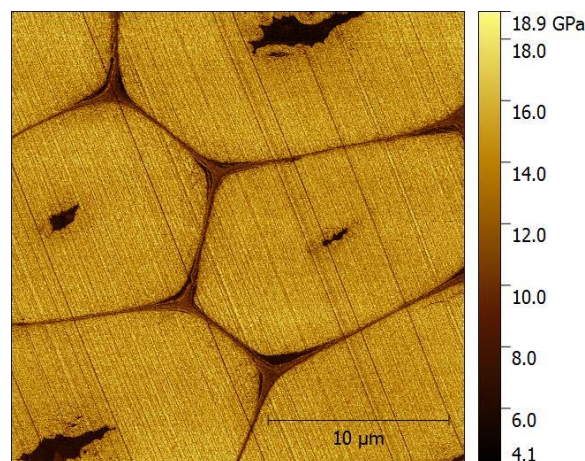


**Figure II-14. AFM PF-QNM mapping of indentation modulus of a flax bundle embedded in epoxy resin.**

The volume fraction of fibers in the bundle shown in Figure II-14 is higher than 95%; this high value is attained owing to the polygonal section of fibers. Moreover, the

thickness of the zone of least stiffness between fibers, corresponding to the middle lamellae and the primary wall [31], varies from 0.3 to 0.8  $\mu\text{m}$  outside cell junctions. In addition, at room temperature and 50% relative humidity, the indentation modulus of the fiber cell wall measured by AFM reaches about 18 GPa, whereas it is about 8 GPa for the middle lamellae.

## 5. Discussion – Reinforcement mechanisms in a flax stem

### 5.1. Anatomical analysis of a stem

Even though the varietal selection has led to changes in stem anatomy through an increase of the fiber yield of the total biomass, the general organization of the flax plant has not changed over time. We can schematically represent the internal structure of a flax stem using a three-part model: an external protection layer (corresponding to the epidermis), a unidirectional ply (simplifying the fiber bundles) and a porous internal core (corresponding to the xylem) whose density decreases toward the center of the stem (Figure II-15).

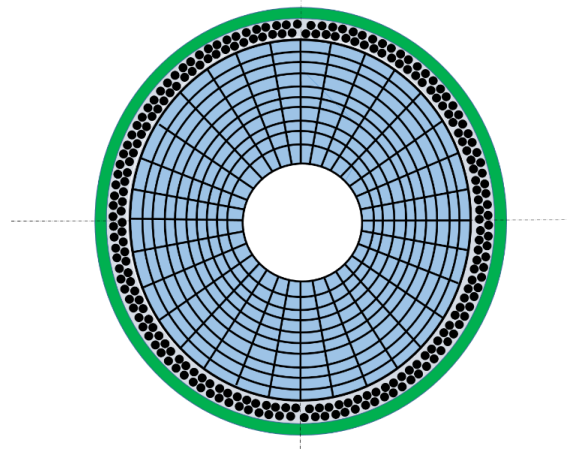


**Figure II-15.** Schematic drawing of a transverse flax stem section composed of a protection layer (green), a unidirectional ply and an alveolar core.

This cylindrical structure is well adapted for recovery-response to flexural loading undergone by the plant. More precisely, fibers take up normal loads whereas the xylem core prevents ovalization of the stem section while reducing the risk of buckling. The ring of fibers so formed is almost continuous for recent varieties for which the neighboring bundles have become increasingly cohesive, to such an extent that it is now very hard to identify single bundles with any certainty. In the stem, fibers are linked together via their pectic junctions, the middle lamellae (Figure II-13) within a

bundle structure, representing a first example at the scale of a composite material. The stresses are transferred to the reinforcing fibers through their junctions, a matrix of pectic polymers. Moreover, this woody core is a low-density cellular core which looks like the core of a sandwich structure and drastically reduces the possibility of Brazier-type buckling [26]. The alternation of layers leads to what biologists refer to as a core-rind structure that increases the effective bending resistance of the stem. Thus, during bending of a flax stem, the xylem would play a key role in the bending resistance by limiting ovalization of the stem and local buckling of bundles in the compressed portion of the plant [46].

## 5.2. Analysis of elementary fibers and bundle characteristics

### 5.2.1. Fiber aspect ratio and mechanical properties

For many years, data sets on the aspect ratio of flax fibers have been available in the literature, as this parameter has been carefully evaluated by spinners. Table II-5 presents some literature data sets extending over more than a century.

**Table II-5. Aspect ratio of elementary flax fibers (data sets from the literature).**

References	$L_f$ (mm)	$D_f$ ( $\mu\text{m}$ )	$L_f/D_f$ (mean)
[37]	20-50 (mean 35)	12-26 (mean 19)	1842
[38]	11-38 (mean 24.5)	12-25 (mean 18.5)	1324
[3]	10-40	15-25	1250
[39]	20-39 (mean 29.5)	11-31 (mean 21)	1404
[40]	27	23	1174
[4]	2-90	12-18	1467
[41]	1.6-24 (mean 7.9)	11.68-31.96 (mean 19)	416
[42]	13-65 (mean 28.8)	12-30 (mean 21)	1190

The cited references do not indicate the area used for sampling fibers in the stem, and no information is given on the flax variety, growing conditions or the technical operations performed on the fibers. However, if we compare the literature data sets

with the values measured in our study (Table II-4), the present aspect ratios fall within the same range of values. Thus, despite an evolution of flax varieties and cultural practices over time, the aspect ratio is a specific criterion of *Linum usitatissimum* L. used for industrial applications.

Complementary, a comprehensive knowledge of plant fibers helps in understanding the origin of their morphology as well as mechanical properties. As described in Chapter I, fiber expansion and thickening of the walls occurs below the snap point, where the bending stiffness of the stem changes, becoming stiffer below this point. Indeed, below the snap point, cell wall thickening takes place in the fibers, with no further elongation. Thus, at the snap point, fiber length is maximal while fibers still have thin cell walls. Structuring of the cell wall is the thickening step, which takes place over about two months and continues to plant maturity, when the fibers are thus best-thickened and exhibit high mechanical properties.

### **5.2.2. Cohesion within a fiber bundle and middle lamellae**

The cell wall of mature fibers reaches about 18 GPa, whereas it is about 8 GPa for the middle lamellae when measured by AFM (Figure II-14). This latter value is very close to the transverse modulus of flax fiber also estimated at 8 GPa by unidirectional transverse tensile tests [47]. Thus, to a first approximation, we can consider the middle lamellae as an isotropic material. The properties of the middle lamellae can also be linked to the plant development, which involves consolidation of the fiber junctions [27]. In a stem, the shared junctions between fibers ensure the transfer of load between fibers (within a bundle). The junctions contain two main types of pectins, homogalacturonans and rhamnogalacturonans [14], and consist of two morphological domains: (1) the middle lamellae between the primary cell walls of two neighboring fibers and (2) the tricellular junctions of three fibers in the corners [14]. The pectic compositions of fiber junctions vary greatly according to sampling area on the stem and time during growth, and adapt to the differentiation stages of fiber development (elongation, expansion, and cell wall thickening). The junctions are generally strengthened during expansion and thickening of the fibers. In addition, the distribution and the tapered geometry of fiber ends represent two criteria limiting strain concentration within the bundles. Indeed, this type of architecture and geometry results in very little disorientation of the reinforcement layer.

Then, if we investigate the transverse behavior of a fiber bundle, an analogy with a unidirectional (UD) fibers can be done. The properties of composite materials reinforced by UD fibers are known to be highly anisotropic, with high values of stiffness and strength in the fiber direction and poor mechanical behavior in the transverse direction. The main inconvenience of composites is their low transverse tensile strength. The initial damage mechanism (first ply failure) is often conditioned by the transverse tensile strength of plies with unidirectional reinforcement. The low value of the transverse tensile strength, and the corresponding transverse failure strain, are due to strain concentration in the matrix (or in the interface) around the fibers. Thus, the strain concentration causes the composite transverse tensile failure strain to be less than the matrix failure strain. In addition, the strain concentration factor in a ply is a function of the distance between fibers (which depends on the volume fraction and distribution of the fibers), the ratio of the matrix modulus ( $E_m$ ) and the transverse modulus of the fibers ( $E_f/T$ ), and the presence of defects such as pore spaces. In other words, the strain concentration factor increases when the fibers are closer together or with decreasing  $E_m/E_fT$  ratio [48]. In a fiber bundle, the volume fraction of the reinforcement is very high. However, no strain concentration appears because the transverse stiffness of fibers is similar to that of the middle lamellae.

### 5.3. Analogy between specific properties of flax fibers and glass ones

Even if the properties of elementary fibers are not necessarily an accurate reflection of performances of their composites, a correlation may exist [21], especially regarding the fiber and composite stiffness. For the strength, the inaccuracy comes from the facts that fibers occur in the form of bundles in a composite [45]. This result means that the individualization of elementary fibers is not optimized. Additionally, the middle lamellae between elementary fibers changes the mechanical general behavior. Moreover, the fiber loading in a composite is much more different than for a single fiber as, in a composite, the surface of fibers is mainly restricted [49]. However, in this study, only the mechanical properties of elementary fibers were studied in order to evaluate the potential of the tested varieties for composite reinforcement. Thus, the specific mechanical properties (*i.e.* tangent modulus or strength at break divided by the density of the material) of the different batches of Liral Prince, Ariane, Eden and Aramis are compared with the values obtained from different batches of glass fibers. For this comparison, densities of 1.53 and 2.54 for flax and glass were assumed,

respectively [15]. Table II-6 reports the results obtained for the different batches from this study and the literature.

**Table II-6. Mechanical properties of flax and glass single fibers from this study and literature. Specific mechanical properties are given for tangent modulus and strength at break (assuming 1.53 and 2.54 as densities of flax and glass, respectively).**

Variety	Diameter ( $\mu\text{m}$ )	Specific tangent modulus (GPa)	Specific strength at break (MPa)	Strain at break (%)	References
Liral Prince	$21.4 \pm 2.5$	$26.9 \pm 6.7$	$574 \pm 186$	$2.40 \pm 0.60$	This study
Ariane	$17.5 \pm 2.8$	$29.0 \pm 6.3$	$712 \pm 238$	$2.53 \pm 0.51$	This study
	$23.2 \pm 5.7$	$35.4 \pm 9.9$	$875 \pm 318$	$3.27 \pm 0.84$	[20]
Eden	$16.2 \pm 3.0$	$36.3 \pm 6.3$	$768 \pm 188$	$2.46 \pm 0.40$	This study
	$16.7 \pm 2.6$	$41.4 \pm 10.4$	$614 \pm 229$	$1.81 \pm 0.71$	[21]
	$13.0 \pm 2.7$	$45.0 \pm 16.1$	$761 \pm 303$	$2.51 \pm 0.97$	[6]
Aramis	$18.6 \pm 2.9$	$30.1 \pm 8.5$	$559 \pm 211$	$1.96 \pm 0.52$	This study
	$14.4 \pm 3.4$	$31.3 \pm 9.3$	$663 \pm 244$	$2.47 \pm 0.85$	[9]
E-Glass	$17.2 \pm 0.7$	$26.8 \pm 4.3$	$772 \pm 180$	$2.87 \pm 0.64$	This study
	$16.0 \pm 0.7$	$26.2 \pm 3.5$	$972 \pm 221$	$3.49 \pm 0.68$	This study
	$19.7 \pm 1.2$	$28.4 \pm 3.1$	$694 \pm 152$	$2.52 \pm 0.53$	This study
	$17.7 \pm 1.8$	$31.0 \pm 2.7$	$720 \pm 152$	$2.44 \pm 0.54$	This study
	$17.9 \pm 1.7$	$27.9 \pm 2.4$	$764 \pm 134$	$2.70 \pm 0.80$	[28]
	$16.6 \pm 1.6$	$30.6 \pm 1.9$	$913 \pm 146$	$3.00 \pm 0.90$	[28]
	$18.0 \pm 1.3$	$28.6 \pm 2.0$	$863 \pm 196$	$3.00 \pm 1.00$	[28]
	$17.9 \pm 1.9$	$27.7 \pm 2.3$	$695 \pm 170$	$2.90 \pm 1.00$	[45]

In addition, Figure II-16 gives the mean values of recent flax varieties, namely Eden and Aramis tested in this study and from literature values, and glass batches tested

in this study. While flax fibers are more scattered in terms of their tangent modulus, the scattering of values for strength and strain at break is of the same order for both types of materials. Although flax fibers are proven to give more scattered properties than glass ones, the deviation in composite properties is not directly implied and has to be investigated further. In addition, even if the strength of flax fiber is generally slightly lower than that of glass, this is not the case for tangent modulus, since the average value of flax fiber stiffness is higher than for glass. This latter property highlights the good mechanical performances of flax and its utility for composite manufacturing. Finally, even though flax fibers are natural materials, the scattering of their properties cannot be attributed to their natural origin or the time of selection but mostly to the uncertainty introduced by their diameter measurements [50].

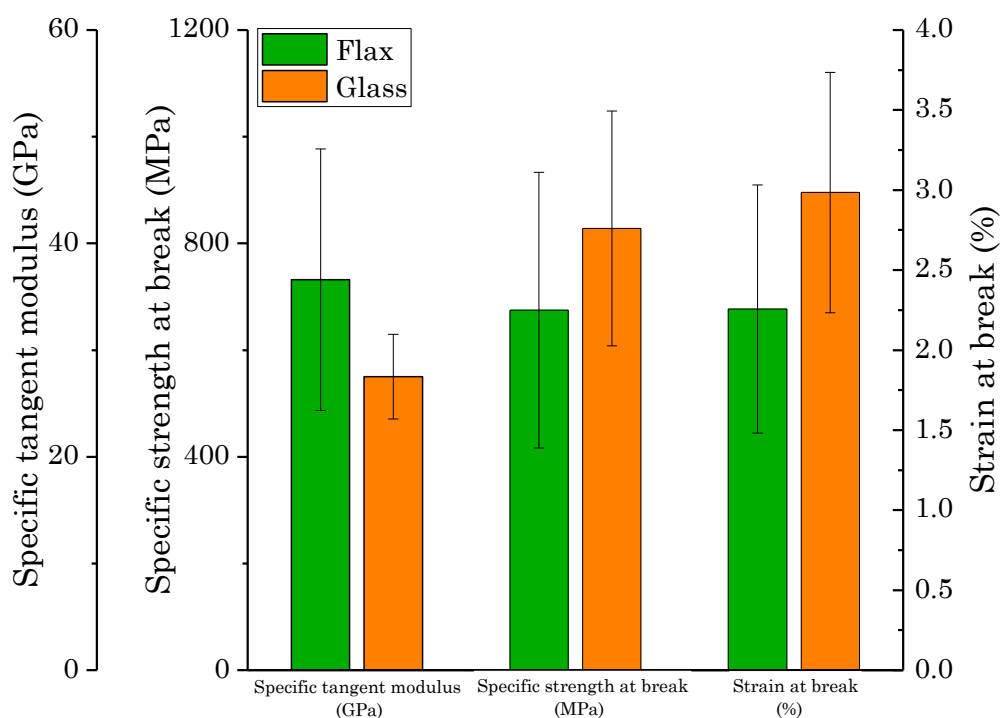


**Figure II-16.** Average specific tensile strength at break, specific tangent modulus and strain at break of recent flax varieties Eden and Aramis (tested in this study and from literature values) [6,9,21] and glass batches tested in this study.

#### 5.4. Analogy between flax stems and composites reinforced by thin plies

The bundles of fibers have moderate thicknesses (a few tens of microns, *i.e.* four times the diameter of a fiber) (Figure II-17 (A)). It is possible to compare these bundles to

the thin-ply laminates used in some composite materials (made by spread tow thin-ply technology). Figure II-17 (B) shows a carbon/epoxy ply made with this technology.

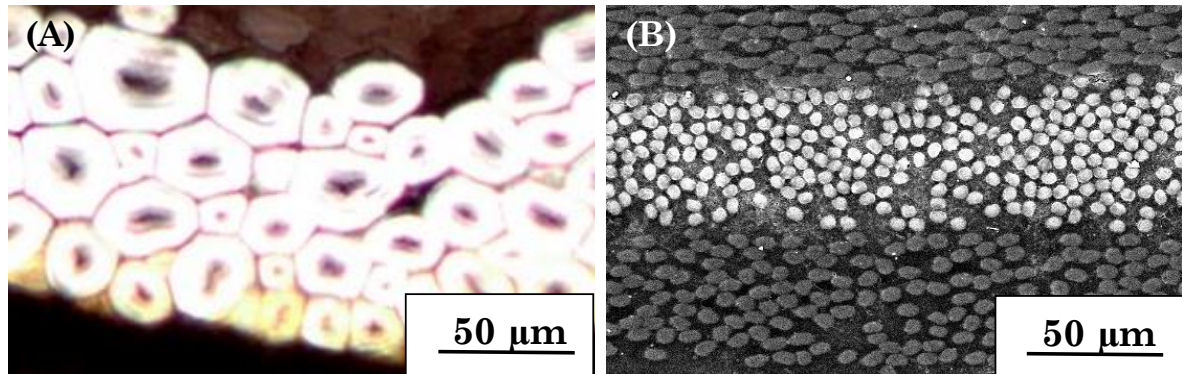


**Figure II-17. Geometry compared between (A) a bundle of flax fibers and (B) a laminate consisting of thin plies ( $\sim 40 \mu\text{m}$ ) reinforced by carbon fibers.**

The bundle thickness is analogous to a thin ply, *i.e.*  $40 \mu\text{m}$ . Even though flax fibers have a polygonal section leading to a higher fiber volume fraction, synthetic fibers are mostly circular to limit the defect content. The development of thinner plies is based on a size effect, with matrix-dominated properties being particularly sensitive to defects (resin-rich zones, porosity, etc.). Rodini and Eisemann [51] used a probabilistic method to show that laminates with thick plies contain statistically more defects than laminates with thin plies. Consequently, the thicker plies are likely to exhibit much lower failure stresses. Among the advantages of this technique, thinner plies are acknowledged to have higher resistance to matrix cracking [52]. Thin ply prepregs are also useful for improving compressive strength properties [52], and the laminate design can be simplified by using a higher allowable strain without carrying out a progressive failure analysis [53]. Thus, a precise analysis of a flax stem is interesting as regards to its general architecture but also in terms of multiscale composites.

## 6. Conclusions

This chapter shows that recent textile flax varieties, such as Eden or Aramis, display a special anatomy, resulting from an extensive selection performed over many years. They differ from older varieties since they lead to much thicker fiber bundles with narrower gaps between them. Consequently, the varietal selection has made possible the increase of the fiber yield, according to the interests of breeders and farmers. This improvement was done without increasing the stem length, thus avoiding the risk of lodging. Interestingly, tensile properties of flax fibers appear to be similar over time

whatever the fiber yield and the variety. This result highlights that varietal selection is an indispensable expertise as well as an essential technique for developing the industrial use of flax fibers in new materials and their wider applications in the future.

Additionally, the architecture of a plant is an important criterion which reflects its external characteristics and anatomical structure; hence, it has to be taken into account for varietal selection and understanding of the mechanical properties of flax fibers. For instance, the length of elementary fibers and their tensile properties change along the stem. Indeed, fibers extracted at middle height of the plant are the longest and give the best mechanical properties. Moreover, a bundle is made up of an assembly of several discontinuous fibers with tapered ends, whose diameter changes along their length. This specific geometry, explained by the intrusive growth of these reinforcement cells, limits the strain concentration to the fiber ends during loading of the bundle. The composition and arrangement of flax fibers and bundles lead to a very cohesive structure in the transverse direction. Moreover, despite their biological origin, the scattering of the specific mechanical performances is within the same range than those of glass fibers. At the composite scale, this scattering could have relatively little impact due to the presence of a high number of single fibers within a composite. Finally, a flax plant is a natural composite having a very slender structure. Its stem can be regarded, from the outer to inner parts, as a cylinder composed of a protective layer, a unidirectional ply and a porous core. The unidirectional ply has a structural function; it is composed of a high volume fraction of reinforcement fibers gathered together in bundles, forming a more or less continuous ring depending on the variety. Analyzing the reinforcement mechanisms of flax stems is a very instructive approach for bioinspiration. Thus, while the role of flax fibers is strictly for reinforcement, the conductive tissues (xylem and phloem) greatly contribute to the bending strength, limiting the risk of ovalization of the stem and local buckling of the bundles.

The results of the present chapter concern dehydrated stems and fibers. During composite manufacturing, the fibers are commonly dehydrated, which provides an interesting example when comparing fibers in the original stems and composite materials. In future research, it could be of a great interest to characterize stem parts in living plants. In fact, the length of elementary fibers does not change significantly with dehydration, but this does not apply to transverse dimensions such as diameter nor mechanical properties of cell wall non cellulosic polymers.

## 7. References

1. Jankauskiene, Z. Results of 90 years of flax breeding in Lithuania. *Proc. Latv. Acad. Sci. Sect. B Nat. Exact, Appl. Sci.* 2014, 68, 184–192, doi:10.2478/prolas-2014-0022.
2. Doré, C.; Varoquaux, F. Histoire et amélioration de cinquante plantes cultivées. In *Medicine*; 2006; pp. 383–396.
3. Plonka, F.; Anselme, C. Les variétés de lin et leurs principales maladies cryptogamiques; Institut National de la Recherche Agronomique, Paris, 1956;
4. Billaux, P. Le lin au service des hommes: sa vie, ses techniques, son histoire; Baillière.; J.-B. Baillière, 1969;
5. Spielmeier, W.; Lagudah, E. S.; Mendham, N.; Green, A. G. Inheritance of resistance to flax wilt (*Fusarium oxysporum* f.sp. lini Schlecht) in a doubled haploid population of *Linum usitatissimum* L. *Euphytica* 1998, 101, 287–291, doi:10.1023/A:1018353011562.
6. Gibaud, M.; Bourmaud, A.; Baley, C. Understanding the lodging stability of green flax stems; The importance of morphology and fibre stiffness. *Biosyst. Eng.* 2015, 137, 9–21, doi:10.1016/j.biosystemseng.2015.06.005.
7. Bert, F. *Lin fibre - Culture et transformation*; Arvalis, Ed.; 2013; ISBN 9782817901572.
8. Vincent, J. F. V A Unified Nomenclature for Plant Fibres for Industrial Use. *Appl. Compos. Mater.* 2000, 7, 269–271, doi:10.1023/A:1026516105382.
9. Bourmaud, A.; Gibaud, M.; Baley, C. Impact of the seeding rate on flax stem stability and the mechanical properties of elementary fibres. *Ind. Crops Prod.* 2016, 80, 17–25, doi:10.1016/j.indcrop.2015.10.053.
10. Le Duigou, A.; Davies, P.; Baley, C. Environmental impact analysis of the production of flax fibres to be used as composite material reinforcement. *J. Biobased Mater. Bioenergy* 2011, 5, 153–165, doi:10.1166/jbmb.2011.1116.
11. Le Duigou, A.; Bourmaud, A.; Balnois, E.; Davies, P.; Baley, C. Improving the interfacial properties between flax fibres and PLLA by a water fibre treatment and drying cycle. *Ind. Crops Prod.* 2012, 39, 31–39, doi:10.1016/j.indcrop.2012.02.001.
12. Dickson, A. R.; Even, D.; Warnes, J. M.; Fernyhough, A. The effect of reprocessing on the mechanical properties of polypropylene reinforced with wood pulp, flax or glass fibre. *Compos. Part A Appl. Sci. Manuf.* 2014, 61, 258–267, doi:10.1016/j.compositesa.2014.03.010.
13. Bourmaud, A.; Akesson, D.; Beaugrand, J.; Le Duigou, A.; Skrifvars, M.; Baley, C. Recycling of L-Poly-(lactide)-Poly-(butylene-succinate)-flax biocomposite. *Polym. Degrad. Stab.* 2016, 128, 77–88, doi:10.1016/j.polymdegradstab.2016.03.018.
14. van Dam, J. E. G.; Gorshkova, T. A. Cell walls and Fibers / Fiber formation. In *Encyclopedia of Applied Plant Sciences*; Elsevier Ltd, 2003; pp. 87–96.
15. Baley, C.; Bourmaud, A. Average tensile properties of French elementary flax fibers. *Mater. Lett.* 2014, 122, 159–161, doi:10.1016/j.matlet.2014.02.030.
16. Shah, D. U. Developing plant fibre composites for structural applications by optimising composite parameters: a critical review. *J. Mater. Sci.* 2013, 48, 6083–6107, doi:10.1007/s10853-013-7458-7.
17. Mohanty, A. K.; Misra, M.; Drzal, L. T. *Natural Fibers, Biopolymers, and Biocomposites*; 2005; ISBN 9780849317415.
18. de Bruyne, N. A. Plastic progress - Some further developments in the manufacture and use of synthetic materials for aircraft construction. *Flight Aircr. Eng.* 1939, 77–79.

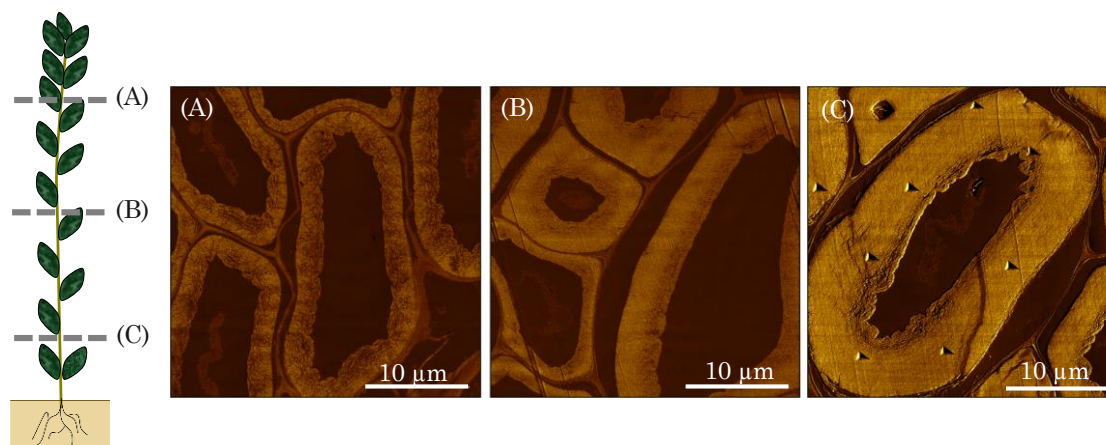
19. Cotterell, B. *Fracture and Life*; Imperial College Press, 2010; ISBN 10 1-84816-282-0.
20. Baley, C. Analysis of the flax fibres tensile behaviour and analysis of the tensile stiffness increase. *Compos. - Part A Appl. Sci. Manuf.* 2002, 33, 939–948, doi:10.1016/S1359-835X(02)00040-4.
21. Lefeuvre, A.; Bourmaud, A.; Baley, C. Optimization of the mechanical performance of UD flax/epoxy composites by selection of fibres along the stem. *Compos. Part A Appl. Sci. Manuf.* 2015, 77, 204–208, doi:10.1016/j.compositesa.2015.07.009.
22. Martin, N.; Mouret, N.; Davies, P.; Baley, C. Influence of the degree of retting of flax fibers on the tensile properties of single fibers and short fiber/polypropylene composites. *Ind. Crops Prod.* 2013, 49, 755–767, doi:10.1016/j.indcrop.2013.06.012.
23. Lefeuvre, A.; Bourmaud, A.; Morvan, C.; Baley, C. Elementary flax fibre tensile properties: Correlation between stress–strain behaviour and fibre composition. *Ind. Crops Prod.* 2014, 52, 762–769, doi:10.1016/j.indcrop.2013.11.043.
24. Ibragimova, N. N.; Ageeva, M. V.; Gorshkova, T. A. Development of gravitropic response: unusual behavior of flax phloem G-fibers. *Protoplasma* 2017, 254, 749–762, doi:10.1007/s00709-016-0985-8.
25. Py, C.; De Langre, E.; Moulia, B.; Hémon, P. Measurement of wind-induced motion of crop canopies from digital video images. *Agric. For. Meteorol.* 2005, 130, 223–236, doi:10.1016/j.agrformet.2005.03.008.
26. Dawson, M. A.; Gibson, L. J. Optimization of cylindrical shells with compliant cores. *Int. J. Solids Struct.* 2007, 44, 1145–1160, doi:10.1016/j.ijsolstr.2006.06.009.
27. Milwich, M.; Speck, T.; Speck, O.; Stegmaier, T.; Planck, H. Biomimetics and technical textiles: Solving engineering problems with the help of Nature’s wisdom. *Am. J. Bot.* 2006, 93, 1455–1465.
28. Lefeuvre, A.; Bourmaud, A.; Morvan, C.; Baley, C. Tensile properties of elementary fibres of flax and glass: Analysis of reproducibility and scattering. *Mater. Lett.* 2014, 130, 289–291, doi:10.1016/j.matlet.2014.05.115.
29. Mattrand, C.; Béakou, A.; Charlet, K. Numerical modeling of the flax fiber morphology variability. *Compos. Part A Appl. Sci. Manuf.* 2014, 63, 10–20, doi:10.1016/j.compositesa.2014.03.020.
30. Ageeva, M. V.; Petrovská, B.; Kieft, H.; Sal’nikov, V. V.; Snegireva, A. V.; Van Dam, J. E. G.; Van Veenendaal, W. L. H.; Emons, A. M. C.; Gorshkova, T. A.; Van Lammeren, A. A. M. Intrusive growth of flax phloem fibers is of intercalary type. *Planta* 2005, 222, 565–574, doi:10.1007/s00425-005-1536-2.
31. Arnould, O.; Siniscalco, D.; Bourmaud, A.; Le Duigou, A.; Baley, C. Better insight into the nano-mechanical properties of flax fibre cell walls. *Ind. Crops Prod.* 2017, 97, 224–228, doi:10.1016/j.indcrop.2016.12.020.
32. Bourmaud, A.; Gibaud, M.; Lefeuvre, A.; Morvan, C.; Baley, C. Influence of the morphology characters of the stem on the lodging resistance of Marylin flax. *Ind. Crops Prod.* 2015, 66, 27–37, doi:10.1016/j.indcrop.2014.11.047.
33. Tiver, N. S. Studies of the flax plant 1. Physiology of growth, stem anatomy and fibre development in fibre flax. *Aust. J. Exp. Biol. Med. Sci.* 1942, 20, 149–160.
34. Charlet, K.; Baley, C.; Morvan, C.; Jernot, J. P.; Gomina, M.; Bréard, J. Characteristics of Hermès flax fibres as a function of their location in the stem and properties of the derived unidirectional composites. *Compos. Part A Appl. Sci. Manuf.* 2007, 38, 1912–1921.
35. Alix, S.; Goimard, J.; Morvan, C.; Baley, C.; Schols, H. A.; Visser, R. G. F.; Voragen, A. G. J. Influence of pectin structure on the mechanical properties of flax fibres: a comparison between linseed-winter variety (Oliver) and a fibre-spring variety of flax. In *Pectins and Pectinases*; 2009; pp. 85–96 ISBN 9789086861088.

36. Bourmaud, A.; Morvan, C.; Bouali, A.; Placet, V.; Perré, P.; Baley, C. Relationships between microfibrillar angle, mechanical properties and biochemical composition of flax fibers. *Ind. Crops Prod.* 2013, 44, 343–351, doi:10.1016/j.indcrop.2012.11.031.
37. Von Wiesner, J. *Einleitung in die technische Mikroskopie nebst mikroskopisch-technischen Untersuchungen*; Wilhelm Braumüller: Wien, 1897;
38. Matthews, J. M. *The textile fibers* (4th edn); John Wiley and Sons, New York, 1931;
39. Koch, P. A. *Microscopie and chemical testing of textiles*; Chapman and Hall, London, 1963;
40. Kirby, R. H. *Vegetable fibres*; Leonard Hill (Books) Ltd, London, 1963;
41. Catling, D.; Grayson, J. *Identification of vegetable fibres*; Springer, Dordrecht, 1982; ISBN 978-94-011-8070-2.
42. Gorshkova, T. A.; Ageeva, M. V.; Salnikov, V. V.; Pavlencheva, N. V.; Snegireva, A. V.; Chernova, T. E.; Chemikosoova, S. B. стадии формирования лубяных волокон *Linum usitatissimum* (Linaceae). *Bot. J.* 2003, 88, 1–11.
43. Gibson, R. *Principles of composites materials mechanics*; 3rd Editio.; Boca Raton: CRC Press., 2012; ISBN 9781439850053.
44. Le Duigou, A.; Bourmaud, A.; Gourier, C.; Baley, C. Multi-scale shear properties of flax fibre reinforced polyamide 11 biocomposites. *Compos. Part A Appl. Sci. Manuf.* 2016, 85, 123–129, doi:10.1016/j.compositesa.2016.03.014.
45. Coroller, G.; Lefeuvre, A.; Le Duigou, A.; Bourmaud, A.; Ausias, G.; Gaudry, T.; Baley, C. Effect of flax fibres individualisation on tensile failure of flax/epoxy unidirectional composite. *Compos. Part A Appl. Sci. Manuf.* 2013, 51, 62–70, doi:10.1016/j.compositesa.2013.03.018.
46. Leblicq, T.; Vanmaercke, S.; Ramon, H.; Saeys, W. Mechanical analysis of the bending behaviour of plant stems. *Biosyst. Eng.* 2015, 129, 87–99, doi:10.1016/j.biosystemseng.2014.09.016.
47. Baley, C.; Perrot, Y.; Busnel, F.; Guezenoc, H.; Davies, P. Transverse tensile behaviour of unidirectional plies reinforced with flax fibres. *Mater. Lett.* 2006, 60, 2984–2987, doi:10.1016/j.matlet.2006.02.028.
48. Kaw, K. *Mechanics of composite materials*; CRC Press, 1997;
49. Joffre, T.; Neagu, R. C.; Bardage, S. L.; Gamstedt, E. K. Modelling of the hygroelastic behaviour of normal and compression wood tracheids. *J. Struct. Biol.* 2014, 185, 89–98, doi:10.1016/j.jsb.2013.10.014.
50. Lefeuvre, A.; Bourmaud, A.; Lebrun, L.; Morvan, C.; Baley, C. A study of the yearly reproducibility of flax fiber tensile properties. *Ind. Crops Prod.* 2013, 50, 400–407, doi:10.1016/j.indcrop.2013.07.035.
51. Rodini, B. T.; Eisenmann, J. R. An Analytical and Experimental Investigation of Edge Delamination in Composite Laminates. In: *Fibrous Composites in Structural Design*; Lenoe, E. M., Oplinger, D. W., Burke, J. J., Eds.; Springer, 1980;
52. Yokozeki, T.; Kuroda, A.; Yoshimura, A.; Ogasawara, T.; Aoki, T. Damage characterization in thin-ply composite laminates under out-of-plane transverse loadings. *Compos. Struct.* 2010, 93, 49–57, doi:10.1016/j.compstruct.2010.06.016.
53. Sihm, S.; Kim, R. Y.; Kawabe, K.; Tsai, S. W. Experimental studies of thin-ply laminated composites. *Compos. Sci. Technol.* 2007, 67, 996–1008, doi:10.1016/j.compscitech.2006.06.008.



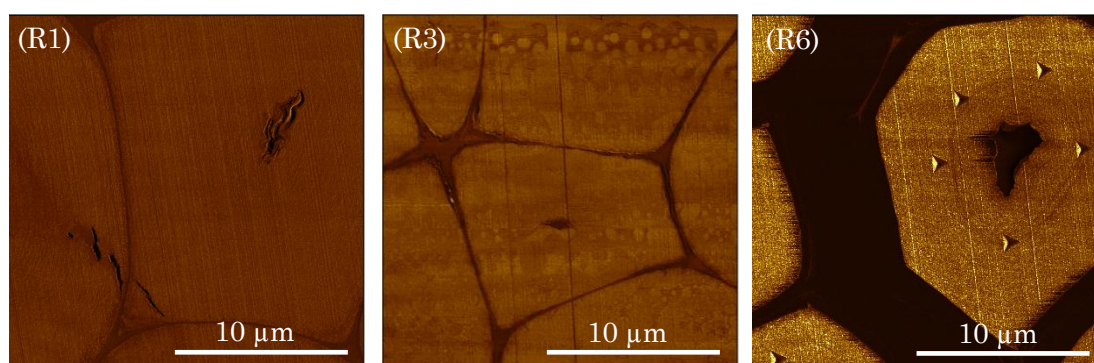
**CHAPTER III –  
EVOLUTION OF FLAX FIBER PROPERTIES  
DURING PLANT DEVELOPMENT AND RETTING**

## Graphical abstract



- ❖ What is the evolution of flax fiber properties during plant development?

**Goudenhoft, C.**; Siniscalco, D.; Arnould, O.; Bourmaud, A.; Sire, O.; Gorshkova, T.; Baley, C. Investigation of the Mechanical Properties of Flax Cell Walls during Plant Development: The Relation between Performance and Cell Wall Structure. *Fibers* **2018**, *6*, 6, doi:10.3390/fib6010006.



- ❖ What is the evolution of flax fiber properties during retting?

Bourmaud, A.; Siniscalco, D.; Falourd, X.; **Goudenhoft, C.**; Foucat, L.; Pontoire, B.; Arnould, A.; Beaugrand, J.; Baley, C. Evolution of the parietal structure and mechanical properties of flax cell walls during the retting step. *Carbohydrate Polymers*, under review.

## CHAPTER III – EVOLUTION OF FLAX FIBER PROPERTIES DURING PLANT DEVELOPMENT AND RETTING

---

Among plant fibers, flax have outstanding mechanical performances which justify their increased use as reinforcement of biocomposite materials. However, the origin of these singular properties remains unclear. The present chapter aims at obtaining better insight on the evolution of fiber mechanical performances, in relation with changes within the fiber cell wall. This investigation is conducted by coupling the innovative technic of atomic force microscopy using peak-force quantitative nanomechanical property mapping (AFM PF-QNM) analysis with biochemical and structural examinations during two major steps of the process of fiber production:

- the plant development, involving fiber formation and maturation *in planta*
- the retting step, major bioprocess linking cultivation and extraction cycles of flax fibers

### 1. Introduction

#### 1.1. The flax fiber: several uncommon features

Over the last few years, flax fibers have demonstrated their great potential as reinforcements of composite materials and their use is developing in several industrial domains, particularly in the transport sector [1]. Flax technical fibers are composed of elementary fibers, whose average performances reach a longitudinal Young's modulus of  $52.5 \pm 8.6$  GPa, a tensile strength of  $945 \pm 200$  MPa, and a strain at break of  $2.07 \pm 0.45\%$  for retted mature fibers [2]. Furthermore, their average specific mechanical properties were proven to compete with those of glass fibers (Chapter II. 5.3). In addition, the geometrical singularities of flax fibers make them an interesting model for studying cell growth [3]. Indeed, its fibers can reach a length of several tens of millimeters [3]. Moreover, the cell wall thickness in fibers is impressively high, as it can reach more than  $10 \mu\text{m}$  at maturity, while most cell walls are less than a few microns thick [4].

## 1.2. From plant development to fiber thickening

For flax, plant development can be divided in several steps (Chapter I. 2.1). The vegetative stage takes place over 50-70 days and plant growth finalizes during flowering [5]. Moreover, plant growth is itself divided into different phases. First, fast growth occurs about a month after sowing, over a 15-day period during which the stem elongates several centimeters per day. The stem grows from 10–20 to 80 cm during fast growth. Once fast growth slows down, the stem keeps growing upon floral budding, *i.e.*, until the plant is about 60–70 days old.

Complementary, the complex mechanism of fiber development (Chapter I. 2.3 to 2.5) can be simplified into two main steps: elongation and thickening [6]. Their elongation appears only at the top part of the stem, above a region called “snap point” [7]. The intensive thickening of the cell walls lasts about 60 days and takes place mainly below the snap point [7]. More precisely, the thick cell wall of fibers, called either the S2 or G-layer, with a gelatinous appearance due to its gel-like matrix similar to tension wood fibers [8], is progressively formed from the conversion of an inner sublayer known as Gn-layer [4]. Later on, the G-layer increases in thickness until complete conversion of Gn-layer which leads to a more homogeneous and compacted layer, over cell maturation [4]. Finally, fiber maturity is reached about 120 days after sowing and plants are pulled out to undergo a dew retting process [5]. Even though the course of fiber development is known, the consequences in terms of mechanical properties over plant growth have yet to be characterized.

## 1.3. The retting step

Due to the industrial potential of flax fibers, the fact that retting often takes place under very different environmental conditions from one year to another, the problem of storage, and the need for ever-increasing productivity leads to new consideration about the control and industrialization of the retting process. During dew retting, flax stems are colonized by fungi and bacteria [9]. These microorganisms secrete enzymes that accelerate the degradation of plant polysaccharides. The enzymatic activity favors the degradation of pectins [10] and the conjugation of wet and mild weather promotes the development of microorganisms (fungi and bacteria) that secrete enzymes such as polygalacturonases or xylanases. The pectins of the middle lamellae of the cortical parenchyma, the epidermis, the xylem and the fiber bundles are gradually degraded, which facilitates the extraction of bundles during scutching. The fiber bundles are also

easier to separate [11], which increases composite mechanical properties due to the improved fiber individualization and the reduction in the number of bundles [12]. Sharma (1988) showed that the limiting factor of retting is the degradation of homogalacturonans, in particular when these constituents are located in the epidermis; over retting results in the loss of the cellulose that makes up the fibers [14], arguably due to the well-known secretion of a second type of enzyme (cellulase). Although the impact of retting on the properties and performances of plant fibers has already been investigated, the conclusions of these studies are unfortunately somewhat contradictory. Van de Weyenberg et al. (2003) obtained similar mechanical properties for fiber bundles of green, half-retted and retted flax, which indicates no significant changes in performances. The same trend was highlighted by Alix et al. (2012). By contrast, other authors [17,18] have measured higher tensile strength at break and Young's modulus values for the most retted elementary flax fibers. Nevertheless, the effects of retting on the cell wall ultrastructure and mechanical properties are poorly known.

This chapter investigates the evolution of cell wall properties of flax fibers both during plant development and during the retting step. In this chapter, nanomechanical measurements were performed through AFM PF-QNM, a powerful tool for imaging possible gradients in stiffness of wood and other plant cell walls [19,20], to highlight the evolution in local indentation modulus of the fiber cell wall over both processes. In a first section, two important stages of the plant development were studied: finalization of crop growth (60 days after sowing) and maturity (120 days after sowing). Moreover, three height positions in the stem were chosen for the investigation, namely top, bottom, and middle parts of the stem. Mechanical properties of extracted single fibers over plant growth were also estimated by tensile tests, a reliable method to evaluate the average apparent tensile properties of flax fibers [2]. The cellulose contribution was also investigated over plant development using confocal Raman spectroscopy [21–23], in order to correlate the indentation modulus and the fiber structure. In a second section, as a complement to AFM PF-QNM measurements, structural and mechanical investigations were conducted at the cell wall scale on fibers from six retting stages, using X-Ray Diffraction (XRD) and solid-state Nuclear Magnetic Resonance (NMR).

## 2. Materials and methods

### 2.1. Plant material, culture conditions and retted fibers

For the study of plant development, flax stems were considered. Flax seeds (Eden variety) were used and provided by Terre de Lin (France). Sowing was done at the end of March 2016 in Lorient (France). A seeding density of 1800 plants/m<sup>2</sup> was chosen, which corresponds to the conventional density for flax cultivation [5]. A first batch of stems was pulled out 60 days after sowing (60 days batch), during the finalization of fast growth period of plant development. The second batch was pulled out at maturity, 120 days after sowing (120 days batch).

For the study of the retting process, fibers were considered. The fiber batches originate from flax plants of the Alizée variety grown in France (Hauts-de-France region) in 2011, pulled at the end of June and dew-retted in the field. These fiber batches were provided by Van Robaey Frères (France) and were carefully stored at controlled humidity and temperature (48% RH and 23°C). They are labelled R1, R2, R3, R4, R5 and R6, which corresponds to retting times of 1, 5, 9, 14, 16 and 19 days, respectively [17]. This short retting stage, which usually lasts from 20 to 50 days, is explained by favorable weather conditions for retting in 2011 [17].

### 2.2. Sample preparation prior AFM PF-QNM measurements

For each batch of stems, samples of 1 cm long were cut from stems using a razor blade, immediately after plants being pulled out. Three samples per stem, using a single stem per sampling date, were taken: the bottom one around 2 cm above cotyledons, one sample from middle height, and one at the top around 2 cm below the snap point (60 days batch) or below the first stem ramification (120 days batch). Samples were immediately placed in an ethanol/deionized water solution (1/1) for several days and stored at 4 °C.

Flax stem samples and fiber batches were then treated with a series of ethanol/deionized water solutions progressively enriched in ethanol (50%, 75%, 90%, and 100%). All dehydrated samples can so be embedded in a mixture of increasing ratios of London Resin (LR)-White acrylic resin/ethanol (25%, 50%, 75%, and 100% resin). Final resin polymerization was performed in an oven (60 °C overnight). Embedded samples were finally machined into a pyramidal shape to reduce their cross-section and cut using an ultramicrotome (Leica Ultracut R) equipped with

diamond knives (Diatome Histo and Ultra AFM). It is well-known that the procedure of sample preparation before embedding as well as the embedding medium itself can modify cell wall properties [24,25] but not that much for LR-White or other acrylic-like resin [26,27], especially with the reduction in time at each step of the embedding process used in the present study. The authors thus consider that stiffness values are not significantly affected by the embedding resin in the present study. Moreover, it is mandatory for the present study to use embedded samples prior to AFM PF-QNM measurements. First of all, the mentioned preparation reduces the artifacts coming from the sample surface roughness or border effect in order to provide reliable contact moduli [19]. In addition, in order to maintain the cell wall structure and avoid G-layer detachment and collapse due to stress release during the sample surface preparation, namely during the cutting process, it is necessary to fill the lumen of fibers by embedding [28]. Nevertheless, the local indentation modulus does not correspond to *in planta* values for stem samples, but to dry ones and cannot be assimilated to absolute values of the longitudinal cell wall stiffness [29]. However, relative values can be taken into account for suitable comparisons.

### 2.3. AFM PF-QNM Measurements

AFM measurements were performed with a Multimode AFM instrument (Bruker Corporation). PF-QNM imaging mode with a RTESPA-525 (Bruker) probe with a spring constant of 139 N/m and a tip radius between 15 and 35 nm were used. The tip and cantilever of the probe were calibrated as detailed in Arnould et al. [20]. A scan rate of 8  $\mu\text{m/s}$  and a maximum load of 200 nN were used for all the measurements. Nanoindentation measurements of the indentation modulus of the embedding resin and at some location in cell wall G-layers of each sample were also done and serve as a control for AFM measurements [20]. Using indentation modulus maps, the cell wall stiffness distribution can be analyzed using the height distribution function (Gwyddion 2.39 software) and then fitted by a Gaussian distribution (OriginPro 2017 software). This distribution yields the mean value (*i.e.* value at the maximum of the distribution) and the standard deviation of the indentation modulus. Finally, these images are used to determine the thickness of the interface between retted fibers. These interfaces are initially composed of middle lamellae, but these are gradually replaced by embedding resin during progression of the retting process.

Lines are sometimes visible on AFM images, which arise from the surface preparation. Moreover, undulations or waves can sometimes be seen too on the indentation

modulus maps. This is due to interference from the AFM laser and its reflection that sometimes occurs on the sample surface, thus inducing a bias, especially in the measurement of the adhesion force.

#### **2.4. Tensile tests on elementary fibers from non-retted stems**

For each batch of stems, samples of 10 cm long were cut from the middle part of the living stems and immediately placed in an ethanol/deionized water solution (1/1) for several days at 4 °C. Then, elementary fibers were extracted manually after immersion of the samples in 1/1-ethanol/water for at least 24h to facilitate the extraction. Fiber strain at break, strength at break, and tangent Young's modulus were determined from tensile tests on elementary fibers (NF T 25-501-2). This fiber testing experiment was performed as detailed in Chapter II. 2.7. To consider the real cell wall contribution to the fiber mechanical performances, *i.e.* to take the presence of the lumen into account, the mean effective cell wall filling ratio of fibers from mid-stem was measured optically on the stem cross-sections.

#### **2.5. Raman spectroscopy**

Raman spectra were obtained using a confocal Raman system (InduRam, Jobin-Yvon). The system consists of a 785 nm laser source with a 2 μm laser spot and a BX41 microscope (Olympus) with an objective of magnitude 50 (NA 0.50). All spectra were obtained on machined LR-White embedded stem samples (previously used for AFM measurements) by averaging 60 measurements (2 s integration time) in the 300–1800 cm<sup>-1</sup> range. Pure resin spectra were also collected to numerically remove its contribution from fibers spectra when necessary.

#### **2.6. Statistical analysis**

Multivariate statistical analyses were performed using Raman spectra. LDA (Linear Discriminant Analysis) was used to discriminate age groups and to correlate the indentation modulus with Raman spectra. All analyses were performed with The Unscrambler® software.

#### **2.7. X-Ray Diffraction**

Flax fiber bundles (diameter ~ 150 μm) were extracted from plants and mounted on a Bruker-AXS D8 Discover diffractometer. Cu Kα<sub>1</sub> radiation ( $\lambda = 1.5405 \text{ \AA}$ ), generated in a sealed tube at 40 kV and 40 mA, was parallelized using a Göbel mirror parallel

optics system and collimated to produce a 500  $\mu\text{m}$  incident beam diameter. Diffraction patterns were obtained by recording scans (10 min for each sample) in the  $2\theta$  angle range between  $10^\circ$  and  $35^\circ$ . The cellulose crystallinity index ( $I_c$ ) of the fiber bundle was calculated using the common method described by Segal et al. [30].

## 2.8. NMR investigations

To improve spectral resolution, samples were firstly hydrated with 40% water (w/w). Solid state  $^1\text{H}/^{13}\text{C}$  CP/MAS NMR experiments were performed on a Bruker Avance III 400 MHz spectrometer operating at a  $^{13}\text{C}$  frequency of 100.62 MHz. A double resonance H/X CP/MAS 4 mm probe was used. The samples were spun at a rate of 9 kHz at room temperature. The cross-polarization pulse sequence parameters were as follows: 3.0  $\mu\text{s}$  proton  $90^\circ$  pulse, 1.75 ms contact time at 37 kHz and 10 s recycle time. Typically, the accumulation of 5120 scans was used. The carbonyl signal of glycine (176.03 ppm) was used as an external standard for the chemical shift of the  $^{13}\text{C}$  NMR spectra. Before performing the Fourier transform, all data sets were processed using Gaussian multiplication parameters of LB = -20 Hz and GB = 0.05.

To determine the cellulose crystallinity and the general morphology of the C4 region of the samples, we adopted the advanced approach published by Larsson & al. [31]. This approach uses four lines for the crystalline part and three lines for the amorphous part. In the crystalline part, three Lorentzian lines correspond to cellulose Cr ( $I_\alpha$ ) (89.4 ppm), cellulose Cr ( $I_{\alpha+\beta}$ ) (88.7 ppm) and cellulose Cr ( $I_\beta$ ) (87.7-87.8 ppm). In addition, a Gaussian line represents the para-crystalline (PCr) contribution (88.5-88.6 ppm). In the amorphous part, two Gaussian lines correspond to accessible surface (AS; 83.2 and 84.1-84.2 ppm) and one stand for inaccessible surface (IAS; 83.5-83.7 ppm). All parameters of these different lines (chemical shift, peak half-width and peak area) were determined with a least squares fitting method using Peakfit® software [32]. The cellulose crystallinity was determined as the peak area ratio between four lines of the crystalline part and seven lines for the cellulose C4 region. Based on NMR signal areas from amorphous cellulose over total cellulose surfaces and a microfibril model comprising cellulose chains having a width of 0.57 nm [33], the lateral fibril dimensions (LFD) and the lateral fibril aggregate dimension (LFAD) can be evaluated considering a square cross-sectional cellulose microfibril model for NMR analysis.

To characterize molecular dynamics, we used variable contact time (VCT)  $^{13}\text{C}$  CP/MAS spectroscopy. Twenty CP/MAS spectra were acquired using contact times from 10  $\mu\text{s}$

to 9 ms, leading to the accumulation of 920 scans. The evolution of carbon line area as a function of the contact time is modelled on the basis of a two-proton reservoir model as previously described in literature [34,35].

### **3. Results and discussion – Fiber properties during plant development**

#### **3.1. Indentation modulus and morphology of fiber cell walls analyzed by AFM Peak Force QNM measurements**

To monitor the fiber indentation modulus along the stem during plant growth, bottom, middle, and top parts of a single stem were analyzed. Figure III-1 shows AFM images from three samples of a single 60-day old plant, where fibers during thickening of the cell wall are visible.

The top part of the stem is characterized by fibers with thinner cell walls (Figure III-1 (A)). Their low indentation modulus ( $13.0 \pm 2.5$  GPa) is attributed to predominant loose portions of the Gn-layer, whereas the G-layer is almost invisible. For this newly formed layer in the thickened cell wall, the loose portions of the Gn-layer (schematized on Figure III-1) might result from long galactan chains present in the nascent version of tissue- and stage-specific rhamnogalacturonan-I. The galactan chains separate cellulose microfibrils, leading to their loose packing [4].

At mid-stem (Figure III-1 (B)), gradients in terms of local indentation modulus are visible on fiber cell walls, with averages values from  $14.0 \pm 1.8$  GPa for the Gn-layer to  $18.0 \pm 1.9$  GPa for the G-layer [20]. The looser appearance of the Gn-layer and its lower indentation modulus compared to the G-layer argue for a mechanism of aggregation of cellulose microfibrils and entrapment of the matrix material, during the maturation of the cell wall from Gn- to G-layer. This maturation could induce a change in the cell wall structure that leads to changes in the mechanical properties; the tensile stress in the transverse direction within the Gn-layer are released with maturation, which leads to the compaction of cellulose microfibrils in the G-layer [8,36]. However, when the fibers from the bottom part of the plant are considered (Figure III-1 (C)), although a thin Gn-layer is still visible at this stage of growth, the major portion of the thickened cell wall is much more homogeneous and gives higher mechanical properties (an indentation modulus of  $19.5 \pm 2.9$  GPa). In fact, the G-layer increased in thickness until the almost complete conversion of the Gn-layer, leading to a more homogeneous and compacted layer [4].

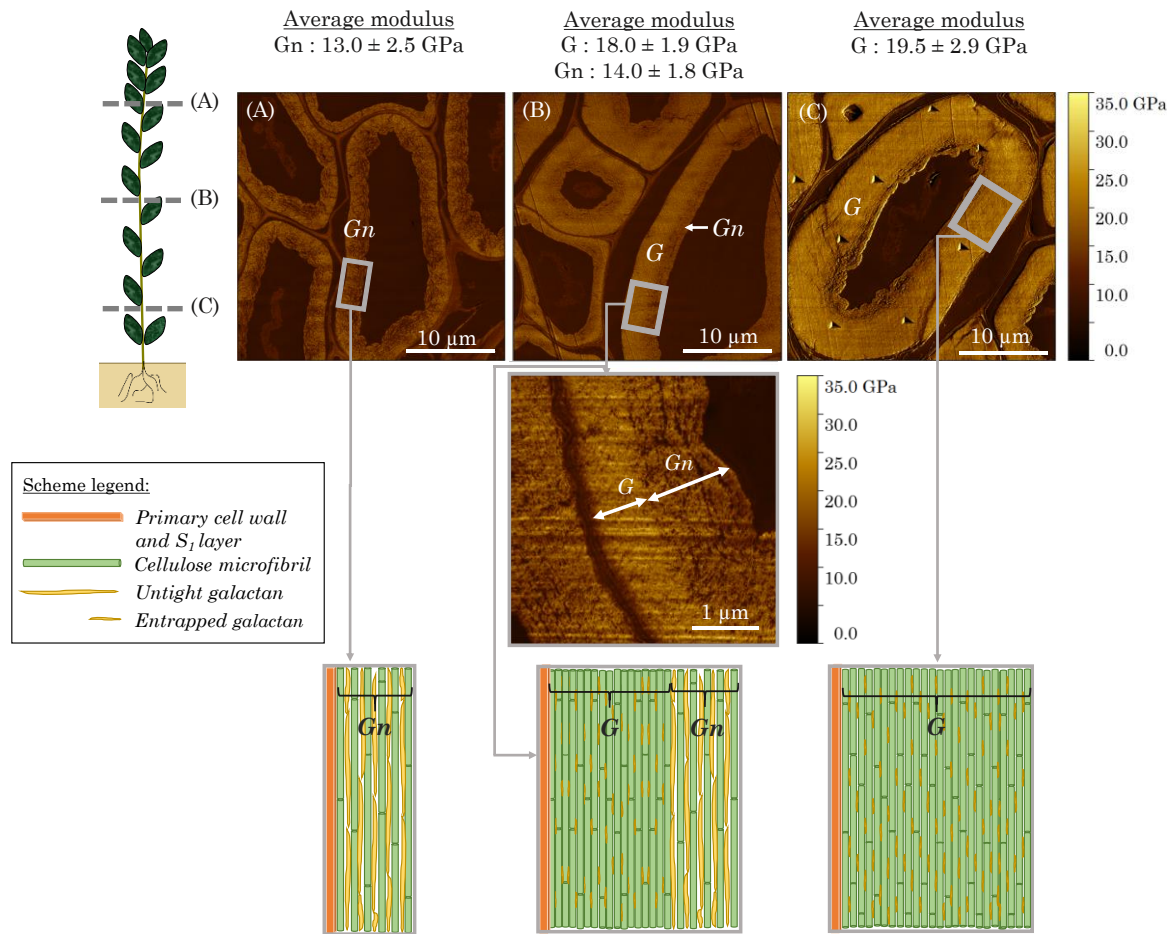


**Figure III-1. AFM PF-QNM mapping of the indentation modulus of developing flax fibers below snap point at top (A), middle (B), and bottom (C) parts of a single stem of Eden at the end of fast growth period (60 days after sowing).**

(A, B): The Gn-layer visible at the top and middle parts is characterized by a low modulus and loose portions. These properties of the Gn-layer are attributed to cellulose microfibrils separated by long galactan chains present in nascent rhamnogalacturonan-I [4].

(B, C): The G-layer at the middle and bottom parts has a higher modulus and is more homogeneous. The G-layer is assumed to be characterized by the entrapped rhamnogalacturonan-I with partially trimmed off galactan side chains and packed due to lateral interactions microfibrils [4]. Indent triangular prints on (C) come from preliminary nanoindentation calibration.

Visualization of the differences in mechanical properties between distinct cell wall layers in developing flax fibers clearly matches the previously published pictures obtained by immunolabeling with LM5 antibody [37,38], with LM5 specifically recognizing beta-1,4-galactans [39]. Based on these works, the Gn-layer has a much higher density of labeling than the G-layer, indicating that modification of the rhamnogalacturonan-I side chains is important for the developing of cell wall mechanical properties. Finally, from a mechanical and structural point of view, at a

given time, the growing flax plant gathers, from its top to its bottom, all developing steps of the fiber cell walls.

To evaluate the development and properties of the fiber cell wall along the stem at fiber maturity (corresponding to the conventional pulling time), additional AFM images were collected. Figure III-2 shows that fibers from all stem locations exhibit thick cell walls with homogeneous indentation moduli within single fibers, but also between fibers ( $17.3 \pm 1.7$  GPa for the top,  $18.4 \pm 1.3$  GPa for the middle, and  $17.7 \pm 1.4$  GPa for the bottom fibers).

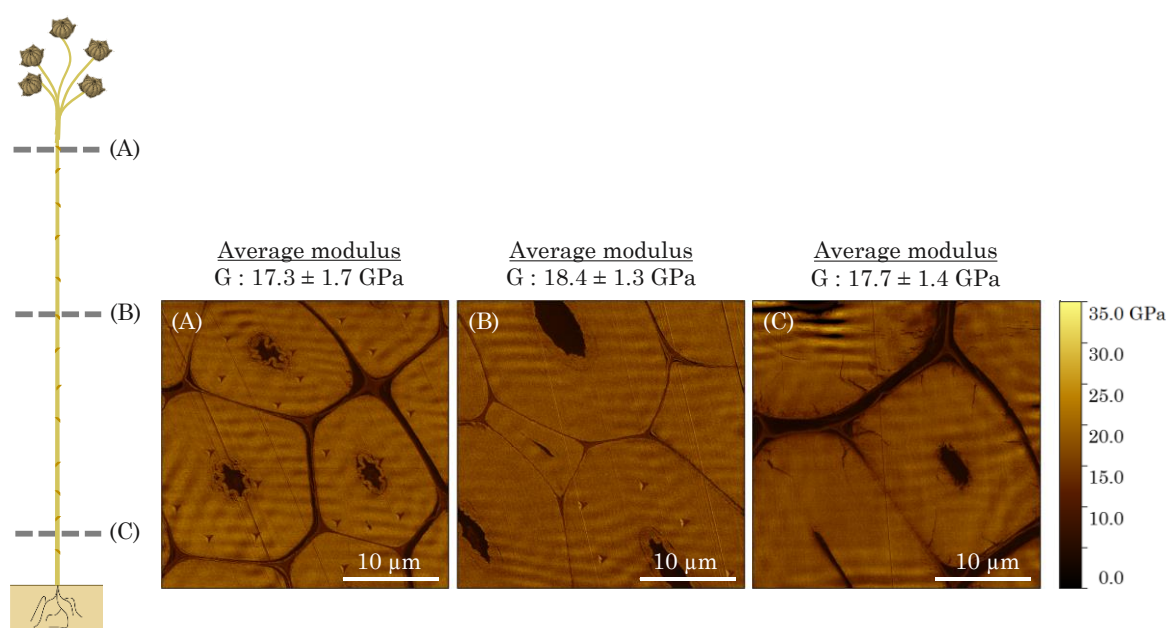


**Figure III-2.** AFM PF-QNM mapping of the indentation modulus of flax fibers from a single mature plant of Eden (120 days after sowing) at the top (A), middle (B), and bottom (C) parts of the stem. Mature fibers are characterized by thick cell walls having a homogeneous modulus for all studied parts of the stem. Apparent waves on the map come from AFM laser interferences that lead to adhesion force artifacts and were not taken into account in the statistical analysis.

The loose Gn-layer is still visible in some fibers, mainly in the top location (Figure III-2 (A)). This unfinished Gn-layer transformation, representing only a negligible part of the whole fiber section, could be attributed to a lack of time to reach fiber maturity at the top level, as these fibers were the latest to be formed. Even though strong but stable wave artifact (coming from AFM laser interferences that lead to adhesion force artifacts) is visible on every image given in Figure III-2, it does not prevent the comparison of neither the changes in the fiber morphology nor the relative average indentation modulus. Finally, at maturity, fibers are well formed with

thickened cell walls, *i.e.* small lumens. Moreover, mature fibers exhibit a high and homogeneous indentation modulus whatever their location along the stem. In addition, diversity in absolute values may exist between plants, since the materials studied are of biological origin. This may explain to a large extent why the indentation moduli of G-layers in Figure III-2 are sometimes slightly lower than those in Figure III-1 (B and C).

### 3.2. Tensile tests performed on elementary fibers

In order to evaluate the influence of the Gn-layer at a larger scale, mechanical properties of elementary fibers were characterized by tensile tests. Fibers from mid-stem for both 60-day-old plants and mature ones were tested, as only the former batch showed a Gn-layer on AFM images. Figure III-3 gives the comparison between the properties of elementary flax fibers extracted from the plants previously mentioned.

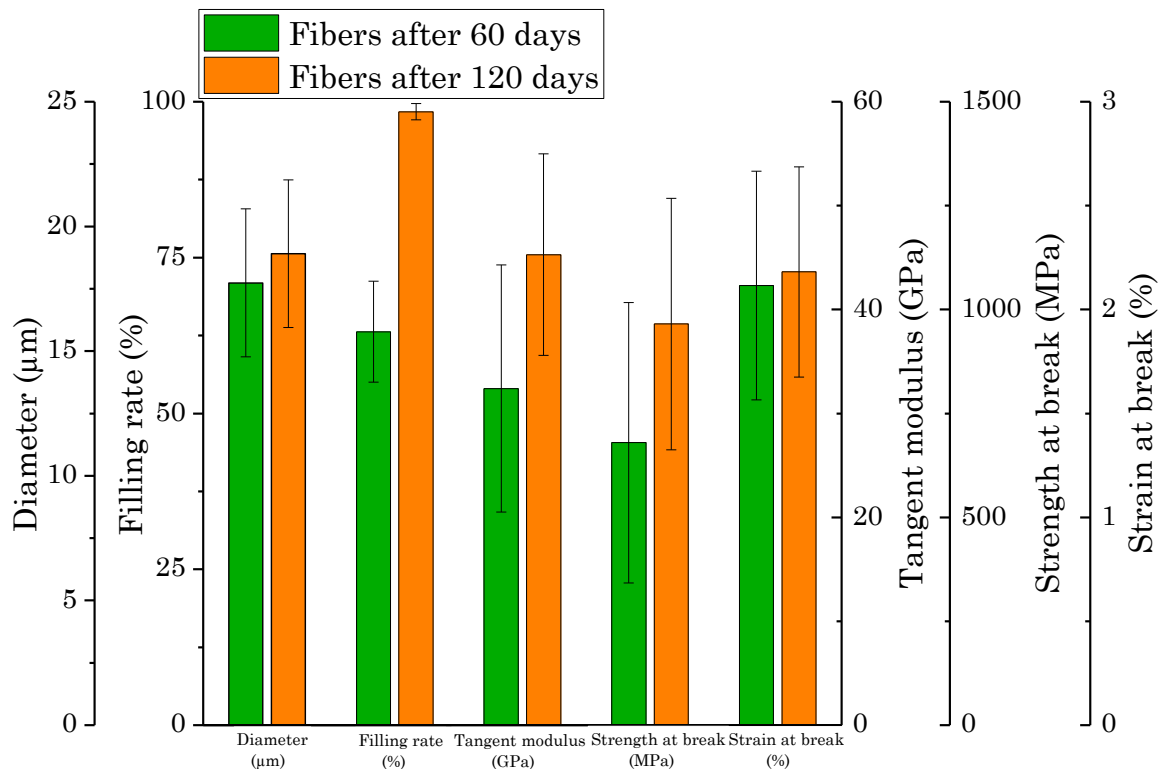


**Figure III-3. Properties of elementary flax fibers at mid-stem height and mechanical performances obtained from tensile tests performed on fibers extracted from plants of 60 days and 120 days after sowing.**

For developing fibers with a filling rate of  $63.1 \pm 8.1\%$ , an average tangent Young's modulus of  $32.4 \pm 11.9$  GPa, and a strength at break of  $680 \pm 337$  MPa were estimated as cell wall properties, whereas much higher performances were observed for mature

cell walls (namely, a tangent modulus of  $45.3 \pm 9.7$  GPa and a strength at break of  $965 \pm 302$  MPa). However, both batches exhibit a similar strain at break, namely  $2.12 \pm 0.55\%$  for developing fibers and  $2.18 \pm 0.51\%$  for mature ones. It is important to keep in mind here that values of indentation modulus in the fiber cell wall are lower than the longitudinal tangent Young's modulus due to the anisotropic behavior of the cell wall layers [29]. In addition, the relationship between the indentation modulus and the tensile modulus of developing fibers as well as of mature fibers is in accordance with the values given in the literature [40].

### 3.3. Composition of the cell wall approached by Raman spectroscopy

To highlight potential differences in terms of composition, an analysis combining Raman spectroscopy with a linear discriminant analysis was performed. The degree of plant maturity was used as a parameter, *i.e.* all Raman spectra from 60 day samples were used as a single batch, while 120 day samples were identified as the other batch.

The LDA led to 89% of correctly discriminated spectra for the 60 days batch and 83% for the 120 days batch. For each batch, an average Raman spectrum was computed from the correctly discriminated spectra only (Figure III-4 (A)). By comparing average spectra, the same Raman lines can be identified, proving that the qualitative cell wall composition is unchanged over cell wall development. In addition, the difference spectrum of the average spectra of the two batches is also displayed (Figure III-4 (B)). From this difference spectrum, several Raman lines allow for distinguishing discriminant between the two levels of maturity. Firstly, the Raman line  $842\text{ cm}^{-1}$  decreases with fiber maturity; this line can be attributed to pectic polysaccharides such as galactans [22,41]. This decrease is in accordance with the changes in the galactan structure occurring during the transformation of the Gn-layer into the G-layer, previously highlighted in Figure III-1, namely long galactan chains are partially trimmed off from the rhamnogalacturonan-I backbone by the action of tissue-specific galactosidase [4].

Secondly, Raman lines  $382\text{ cm}^{-1}$ ,  $1097\text{ cm}^{-1}$ ,  $1123\text{ cm}^{-1}$ , and  $1385\text{ cm}^{-1}$  also differentiate the fiber maturity. Similar wavelengths ( $379\text{ cm}^{-1}$ ,  $1095\text{ cm}^{-1}$ ,  $1120\text{ cm}^{-1}$ , and  $1379\text{ cm}^{-1}$ ) have been reported in the literature as characterizing microcrystalline cellulose [22], while  $1380\text{ cm}^{-1}$  was found to selectively characterize the G-layer of poplar wood [42]. Moreover, these wavelengths were also assigned to specific vibrational modes related to molecular groups of cellulose [23]. It can be assumed that

changes in the cellulose microfibrils appear with fiber maturity; this could be linked to the increase of the microfibrils volume fraction during their aggregation (scheme in Figure III-1), leading to better mechanical properties, namely a higher cell wall indentation modulus characterizing the mature fibers.

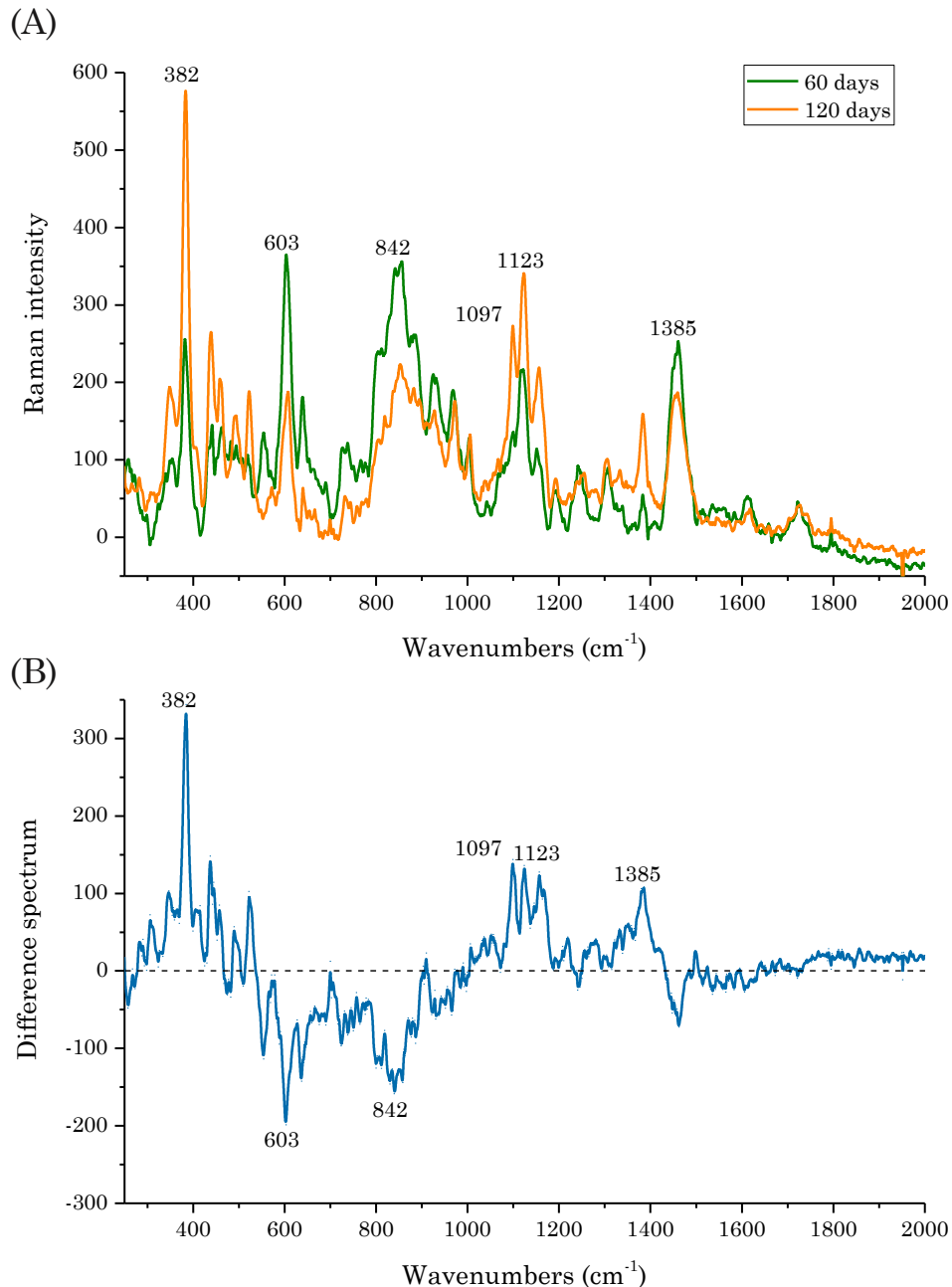


**Figure III-4. Average Raman spectra obtained from the correctly discriminated spectra of the 60 day and 120 day samples (A) and their difference spectrum (B). Raman lines 382 cm<sup>-1</sup>, 1097 cm<sup>-1</sup>, 1123 cm<sup>-1</sup>, and 1385 cm<sup>-1</sup> (attributed to cellulose) increases with fiber maturity. The Raman line 842 cm<sup>-1</sup> (attributed to galactans) decreases with fiber maturity, as does the 603 cm<sup>-1</sup> one (which corresponds to the embedding resin, whose content decreases as lumen size decreases with fiber wall thickening).**

## 4. Results and discussion – Fiber properties during retting

### 4.1. Indentation modulus and morphology of fiber cell walls analyzed by AFM Peak Force QNM measurements

For all levels of retting, AFM PF-QNM modulus mapping (Figure III-5) reveals a homogenous indentation modulus across the flax cell walls without any gradient (*i.e.* the Gn-layer is not visible at these stages). This homogeneity indicates that the fibers are well-matured, including the R1 level which is the batch corresponding to the pulling-out stage. Moreover, the indentation modulus of R1 is of the same order of magnitude as values obtained on the mature G-layer measured on non-retted fibers based on stem cross-sections from mature plants (Figure III-2).

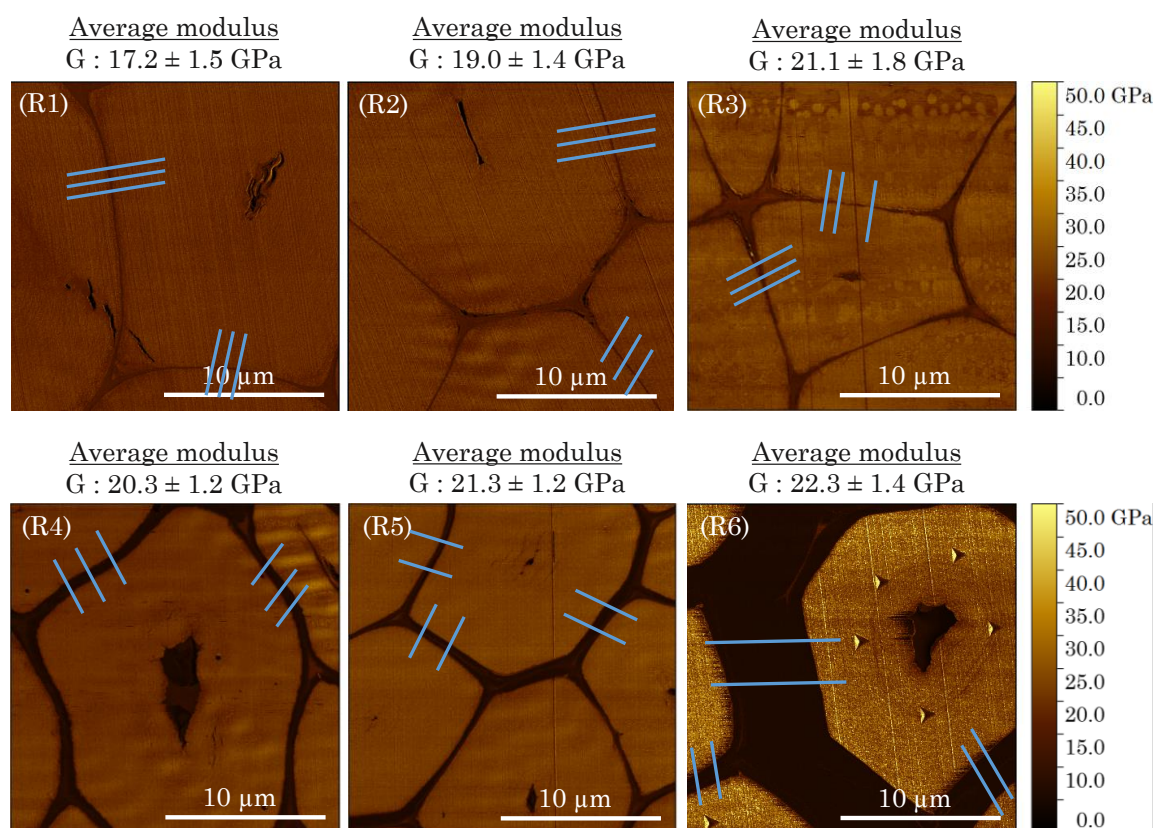


**Figure III-5. AFM PF-QNM modulus mapping from R1 to R6 retting degree of Alizée scutched fibers. The blue lines correspond to the direction and position where the thickness of the interfaces between fibers were measured.**

Interestingly, a general increase of the indentation modulus of fiber cell walls is obtained during retting (about +30% from levels R1 to R6). To our knowledge, this stiffening has never been demonstrated at the cell wall scale; however, a similar tendency of increased mechanical properties with retting has been demonstrated on

the same fiber batches, in another study focused on the tensile characterization of single flax fibers [17]. In this latter study, the fiber Young's modulus was shown to increase by +44% between levels R1 and R6. The difference in increase between Young's modulus and indentation modulus is due to the anisotropic nature of the cell wall (Eder et al, 2013) as well as the order of magnitude of the scale of investigation. Therefore, there is a significant evolution of the overall fiber and cell wall stiffness during the retting process, whatever the investigation scale. Although (Martin et al., 2013) did not conduct a structural investigation, these authors used TGA analysis and hot-water/EDTA extraction to show a decrease in cortical parenchyma and middle lamellae components, which is consistent with a dew-retting process. Similar conclusions were obtained for hemp fibers by Placet et al. [14], as these authors demonstrated a significant decrease of pectic components. Moreover, for hemp, a decrease of xylan components was observed; xylan plays a determining role in the cell wall architecture and could potentially be linked to changes in the stiffness of the cell wall. According to Placet et al. [14], this major structural evolution is linked to the worsened mechanical performance of single fibers, demonstrating that the tested hemp batch was over-retted and exposed to a profound, and therefore detrimental, enzyme degradation. These authors also highlight the great uncertainty in monitoring hemp retting compared to flax cultivation. In the latter case, exogenous parameters (such as temperature) are constantly checked by calculating cumulated temperature data [43]. In view of these considerations, we can exclude over-retting in the present case and the positive evolution of cell wall mechanical properties should be linked rather to a change in the cell wall ultrastructure or conformation, such as an evolution of the cellulose crystallinity. These points are explored further in the next subsection.

Complementary, AFM PF-QNM investigations also provide interesting information about the bundle structure during the retting process. As shown in Figure III-5, middle lamellae are visible for the first three retting levels (R1-R3) and brings cohesion between surrounding fibers, especially at the fibers junctions. With the increase of retting level and development of enzymatic action, the middle lamellae progressively disappear until it represents only a few fragments, as in the case of the R4 sample where it is still present but not physically linked with the fiber primary wall. At the same time, the interfiber space is filled with embedding resin, indirectly showing the importance of retting for enhancing the fiber impregnation in composite materials. Figure III-6 (A) illustrates the qualitative evolution of the thickness of the interface between fibers (*i.e.* middle lamellae and/or embedding resin) throughout the

retting process and the impact on fiber divisibility. Distance values correspond to the average interface length between fibers calculated from ten profile measurements, as represented by blue lines on Figure III-5. These observations are supported by additional mechanical investigations (Figure III-6 (B)). In fact, local measurements performed by AFM PF-QNM in the middle lamellae region yield indentation moduli of  $12.5 \pm 0.7$  GPa,  $13.6 \pm 0.8$  GPa and  $12.4 \pm 1.7$  GPa, for R1, R2 and R3 samples, respectively. On the other hand, similar investigations carried out on the most retted samples (R4, R5 and R6) give results between  $5.4 \pm 0.2$  GPa and  $6.0 \pm 0.3$  GPa, which correspond to the resin indentation modulus.

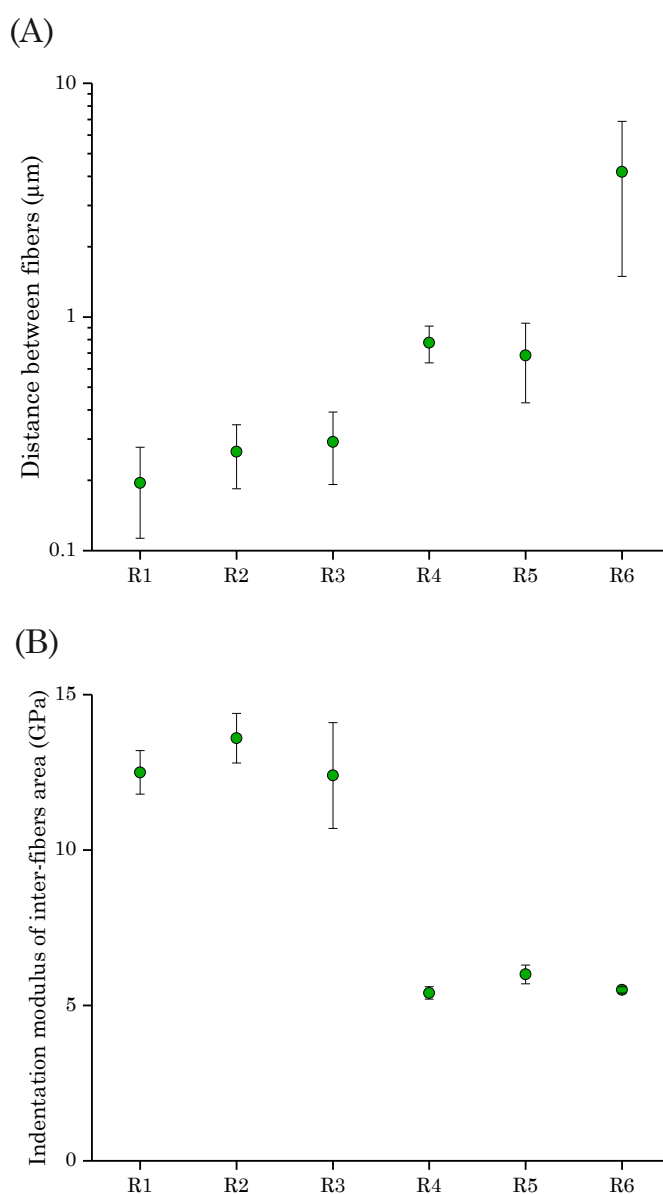


**Figure III-6. Evolution of the distance (A) and indentation modulus (B) between fibers along the retting process.**

The resin indentation modulus is slightly higher here than the literature value [20], presumably due to the presence of a residual middle lamellae fraction in the interfiber space, especially in R4 and R5 samples. Values obtained in the middle lamellae region are slightly higher than those reported in the literature for wood by nanoindentation in the cell corner middle lamellae [44]. A knowledge of middle lamellae is of great interest here, especially to highlight their cohesive function in fiber bundles; nevertheless, these data sets must be considered with caution, being only of relative value to compare cell wall indentation moduli, and should not be used, for example, to establish an absolute value of the longitudinal Young's modulus in numerical or micromechanical modelling.

#### **4.2. Monitoring of crystallinity degree during retting using X-ray diffraction and NMR analysis**

In the literature, an increase in the crystallinity of plant fibers during retting has been demonstrated based on crystallinity index measurements obtained by X-Ray diffraction. Zafeiropoulos et al. [45] reported an increase of the crystallinity index from 64.55% for green flax to 71.64% for dew-retted flax. Moreover, Marrot et al. [46] reported an increase in the degree of crystallinity of hemp fibers following retting of the plant in the field. These authors showed that the crystallinity index increased from 45.8% for green hemp, to 71.3%, 71.2% and 74.5% after 14, 31 and 45 days, respectively, of dew-retting.

In the present case, the cellulose crystallinity of fiber cell walls of R1 and R6 only was investigated by both NMR and XRD. Indeed, NMR experiments are time-consuming to prepare and carry out, and require considerable processing time which leads us to concentrate on these two extreme cases. Figure III-7 shows the  $^{13}\text{C}$  CP/MAS NMR spectra obtained for R1 and R6 samples. These spectra are characteristic of type-I cellulose [47] for the two samples studied. Characteristic hemicelluloses signals are also observed as part of the main constituents of flax plant cell walls. To obtain information on the supramolecular structure of cellulose fibrils in the plant cell walls, the C4 region between 77 and 92 ppm is deconvoluted here using the model of Larsson and Wickholm [31].

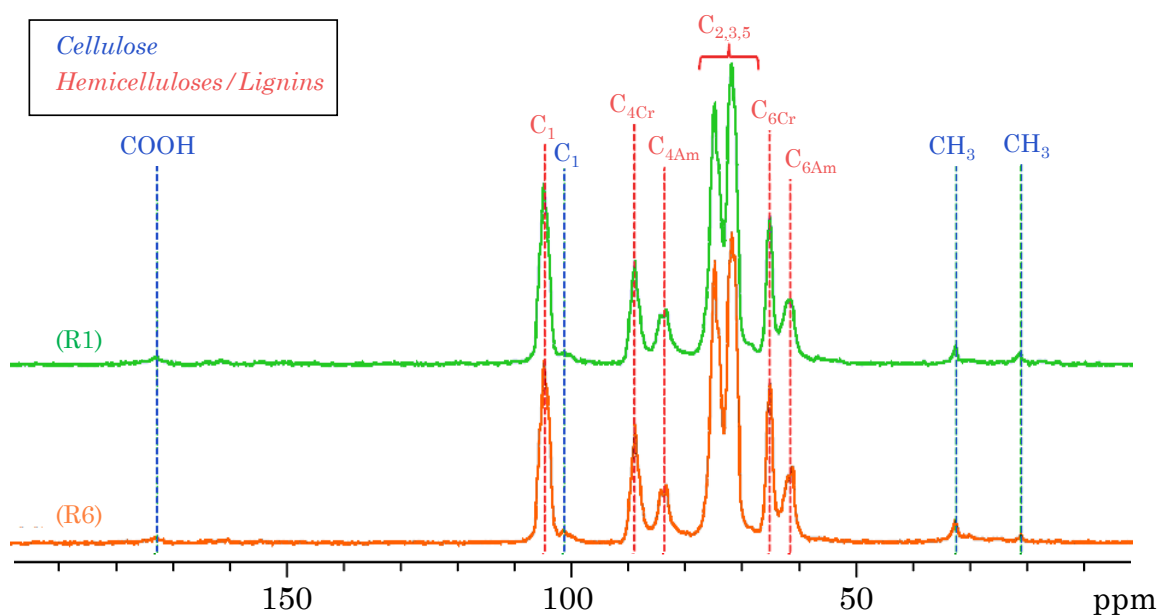
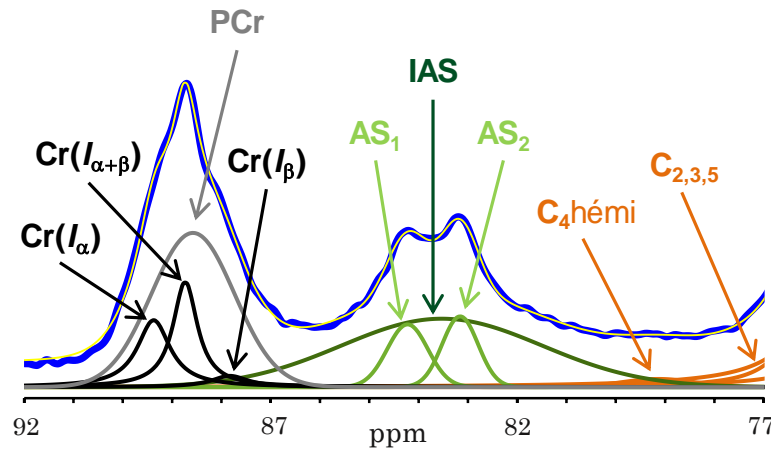


Figure III-7. Solid state  $^{13}\text{C}$  CP/MAS NMR spectra for R1 and R6 samples.

Figure III-8 illustrates this deconvolution, while Table III-1 reports the signal assignments with their corresponding values of full width at half maximum (FWHM) and normalized areas. The crystallinity appears higher for the R6 sample (56%) than for the R1 sample (52%). Although the NMR-derived crystallinity values are lower than those obtained by XRD, the observed trend is in line with the measurements already available on non-retted and retted flax or hemp fibers. These literature measurements were carried out using XRD on fiber bundles, which can make their interpretation more complex. Indeed, during the data processing of bundles, the signal corresponding to the amorphous constituents can be influenced by components outside the cell walls, in particular the residues of middle lamellae which may be present, especially for samples with a low retting level. In the case of NMR analysis, this problem does not arise, as the processing of data from C4 cellulose-related signals restricts the scope of investigation solely to the cell wall components.

(A) R1 (crystallinity: 52%)



(B) R6 (crystallinity: 56%)

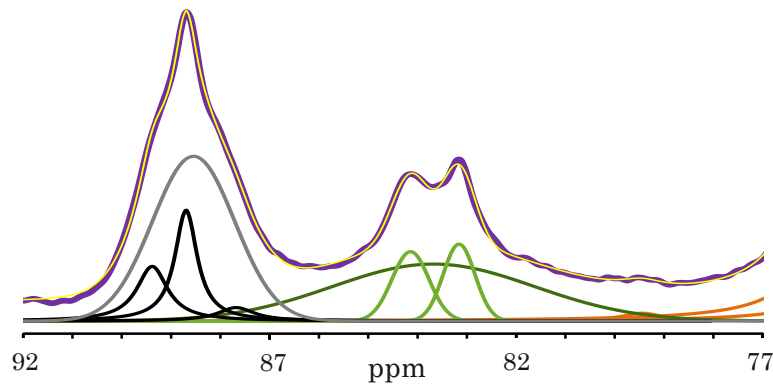
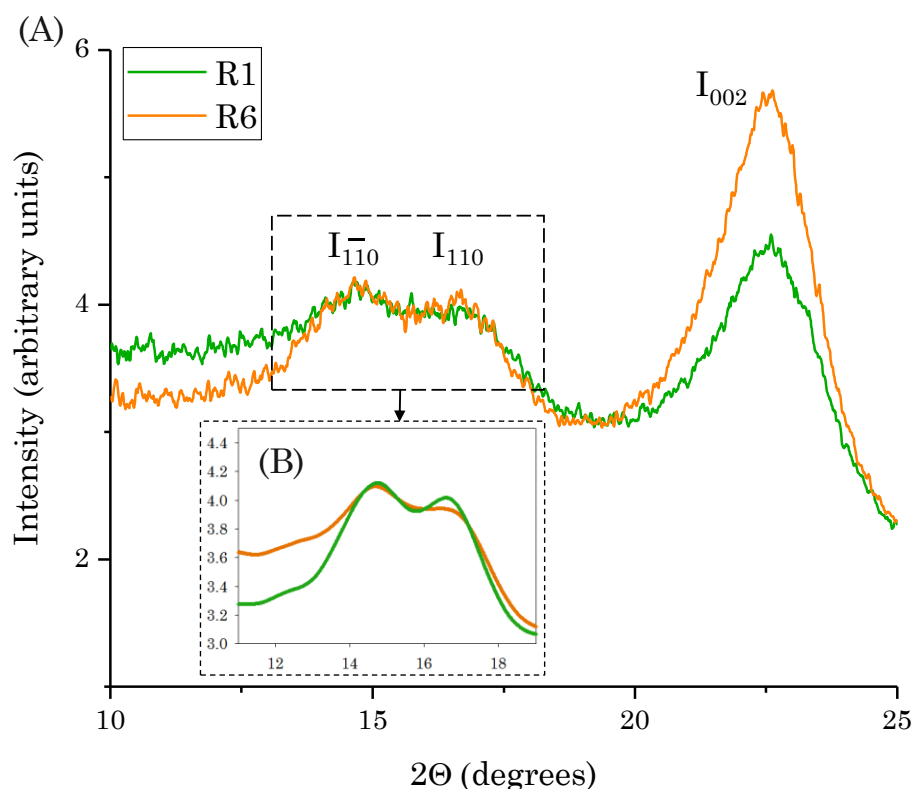


Figure III-8. Deconvolution of C4 region with crystalline forms Cr ( $I_{\alpha}$ ), Cr ( $I_{\beta}$ ) and Cr ( $I_{\alpha+\beta}$ )(black), para-crystalline form (PCr)(grey), accessible fibril surface (AS)(green), and inaccessible fibril surface (IAS)(dark green) signals for R1 (A) and R6 (B).

Table III-1. Calculated parameters obtained from the C4 region deconvolution of  $^{13}\text{C}$  CP/MAS NMR spectra for R1 and R6 samples. FWHH = Full Width at Half Height.

		Peak assignment						
		Cr( $I_{\alpha}$ )	Cr( $I_{\alpha+\beta}$ )	PCr	Cr( $I_{\beta}$ )	AS	IAS	AS
$\delta$ (ppm)	R1	89.37	88.73	88.58	87.83	84.22	83.53	83.16
	R6	89.38	88.70	88.54	87.68	84.14	83.68	83.16
FWHH (Hz)	R1	81	60	199	90	98	482	86
	R6	76	55	197	90	88	484	76
Normalized area (%)	R1	8	10	32	2	6	35	7
	R6	7	10	37	2	7	31	7

To supplement the crystallinity data obtained by NMR, the XRD patterns of R1 and R6 samples are presented in Figure III-9.



**Figure III-9. X-Ray Diffraction patterns of R1 and R6 flax samples.**

As usual for plant samples, the major crystalline peak occurs at around  $22.4^\circ$ , which corresponds to the crystallographic plane (002) representative of type-1 cellulose. In the case of cellulose II conversion, new peaks attributed to (110) and (012) planes could be observed around  $20^\circ$  [48], but are not present here. The crystallinity index (CI) is calculated according to the Segal method; although this method is questionable [49], it is suitable for obtaining rapid measurements and therefore abundant published data are available for purposes of comparison. Estimated CI for R1 and R6 are 31% and 44%; thus, R1 exhibits a low CI compared to R6. As observed by NMR analysis, an increase of the CI is highlighted between R1 and R6 samples, but this latter is more pronounced by XRD analysis. This is probably due to the large amount of residual amorphous components remaining in the middle lamellae areas and inducing an error into the calculation of CI, based on the ratio between crystalline and amorphous materials at the bundle scale. For this reason, the CI of R1 sample is probably underestimated. To check this hypothesis, it is possible to study the behavior of the diffraction peaks at  $2\theta = 14.8^\circ$  and  $2\theta = 16.4^\circ$ , corresponding to the  $(\bar{1}10)$  and (110)

crystallographic planes, respectively. When the crystalline cellulose content is high, these two peaks are more pronounced [50], but when the fibers contain large amounts of amorphous material (such as lignin, hemicelluloses, pectins and amorphous cellulose), these two peaks are smoothed out and appear as a single broad peak. The smoothing of this specific area leads to the result shown in Figure III-6. Interestingly, the two peaks appear to be more clearly defined for R6 than R1, suggesting that the content of amorphous components is higher in the R1 sample.

### **4.3. Investigation of cell wall biochemical structure using NMR**

As mentioned, Table III-1 gives the detailed characteristics of the different lines obtained after deconvolution (Figure III-8) of the C4 region of the NMR spectra presented in Figure III-7. Two main observations can be drawn from the data set. Firstly, the inaccessible surface of cellulose decreases significantly with retting, decreasing from 35 to 31% and, at the same time, the fraction of paracrystalline cellulose increases from 32 to 37%. The paracrystalline cellulose is an intermediate form of cellulose, but which is considered as crystalline. It is noteworthy that, at the same time, the proportion of crystalline cellulose (Cr) remains unchanged at 20% and 19%, respectively, for R1 and R6. The same applies to the accessible surface, which remains constant (about 13%) for both levels of retting. These data indicate that the inaccessible fraction of cellulose is the main component impacted by retting, representing a component evolving towards paracrystalline cellulose. Owing to this data set, it is possible to determine morphological parameters related to the structure of cellulose and microfibrils. From the determination of crystallinity, we can estimate the LFD (Lateral Fibril Dimension) and the LFAD (Lateral Fibril Aggregate Dimension) according to the method of Zuckerstätter et al. [51]. The LFD of samples R1 and R6 are 4.1 and 4.5 nm, respectively, while the LFAD slightly decreases during retting from 17.1 nm for R1 to 16.3 nm for R6.

Figure III-10 gives a schematic representation of the flax cellulose elementary microfibrils that reflects the differences in structure highlighted by the solid NMR spectra. The basic pattern chosen here with 16 fibrils is compatible with the relative scale of the constituents, the aggregate being approximately 4 times larger than the elementary fibril.

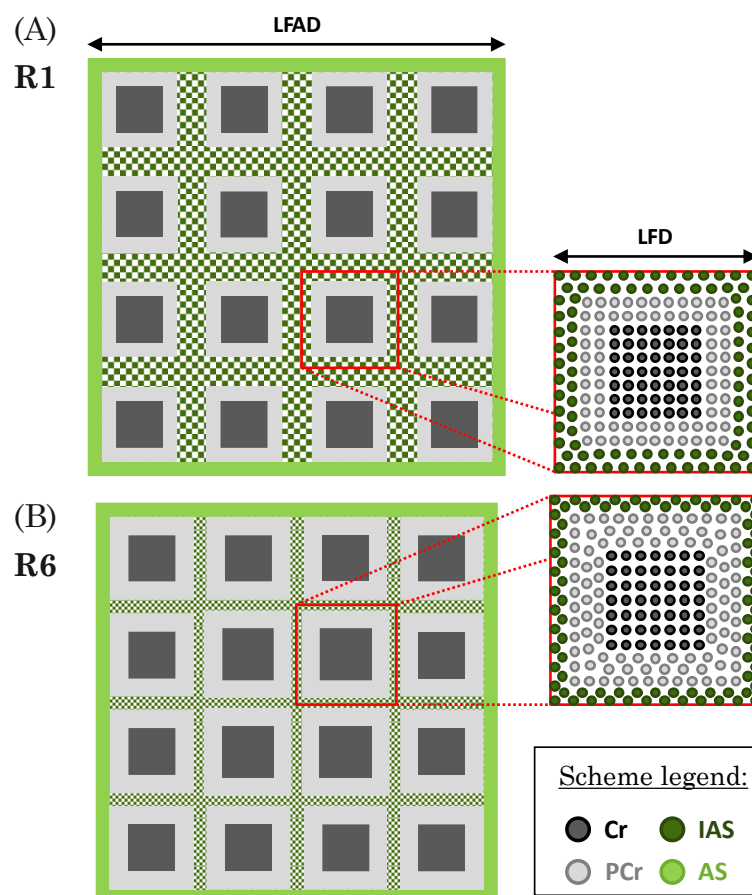


**Figure III-10. Schematic representation of the flax cellulose elementary microfibrils structure. Cr: crystalline cellulose, PCr: paracrystalline cellulose, IAS: inaccessible surface, AS: accessible surface, LFD: lateral fibril dimension and LAFD: lateral fibril aggregate dimension. The surface areas (left part) and the number of points (zoomed views) in the scheme are proportional to the area of the corresponding NMR signals.**

Thus, a slight decrease in LAFD corresponding to a densification in aggregate size is visible, which is well correlated with the decrease in inaccessible surface area (IAS). This is probably caused by a decrease in porosity (as illustrated in Figure III-10) within cell wall polymers, and consequently a compaction of cellulose within the walls in which the cellulose microfibrils are located. The flax cell walls evolve during their maturation, in particular with a transition from the Gn- to the G-layer. This phenomenon is assumed to result in a compaction of the cell walls under the action of galactosidases, responsible for the cutting of the long galactan chains which are then easily entrapped between the cellulose fibrils (Figure III-1). Even if this compaction occurs throughout plant growth, it is not excluded that maturation could be completed during the retting period. Thus, most of the cellulosic components in the R6 sample become truly isolated, being surrounded by densified layers of inaccessible surfaces (IAS). This does not apply in the case of degradation of surrounding layers, which

could occur due to over retting [14] or prolonged thermal exposure [18]. The phenomenon of shrinkage described above can be linked to the increase of paracrystalline cellulose; in fact, under the effect of compression, a fraction of amorphous cellulose can evolve towards a paracrystalline form.

The last part of this NMR investigation involves using the two-proton reservoir model [34,35] to study the evolution of the crystalline and amorphous C4 phase areas as a function of the contact time. Figure III-11 shows the experimental data obtained for R1 and R6 samples along with model estimates. The associated relaxation time values are summarized in Table III-2.

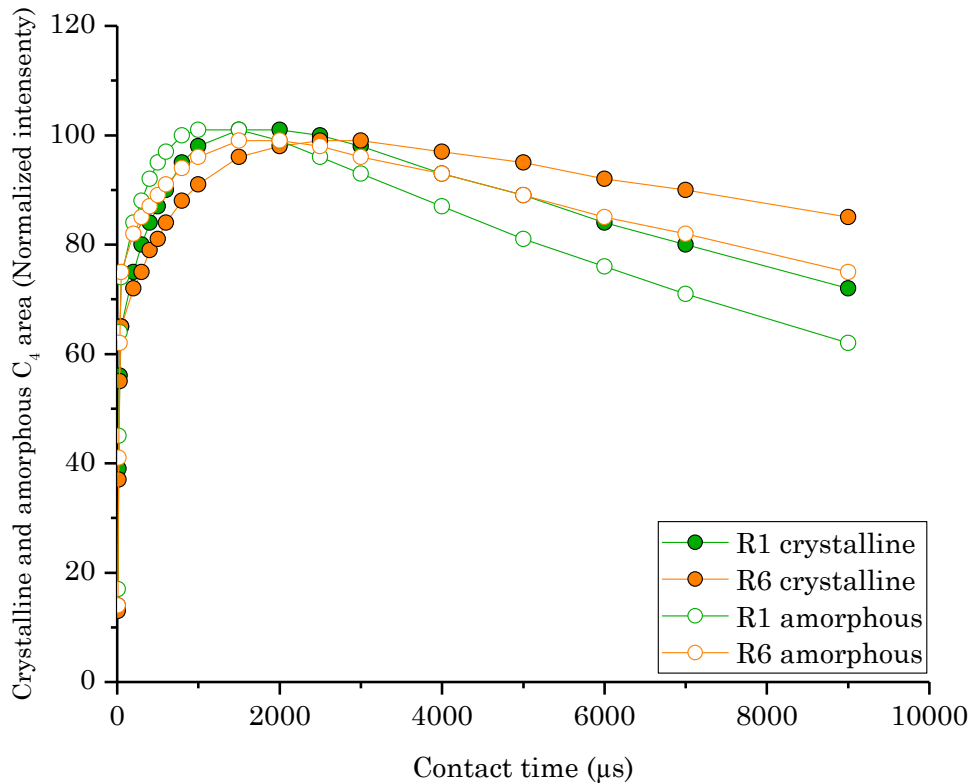


**Figure III-11. Evolution of the crystalline and amorphous C4 area according to the contact time. Points showed correspond to experimental values, and curves have been obtained through the use of a two proton reservoir model [34,35].**

**Table III-2. Relaxation time values extracted from the two proton reservoir model [34,35] for the crystalline and amorphous C4 phase areas of R1 and R6 samples.**

	$T_{1\rho}^H$ (ms)		$T_{CH}$ ( $\mu$ s)		$T_{HH}$ ( $\mu$ s)	
	R1	R6	R1	R6	R1	R6
$C_{4cr}$	19.3	34.7	15	16	687	947
$C_{4am}$	14.7	23.0	15	16	501	772

Higher values of  $T_{1\rho}^H$  for the R6 sample compared to R1 are observed. The increase of these values highlights a drop in the mobility, which could be associated with a higher degree of molecular order. As shown on Figure III-11 and Table III-2, the amorphous C4 yields lower values than crystalline forms and the increase in  $T_{1\rho}^H$  with retting is reduced, being +56% instead of +80% for crystalline C4. These results indicate that the amorphous components are probably more affected by retting than crystalline components. This suggested decrease in crystalline component mobility is consistent with the hypothesis of compaction of the inaccessible parts of the cell walls. Zhang et al. [52] have already shown that the increase in Young's modulus may be related to an increase in  $T_{1\rho}^H$ . This hypothesis, combined with the densification of the walls, allows us to explain the evolution of the mechanical properties of the cell walls highlighted by AFM PF-QNM as shown in Figure III-5.

## 5. Conclusions

This chapter aims at improving our knowledge of flax fiber characteristics at the cell wall scale during the plant development and during field retting of flax.

AFM PF-QNM was used to investigate the mechanical and morphological properties of flax fiber cell walls, over plant development based on stem cross-sections and over retting based on scutched fibers. The lowest indentation modulus (13–14 GPa), characterizing the Gn-layer, were measured for developing fibers during plant growth. The homogeneous and mature G-layer exhibits a greater indentation modulus, namely about 18 GPa both in the stem at plant maturity and for scutched fibers from the fiber batch R1 sampled at the pulling-out time. The evolution of mechanical properties over fiber development was confirmed by tensile tests, as it was performed in literature to highlight the increase of fiber tensile properties. Moreover, AFM PF-QNM results

highlight a significant increase in the indentation modulus with retting time, up to +30% at the end of a conventional retting process. In addition, thickened cell walls in mature fibers have a homogeneous morphology, including during retting, as the Gn-layer was completely transformed in the G-layer over cell maturation. Furthermore, morphological analyses on AFM images show a progressive increase in the distance between fibers, associated with the disappearance of the middle lamellae with the retting levels, illustrating the progressive action of enzymes on the digestion of middle lamellae.

Raman spectroscopy highlights a change in cellulose over fiber thickening. Thus, for the flax fiber cell wall, changes in the mechanical properties measured by AFM could be attributed to the microfibril aggregation (transforming Gn into G) that takes place over cell wall development. A precise description of the changes in the cellulose structure could not be performed in this study and would require further investigations; in addition, NMR and XRD were not performed regarding plant development due to the too low availability of fiber materials. Nevertheless, during retting, the degree of crystallinity of scutched fibers is studied using both solid-state NMR and XRD. Indeed, these methods of analysis are quite different, as well as their scales of analysis. The global signal obtained on fiber bundles measured by XRD probably overestimates the differences in crystallinity between the retting states. The calculation protocol is based on a comparison between amorphous and crystalline components, including the amorphous residues of middle lamellae whose abundance varies greatly between samples. Thus, the modest increase in crystallinity highlighted by NMR is probably more consistent with the physicochemical phenomena involved in retting at the cell wall scale. NMR results also show a significant evolution in the cell wall ultrastructure of flax during the retting stages. Thus, the improvement in the mechanical performance of plant cell walls can be explained by the compaction of inaccessible zones, combined with an increase in contact time, as demonstrated by modelling with the two-reservoir method showing a decrease in mobility. The original coupling of NMR and XRD for the analysis of ultrastructure provides a significant contribution to the understanding of the mechanisms involved in retting.

Finally, this chapter represents a further step in understanding the origin and evolution in mechanical performances of flax fibers in view of their use as reinforcements in composite materials.

## 6. References

1. Witayakran, S.; Smitthipong, W.; Wangpradid, R.; Chollakup, R.; Clouston, P. L. Natural Fiber Composites: Review of Recent Automotive Trends. In *Reference Module in Materials Science and Materials Engineering*; Elsevier, 2017 ISBN 9780128035818.
2. Baley, C.; Bourmaud, A. Average tensile properties of French elementary flax fibers. *Mater. Lett.* **2014**, *122*, 159–161, doi:10.1016/j.matlet.2014.02.030.
3. Snegireva, A. V.; Ageeva, M. V.; Amenitskii, S. I.; Chernova, T. E.; Ebskamp, M.; Gorshkova, T. A. Intrusive growth of sclerenchyma fibers. *Russ. J. Plant Physiol.* **2010**, *57*, 342–355.
4. Mikshina, P.; Chernova, T.; Chemikosova, S.; Ibragimova, N.; Mokshina, N.; Gorshkova, T. Cellulosic fibers: Role of matrix polysaccharides in structure and function. In *Cellulose - Fundamental Aspects*; InTech, 2013; pp. 91–112 ISBN 978-953-51-1183-2.
5. Bert, F. *Lin fibre - Culture et transformation*; Arvalis, Ed.; 2013; ISBN 9782817901572.
6. van Dam, J. E. G.; Gorshkova, T. A. Cell walls and Fibers / Fiber formation. In *Encyclopedia of Applied Plant Sciences*; Elsevier Ltd, 2003; pp. 87–96.
7. Gorshkova, T. A.; Sal'nikov, V. V.; Chemikosova, S. B.; Ageeva, M. V.; Pavlencheva, N. V.; Van Dam, J. E. G. The snap point: A transition point in *Linum usitatissimum* bast fiber development. *Ind. Crops Prod.* **2003**, *18*, 213–221, doi:10.1016/S0926-6690(03)00043-8.
8. Gorshkova, T.; Mokshina, N.; Chernova, T.; Ibragimova, N.; Salnikov, V.; Mikshina, P.; Tryfona, T.; Banasiak, A.; Immerzeel, P.; Dupree, P.; Mellerowicz, E. J. Aspen tension wood fibers contain  $\beta$ -(1→4)-galactans and acidic arabinogalactans retained by cellulose microfibrils in gelatinous walls. *Plant Physiol.* **2015**, *169*, 2048–2063, doi:10.1104/pp.15.00690.
9. Djemiel, C.; Grec, S.; Hawkins, S. Characterization of bacterial and fungal community dynamics by high-throughput sequencing (HTS) metabarcoding during flax dew-retting. *Front. Microbiol.* **2017**, *8*, 1–16, doi:10.3389/fmicb.2017.02052.
10. Sharma, H. S. S.; Faughey, G.; McDall, D. Effect of sample preparation and heating rate on the differential thermogravimetric analysis of flax fibres. *J. Text Inst.* **1996**, *87*, 249.
11. Akin, D. E.; Foulk, J. A.; Dodd, R. B.; McAlister, D. D.; Akin, D. E.; Foulk, J. A.; Dodd, R. B.; McAlister, D. D. Enzyme-retting of flax and characterization of processed fibers. *J. Biotechnol.* **2001**, *89*, 193–203, doi:10.1016/S0168-1656(01)00298-X.
12. Coroller, G.; Lefeuvre, A.; Le Duigou, A.; Bourmaud, A.; Ausias, G.; Gaudry, T.; Baley, C. Effect of flax fibres individualisation on tensile failure of flax/epoxy unidirectional composite. *Compos. Part A Appl. Sci. Manuf.* **2013**, *51*, 62–70, doi:10.1016/j.compositesa.2013.03.018.
13. Sharma, H. S. S. Chemical retting of flax using chelating compounds. *Ann. Appl. Biol.* **1988**, *113*, 159–165, doi:10.1111/j.1744-7348.1988.tb03292.x.
14. Placet, V.; Day, A.; Beaugrand, J. The influence of unintended field retting on the physicochemical and mechanical properties of industrial hemp bast fibres. *J. Mater. Sci.* **2017**.
15. Van de Weyenberg, I.; Ivens, J.; De Coster, A.; Kino, B.; Baetens, E.; Verpoest, I. Influence of processing and chemical treatment of flax fibres on their composites. *Compos. Sci. Technol.* **2003**, *63*, 1241–1246, doi:10.1016/S0266-3538(03)00093-9.
16. Alix, S.; Lebrun, L.; Marais, S.; Philippe, E.; Bourmaud, A.; Baley, C.; Morvan, C. Pectinase treatments on technical fibres of flax: Effects on water sorption and mechanical properties. *Carbohydr. Polym.* **2012**, *87*, 177–185, doi:10.1016/j.carbpol.2011.07.035.
17. Martin, N.; Mouret, N.; Davies, P.; Baley, C. Influence of the degree of retting of flax fibers on the tensile properties of single fibers and short fiber/polypropylene composites. *Ind. Crops Prod.* **2013**, *49*, 755–767, doi:10.1016/j.indcrop.2013.06.012.

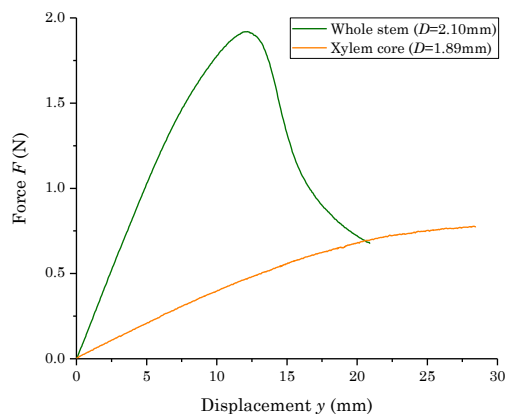
18. Velde, K. Van de; Baetens, E. Thermal and mechanical properties of flax fibres as potential composite reinforcement. *Macromol. Mater. Eng.* **2001**, *286*, 342–349.
19. Arnould, O.; Arinero, R. Towards a better understanding of wood cell wall characterisation with contact resonance atomic force microscopy. *Compos. Part A* **2015**, *74*, 69–76, doi:10.1016/j.compositesa.2015.03.026.
20. Arnould, O.; Siniscalco, D.; Bourmaud, A.; Le Duigou, A.; Baley, C. Better insight into the nano-mechanical properties of flax fibre cell walls. *Ind. Crops Prod.* **2017**, *97*, 224–228, doi:10.1016/j.indcrop.2016.12.020.
21. Agarwal, U. P. Raman imaging to investigate ultrastructure and composition of plant cell walls: Distribution of lignin and cellulose in black spruce wood (*Picea mariana*). *Planta* **2006**, *224*, 1141–1153, doi:10.1007/s00425-006-0295-z.
22. Himmelsbach, D. S.; Akin, D. E. Near-infrared Fourier-transform Raman spectroscopy of flax (*Linum usitatissimum* L.) stems. *J. Agric. Food Chem.* **1998**, *46*, 991–998, doi:10.1021/jf970656k.
23. Edwards, H. G. M.; Farwell, D. W.; Webster, D. FT Raman microscopy of untreated natural plant fibres. *Spectrochim. Acta - Part A Mol. Biomol. Spectrosc.* **1997**, *1425*, 2383–2392.
24. Matsko, N.; Mueller, M. AFM of biological material embedded in epoxy resin. *J. Struct. Biol.* **2004**, *146*, 334–343, doi:10.1016/j.jsb.2004.01.010.
25. Meng, Y.; Wang, S.; Cai, Z.; Young, T. M.; Du, G.; Li, Y. A novel sample preparation method to avoid influence of embedding medium during nano-indentation. *Appl. Phys. A* **2013**, 361–369, doi:10.1007/s00339-012-7123-z.
26. Konnerth, J.; Harper, D.; Lee, S. H.; Rials, T. G.; Gindl, W. Adhesive penetration of wood cell walls investigated by scanning thermal microscopy (SThM). *Holzforschung* **2008**, *62*, 91–98.
27. Wagner, L.; Bader, T. K.; De Borst, K. Nanoindentation of wood cell walls: Effects of sample preparation and indentation protocol. *J. Mater. Sci.* **2014**, *49*, 94–102, doi:10.1007/s10853-013-7680-3.
28. Clair, B.; Gril, J.; Baba, K.; Thibaut, B.; Sugiyama, J. Precautions for the structural analysis of the gelatinous layer in tension wood. *IAWA J.* **2005**, *26*, 189–195, doi:10.1163/22941932-90000110.
29. Jäger, A.; Bader, T.; Hofstetter, K.; Eberhardsteiner, J. The relation between indentation modulus, microfibril angle, and elastic properties of wood cell walls. *Compos. Part A Appl. Sci. Manuf.* **2011**, *42*, 677–685, doi:10.1016/j.compositesa.2011.02.007.
30. Segal, L.; Creely, J. J.; Martin, A. E.; Conrad, C. M. An empirical method for estimating the degree of crystallinity of native cellulose using the X-Ray diffractometer. *Text. Res. J.* **1959**, *29*, 786–794, doi:10.1177/004051755902901003.
31. Larsson, P. T.; Wickholm, K.; Iversen, T. A CP/MAS<sup>13</sup>C NMR investigation of molecular ordering in celluloses. *Carbohydr. Res.* **1997**, *302*, 19–25, doi:https://doi.org/10.1016/S0008-6215(97)00130-4.
32. Villares, A.; Moreau, C.; Bennati-Granier, C.; Garajova, S.; Foucat, L.; Falourd, X.; Saake, B.; Berrin, J.-G.; Cathala, B. Lytic polysaccharide monoxygenases disrupt the cellulose fibers structure. *Sci. Rep.* **2017**, *7*, 40262–40270, doi:10.1038/srep40262.
33. Newman, R. H. Estimation of the lateral dimensions of cellulose crystallites using C-13 NMR signal strengths. *Solid State Nucl. Magn. Reson.* **1999**, *15*, 21–29.
34. Kolodziejski, W.; Klinowski, J. Kinetics of cross-polarization in solid-state NMR: A Guide for chemists. *Chem. Rev.* **2002**, *102*, 613–628, doi:10.1021/cr000060n.
35. Paris, M.; Bizot, H.; Emery, J.; Buzaré, J. ; Buléon, A. NMR local range investigations in amorphous starchy substrates: II-Dynamical heterogeneity probed by <sup>1</sup>H/<sup>13</sup>C magnetization transfer and 2D WISE solid state NMR. *Int. J. Biol. Macromol.* **2001**, *29*, 137–143, doi:S0141-8130(01)00161-1.

36. Alméras, T.; Clair, B. Critical review on the mechanisms of maturation stress generation in trees. *J. R. Soc. Interface* **2016**, *13*, 20160550, doi:10.1098/rsif.2016.0550.
37. Roach, M. J.; Mokshina, N. Y.; Badhan, A.; Snegireva, A. V.; Hobson, N.; Deyholos, M. K.; Gorshkova, T. A. Development of cellulosic secondary walls in flax fibers requires b-galactosidase. *Plant Physiol.* **2011**, *156*, 1351–1363, doi:10.1104/pp.111.172676.
38. Gorshkova, T. A.; Chemiksova, S. B.; Sal'nikov, V. V.; Pavlencheva, N. V.; Gur'janov, O. P.; Stolle-Smits, T.; Van Dam, J. E. G. Occurrence of cell-specific galactan is coinciding with bast fiber developmental transition in flax. *Ind. Crops Prod.* **2004**, *19*, 217–224, doi:10.1016/j.indcrop.2003.10.002.
39. Jones, L.; Seymour, G. B.; Knox, J. P. Localization of pectic galactan in tomato cell walls using a monoclonal antibody specific to (1/4)-b-D-galactan. *Plant Physiol.* **1997**, *113*, 1405–1412.
40. Tanguy, M.; Bourmaud, A.; Baley, C. Plant cell walls to reinforce composite materials: Relationship between nanoindentation and tensile modulus. *Mater. Lett.* **2016**, *167*, 161–164, doi:10.1016/j.matlet.2015.12.167.
41. Christophe, F.; Séné, B.; Mccann, M. C.; Wilson, R. H.; Crinter, R. Fourier-Transform Raman and Fourier-Transform Infrared Spectroscopy. *Plant Physiol.* **1994**, *106*, 1623–1631, doi:10.1104/pp.106.4.1623.
42. Gierlinger, N. New insights into plant cell walls by vibrational microspectroscopy. *Appl. Spectrosc. Rev.* **2017**, *4928*, 1–35, doi:10.1080/05704928.2017.1363052.
43. Lefeuvre, A.; Bourmaud, A.; Morvan, C.; Baley, C. Tensile properties of elementary fibres of flax and glass: Analysis of reproducibility and scattering. *Mater. Lett.* **2014**, *130*, 289–291, doi:10.1016/j.matlet.2014.05.115.
44. Gindl, W.; Gupta, H.-S.; Schöberl, T.; Lichtenegger, H.-C.; Fratzl, P. Mechanical properties of spruce wood cell walls by nanoindentation. *Appl. Phys. A* **2004**, *79*, 2069–2073.
45. Zafeiropoulos, N. E.; Baillie, C. A.; Matthews, F. L. A study of transcrystallinity and its effect on the interface in flax fibre reinforced composite materials. *Compos. Part A Appl. Sci. Manuf.* **2001**, *32*, 525–543, doi:http://dx.doi.org/10.1016/S1359-835X(00)00058-0.
46. Marrot, L.; Lefeuvre, A.; Pontoire, B.; Bourmaud, A.; Baley, C. Analysis of the hemp fiber mechanical properties and their scattering (Fedora 17). *Ind. Crops Prod.* **2013**, *51*, 317–327, doi:10.1016/j.indcrop.2013.09.026.
47. Dinand, E.; Vignon, M.; Chanzy, H.; Heux, L. Mercerization of primary wall cellulose and its implication for the conversion of cellulose I to cellulose II. *Cellulose* **2002**, *9*, 7–18.
48. Ouajai, S.; Shanks, R. A. Composition, structure and thermal degradation of hemp cellulose after chemical treatments. *Polym. Degrad. Stab.* **2005**, *89*, 327–335.
49. Thygesen, A.; Oddershede, J.; Lilholt, H.; Thomsen, A.; Sta, K. On the determination of crystallinity and cellulose content in plant fibres. *Cellulose* **2005**, *12*, 563–576.
50. Tserki, V.; Zafeiropoulos, N. E.; Panayiotou, C.; Zafeiropoulos, N. E.; Simon, F.; Panayiotou, C. A study of the effect of acetylation and propionylation surface treatments on natural fibres. *Compos. Part A Appl. Sci. Manuf.* **2005**, *36*, 1110–1118.
51. Zuckerstätter, G.; Schild, G.; Wollboldt, P.; Röder, T.; Weber, H.; Sixta, H. The elucidation of cellulose supramolecular structure by <sup>13</sup>C CP-MAS NMR. *Lenzinger Berichte* **2009**, *87*, 38–46.
52. Zhang, X.; Wu, X.; Haryono, H.; Xia, K. Natural polymer biocomposites produced from processing raw wood flour by severe shear deformation. *Carbohydr. Polym.* **2014**, *113*, 46–52.

**CHAPTER IV –  
BENDING PROPERTIES OF FLAX PLANTS – ROLE  
OF THE FIBERS WITHIN THE STEM**

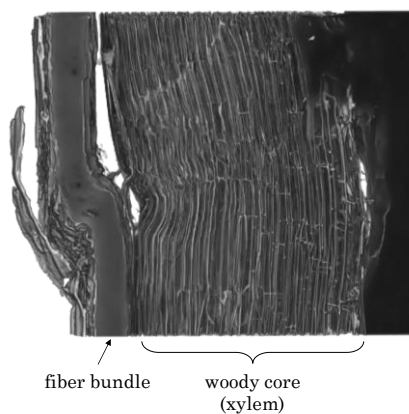
## Graphical abstract

---



- ❖ What is the link between bending behavior of flax stems and fiber stiffness?

Réquilé, S.; Goudenhoft, C.; Bourmaud, A.; Duigou, A. Le; Baley, C.; Le Duigou, A.; Baley, C. Exploring the link between flexural behaviour of hemp and flax stems and fibre stiffness. *Ind. Crops Prod.* **2018**, *113*, 179–186, doi:10.1016/j.indcrop.2018.01.035.



- ❖ What is the compressive strength of flax fibers within the stem?
- ❖ What is the relationship between compressive properties of UD flax/epoxy composites and fiber bundles within the stem?

Baley, C.; Goudenhoft, C.; Perré, P.; Liu, P.; Pierre, F.; Bourmaud, A. Compressive strength of flax fibre bundles within the stem and comparison with unidirectional flax/epoxy composites. *Ind. Crops Prod.*, *under review*.

## CHAPTER IV – BENDING PROPERTIES OF FLAX PLANTS – ROLE OF THE FIBERS WITHIN THE STEMS

---

Flax is one of the most commonly cultivated industrial fiber plant in Europe. The use of its fibers as reinforcement of composite materials covers a wide range of applications, which requires a precise knowledge of fiber mechanical properties. Nevertheless, the compressive strength of flax-based composites is known to be rather modest compared with materials reinforced by synthetic fibers [1,2]. This chapter explores the role of flax fibers in the mechanical properties and behavior of the stems under a flexural load. It also investigates the compressive performances of flax fibers to evaluate their potential as limiting factor for structural applications of flax-based composite materials. A first section is dedicated to the study of flax fiber contribution to the stiffness of dry stems, *i.e.* in a state similar to fibers used during processing of composite materials, subjected to a simple three-point bending test. The analysis is based on measuring the difference of bending stiffness between stems with fibers and stems without fibers, after removal by manual peeling. The second section of the present chapter investigates the compressive strength of flax fiber bundles both within the stems and in unidirectional (UD) flax/epoxy composites. In this way, an optimized arrangement of fiber bundles inside the plant is assumed, and damage mechanisms are analyzed. Within stems, failure is highlighted by nanotomography, whereas for UD, it is studied by scanning electron microscopy (SEM).

### 1. Introduction

Ecological and environmental concerns have increased interest in the use of natural fibers from plants for the development of biocomposites. Flax fibers are ideal candidates to be used as substitutes for synthetic fibers as reinforcements in composite materials, the main purposes of flax-based composite development being for instance the reduction of weight of manufactured parts or the decrease of their environmental impacts [3]. Interestingly, seeds and woody core of flax also have specific markets, thus increasing the profitability of cultivation. Since this annual crop is also favored by a short life cycle, they are easily integrated into farmers' crop rotations.

## 1.1. Description of a flax stem

### 1.1.1. General features and organization

Flax stems can be considered as hollow cylinders of variable length and diameter depending on growth conditions [4], variety (Figure II-3) and the stage of development of the plant (Figure I-1). In the case of flax, the plant height reaches around 1 m with a basal diameter of about 3 mm [5]. The flax stem is made up of several tissues arranged in the form of successive rings affording protection, support, conduction and various metabolic functions (Figure I-2). At the stem scale, from the center to the periphery, the structure within the stem is as follows: pith, xylem, vascular cambium, phloem, fibers, cortical parenchyma and epidermis. Among those tissues, two main ones can be identified: fibers at the periphery of the stem, and woody core (or xylem) at the center of the stem.

### 1.1.2. Two main mechanical tissues – Flax fiber crown and xylem

Flax primary fibers are located between the epidermis and the vascular cambium, forming a crown surrounding the xylem core. The fibers are arranged in various size bundles influenced by plant growth or variety and they ensure the plant stability thanks to noteworthy mechanical properties (Chapter II). The outstanding properties of flax fibers, and more specifically the length of elementary cells and associated mechanical properties, are the results of an intrusive fiber development in a first place [6], which is followed by the thickening of the fiber cells through the deposition of cellulose [7]. This latter process provides fibers exhibiting a very thick secondary cell wall and small lumen [8]. Within the stem, pectic junctions bond the fibers together and ensure the bundle arrangement. This structure gives a first model of a composite material at the bundle scale. In this latter, the stresses are transferred to the reinforcing fibers through a polymer matrix, made of pectic junctions, mainly composed of homogalacturonans and rhamnogalacturonans [9]. This matrix can be found in two different areas: the middle lamella (*i.e.* between the primary cell walls of two neighboring fibers) and the tri-cellular junctions (*i.e.* in the corner between three fibers)[10].

The woody core (also called shives after industrial fiber extraction) is a highly lignified alveolar structure [11]. The xylem is responsible for the conduction of raw sap from the roots to the vegetative parts. This structure also plays the role of a supporting element [10].

## 1.2. Bending properties of stems

Previous studies have focused on exploring the behavior of stems. In these studies, stems are commonly considered as thin-walled circular structures, for which bending can be divided in two consecutive phases, namely ovalization and Brazier-type buckling [13–15]. Different research teams have studied the lodging resistance of stems against external loads [16,17], while Niklas investigated the influence of sample geometry on the bending response of hollow stems [18]. Experimental studies have also been performed on stems from different plants to establish reliable methodologies for measurement of their bending stiffness [13]. These studies provide information to better understand the biomechanics of plants by determining their mechanical properties and their response to bending. However, to the best of our knowledge, little information is available on the contribution of the different tissues to the bending stiffness of the stem.

## 1.3. Compressive strength of flax-based composites

Despite this remarkable structure and tissue organization of plant fiber reinforcement, the resistance to compressive strength of flax-based composites is rather limited, whatever the type of matrix or the fiber volume fraction, when compared to their resistance to tensile strength [19]. Table IV-1 shows the longitudinal compressive mechanical properties of different unidirectional (UD) of flax-reinforced composites [1,2,20–23].

**Table IV-1. Properties of unidirectional composites reinforced by flax fibers provided in literature, highlighting longitudinal compressive and tensile properties.**

Matrix	Fiber volume fraction (%)	Compressive modulus (GPa)	Compressive strength (MPa)	Tensile modulus (GPa)	Tensile strength (MPa)	References
Phenol formaldehyde	~ 70	41.4	163	41.4	310	[23]
	~ 75	48.3	182	48.3	414	[20]
	43.9	24.7	136	22.8	318	[21]
Epoxy	40	15.1	137	23.9	223	[2]
	51	30.3	127	31.4	287	[22]

For all the data sets given in Table IV-1, the compressive strength is lower than 200 MPa. In addition, it is always poorer than the tensile strength (which is about two

times higher). Therefore, this mechanical parameter is of significance for the improvement of flax biocomposites. Numerous parameters can influence the compressive behavior of composite materials, such as fiber volume fraction, the fiber and matrix properties, the interface bond strength, the porosity, the fiber misalignment, as well as the difference in Poisson ratio between fiber and matrix [2,20–23]. In the case of a unidirectional ply under longitudinal compression, the failure takes place due to fiber kinking; this result was demonstrated for natural fibers [24] as well as synthetic ones [25].

The present chapter aims, at first, to improve our understanding of the mechanical contribution of flax fibers within dry stems under flexural load, which is potentially linked to their mechanical performance. After defining optimal testing parameters, bending tests are carried out on stems with and without fibers. The bending stiffness of the samples is studied taking into account both the contribution of the fibers and the xylem geometries. A comparison between the longitudinal modulus of fibers, estimated by bending tests, and the modulus measured by tensile tests on elementary fibers is proposed. Secondly, the present chapter also investigates the compressive behavior of flax fiber bundles within the stem. In this way, fibers are considered under an optimal situation within the stem, *i.e.* cohesive and oriented in the longitudinal direction of the stem, leading to a model of natural composite structure. First, loading is performed through bending of the stems. Then, the induced damaging and failure mechanisms of fiber bundles are observed by nanotomography. Complementary experiments are performed on several flax varieties to evaluate the influence of the varietal selection work on the bundle compressive strength. In addition, the compressive strength at break of fiber bundles within the stems is compared with the ones of unidirectional plies. Finally, the estimation of the role in compression of the xylem, also called woody core, is given.

## 2. Materials and methods

### 2.1. Plant materials – Stems and fibers

All flax plants were provided by Terre De Lin. Two recent and two ancient textile flax varieties were studied. The recent varieties are Bolchoï (registered in 2014) and Eden (registered since 2009), selected by Terre De Lin and both currently commercialized. Liral Prince comes from a selection made in 1944 by the Linen Industry Research Association (L.I.R.A, Ireland). Ariane was registered in 1978 (Coopérative Linière de

Fontaine Cany, France). These two ancient varieties are not commercialized anymore. For this chapter, Bolchoï is used as the reference variety for the tests, being an increasingly cultivated recent variety which leads to high fiber yields and good lodging stability. Plants were cultivated in Saint-Pierre le Viger (France) in 2016. Conventional seeding rates and culture conditions were used [26]. Plants were pulled out at maturity and subsequently dried under a standard atmosphere (temperature of  $23 \pm 2^\circ\text{C}$  and relative humidity of  $50 \pm 4\%$ ) until stabilization of the stem weight. Some of the dried stems were water-retted (in order to facilitate the extraction of fibers for tensile tests). Prior to bending and tensile tests, stems and fibers were conditioned under the mentioned standard atmosphere for at least 24h. Water contents of both stems and fibers were measured to be  $7.8 \pm 0.4\%$  after conditioning.

## 2.2. Anatomical analysis of the stems

Sample anatomy and fiber geometry were characterized using stem transverse sections. Stem portions were taken at the middle height of the flax plants. To facilitate the cut, the portions were immersed in water at least 24h. Then, they were embedded in elder marrow and semi-thin sections were cut transversally using a razor blade and a hand microtome to clamp the sample. Optical images were taken under the microscope and used to carry out different measurements of the tissue features present in the stem, such as the bundle thickness. To do so, the images were processed with Gimp® and then analyzed with ImageJ®.

## 2.3. Specific gravity measurements

The specific gravity of the xylem core was determined. The experiment was performed in duplicate on 1 cm sized samples extracted from hand-peeled stems of various diameters. Prior to measurement, the samples were weighted in air. They were then immersed in ethanol at  $22^\circ\text{C}$ , using an ultrasonic bath for degassing for 30 minutes. Samples were then weighed in ethanol solution and the values were taken once stabilization of the mass. The specific gravity of a sample is expressed by Equation IV-1.

$$\text{Specific gravity} = \left[ \frac{w_{Air} \cdot (\rho_{EtOH} - \rho_{Air})}{w_{Air} - w_{EtOH}} \right] + \rho_{Air}$$

**Equation IV-1. Calculation of the specific gravity of xylem samples, where  $w_{Air}$  is the weight of the sample in air,  $w_{EtOH}$  is the weight of the sample in ethanol, while  $\rho_{Air}$  ( $0.0012 \text{ g/cm}^3$ ) and  $\rho_{EtOH}$  ( $0.78763 \text{ g/cm}^3$ ) are the specific gravities at  $22^\circ\text{C}$  of air and ethanol, respectively.**

## 2.4. Three-point bending test

Three-point bending tests were carried out at controlled temperature ( $23 \pm 2$  °C) and relative humidity ( $50 \pm 4$  %). Tests were performed using a universal MTS tensile testing machine equipped with a 50 N capacity load cell. The displacement rate was fixed at 0.1 mm/s. Prior to experiments, both load cell and cross head were calibrated. Flax stem samples were cut from the middle height of the stem, corresponding to a position where the fibers exhibit optimal mechanical properties [27]. Experiments were conducted on flax stems to study the test set-up conditions, thereby allowing pure bending stress to be applied. This analysis reveals the influence of the  $L/D$  ratio on the bending stiffness of the stems, which varies from 18 to 88 for flax, with  $L$  being the span length and  $D$  the stem diameter. Some stems were then carefully hand peeled and similarly tested to determine the mechanical properties of their xylem core.

By considering both the entire stem and the xylem as a uniform beam with a circular cross section, displacement  $y$  in the middle of the section is given by Equation IV-2 for small displacements [28].

$$y = \frac{FL^3}{48EI}$$

**Equation IV-2. Calculation of the displacement  $y$  in the middle of the sample section, where  $F$  is the applied force,  $L$  the span length and  $EI$  the bending stiffness,  $I$  the quadratic momentum given as  $I = \frac{\pi}{64}D^4$  ( $D$  being the sample diameter) and  $E$  the bending modulus of the sample.**

The stem or xylem apparent modulus is then obtained by applying Equation IV-3.

$$E = \frac{dF}{dy} \frac{L^3}{48.I}$$

**Equation IV-3. Calculation of the sample apparent modulus, where  $dF/dy$  is the slope on the linear part of the force-displacement curve,  $L$  the span length and  $I$  the quadratic momentum of the sample.**

The stem is assimilated to a composite tube of two layers: the fiber and the xylem layer. For each layer constructing the tube, the bending stiffness is obtained by multiplying the stiffness ( $E$ ) to the quadratic momentum ( $I$ ). Finally, the bending stiffness of the stem is obtained by adding the bending stiffness of each layer.

Figure IV-1 illustrates the modelling of the entire stem with a circular cross section, the exterior ( $D_{ext}$ ) and interior ( $D_{int}$ ) diameters of the different layers used for the calculation of the quadratic momentum.

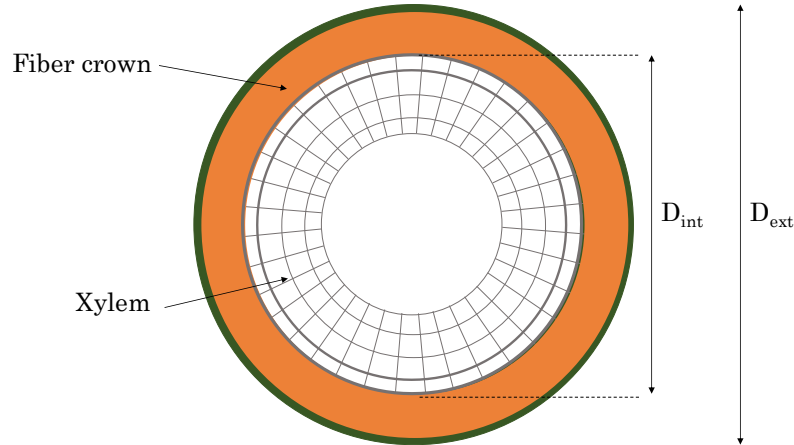


**Figure IV-1. Scheme illustrating the modeling of a stem with a circular cross section. This stem geometry was used for the calculation of bending properties.**

Their modulus can then be estimated by taking into account the difference in bending stiffness of the stem and the xylem (Equation IV-4).

$$E_{f,b} = \frac{(EI)_s - (EI)_x}{I_f}$$

**Equation IV-4. Calculation of the fiber modulus  $E_{f,b}$ , where  $(EI)_s$  and  $(EI)_x$  are the bending stiffness of the stem and the xylem, respectively, and  $I_f$  is the quadratic momentum of the fibers present in the stem and expressed as  $I_f = \frac{\pi}{64} (D_{ext}^4 - D_{int}^4)$ .**

Additionally, the maximal force  $F_{max}$  damaging the sample can be determined; the corresponding maximum bending moment  $M_{max}$  at the center of the sample is estimated by Equation IV-5.

$$M_{max} = \frac{F_{max}L}{4}$$

**Equation IV-5. Calculation of the maximum bending moment  $M_{max}$  at the center of the sample, where  $F_{max}$  is the maximal force at failure and  $L$  the span length.**

At mid-length of the beam, the maximal strain  $\varepsilon_{max}$  is expressed by Equation IV-6.

$$\varepsilon_{max} = \frac{M_{max}D}{EI^2}$$

**Equation IV-6. Calculation of the maximal strain  $\varepsilon_{max}$  in the center of the section, where  $M_{max}$  is the maximum bending moment,  $D$  the sample diameter and  $EI$  the bending stiffness.**

In the case of the peeled stem, the sample is considered as a homogeneous material having a linear mechanical behavior (validated Hooke's law). The strength is thus calculated as the multiplication of the maximal strain by the apparent elastic modulus determined through bending tests.

However, for the entire stem, a sandwich composite beam is considered, having an unidirectional ply on the outermost side (assembly of fibers in the form of bundles forming an external fibrous ring). The elastic modulus of the fibers  $E_{f,t}$  is measured by tensile tests. In the present case, the fiber behavior is simplified as being elastic linear. Thus, the bundles compressive strength at break  $\sigma_{f,max}$  is expressed by Equation IV-7.

$$\sigma_{f,max} = \varepsilon_{max} E_{f,t}$$

**Equation IV-7. Calculation of the fiber compressive strength at break  $\sigma_{f,max}$ , where  $\varepsilon_{max}$  is the maximal strain and  $E_{f,t}$  is the elastic modulus of the fibers.**

## 2.5. Tensile test on elementary fibers

Tensile tests on elementary fibers were carried out according to the NF T 25-501-2 standard which takes into consideration the compliance of the load sensor. Before fiber extraction, the stems were retted using running water for 10 days to facilitate peripheral tissue peeling, and to avoid fiber damage during the extraction phase. Fibers were then extracted manually and bonded onto a paper frame to obtain a fixed gauge length of 10 mm. The samples were conditioned for 24h at a controlled temperature and humidity. The diameter of each fiber was determined using an optical microscope, the value corresponding to the mean of six measurements taken at different locations along the fiber [29]. The samples were then clamped on a universal MTS tensile testing machine equipped with a 2 N capacity load sensor. The crosshead speed was fixed at 1 mm/min. For each batch of fibers, a minimum of 50 fibers were tested. The fiber Young modulus is assimilated to the tangent modulus, obtained from the linear part of the force/displacement curve (NF T 25-501-2).

## 2.6. Nanotomography

samples were scanned with a nanotomograph EasyTom XL 150/160 manufactured by RX-solutions (Annecy, France). The nano-focus X-ray sources (an open nano-focus tube with a tungsten filament) and a CCD detector of  $2004 \times 1336$  pixels were selected to obtain a voxel size of  $1.7 \mu\text{m}$ , the best possible compromise to scan the entire stem diameter. The region of interest of the flax stem after bending was glued on the top of the 2 mm-carbon rod of the sample holder. This protocol allows the flax stem to be close enough the X-ray tube to obtain this resolution. These conditions impose an acquisition time of about 3h.

## 2.7. Unidirectional composites

The matrix used is an epoxy resin (Axson, Epolam 2020). Its tensile Young's modulus, strength and strain at break are  $3.10 \pm 0.01$  GPa,  $78 \pm 6$  MPa, and  $3.1 \pm 0.5$  %, respectively. The reinforcement consists of a tape of unidirectional fibers without any twist (Flax-Tape, Lineo®)[30] with an area weight of  $200 \text{ g/m}^2$ . The unidirectional laminates of different fiber volume fractions were obtained by impregnating and then pressing to eliminate voids (Labtech© 50T molding press). After hardening for 24h at  $25^\circ\text{C}$ , samples were post-cured (3 h at  $40^\circ\text{C}$ ; 2 h at  $60^\circ\text{C}$ ; 2 h at  $80^\circ\text{C}$ ; 5 h at  $100^\circ\text{C}$ ). For compressive characterization and after preliminary tests, the thickness of samples is set at 2.5 mm. For the test, two gauges were bonded, one on each face, in order to monitor the compressive behavior.

## 2.8. Scanning electron microscopy (SEM)

Unidirectional composite samples were embedded in an epoxy resin before polishing. They were then metalized with gold before being observed under a JEOL JSM 6460LV scanning electron microscope (SEM). Fiber volume fractions from 20% to 52% were measured by image analysis from SEM observations on the transverse section after polishing.

# 3. Results and discussion – Link between bending behavior of flax stems and fiber stiffness

## 3.1. Architecture and morphology of stems

Figure IV-2 shows some an example of a transverse section of a flax stem at the middle height. Fibers are arranged in bundles forming a continuous ring on the periphery of

the stem. Moreover, the flax xylem is a dense and homogeneous structure quite similar to the xylem from softwood [31].

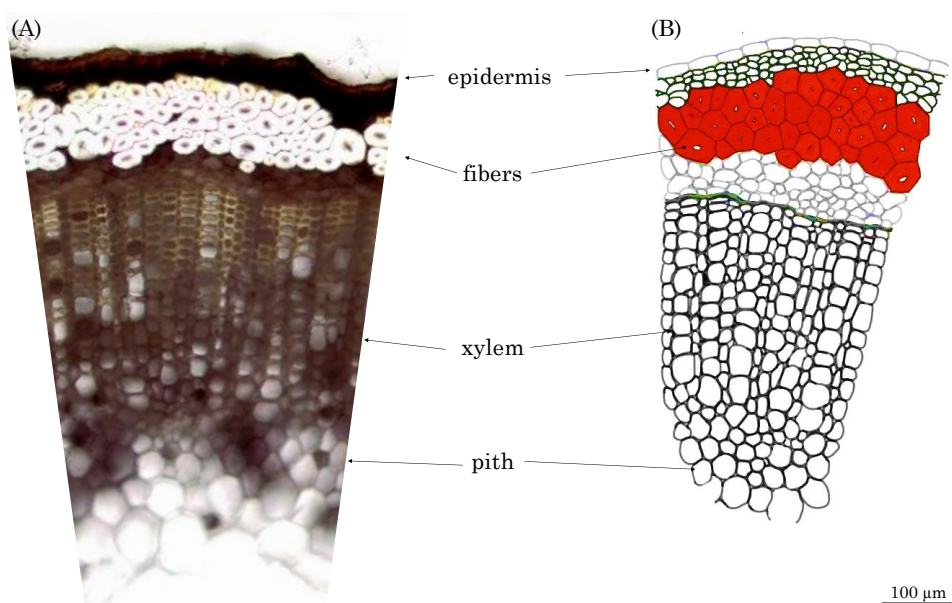


**Figure IV-2. Transverse cross-section (A) and corresponding scheme (B) of the middle part of a flax stem.**

Table IV-2 summarizes the values of the morphological parameters obtained from the analysis of the stem section, partially shown in Figure IV-2, considering a circular cross-section calculated from the section area.

**Table IV-2. Morphological parameters of flax resulting from image analysis. All percentages are calculated with respect to the stem section.**

	Stem diameter (mm)	Tissue content (%)	Xylem content (%)	Fiber content (%)	Epidermis and cortical parenchyma content (%)
Flax stem (Bolchoï)	2.85	82.7	63.3	13.0	6.4

By way of illustration, the fraction of different tissues with respect to the total cross-section area of the stem is calculated. The estimation of the tissue content in the stem, including porosities, shows the presence of a central void representing 17.3 % for flax. Within these tissues, the xylem and fibers account for 63.3 % and 13.0 % of the total area of the stem, demonstrating the small area occupied by the fibers within the stem.

### 3.2. Analysis of bending characterization conditions

To obtain accurate data on stem stiffness, careful attention must be paid to the three-point bending test set-up. The results presented in Figure IV-3 show the influence of the  $L/D$  ratio,  $L$  being the span length and  $D$  the diameter of the sample, on the bending stiffness of the stem samples.

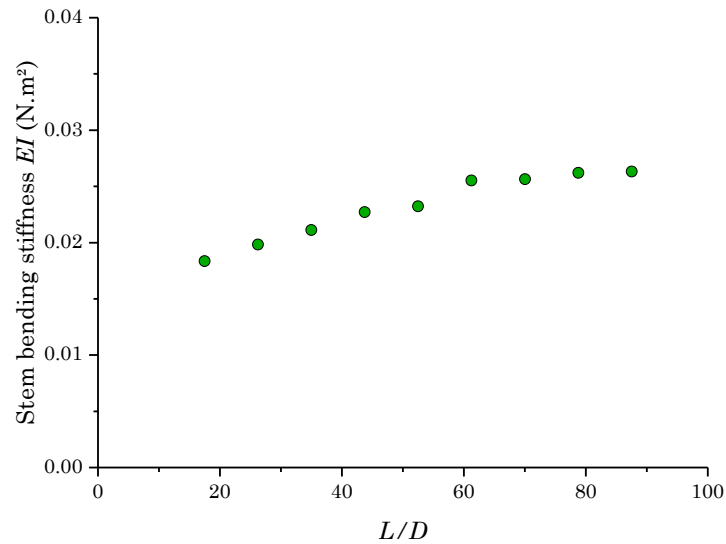


**Figure IV-3. Bending stiffness ( $EI$ ) of a flax stem obtained from a three-point bending test, which highlight the influence of the ratio of the span length ( $L$ ) over the diameter ( $D$ ) of the sample.**

Flax stems show a slight increase of the stiffness from  $0.018 \text{ N.m}^2$  to  $0.026 \text{ N.m}^2$  for  $L/D$  ratios of 18 to 88. These disparities lead to inaccurate measurements of the mechanical properties of the samples when using a small span length. This effect can be associated with the presence of shear stresses, ovalization and squashing of the stem. Indeed, when a bending force is applied to a tubular structure, two consecutive phenomena occur: a first phase is characterized by the flattening of the cross-section of the sample, leading to a reduction of the bending stiffness. This ovalization phase is followed by a buckling phase, during which the system loses its stability and the cross-section flattens out [14]. Thus, increasing the span length of the experimental set-up leads to a reduction in the applied force required to obtain a given moment. Therefore, other than reducing shear stresses in the stem, the ovalization phenomenon is minimized. Experimental parameters need to be precisely determined to be able to characterize the bending stiffness of the samples without being impacted by the set-up parameters. Indeed, the  $L/D$  ratio needs to be sufficiently high so the sample remains stable while exploring a specific localization on the stem. For the experiments

carried out in this study, a  $L/D$  ratio of 80 (*i.e.*  $L$  of 18 cm) is selected for flax samples, which is much higher than values typically chosen in literature ( $L/D$  ranging from 10 to 40, as larger span-to-depth ratios are often limited by the presence of nodes or by sagging of non-rigid stem samples)[15].

### 3.3. Characterization of the bending stiffness of flax stems

#### 3.3.1. Stress-strain behavior of stems and xylem cores

The bending stiffness of flax stems and xylem are evaluated by three-point bending tests. Figure IV-4 presents the force-displacement profiles for both the flax stem and the woody part, with a diameter of 2.10 mm and 1.89 mm, respectively.

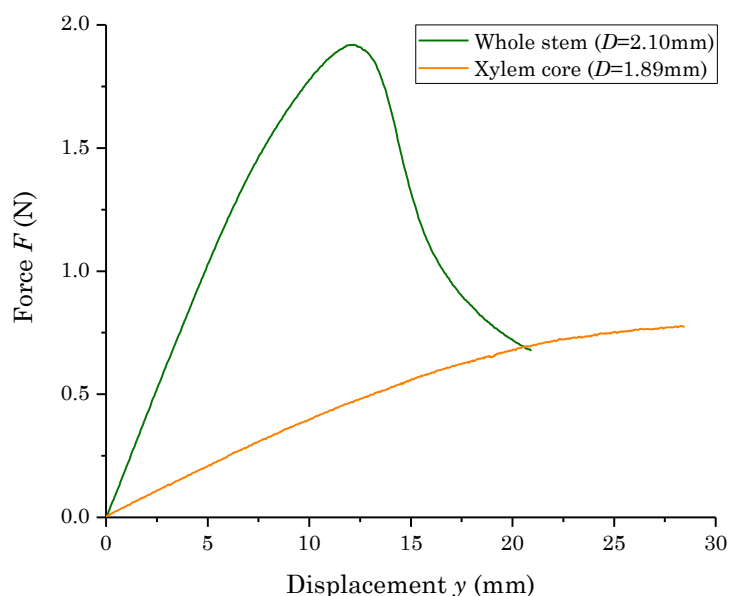


**Figure IV-4. Typical stress-strain curve for a three-point bending test on a whole flax stem and of a xylem core.**

Similar elastic and linear behaviors are exhibited at the beginning of the test for both the stem and the xylem core, which allow us to define the bending modulus of the samples, based on Equation IV-3. Considerably lower values are highlighted for the woody core in terms of maximal strength compared to an entire stem. This result underlines the key role of fiber part in stem stability. Flax stems can be assimilated to cylindrical tubes of small diameter, taking into consideration the thickness of the fiber ring. Therefore, the bending behavior of these stems can be described as analogous to those of tubes with thin walls [14]. Considering the large  $L/D$  taken for the bending tests, the loss of linearity of the curve is explained by a large displacement of the central support just before breakage (Figure IV-4).

In addition, the ovalization and squashing effects are negligible for all the performed tests thanks to the use of a pertinent span length. The stem damage actually happens on the face in compression, and is often located close to the central support of the bending device. This observation is consistent with a three-point bending test, for which the bending moment is maximum at mid-length, which confirms the hypothesis of a behavior very similar to pure bending.

### 3.3.2. Bending stiffness of stems and xylem cores

Figure IV-5 shows the evolution of bending stiffness of flax whole stems and xylem cores (peeled stems) according to their respective diameter.

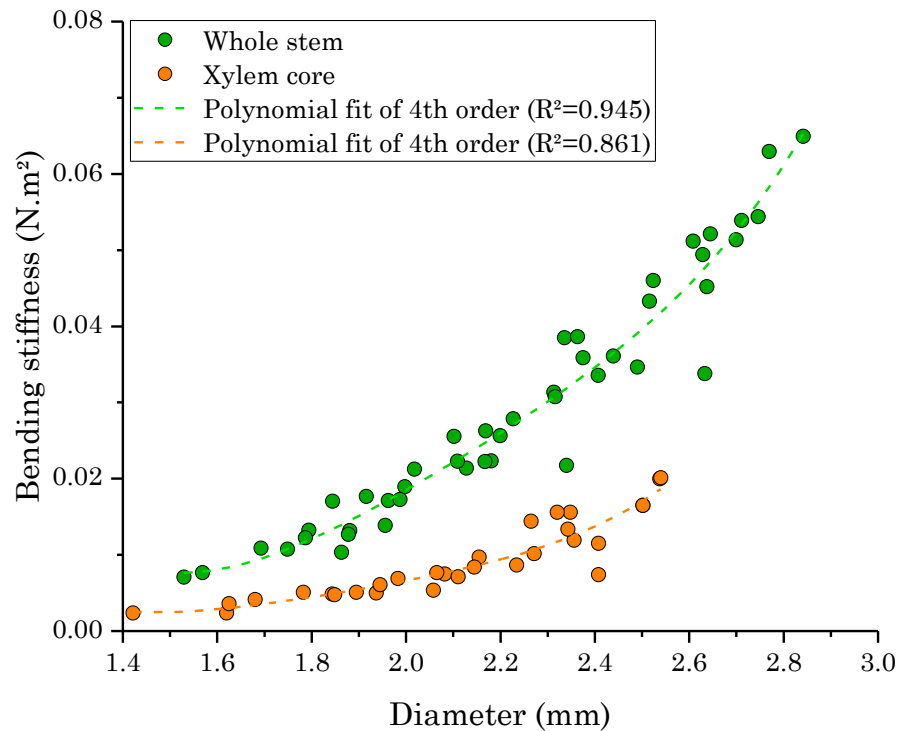


**Figure IV-5. Bending stiffness of flax samples (whole stem and xylem core) according to the sample diameter.**

Measured diameters of whole flax stems are in the range of 1.53 mm to 2.84 mm, while samples of xylem core vary from 1.42 mm to 2.54 mm, as we decided to use samples having dispersed diameters in order to validate the method. The results show an expected increase of bending stiffness of stems and equivalent xylem with increasing diameter. Similar behavior has been found by Gibaud et al. (2015) on flax stems, explaining their stability, *i.e.* resistance to lodging. Two distinct regions can be observed on the stem stiffness curves: a first region is characterized by a slight

increase of stiffness with increasing diameter for stems smaller than 2 mm for flax, followed by a faster gain of stiffness for larger diameters, explained by the dependence of stem bending stiffness to the diameter  $D$  of the stem (namely  $D^4$ ).

Figure IV-5 also presents the evolution of bending stiffness of the xylem core. Unlike the behavior of stem samples, the bending stiffness of flax xylem appears to be less diameter dependent. Apart from being solely affected by the diameter of the plant, the stem bending stiffness may also be governed by the presence of fibers in the stem. Indeed, Figure IV-5 also shows a clear loss of stiffness between stems before and after peeling. In fact, this loss reaches 50 to 80% (with a mean loss of  $70 \pm 8\%$ ). These results confirm the important role of fibers in the peripheral tissue to ensure stability of the plant and the fact that they are commonly referred to as ‘supporting tissue’.

### 3.3.3. Apparent bending moduli of stems and xylem cores

Knowing the bending stiffness of the samples and their geometry (determined by the transversal section microscopy, as presented in Figure IV-2), it is possible to calculate, using Equation IV-3, the apparent modulus of stem samples (Figure IV-6), if considering them as plain cylindrical homogeneous materials.

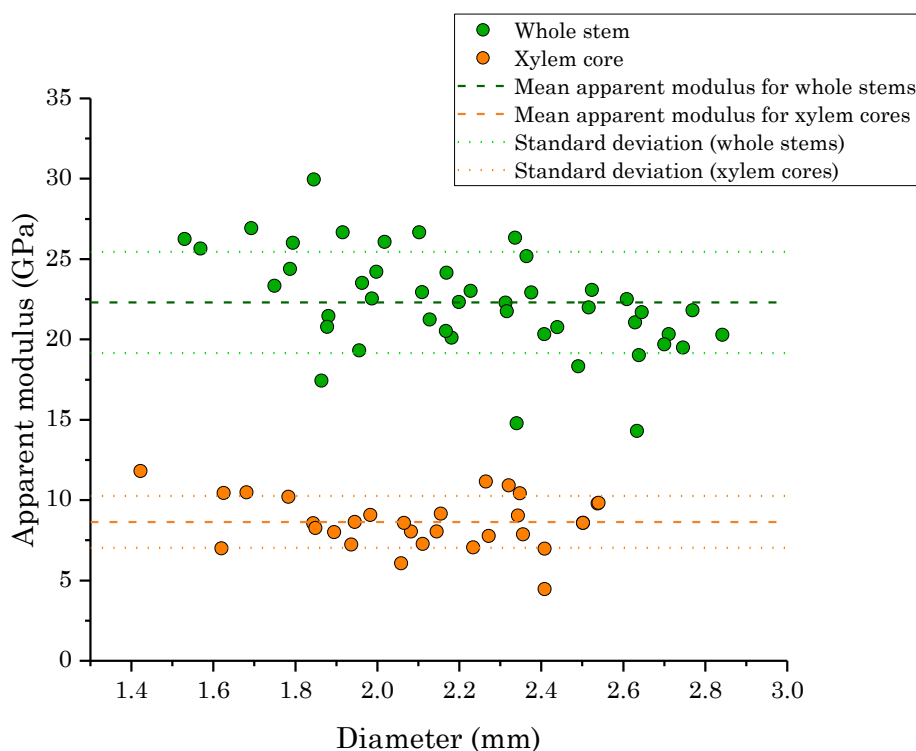


**Figure IV-6. Apparent bending modulus of flax samples (whole stem and xylem core) according to the sample diameter.**

Regardless of the sample diameter, the apparent modulus of both whole stems and xylem samples reaches values of  $22.3 \pm 3.1$  GPa for the entire stem and  $8.6 \pm 1.6$  GPa for the xylem. These values remain rather persistent between samples as the dispersion of the results is modest for a natural material such as flax stems (less than 20%).

The general contribution of fibers to the mechanical properties of the stems was studied by bending tests. In the case of flax, the xylem accounts for less than half of the global bending stiffness, as the fiber contribution reached up to an average of  $70 \pm 8$  % of the bending stiffness of the stems. These results confirm the important contribution of fibers to the bending mechanical properties of stems and the mechanical properties of the fibers themselves also need to be considered.

### 3.4. Longitudinal modulus of flax fibers estimated by bending tests

This section presents an analysis of flax fiber modulus. Knowing the bending stiffness of the complete stem and its xylem, it is possible to estimate the stiffness imparted by the fibers, and therefore their apparent modulus.

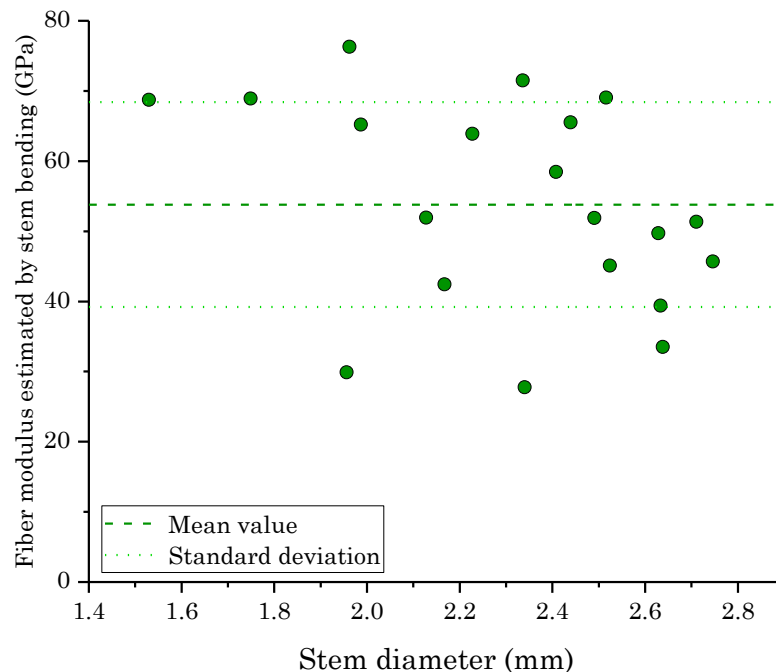


**Figure IV-7. Modulus of flax fibers estimated by bending test on stems.**

Only fibers are assumed to contribute to the bending stiffness within peeled tissues. Figure IV-7 gives the apparent moduli of flax fibers estimated by bending tests, showing no correlation between the modulus of flax fibers and the diameter of the

stem from which they are extracted. Equation IV-4 yields mean values of  $53.8 \pm 14.6$  GPa for flax fibers.

From a broader standpoint, it is possible to correlate the fiber mechanical properties to the morphology of the stem, particularly their slenderness. Indeed, the flax plants tested in this study reach a height of 1 m for a diameter ranging from 1.5 to 2.8 mm. The great mechanical properties of flax fibers as well as their contribution within the stem can be linked to the high length-to-diameter ratio of the plant.

To validate the method used for estimating fiber modulus from stem bending tests, the results are compared with the elementary fiber modulus measured by tensile tests. Figure IV-8 shows the mean longitudinal apparent modulus of flax fibers as a function of their diameter.

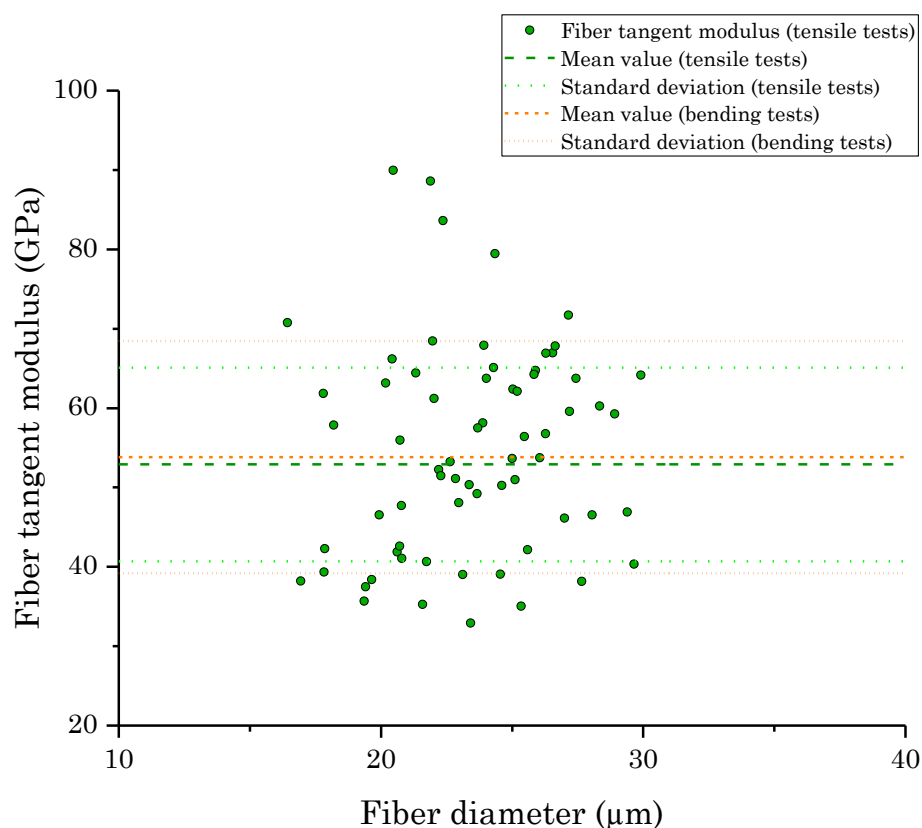


**Figure IV-8. Tangent modulus of flax elementary fibers measured by tensile test. Dashed lines represent the average fiber modulus value estimated by bending tests.**

Despite a wide scattering of the mechanical properties, the results show similar moduli for both types of experiments, namely an average tangent modulus reaching  $52.9 \pm 12.2$  GPa by tensile tests and a modulus of  $53.8 \pm 14.6$  GPa estimated by bending

tests. In addition, these values are well correlated with literature [8,29] and results given in previous chapters, showing an apparent modulus of about 50 GPa for flax.

Finally, it is possible to relate the stiffness of the stem to that of elementary fibers; three-point bending tests on stems could become a standard method for estimating the apparent modulus of flax fibers.

## 4. Results – Compressive strength of flax fibers within stems

### 4.1. Mechanical properties of elementary flax fibers

In order to analyze the compressive behavior of flax stems, it is necessary to know the mechanical properties of the elementary fibers composing their bundles. More particularly, the fiber Young’s modulus is required for the studied batches. Table IV-3 presents the average tensile properties of elementary fibers extracted after water retting of the related stem batches of different flax varieties.

**Table IV-3. Tensile mechanical properties of elementary fibers of the four flax varieties.**

Variety	Fiber diameter (μm)	Tangent modulus (GPa)	Strength at break (MPa)	Strain at break (%)
Bolchoï	22.7 ± 3.9	52.9 ± 12.2	1012 ± 283	2.12 ± 0.59
Eden	16.6 ± 2.8	54.9 ± 10.5	1056 ± 310	2.22 ± 0.62
Ariane	17.4 ± 2.6	43.6 ± 9.6	960 ± 288	2.39 ± 0.49
Liral Prince	21.8 ± 2.4	40.9 ± 10.2	860 ± 268	2.39 ± 0.62

These performances can be compared with the work of Baley and Bourmaud [3] which have analyzed numerous batches of elementary fibers, tested under a similar standard atmosphere and the same protocol than the present study. Average mechanical properties available in the mentioned literature are a Young’s modulus reaching  $52.5 \pm 8.6$  GPa, a strength at break of  $945 \pm 200$  MPa and a strain at break of  $2.07 \pm 0.45$  % for an average fiber diameter of  $16.8 \pm 2.7$  μm. One can notice that, despite slightly lower tensile Young’s modulus and strength at break for the oldest varieties (Liral Prince and Ariane), the diameters and mechanical properties of elementary fibers measured in the present work belong to the same ranges as literature values [3] and in Chapter II-3.3. These similarities confirm the good reproducibility of flax fibers mechanical properties, despite differences of flax varieties and retting methods.

#### 4.2. Failure mechanisms of flax stems during bending tests

Observations of a damaged stem (Bolchoï) through nanotomography highlights the mechanism of local buckling in the part of the stem in compression (Figure IV-9).

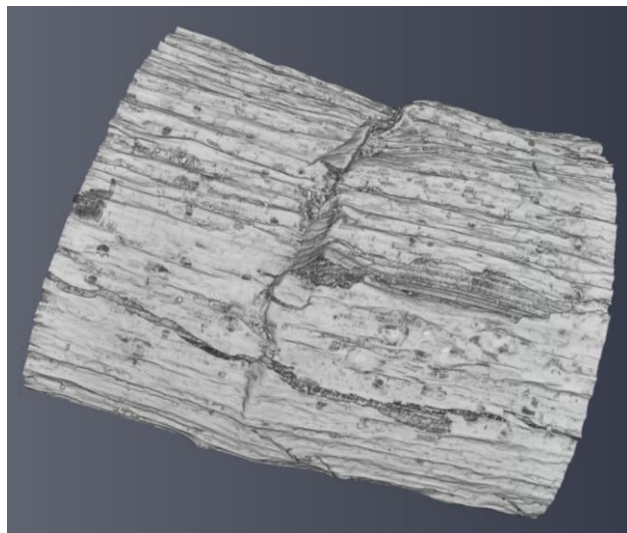


**Figure IV-9.** Nanotomographic image of a flax stem in the damaged area after a bending test. Local buckling is visible, due to excessive compressive strength.

In addition, the nanotomographic investigations enable to visualize a longitudinal section of the stem within the damaged zone (Figure IV-10).

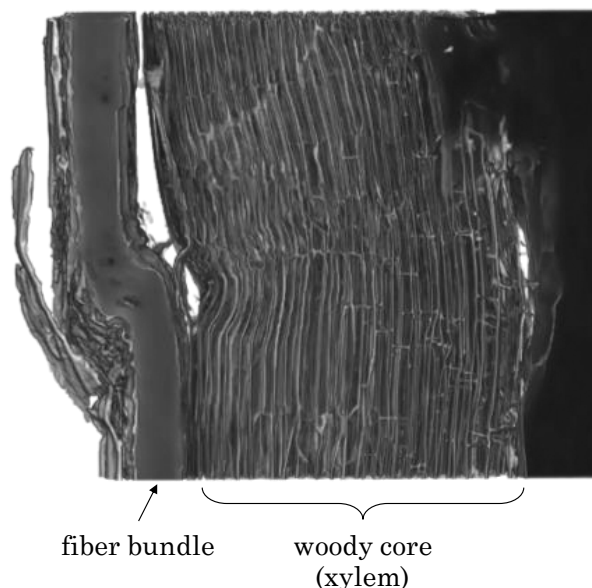


**Figure IV-10.** Nanotomographic image of a stem longitudinal section after the bending test, in the damaged area. The local buckling of the bundle is visible, as well as other cell types. The apparition of a kink-band is also highlighted.

Thanks to these observations, successive damages can be identified within a stem with, first, the local buckling of a fiber bundle together with the formation of a kink-band. The latter phenomenon is also visible on elementary fibers while bending [32], but also for wood under compressive strength [33,34] as well as for synthetic fibers such as ultra-high molecular weight polyethylene (UHMWPE) [35] or aramid [36]. Then, the detachment of the bundle from the woody core is visible in a small part of the stem. Finally, the local buckling of other cell types, namely conduction cells within the xylem core, is also visible on Figure IV-10. This latter figure also shows that the cohesion between the fiber bundles and xylem is a key parameter to the resistance of fiber bundles to local buckling, while both fibers and xylem provide the plant with mechanical support. However, one can notice that nanotomographic images do not allow to distinguish elementary fibers given the absence of density difference between fibers within the bundle.

### 4.3. Compressive properties of Bolchoï stems through bending tests

Figure IV-5 highlighted a good correlation between the diameter of a flax stem (Bolchoï) and its bending stiffness measured by three-point bending tests. When estimating the apparent bending modulus of the stem (Figure IV-6), the results showed that values are slightly dispersed, with a mean value of  $22.3 \pm 3.1$  GPa.

For some of the tested stem samples (namely 20 samples for which the diameter ranges from 1.57 mm to 2.84 mm), the maximal force damaging the sample ( $F_{max}$ ) is also measured. In addition, the average modulus of elementary fibers of Bolchoï was previously determined ( $E_{fibers,t} = 52.9$  GPa, see Table IV-3). From this set of data and through related equations, Table IV-4 gives the resulting stem apparent bending modulus, the maximal compressive strain at break ( $\epsilon_{max}$ ) and the bundle compressive strength at break ( $\sigma_{fmax}$ ).

**Table IV-4. Stem properties obtained from three-point bending tests on Bolchoï stems.**

Stem diameter (mm)	Bending stiffness (N.m <sup>2</sup> )	Apparent bending modulus (GPa)	Compressive strain at break (%)	Compressive strength at break (MPa)
$2.11 \pm 0.34$	$0.025 \pm 0.015$	$23.8 \pm 2.8$	$0.39 \pm 0.05$	$206 \pm 26$

In order to illustrate the scattering of the results, Figure IV-11 presents the compressive strength at break of fiber bundles as a function of the stem diameter.

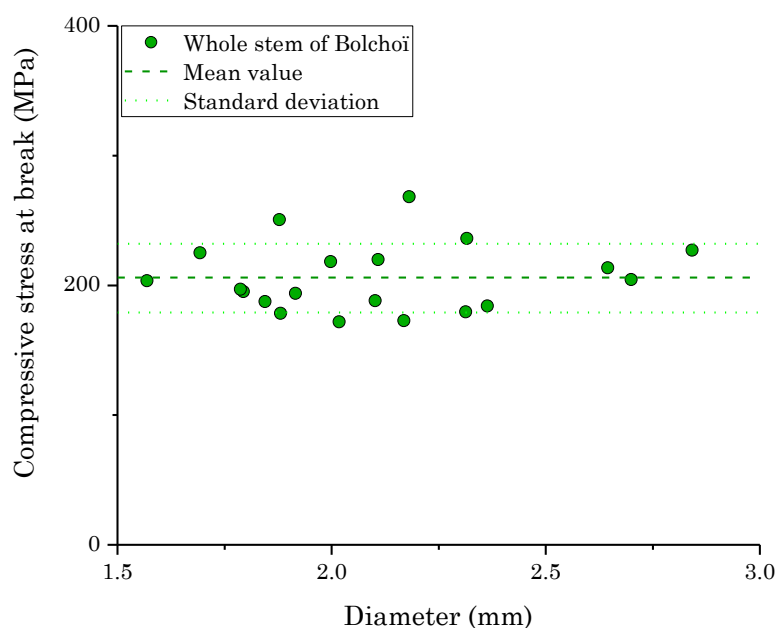


**Figure IV-11. Compressive strength at break of the fiber bundles as a function of the stem diameter.**

An absence of correlation between the mentioned properties is noticeable, *i.e.* there is no link between the compressive failure strength and the stem diameter. Moreover, the values are slightly scattered ( $206 \pm 26$  MPa) despite the difficulty to precisely achieve the stress value leading to local buckling in the part of the stem under compression. The maximal damaging force was used for calculations, but it is possible that the local buckling appears due to an accumulation of damages. This scenario is well described in literature for unidirectional plies reinforced by synthetic fibers solicited in compression [25]. In this case, the mechanism of kink-band formation is described as a succession of several steps; namely, the fiber breaks first by microbuckling, followed by the subsequent development of a damaged zone. Finally, the kink-band is formed from the shear instability, originated and visible in the damage zone.

#### 4.4. Compressive properties of flax stems of different varieties

The flax variety previously studied is Bolchoï; a recent one having a high fiber content. This later parameter is a major criterion of selection for flax breeders. Thus, one can wonder what would be the influence of the fiber content, *i.e.* of the variety, on the compressive resistance of flax bundles. In Chapter II-3.2, we investigated the impact

of the varietal selection on the stem architecture (namely the plant anatomy) thanks to an analysis of 4 different varieties selected at different times but cultivated during the same year, in the same location and under the same cultural conditions. The evolution of the fiber content over selection, namely increased fiber contents for more recent varieties, was highlighted. Figure IV-13 presents a transverse stem section of a more recent variety, Bolchoï, having thick fiber bundles and a high fiber yield.

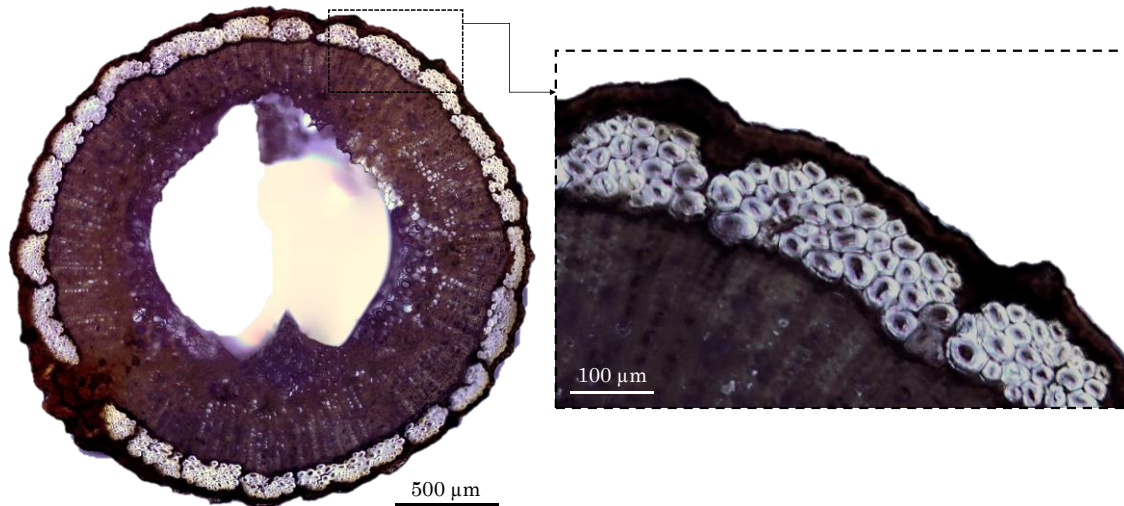


**Figure IV-12. Transverse cross-section of a stem of Bolchoï exhibiting thick fiber bundles (100 µm in average).**

Based on image analysis and three-point bending tests, Table IV-5 presents the results and links between the compression resistance of the stem and the thickness of their respective fiber bundles. Thus, a general increase of the compressive strength at break is visible with increasing bundle thickness in the plant.

**Table IV-5. Influence of the flax variety and fiber bundle thickness on the compression resistance of the stems.**

Variety	Stem diameter (mm)	Fiber bundles thickness (µm)	Bending stiffness (N.m <sup>2</sup> )	Apparent bending modulus (GPa)	Compressive strain at break (%)	Compressive strength at break (MPa)
Bolchoï	2.11 ± 0.34	102 ± 18	0.025 ± 0.015	23.8 ± 2.8	0.39 ± 0.05	206 ± 26
Eden	2.02 ± 0.23	99 ± 16	0.018 ± 0.006	20.8 ± 2.2	0.38 ± 0.02	207 ± 8
Ariane	2.11 ± 0.34	70 ± 18	0.020 ± 0.012	18.2 ± 1.7	0.43 ± 0.04	189 ± 16
Liral Prince	2.10 ± 0.29	73 ± 13	0.019 ± 0.009	18.4 ± 2.4	0.45 ± 0.04	183 ± 15

In addition, as visible on the cross-section of Bolchoï (Figure IV-12), the fibrous ring is continuous along the stem periphery, which decreases the risk of buckling; this result is true for recent varieties, whereas ancient ones exhibit gaps between neighboring bundles (Chapter II-3.2). Moreover, the elastic modulus of elementary fibers is greater for recent varieties (Table IV-3), which strengthens the stems.

#### **4.5. Compressive properties of xylem cores through bending tests**

Complementary, peeled stems of Bolchoï (considered as only composed of the xylem core) are submitted to three-point tests. The main aim of this analysis is to achieve the strain capacity of the woody core than cannot withstand buckling. This component of the stem is constituted of cells of short length (about 250  $\mu\text{m}$  long), which are responsible for the conduction of the raw sap (Chapter II-4.1). These conductive cells have a great lumen size and thin cell walls, as shown in Figure IV-2 and Figure IV-10. Furthermore, the biochemical composition of woody cells differs from the fiber ones [37], mainly in terms of cellulose content but also of non-cellulosic polymer fraction and nature. On average, when expressed in percentage of cellulose in the dry matter, the woody core reaches 45.6% whereas it reaches 78.7% for the fibers [37]. The mechanical behavior of a peeled stem was shown in Figure IV-4. Additionally, such as for entire stems, the bending stiffness of samples with scattered diameters was analyzed (Figure IV-5), highlighting a good correlation between the bending stiffness of the woody core and the sample diameter. By measuring the bending stiffness of the peeled stems, the apparent bending modulus was calculated by considering the woody core as a homogeneous material (Figure IV-6).

Complementary, the compressive strain at break obtained from the maximal force damaging the sample is estimated for ten specimens, with diameter ranging from 1.62 mm to 2.54 mm (Figure IV-13). For the woody core, there is a slight correlation between the strain at break and the sample diameter, and a better understanding of the phenomenon would require further investigations.

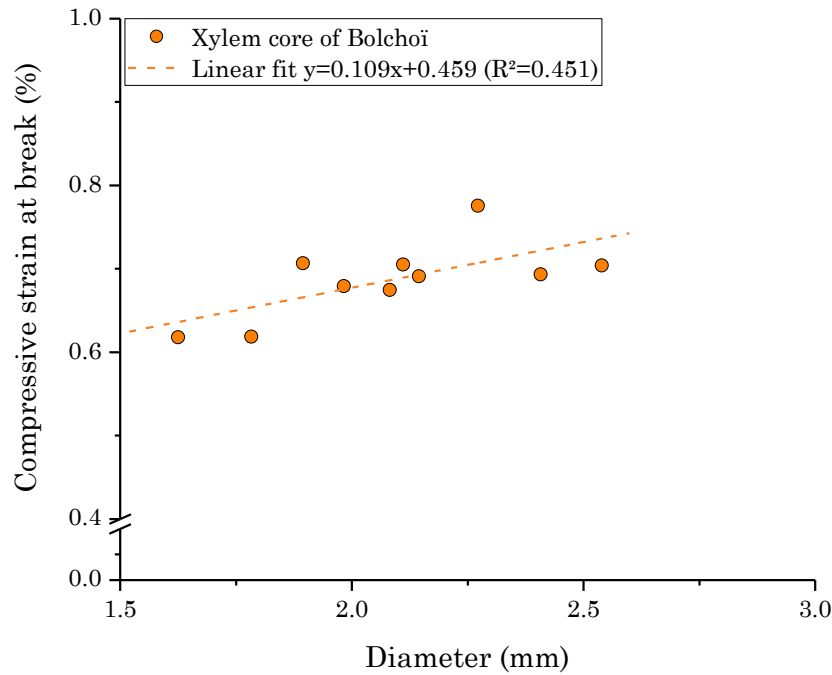


**Figure IV-13. Compressive strain at break of the xylem core as a function of the sample diameter.**

Table IV-6 reports the mechanical properties resulting from three-point bending tests on peeled samples. In comparison with entire stem samples (Table IV-4), a superior strain at break of the woody core ( $0.69\% \pm 0.05$ ) is demonstrated compared with the one of fiber bundles ( $0.39\% \pm 0.05$ ).

**Table IV-6. Xylem properties obtained from three-point bending tests on peeled samples of Bolchoï.**

Sample diameter (mm)	Bending stiffness (N.m <sup>2</sup> )	Apparent bending modulus (GPa)	Compressive strain at break (%)	Compressive strength at break (MPa)
$2.08 \pm 0.28$	$0.009 \pm 0.005$	$8.5 \pm 4.7$	$0.69 \pm 0.05$	$59 \pm 6$

Through a greater strain capacity, the contribution of the woody core in limiting the buckling risk of flax stems under compression is confirmed. However, the compressive strength at break of this porous structure is rather low (59 MPa on average in Table IV-6) compared to fiber bundles (206 MPa in Table IV-4).

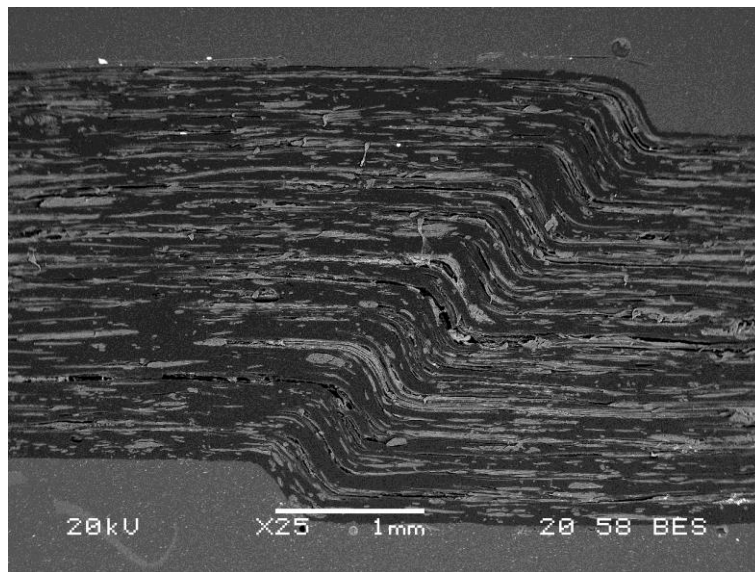
In this study, the mean apparent density of flax xylem reaches  $0.455 \pm 0.113 \text{ g/cm}^3$ . When compared to the compressive strength at break of wood, estimated by the wood

density [38], a mean value of 45 MPa is expected for wood when using the flax xylem density of 0.455 (as a change in density of wood samples is known to influence their mechanical properties [39]). Finally, for an equivalent density, the compressive strength at break of the woody core belongs to the same range of values as for wood, and is even somewhat superior.

## 5. Discussion – Correlation between compressive properties of UD (flax/epoxy) and fiber bundles within a stem

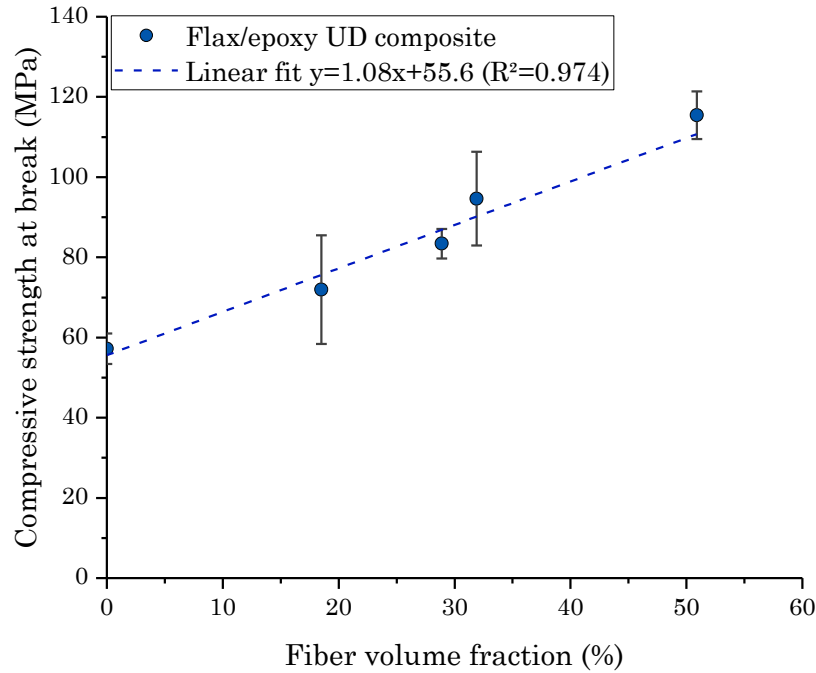
### 5.1. Compressive properties of unidirectional flax/epoxy composites

Figure IV-14 shows the buckling of flax fibers inside a unidirectional laminate flax/epoxy loaded in compression. This type of phenomenon is a standard behavior and failure mode of composite materials.



**Figure IV-14. Typical kinking failure in a flax-epoxy after compressive loading.**

Complementary, Figure IV-15 shows the longitudinal compressive strength of flax/epoxy composites as a function of fiber volume fraction. The strength increasing with the fiber volume fraction illustrates a reinforcing effect.



**Figure IV-15. Compressive strength as a function of fiber volume fraction for unidirectional flax/epoxy composite.**

The maximum measured strength is 115 MPa for a fiber volume fraction of 50.9%. This limited value confirms the literature data sets presented in Table IV-1 for composites reinforced by flax fibers. Moreover, this value is significantly lower than that measured for glass-fiber reinforced composites [40] (*e.g.* for glass/epoxy UD with 45% of fiber volume fraction, the longitudinal compressive strength is 621 MPa [41]).

Obviously, other parameters could be taken into account to refine these results, such as the bundle division and distribution in a ply cross section as well as the fiber orientation inside the composites. Indeed, flax fibers have a limited length, and it is not possible to apply a tensile load during the process to obtain their perfect orientation. Additionally, the bonding between fiber and matrix with this batch of fibers is another parameter to consider. However, the good adhesion between flax and epoxy is described in the literature [42]. Finally, the possible evolution of the cell wall properties during the transformation cycle (*e.g.* retting, scutching, combing, manufacturing of unidirectional preform, *etc.*) could be investigated.

Furthermore, by an inverse approach, the compressive strength leading to fiber buckling can be estimated through different approaches. These approaches aim at comparing the properties of flax stems with unidirectional composites, rather than providing a micromechanical model to predict the compressive strength of flax bundles.

## 5.2. First approach to estimate the fiber compressive strength

Fiber compressive strength ( $\sigma_f$ ) can be estimated from the compressive strength of the unidirectional composite ( $\sigma_{UD}$ )(Equation IV-8).

$$\sigma_f = \frac{\sigma_{UD}}{V_f}$$

**Equation IV-8. Estimation of the fiber compressive strength ( $\sigma_f$ ), where  $\sigma_{UD}$  is the compressive strength of the UD composite and  $V_f$  the fiber volume fraction [43].**

The hypothesis is that the compressive strength is linearly proportional to the fiber volume fraction ( $V_f$ ), which is validated for glass fibers [40]. With our set of results, the longitudinal compressive strength of flax fibers is estimated to  $260 \pm 59$  MPa (average of the measured values by taking all the specimens).

## 5.3. Second Approach to estimate the fiber compressive strength

In a second approach, the contribution of the matrix is considered. In this case, the fiber buckling strain is much lower than the strain at break of the epoxy resin. The longitudinal compressive strength of a unidirectional ( $\sigma_{UD}$ ) can be approached using a mixture law (Equation IV-9).

$$\sigma_{UD} = V_f \sigma_f + (1 - V_f) \sigma_m$$

**Equation IV-9. Mixture law to calculate the UD compressive strength ( $\sigma_{UD}$ ), where  $V_f$  is the fiber volume fraction,  $\sigma_f$  the compressive strength causing fiber buckling and  $\sigma_m$  the stress in the matrix during fiber buckling.**

Considering an elastic and linear behavior, Equation IV-9 becomes Equation IV-10.

$$\sigma_{UD} = V_f \sigma_f + (1 - V_f) \varepsilon_f E_m$$

**Equation IV-10. Calculation of the UD compressive strength ( $\sigma_{UD}$ ), where  $E_m$  is the matrix modulus (3 GPa here) and  $\varepsilon_f$  is the strain causing fiber buckling.**

$\varepsilon_f$  is determined by bending tests on stem ( $0.39 \pm 0.05$  %, see Table IV-4). Finally, the longitudinal compressive strength of flax fibers can be estimated by Equation IV-11.

$$\sigma_f = \frac{\sigma_{UD} - (1 - V_f) \varepsilon_f E_m}{V_f}$$

**Equation IV-11. Calculation of compressive strength of flax fibers ( $\sigma_f$ ), where  $\sigma_{UD}$  is the UD compressive strength,  $E_m$  is the matrix modulus,  $\varepsilon_f$  is the strain causing fiber buckling and  $V_f$  is the fiber volume fraction.**

With the set of results of the present study, the longitudinal compressive strength of flax fibers is estimated to  $242 \text{ MPa} \pm 44 \text{ MPa}$ . For comparison, Table IV-7 shows the estimated compressive strength of flax fibers from tests on both UD composite and stems.

**Table IV-7. Estimated compressive strength of flax fibers from unidirectional composite tests and stem bending tests.**

	Compressive strength at fiber buckling (MPa)
UD - First approach	$260 \pm 59$
UD - Second approach	$242 \pm 44$
Stem - Bolchoï	$206 \pm 26$
Stem - Eden	$207 \pm 8$
Stem - Ariane	$189 \pm 16$
Stem - Liral Prince	$183 \pm 15$

The estimated values given in Table IV-7 are of the same order of magnitude, with a difference of less than 10% between the two approaches regarding UD ( $260 \text{ MPa}$  and  $242 \text{ MPa}$  respectively), and a difference of less than 15% between average values of flax varieties (from  $183 \text{ MPa}$  to  $207 \text{ MPa}$  for Liral Prince and Eden, respectively). The estimated strength is slightly lower for the old varieties (Liral Prince and Ariane) due to their low fiber content. The poor compression strength of flax fibers in a unidirectional composite is also observed within the stems. This is a limit for the use of flax for the reinforcement of a polymer, as in the case of organic fibers [43].

A comparison with wood is also possible. In fact, wood is a composite material composed of an assembly of fibers mainly oriented along the axis of primary growth. The mechanism leading to the compressive break of wood is a kink banding phenomenon [24], such as observed in unidirectional composites reinforced by flax. The compressive behavior of wood is linearly proportional to the specific gravity [38]. This relationship allows the modelling of structures, and remains valid whether the wood is green or air dried. Thus, Gibson [44] estimated the axial compressive strength of a wood cell wall as  $120 \text{ MPa}$ , which corresponds to a densified wood with no lumen.

Higher values are obtained for flax, mainly due to higher cellulose content and lower microfibrillar angle.

#### **5.4. Is the modest compression strength of flax fibers a problem for living plants?**

In the living plant, the fiber state is different, mainly because living tissues have a higher water content. Water is known to be a plasticizer of plant cell walls. For example, the compressive strength of wood decreases with increasing moisture content [38] to the saturation point of the cell walls. Theoretically, the fiber saturation point corresponds to the moisture content of wood when placed under 100% relative humidity. The same behavior is observed for the stiffness, which decreases with the increase in water content absorbed by the plant walls [38] while, on the other hand, the strain at break increases. To our knowledge, the whole mechanical properties of fibers in a living flax stem are unidentified. Nevertheless, by bending tests on green or dried stems, the fiber modulus of elasticity was compared [16], and was shown to be 25% lower for green flax fibers (in the living plant) than that of dried fibers.

Moreover, in the living plant, it is important to consider the turgor pressure, which greatly increases the transverse stiffness of the stems [45]. For example, in the case of *Equisetum giganteum*, the turgor pressure insures the resistance against stem ovalization (e.g. the turgor loss decreases the transverse stem stiffness by a factor of five for this latter plant [45]).

Furthermore, plants develop themselves by limiting the risk of buckling instability, a result that has been analyzed for trees [46,47]. For slender beams subjected to buckling, the criterion to compare two solutions is  $(E^{1/2}/d)$ , where  $E$  is the apparent bending modulus and  $d$  the density. In spite of having a limited bending stiffness, the flax stem has a low density which is a favorable element. Flax plants are therefore very lightly loaded structures. The stem flexibility also allows them to accommodate wind loads by reducing their aerodynamic drag [48]. By experience of flax farmers, in a field, the flax plants are able to resist wind gusts up to 120 km/h.

## 6. Conclusions

This chapter sets up a new method of estimating the apparent modulus of flax fibers, through a simple three-point bending test. The first results have led to a better understanding of the role of the fibers within the dry stem. The bending tests on stems with and without fibers allow a determination of their stiffness and bending modulus, with a loss of  $70 \pm 8\%$  of these values for fiber-free samples. This high value confirms the important contribution of flax fibers to the stiffness of the stems.

Fibers moduli obtained by stem bending ( $53.8 \pm 14.6$  GPa) are very close to those measured by tensile tests on elementary fibers ( $52.9 \pm 12.2$  GPa) extracted from the same batch of stems, which validate this new approach. However, this protocol requires a delicate morphological analysis and does not take into consideration the detailed behavior of these natural fibers. Nevertheless, bending tests on stems represent an original and rapid method for estimating the apparent moduli of fibers.

In addition, this chapter illustrated the compression buckling mechanisms of flax fiber bundles within a stem. The analysis of the measured values made it possible to estimate the stress causing bundle instability within a flax stem ( $206 \pm 26$  MPa for Bolchoï stems). The stem organization influences the behavior; as the compression strength of the bundles was slightly lower for the older varieties having a smaller fraction of fibers (the lowest value reaches  $183 \pm 15$  MPa for Liral Prince). In addition, thanks to longitudinal compressive tests on unidirectional laminates, the limited reinforcement of flax fibers was illustrated. By an inverse method using two different approaches, the theoretical compressive strength of flax fibers was estimated and both approaches led to the same orders of magnitude ( $242 \pm 44$  MPa and  $260 \pm 59$  MPa). Thus, despite an assumed optimal arrangement of the fibers in the stems and a strong fiber cohesion, the fiber compression strength remains limited. This assessment is a limit of the use of flax fibers as polymer reinforcement, especially when significant compressive properties are required. The central part of the stem, namely the xylem core, exhibits a higher apparent strain in compression despite the thin xylem cell walls and large lumens, which can be explained by the conductive function of this inner core. This xylem tissue significantly contributes to the compressive strength of the stem, such as in a structure sandwich. To go further, future works should be carried out on living plants for a better understanding of their strengthening mechanisms.

## 7. References

1. Bos, H. L.; Molenveld, K.; Teunissen, W.; Van Wingerde, A. M.; Van Delft, D. R. V. Compressive behaviour of unidirectional flax fibre reinforced composites. *J. Mater. Sci.* 2004, 39, 2159–2168, doi:10.1023/B:JMSC.0000017779.08041.49.
2. Van Vuure, A. W.; Baets, J.; Wouters, K.; Hendrickx, K. Compressive properties of natural fibre composites. *Mater. Lett.* 2015, 149, 138–140, doi:10.1016/j.matlet.2015.01.158.
3. Baley, C.; Bourmaud, A. Average tensile properties of French elementary flax fibers. *Mater. Lett.* 2014, 122, 159–161, doi:10.1016/j.matlet.2014.02.030.
4. Bourmaud, A.; Gibaud, M.; Baley, C. Impact of the seeding rate on flax stem stability and the mechanical properties of elementary fibres. *Ind. Crops Prod.* 2016, 80, 17–25, doi:10.1016/j.indcrop.2015.10.053.
5. Kulma, A.; Zuk, M.; Long, S. H.; Qiu, C. S.; Wang, Y. F.; Jankauskiene, S.; Preisner, M.; Kostyn, K.; Szopa, J. Biotechnology of fibrous flax in Europe and China. *Ind. Crops Prod.* 2015, 68, 50–59, doi:10.1016/j.indcrop.2014.08.032.
6. Snegireva, A. V.; Ageeva, M. V.; Amenitskii, S. I.; Chernova, T. E.; Ebskamp, M.; Gorshkova, T. A. Intrusive growth of sclerenchyma fibers. *Russ. J. Plant Physiol.* 2010, 57, 342–355, doi:10.1134/S1021443710030052.
7. Rihouey, C.; Paynel, F.; Gorshkova, T.; Morvan, C. Flax cellulosic fibres: how to assess the non-cellulosic polysaccharides and to approach cell wall supramolecular design. *Cellulose* 2017, In press.
8. Charlet, K.; Jernot, J. P.; Gomina, M.; Bréard, J.; Morvan, C.; Baley, C. Influence of an Agatha flax fibre location in a stem on its mechanical, chemical and morphological properties. *Compos. Sci. Technol.* 2009, 69, 1399–1403, doi:10.1016/j.compscitech.2008.09.002.
9. Andème-Onzighi, C.; Girault, R.; His, I.; Morvan, C.; Driouich, A. Immunocytochemical characterization of early-developing flax fiber cell walls. *Protoplasma* 2000, 213, 235–245, doi:10.1007/BF01282161.
10. Baley, C.; Le Duigou, A.; Bourmaud, A.; Davies, P.; Nardin, M.; Morvan, C. Reinforcement of polymers by flax fibers: role of interfaces. In *Bio-Based Composites for High-Performance Materials*; CRC Press, 2014; pp. 87–112 ISBN 978-1-4822-1448-2.
11. Day, A.; Ruel, K.; Neutelings, G.; Crônier, D.; David, H.; Hawkins, S.; Chabbert, B. Lignification in the flax stem: Evidence for an unusual lignin in bast fibers. *Planta* 2005, 222, 234–245, doi:10.1007/s00425-005-1537-1.
12. Deger, G. G.; Pakdemirli, M.; Candan, F.; Akgün, S.; Boyacı, H.; Akgun, S.; Boyaci, H. Strength of wheat and barley stems and design of new beam/columns. *Math. Comput. Appl.* 2010, 15, 1–13, doi:10.3390/mca15010001.
13. Robertson, D. J.; Smith, S. L.; Cook, D. D. On measuring the bending strength of septate grass stems. *Am. J. Bot.* 2015, 102, 5–11, doi:10.3732/ajb.1400183.
14. Leblicq, T.; Vanmaercke, S.; Ramon, H.; Saeys, W. Mechanical analysis of the bending behaviour of plant stems. *Biosyst. Eng.* 2015, 129, 87–99, doi:10.1016/j.biosystemseng.2014.09.016.
15. Shah, D. U.; Reynolds, T. P.; Ramage, M. H. The strength of plants: theory and experimental methods to measure the mechanical properties of stems. *J. Exp. Bot.* 2017, 68, 4497–4516, doi:10.1093/jxb/erx245.
16. Gibaud, M.; Bourmaud, A.; Baley, C. Understanding the lodging stability of green flax stems; The importance of morphology and fibre stiffness. *Biosyst. Eng.* 2015, 137, 9–21, doi:10.1016/j.biosystemseng.2015.06.005.

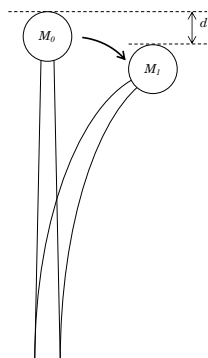
17. Berry, P. M.; Sylvester-Bradley, R.; Berry, S. Ideotype design for lodging-resistant wheat. *Euphytica* 2007, 154, 165–179, doi:10.1007/s10681-006-9284-3.
18. Niklas, K. J. Responses of hollow, septate stems to vibrations: Biomechanical evidence that nodes can act mechanically as spring-like joints. *Ann. Bot.* 1997, 80, 437–448, doi:10.1006/anbo.1997.0463.
19. Roussi re, F.; Baley, C.; Godard, G.; Burr, D. Compressive and tensile behaviours of PLLA matrix composites reinforced with randomly dispersed flax fibres. *Appl. Compos. Mater.* 2012, 19, 171–188, doi:10.1007/s10443-011-9189-8.
20. Livingston Smith, S.; Mech, M. A survey of plastics from the viewpoint of the mechanical engineer. *Inst. Mech. Eng.* 1945, 29–43.
21. Liang, S.; Gning, P.-B.; Guillaumat, L. Quasi-static behaviour and damage assessment of flax/epoxy composites. *Mater. Des.* 2015, 67, 344–353, doi:10.1016/j.matdes.2014.11.048.
22. Mahboob, Z.; El Sawi, I.; Zdero, R.; Fawaz, Z.; Bougherara, H. Tensile and compressive damaged response in Flax fibre reinforced epoxy composites. *Compos. Part A Appl. Sci. Manuf.* 2017, 92, 118–133, doi:10.1016/j.compositesa.2016.11.007.
23. de Bruyne, N. A. Plastic progress - Some further developments in the manufacture and use of synthetic materials for aircraft construction. *Flight Aircr. Eng.* 1939, 77–79.
24. Poulsen, J. S.; Moran, P. M.; Shih, C. F.; Byskov, E. Kink band initiation and band broadening in clear wood under compressive loading. *Mech. Mater.* 1997, 25, 67–77, doi:10.1016/S0167-6636(96)00043-9.
25. Garland, B. D.; Beyerlein, I. J.; Schadler, L. S. The development of compression damage zones in fibrous composites. *Compos. Sci. Technol.* 2001, 61, 2461–2480, doi:10.1016/S0266-3538(01)00176-2.
26. Bert, F. *Lin fibre - Culture et transformation*; Arvalis, Ed.; 2013; ISBN 9782817901572.
27. Charlet, K.; Baley, C.; Morvan, C.; Jernot, J. P.; Gomina, M.; Br ard, J. Characteristics of Herm s flax fibres as a function of their location in the stem and properties of the derived unidirectional composites. *Compos. Part A Appl. Sci. Manuf.* 2007, 38, 1912–1921, doi:10.1016/j.compositesa.2007.03.006.
28. Timoshenko, S. P. *Strength of Materials - part 2 - Advanced Theory and Problems*. 9th printing.; Van, N., Ed.; van, Nostrand, 1947; ISBN 0898746213.
29. Lefeuvre, A.; Bourmaud, A.; Lebrun, L.; Morvan, C.; Baley, C. A study of the yearly reproducibility of flax fiber tensile properties. *Ind. Crops Prod.* 2013, 50, 400–407, doi:10.1016/j.indcrop.2013.07.035.
30. Khalfallah, M.; Abb s, B.; Abb s, F.; Guo, Y. Q.; Marcel, V.; Duval, A.; Vanfleteren, F.; Rousseau, F. Innovative flax tapes reinforced Acrodur biocomposites: A new alternative for automotive applications. *Mater. Des.* 2014, 64, 116–126, doi:10.1016/j.matdes.2014.07.029.
31. Siau, J. F. *Transport Processes in Wood*; Timell, T. E., Ed.; Springer S.; Springer Science & Business Media, 1984; ISBN 9783642692154.
32. Baley, C. Analysis of the flax fibres tensile behaviour and analysis of the tensile stiffness increase. *Compos. - Part A Appl. Sci. Manuf.* 2002, 33, 939–948, doi:10.1016/S1359-835X(02)00040-4.
33. Benabou, L. Kink band formation in wood species under compressive loading. *Exp. Mech.* 2008, 48, 647–656, doi:10.1007/s11340-007-9098-9.
34. Zaune, M.; Stampanoni, M.; Niemz, P. Failure and failure mechanisms of wood during longitudinal compression monitored by synchrotron micro-computed tomography. *Holzforschung* 2016, 70, 179.

35. Attwood, J. P.; Fleck, N. A.; Wadley, H. N. G.; Deshpande, V. S. The compressive response of ultra-high molecular weight polyethylene fibres and composites. *Int. J. Solids Struct.* 2015, 71, 141–155, doi:10.1016/j.ijsolstr.2015.06.015.
36. Deteresa, S. J.; Porter, R. S.; Farris, R. J. Experimental verification of a microbuckling model for the axial compressive failure of high performance polymer fibres. *J. Mater. Sci.* 1988, 23, 1886–1894, doi:10.1007/BF01115735.
37. Evon, P.; Barthod-Malat, B.; Grégoire, M.; Vaca-Medina, G.; Labonne, L.; Ballas, S.; Véronèse, T.; Ouagne, P. Production of fiberboards from shives collected after continuous fiber mechanical extraction from oleaginous flax. *J. Nat. Fibers* 2018, 0, 1–17, doi:10.1080/15440478.2017.1423264.
38. Domone, P.; Illston, J. *Construction materials: Their nature and behaviour* Fourth edition; Spon Press, 2010; ISBN 0-203-92757-5.
39. Bardet, S.; Beauchene, J.; Thibaut, B. Influence of basic density and temperature on mechanical properties perpendicular to grain of ten wood tropical species. *Ann. For. Sci.* 2003, 60, 49–59, doi:10.1051/forest.
40. Lo, K. H.; Chim, E. . Compressive strength of unidirectional composites. *J. Reinf. Plast. Compos.* 1992, 11, 838–896.
41. Gibson, R. *Principles of composites materials mechanics*; 3rd Editio.; Boca Raton: CRC Press., 2012; ISBN 9781439850053.
42. Le Duigou, A.; Kervoelen, A.; Le Grand, A.; Nardin, M.; Baley, C. Interfacial properties of flax fibre-epoxy resin systems: Existence of a complex interphase. *Compos. Sci. Technol.* 2014, 100, 152–157, doi:10.1016/j.compscitech.2014.06.009.
43. Kozez, V.; Jiang, H.; Mehta, V.; Kumar, S. Compressive behavior of materials: Part II. High performance fibers. *Mater. Resarch Soc.* 1995, 10, 1044–1061.
44. Gibson, L. J. The hierarchical structure and mechanics of plant materials. *J R Soc Interface* 2012, 9, 2749–2766, doi:10.1098/rsif.2012.0341.
45. Spatz, H. C.; Köhler, L.; Speck, T. Biomechanics and functional anatomy of hollow-stemmed sphenopsids. I. *Equisetum giganteum* (Equisetaceae). *Am. J. Bot.* 1998, 85, 305–314, doi:10.2307/2446321.
46. Jaouen, G.; Alméras, T.; Coutand, C.; Fournier, M. How to determine sapling buckling risk with only few measurements. *Am. J. Bot.* 2007, 94, 1583–1593.
47. Niklas, K. J.; Spatz, H.-C. Growth and hydraulic (not mechanical) constraints govern the scaling of tree height and mass. *Proc. Natl. Acad. Sci. U. S. A.* 2004, 101, 15661–15663, doi:10.1073/pnas.0405857101.
48. de Langre, E. Effects of wind on plants. *Annu. Rev. Fluid Mech.* 2008, 40, 141–168, doi:10.1146/annurev.fluid.40.111406.102135.

**CHAPTER V – INFLUENCE OF CULTURAL  
CONDITIONS AND STIMULI ON FLAX STEMS AND  
FIBERS**

## Graphical abstract

---



- ❖ How can such a slender plant be mechanically stable?

**Goudenhooff, C.;** Alméras, T.; Bourmaud, A.; Baley, C. The remarkable slenderness of flax plant and pertinent factors affecting its mechanical stability. *Biosyst. Eng.*, *under review*.



- ❖ What is the influence of greenhouse cultivation on the properties of flax stems and fibers?

**Goudenhooff, C.;** Bourmaud, A.; Baley, C. Conventional or greenhouse cultivation of flax: What influence on the number and quality of flax fibers?. *Ind. Crops Prod.* **2018**, *accepted on 06/18/2018*.



- ❖ Are plant characteristics impacted by lodging and recovery?

**Goudenhooff, C.;** Bourmaud, A.; Baley, C. Study of plant gravitropic response: exploring the influence of lodging and recovery on the mechanical performances of flax fibers. *Ind. Crops Prod.*, *under review*.

## **CHAPTER V – INFLUENCE OF CULTURAL CONDITIONS AND STIMULI ON FLAX STEMS AND FIBERS**

---

The use of flax fibers for industrial purposes requires increasing quantities and constant quality. To increase fiber yields, the varietal selection has been used to develop varieties having great fiber content, while keeping a good resistance to lodging. This selection has led to impressively slender structures of flax compared to other herbaceous plants. The first section of the present chapter consists of a study of the mechanical stability of the flax stem related to its specific architecture when grown under conventional cultural conditions. Moreover, plants can change their morphology and mechanical properties when submitted to stress. It is the case of the reaction of plants to wind, a phenomenon known as seismomorphogenesis. To get better insights on the influence of wind on flax properties, greenhouse and field cultivations are compared in the second section, both at stem and fiber scales. The last section of this chapter focuses on lodging, which sometimes happens within flax fields, complicating plant harvest and compromising yields. Interestingly, it sometimes occurs that flax stems restore from lodging through a gravitropic reaction. The effects of lodging on the fiber mechanical performances are explored to evaluate the suitability of fibers from lodged plants for composite reinforcement.

### **1. Introduction**

Flax is highly valued for its fibers, a distinctive feature explaining the development of practices for its varietal selection, aiming at increasing the fiber yields, plant stability to lodging and resistance against diseases [1]. Although the influence of varietal selection can be currently seen in terms of effective yields, it has also affected the plant anatomy. Nevertheless, under conventional cultural conditions, the mechanical properties of flax elementary fibers remain reliable whatever the fiber yield and only slightly influenced by flax variety (Chapter II. 3.3). Moreover, even though the varietal selection of flax also aims at improving the lodging stability, this natural phenomenon remains a major problem for flax as well as other crop plants such as wheat or barley, as it compromises yield and quality [2–4].

### 1.1. Slenderness of plants and mechanical stability

In addition to its industrial advantages, flax stems possess outstanding morphological properties. To our knowledge, the slenderness factor (*i.e.* the ratio between height and diameter of the stem) of flax has no competitor among herbs and trees. In fact, when compared to the 76 species of herbaceous stems studied by Niklas [5], flax possesses a much greater slenderness (Figure V-1) taking an average basal diameter of 3 mm and a total height of 1.17 m as measured in the present work.

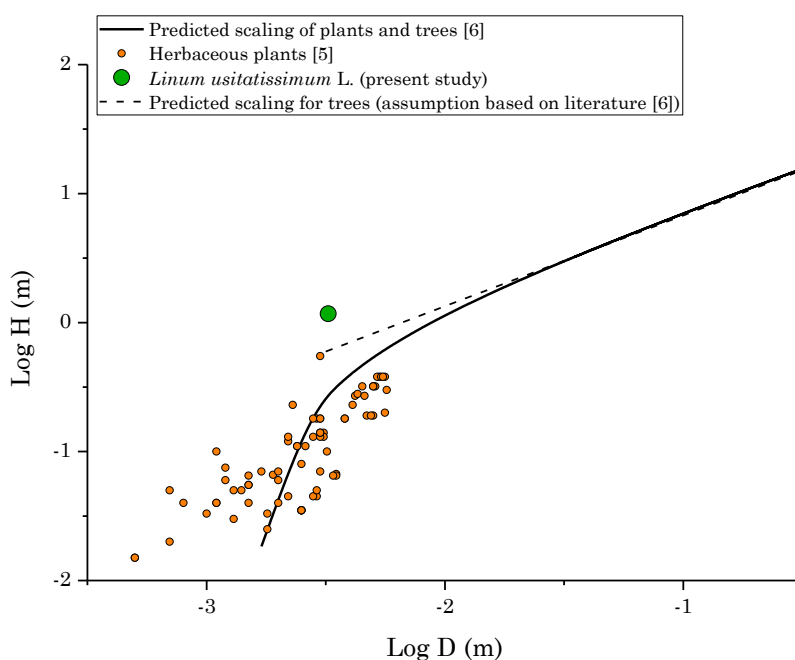


**Figure V-1. Scaling relationship for plant height ( $H$ ) and basal diameter ( $D$ ) measured on flax (*Linum usitatissimum* L) in this chapter, in comparison with herbaceous plants analyzed by Niklas [5] and using the predicted scaling of plants and trees given by Niklas and Spatz [6] by  $H = 34.64 \times D^{2/3} - 0.475$ . The assumption made here to predict the scaling of trees is based on the study of Niklas and Spatz [6].**

The value for flax given here refers to a recent variety and is based on plants cultivated using a conventional seeding rate, *i.e.* making a compromise between fiber yields and plant stability [7]. Finally, even though flax is an herbaceous plant with a limited secondary growth, this plant appears to follow a scaling relationship more closely resembling trees rather than herbaceous plants (Figure V-1), according to our assumption based on literature [6]. Additionally, to quantify the impact of varietal selection on the lodging stability of flax stems, a crucial parameter to consider is the mechanical stability of the plant [8]. Indeed, for flax, the risk of lodging increases with

rainfall and wind, but a high slenderness ratio also implies a risk of elastic buckling due to self-weight and additional loads such as rain. The degree of mechanical stability can be accessed through the safety factor against buckling, defined as the ratio between the critical buckling height and actual height of the plant [9]. The critical buckling height [10] is the maximal height that the plant can reach while remaining stable, given its diameter and material properties. In a study on tree saplings grown in a tropical environment, Jaouen et al. [11] showed that variations in critical buckling height also strongly depend on “form” parameters, namely the distribution of mass and diameters along the stem. The stability of the plant may also depend on gradients in mechanical properties along the stem, but the case of flax remains to be explored.

## **1.2. Plant response to a mechanical stress: case of wind**

Studies have been conducted on the impact of mechanically-induced stress (MIS) on plant properties such as yield or anatomy. MIS can be of natural origin, resulting from the action of wind, rain or animals, but it can also be induced indoors, for example by rubbing or brushing plants [12]. The plant response is termed thigmomorphogenesis in the case of physical contact [13] and seismomorphogenesis when it is due to the action of wind [14]; the plant response can radically differ between unstressed and stressed plants.

A first example of such responses is the reduction in plant height often observed on plants exposed to wind or other MIS [12]. For instance, it has been shown that wind-exposed trees are shorter and more tapered, but exhibit an overall lower stiffness, even though their mechanical properties are less affected than their morphology [15]. On the contrary, wheat plants are stronger and less flexible, but show no significant change in stem height under the influence of wind sway [16]. Seismomorphogenesis also induces changes in plant characteristics such as stem diameter or chlorophyll content, with different responses being observed between species [12]. Besides causing morphological and mechanical changes at the stem scale, seismomorphogenesis often leads to a considerable increase of crop yields when plants are grown under optimal conditions in a greenhouse [17]. Thus, the greenhouse cultivation of flax is of interest for the study of fiber yields; in fact, flax is an industrial crop commonly grown in fields, and we might expect changes in morphology and fiber yield when flax is cultivated under much gentler wind conditions. However, no such study of greenhouse cultivation can be found in the literature. Furthermore, little is known on the effect of

seismomorphogenesis on the mechanical properties at the fiber scale, which represent an essential criterion for composite reinforcements.

### **1.3. Lodging and plant gravitropic response**

Lodging is defined as the natural phenomenon through which the plant is displaced from its vertical position after rainfall and wind [18]; for flax, it comes out as stem lodging [7]. The lodging stability of flax is of crucial priority for breeders, as this accident constrains plants to lie on the ground, at times permanently; thus, it can greatly complicate flax harvesting and consequently decreased fiber yields. However, it sometimes happens that plants, including flax [19], restore a vertical position thanks to the plant ability to respond to gravity, so-called gravitropism [20]. In response to stem lodging, gravitropism is negative as the plant moves against the direction of gravity and it is accompanied by a stem curvature [19]. The study of flax gravitropism is of great interest in agricultural and industrial views, but also because this plant naturally generates fibers exhibiting a G-layer over a normal plant development (Chapter III. 3.). It makes fibers analogous to tension wood of angiosperm woody species [21], thus interrogates about the involvement of flax fibers in the gravitropic response of the plant. Ibragimova et al. [19] demonstrated that, even if stem curvature occurs in a part where fiber elongation no longer happens, fiber thickening is still taking place there. In addition, when comparing fibers on transverse stem cross-sections of control plants and fibers from inclined ones, a significant increase of fiber diameters is obtained on the pulling side together with significantly enlarged lumens in fibers from tilted plants on both sides of the stem [19]. To the authors' knowledge, the impact of lodging on the mechanical properties of flax fibers has not been studied.

The first results section investigates the stability of flax in order to understand how this plant can reach such a slender structure while remaining mechanically stable. The architecture of flax plants is first studied through an anatomical analysis. Then, the mechanical stability of the plants is assessed by determining their safety factor, taking into account the distribution of diameters and mass along the stem. The effect of gradients in elasticity modulus is also investigated, using a numerical model of buckling. The second section explored the impact of seismomorphogenesis on flax stems and fibers in terms of architecture, anatomy and mechanical properties. This approach involves a comparison between field and greenhouse cultivated flax at plant maturity. This comparison is based on a morphological analysis of flax stems and an

estimation of their fiber content. Then, the changes in mechanical performances of flax stems are evaluated by bending tests. These tests are used to establish a comparison between the tensile performances of elementary flax fibers. Finally, changes in fiber mechanical properties after lodging, simulated at different key stages of plant development by tilting of the plants, are investigated. Four days after inclination, living plants are samples in order to extract unitary fibers for tensile tests. Three stages of plant growth were chosen for plant inclination, namely (i) the beginning of the vegetative stage (VS), for which the stem slowly elongates; (ii) during fast growth (FG) of the stem and (iii) at plant maturity (M).

## 2. Materials and methods

### 2.1. Plant materials and measurements

Two different types of plant materials were used for experiments: either living plants and dried ones, all of the variety Bolchoï (recently selected, in 2014, by Terre de Lin). This variety was chosen for the present chapter due its high fiber yield, its resistance toward lodging, its ease of cultivation and its triple resistance to diseases (*i.e.* against fusarium wilt (*Fusarium oxysporum*), powdery mildew (*Oidium lini*) and scorch (*Phytium megalacanthum*)).

#### 2.1.1. Plant materials for the study of the mechanical stability

Flax seeds were provided by Terre de Lin and sown in pots outdoor in 2017 in Lorient (France), using a conventional seeding density of about 1800 seeds/m<sup>2</sup> [7]. Ten stems were pulled out 100 days after sowing, duration corresponding to an accumulated temperature of 1010°C and indicating plant maturity (Equation I-1). Immediately after being pulled out, the technical stem height (stem part located below the first floral ramification) and the total height of each living stem were determined using a measuring tape. Then, the technical stem was cut from the basal part into 4 portions of 20 cm to make the samples (the last portion is generally less than 20 cm). For each sample, the diameter was measured at mid-height using a caliper and its weight recorded; the inflorescence was also weighed. These stem segments were used for anatomical analysis and bending tests.

#### 2.1.2. Plant materials for the study of the influence of wind

Plants were cultivated in 2016 at Saint-Pierre le Viger (France). A first batch of plants, corresponding to field trials, was grown in fields under normal conditions (*i.e.* without

any climatic perturbation such as drought or severe rainfalls [22]). The second batch was cultivated in a greenhouse to restrict the impact of the wind, and we assumed that the major differences between both batches result from seismomorphogenesis. The greenhouse is commonly used by the breeder for the flax varietal selection. Thus, the composition of the soil and nitrogen fertilization used in the greenhouse were similar as the outside. Field cultivated plants were only submitted to natural watering provided by rainfalls, whereas the plants cultivated in the greenhouse were submitted to an artificial watering as well as gentle heating or airing to keep a temperate atmosphere. If the moisture and temperature were not similar as the outside ones, the conditions in the greenhouse were kept as mild as possible, *i.e.* as suitable as possible for the cultivation of flax.

Both batches were pulled out at maturity. Plants were sampled and dried at this step at  $23 \pm 2^\circ\text{C}$  and  $50 \pm 4\%$  of relative humidity until stabilization of the stem weight, prior architectural and mechanical analysis of the stems. The total and technical heights of the plants were determined for 15 stems per batch. Basal diameters of each stem were measured at 10 cm height, and the technical diameters were measured at mid-height of the technical stem from 3 measurements at mid-sample using a caliper. The mid-height of flax stems is a location of interest, since it is known to yield the greatest number of fibers [23]. The total height-to-basal diameter ratio is calculated as the total height (in mm) divided by the basal diameter (in mm), used here to estimate the slenderness of the whole plant. However, the technical height-to-diameter ratio is calculated as the technical height (in mm) divided by the technical diameter (in mm), used here to illustrate the technical characteristics of flax stems. Finally, total and technical stem weights were measured to allow determination of the total and technical linear weights, respectively.

### **2.1.3. Plant materials for the study of gravitropic reaction**

Seeds were sown in pots in 2017 (Lorient, France) using a conventional seeding rate of about 1800 seeds/m<sup>2</sup> [7] and cultivated outdoor. Plant growth stages were evaluated based on the average plant height as well as days after sowing and cumulated temperature (Equation I-1). The different steps mentioned in the following procedure are illustrated in Figure V-2.

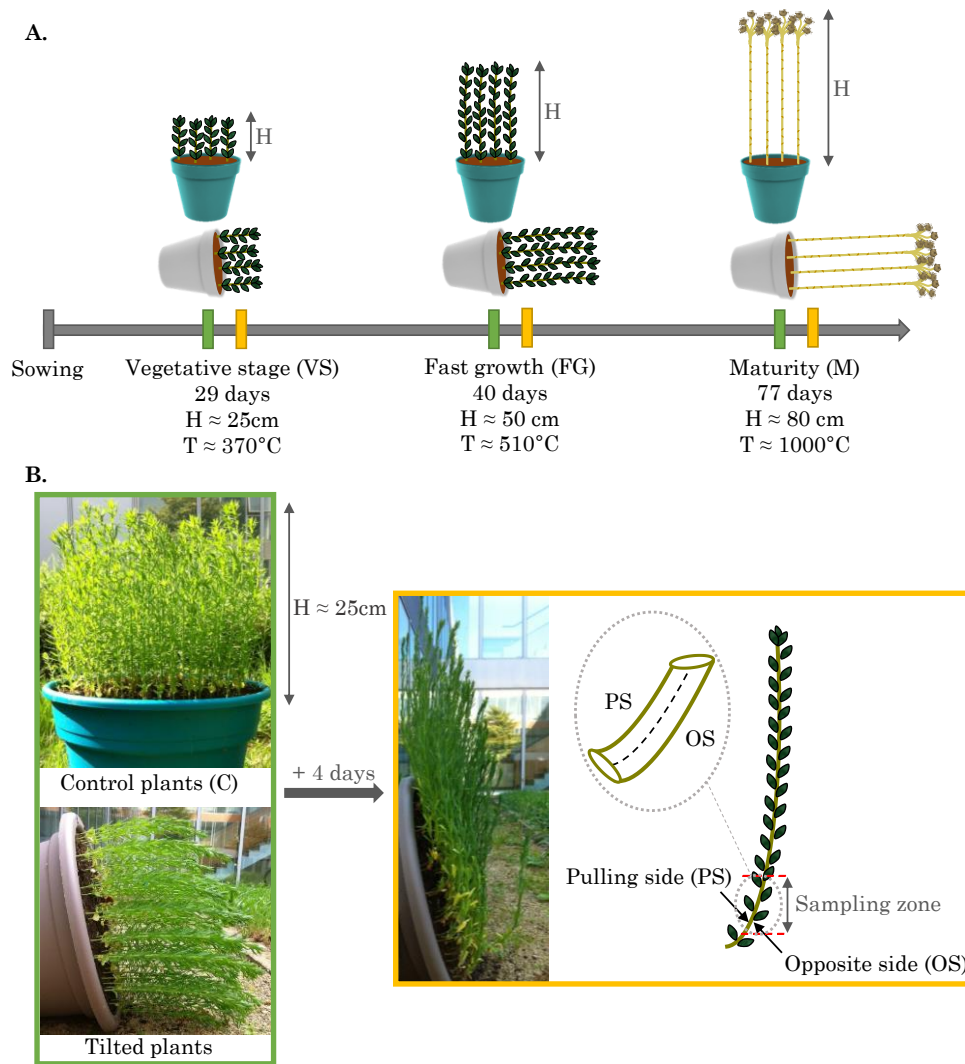


**Figure V-2. A. Scheme of consecutive steps of the experiment. A pot is left as a control whereas three other pots are tilted at a key stage of plant development (green symbols), considering the time after sowing, mean plant height (H) and cumulated temperature (T). Four days after inclination (yellow symbols), some plants are sampled. B. Pictures of the experiment at tilting (green) and at sampling (yellow)(portions of 10 cm are sampled from the curvature area, differentiating the pulling side and the opposite side of each plant.**

A pot was named as a control (C), *i.e.* it contained plants never inclined. Three other pots were used for the experiments, consisting of inclining pots at about 90°, consecutively at different key stages of plant development, and left inclined until the end of the experiment. The first pot was tilted at the beginning of the vegetative stage (VS), when plants reached about 25 cm *i.e.* 29 days after sowing for a cumulated temperature of 370°C. The second pot was tilted during the fast growth period (FG), when the plant height was about 50 cm corresponding to 40 days after sowing and 510°C of cumulated temperature. Finally, the third pot was inclined at plant maturity (M), in the present case 77 days after sowing when plants were about 80 cm high and

the temperature reached the expected cumulated temperature of 1000°C. Plants were sampled from the control pot and the inclined one 4 days after tilting, for each step respectively, which is the time required by the plants to restore their vertical position [19]. At maturity, sampling was performed in all pots. All samplings consisted of collecting samples of 10 cm (starting from 2 cm above the cotyledons) corresponding to the remaining curvature zone when recovery takes place. The pulling side (PS) and opposite side (OS) of each tilted plant were separated by longitudinally cutting 6 plants per pot; for similarity, control plants were also longitudinally split in two. Immediately after the cut, the resulting stem portions were placed in a 50% ethanol solution for several days at 4°C to facilitate the fiber extraction. For each sampling, additional samples were also taken from the same locations for anatomical analysis.

## **2.2. Anatomical analysis**

### **2.2.1. Samples from living materials**

Stem portions about 1 cm in length were cut from the middle of the samples collected from an average plant. 1 cm portions were fixed in a solution of 4% v/v formaldehyde in 0.1 M phosphate buffer (pH 7.2) at 4°C overnight. These samples were gradually dehydrated in a series of ethanol solutions. Then, samples were cleaned using increasing concentrations of HistoClear® in ethanol/HistoClear solutions. Later, samples were immersed in HistoClear/paraffin (Paraplast Plus, Leica) baths with gradually increasing concentrations of paraffin. Samples were finally embedded in pure paraffin at 60°C and immediately stored at 4°C. Sections (20 µm thick) were cut using a microtome (Leica RM2135 equipped with disposable blade) and placed on Superfrost Plus® slides on a hot plate (35°C). Slides were stored at 40°C overnight. Then, sections were dewaxed by immersion in two pure HistoClear baths followed by a series of solutions with decreasing ethanol concentrations. Finally, sections were rinsed in distilled water, stained with toluidine blue and covered with Eukitt® and a glass coverslip. The stained slides were observed under a microscope (Olympus AX70). Pictures were taken with an Olympus DP25 camera and anatomical parameters were analyzed using image analysis. Namely, the outline of the central lacuna, of the xylem tissue and of each fiber bundle visible on pictures of stem cross-sections are manually drawn using Gimp®. Then, the tissue content (% of the stem area devoid of lacuna area) and the fiber content (total bundle area expressed in % of the stem area and % of tissue content) are automatically evaluated using ImageJ®. The average bundle thickness is calculated from 30 measurements around the stem cross-section with

ImageJ®. Moreover, from the resulting pictures, the number of fibers and average fiber diameter can be estimated. The mean cell wall filling rate of flax fibers was calculated based on a minimum of 50 measurements per batch, by Equation V-1.

$$\text{Filling rate (\%)} = \left(1 - \frac{\text{lumen area}}{\text{total fiber area}}\right) \times 100$$

**Equation V-1. Calculation of the filling rate, as a function of the lumen area and total fiber area.**

### 2.2.2. Samples from dried materials

Samples of 1 cm length were cut from the middle height of the technical stems and immersed in 50/50-water/ethanol solution for 24h prior to embedding in elder marrow and cutting of cross-sections. The stem cross-sections used for anatomical analysis were obtained according to the method described in Chapter 2, *i.e.* by cutting transversal stem sections from embedded samples using a razor blade combined with a hand microtome. A microscope (Olympus AX70) equipped with a Olympus DP25 camera was used to acquire images of the resulting stem cross-sections. Anatomical parameters such as tissue content, fiber content, number of fibers or average fiber diameter were characterized based on image analysis as described above.

### 2.3. Three-point bending tests

Three-point bending tests were carried out on flax samples using a universal MTS tensile testing machine equipped with a 50 N capacity load cell. A displacement rate of 0.1 mm/sec was used and a span length ( $L$ ) of 18 cm was fixed to allow pure bending stress during tests, as demonstrated in Chapter IV. Tested stem samples were all 20 cm long, with a diameter of approximately 3 mm, in order to be sufficiently slender to prevent significant shearing of the stem as well as crushing by the support during bending [24].

Assuming the stem sample is a uniform beam loaded by a three-point bending test with a central support localized at mid-span length, the displacement ( $y$ ) at the middle of the sample is given by Equation V-2 [25].

$$y = \frac{FL^3}{48EI}$$

**Equation V-2. Calculation of the displacement  $y$  at the middle of the sample.  $F$  is the applied force,  $L$  the span length and  $EI$  the bending stiffness of the sample, while  $E$  is the apparent bending modulus and  $I$  the second moment of area given as  $I = \frac{\pi}{64}D^4$  for a circular cross-section of diameter  $D$  [25].**

This formula is exact for a cylindrical stem, but also valid for a conical sample if the diameter at the middle is taken as the representative value [26].

Finally, the apparent bending modulus of the sample is obtained Equation V-3.

$$E = \frac{dF}{dy} \cdot \frac{L^3}{48I}$$

**Equation V-3. Formula for the calculation of the apparent bending modulus  $E$ , where  $dF/dy$  is the slope of the linear part of the force-displacement curve, from the beginning of the test and for small strains,  $L$  the span length and  $I$  the second moment of area.**

#### 2.4. Greenhill's model

Greenhill's model [10] can be used to determine the critical buckling height, *i.e.* the maximum height that a plant can reach while remaining stable, given its diameter  $D$ , elastic modulus  $E$ , and loads. The classically used formula is Equation V-4.

$$H_{cr} = K \left( \frac{E \times D^2}{\rho} \right)^{1/3}$$

**Equation V-4. Greenhill equation for a vertical stem.  $H_{crit}$  is the critical buckling height,  $K$  is a proportionality constant depending on the distribution of diameters and loads,  $E$  is the elastic modulus of the stem,  $D$  is the diameter at the base and  $\rho$  is the bulk density of the material [10].**

Starting from Greenhill's formulation, the dependence of the critical buckling height in the distributions of diameters and masses can be made explicit. The trunk taper and load distribution are given by power laws characterized by parameters  $n$  and  $m$  as described by Jaouen et al. [11] ( $n = 0$  for a cylindrical stem and 1 for a conical stem,  $m = 0$  if load is concentrated at the top and 1 if load is uniformly distributed). Rearranging the equation of Jaouen et al. [11], the critical buckling height  $H_{cr}$  can be expressed as Equation V-5.

$$H_{cr} = \left( \frac{E \times F'^2 \times D^2}{64g \times L} \right)^{1/3}$$

**Equation V-5. Formula for the calculation of the critical buckling height  $H_{cr}$ , where  $g$  is the acceleration due to gravity,  $L$  is a load factor defined as the ratio of total plant mass to stem volume, and  $F'$  is a form factor given by  $F' = c(n, m) \times |m - 4n + 2| \times \sqrt{2n + 1}$ , while  $c$  is a function of  $n$  and  $m$ , whose numerical expression can be found in the study of Jaouen et al. [11]. Note that, because of a different formulation,  $F'$  slightly differs from the form factor  $F$  defined by Jaouen et al. [11].**

The critical buckling height of each plant is computed from Equation V-5, with  $D$  being the diameter of the basal segment,  $E$  the mean elastic modulus over the four tested segments.  $L$  is estimated from the volume of the segments and the total mass of the plant,  $n$  is obtained by log/log regression of the segment diameter versus its relative position along the stem and  $m$  is computed so the height of the center of mass of the modeled plant matches that of the real plant. The safety factor of each plant is obtained by Equation V-6.

$$SF = H_{cr}/H$$

**Equation V-6. Formula for the calculation of the safety factor  $SF$ , where  $H_{cr}$  is the critical buckling height and  $H$  the real plant height.**

## 2.5. Effect of a gradient in elastic modulus

Greenhill's model (Equation V-4) assumes that the elastic modulus of the stem is uniform. However, gradients in elastic modulus along the stem may contribute to the stability of the plant. To test this hypothesis, a numerical buckling model that can be applied to any distribution of diameters, loads and elastic moduli along the stem is used. The principle of this model is to set an initial small disturbance (inclination angle of  $1^\circ$ ) and compute the shape of the deformed stem submitted to its self-weight, accounting for the non-linear effect of large displacements [27]. If the plant is stable, the deflection remains small; if the plant is close to buckling, the deflection becomes large. This model is applied to the case of conical stem topped with a load corresponding to the inflorescence, setting average values of flax stem properties (Figure V-3 (A)). The critical load of the plant was computed by varying the top load and calculating the deflection, and taken as the intersection point of the two regimes (Figure V-3 (B)). To assess the effect of the gradient in elastic modulus, this computation is carried out for a stem with uniform elastic properties, and for stems with variable gradients in elastic modulus, keeping the same average elastic modulus.

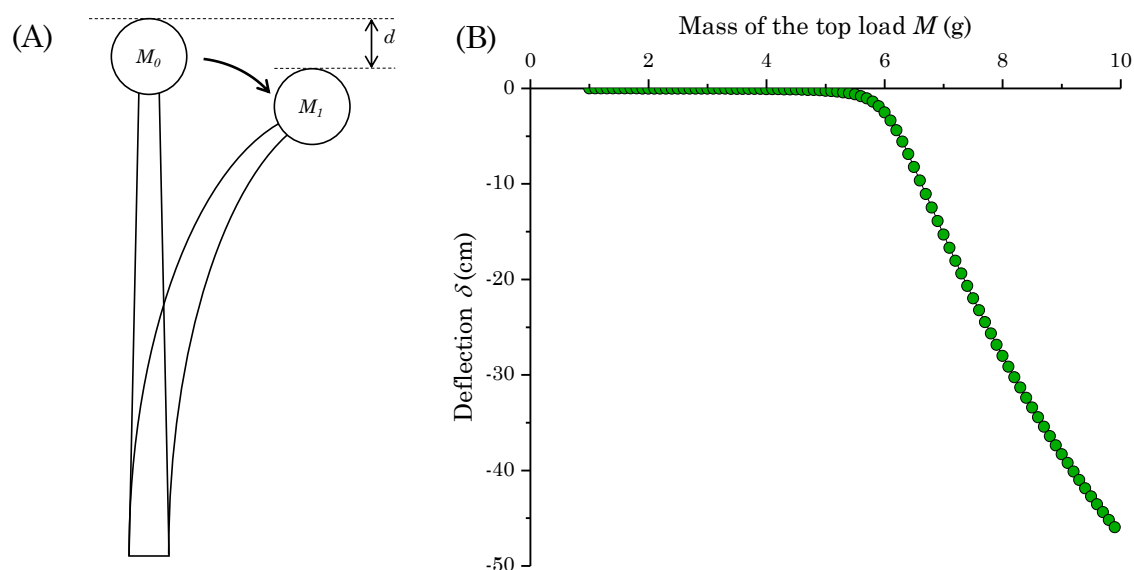


**Figure V-3. Numerical computation of the critical buckling height accounting for gradients in elastic modulus. (A) Representation of the plant as a conical stem topped with the load of inflorescence. When the top load  $M$  is increased above the critical limit, the stem starts bending, yielding in a deflection  $\delta$ . (B) Deflection  $\delta$  as a function of the top load  $M$ . The curve shows two regimes: below the critical load, the deflection remains small because the stem is loaded in pure compression; above the critical load, the stem bends and the deflection increases linearly. The critical load is computed as the intersection of these two lines.**

## 2.6. Measurements of elementary fiber length

Some selected batches of dried stems were retted in cold water in buckets for about ten days [28]. This natural and slow process facilitates fiber individualization owing to the action of bacteria, while avoiding over retting (the progress of retting was regularly checked, and then halted upon decohesion of fibers from the stems). Retted samples were then air dried. Finally, elementary fibers were manually extracted one by one from the retted samples, using tweezers. Extraction was performed from 15 cm-long bundles located at mid-height of the technical stems in each batch of retted samples. To facilitate handling for length measurement, fibers were manually aligned on glass slides and covered with mounting media (Eukitt®). Glass slides were then covered with coverslips and air-dried. Then, the slides were placed under the microscope and each fiber length was measured, after ensuring the presence of pointed ends to check the integrity of the fibers. To estimate the average fiber length, at least 30 fibers were measured.

## **2.7. Tensile tests on elementary fibers**

To estimate changes in fiber mechanical performances, tensile tests (in accordance with NF T 25-501-2) were performed on elementary fibers manually either extracted from stem portions stored in a 50% ethanol solution at 4°C or from retted stems originally dried. The elementary fibers of each batch were bonded onto a paper frame, having a gauge length of 10 mm, and conditioned at  $23 \pm 2^\circ\text{C}$  and  $50 \pm 4\%$  of relative humidity for a minimum of 24h. Then, the average fiber diameter was estimated through six measurements along each elementary fiber. Formerly, bonded fibers were conditioned once again for at least 24h. Finally, a minimum of 30 elementary fibers were placed in a universal MTS-type tensile-testing machine equipped with a 2 N capacity load using a displacement speed of 1 mm/min until rupture of the fiber. Both fiber mechanical properties and cell wall contribution were evaluated for the study on tilted plants.

## **2.8. Statistical analysis**

To evaluate the statistical difference in terms of mean values of stem measurements and fiber mechanical performances, the results were analyzed using a bilateral t-test with a 95% confidence interval. If resulting P-values are lower than 0.05, the difference in properties is considered being statistically significant. Regarding tilted plants, for a given development stage, both sides of inclined plants are analyzed in comparison with the control and between each other. At maturity, all batches are compared with mature control plants, and different sides of the plants from the same pot only are also compared.

### 3. Results – Slenderness and stability of flax plants

#### 3.1. Stem properties and anatomy obtained from living plants

By taking into account the diameter of the very base of the stem and the related total stem height, the average slenderness  $H/D$  of flax is evaluated to be  $365 \pm 33$ , highlighting the impressive feature of this plant. Changes in stem properties are then evaluated in samples collected along the stem, as illustrated in Figure V-4, and the associated average characteristics are presented in Table V-1.

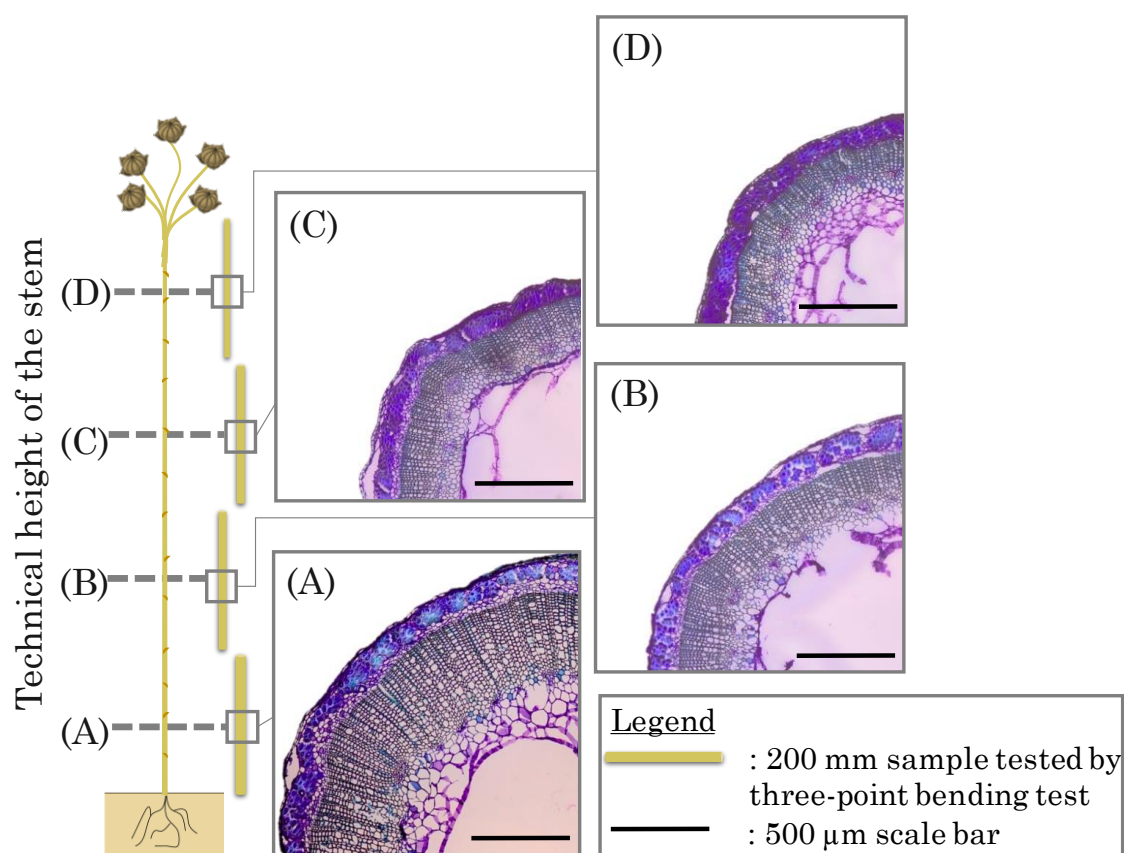


**Figure V-4.** Schematic diagram of sampling along a flax stem and associated transverse sections (A, B, C and D) of a single plant, with (A) being the basal sample and (D) the apical one.

The linear weight of the stem greatly decreases along the height, varying on average from  $7.06 \times 10^{-2}$  g/cm for the basal samples to  $3.16 \times 10^{-2}$  g/cm for the apical samples. This can be explained by the taper of the stem, reflecting the changes in diameter along the stem height, which decreases acropetally from 3.12 mm at a height of 10 cm to 2.09 mm at 70 cm (Figure V-4).

**Table V-1. Characteristics of flax stem samples along the stem; means and standard deviations are calculated on 10 tested plants.**

Sample	Height (cm)	Linear weight ( $\times 10^{-2}$ g/cm)	Stem diameter (mm)
A	10	7.06 $\pm$ 2.01	3.12 $\pm$ 0.38
B	30	5.08 $\pm$ 1.58	2.88 $\pm$ 0.41
C	50	3.83 $\pm$ 0.93	2.56 $\pm$ 0.41
D	70	3.16 $\pm$ 0.90	2.09 $\pm$ 0.34

Table V-2 gives the anatomical criteria corresponding to the cross-sections illustrated in Figure V-4.

**Table V-2. Analyses of stem samples corresponding to transverse sections visible on Figure V-4 for illustrative purposes.**

Sample	Tissue content (% of stem area)	Fiber content (% of stem area)	Fiber content (% of tissue area)	Bundle thickness ( $\mu$ m)
A	68	17	25	77 $\pm$ 8
B	62	21	34	82 $\pm$ 12
C	55	20	36	83 $\pm$ 8
D	63	23	36	73 $\pm$ 11

This analysis only takes into account the tissues having a mechanical key role, namely the fiber bundles and the xylem. The tissue content is at a maximum toward the base of the technical stem, whereas it reaches a minimum around mid-height *i.e.* around 50 cm height. The fiber content is lower in the basal region of the stem (Table V-2) and does not change significantly between 30 and 70 cm. Fiber bundles have a similar thickness along the stem despite the changes in stem diameter.

### 3.2. Bending properties along the stem

Samples from living stems collected as illustrated in Figure V-4 were evaluated by three-point bending tests. Resulting properties are presented in Table V-3.

**Table V-3. Characteristics of flax stem samples along the stem obtained from three-point bending test. Means and standard deviation are calculated on 10 plants.**

Sample	Second moment of area (mm <sup>4</sup> )	Bending stiffness (N.m <sup>2</sup> )	Apparent bending modulus (GPa)
a	5.0 ± 2.3	0.044 ± 0.020	8.7 ± 0.5
b	3.7 ± 1.9	0.036 ± 0.016	10.0 ± 1.1
c	2.3 ± 1.1	0.024 ± 0.016	10.5 ± 1.1
d	1.1 ± 0.6	0.013 ± 0.006	12.9 ± 1.8

The tests show that stem bending stiffness increases with the diameter, *i.e.* the closer to the apex the tested sample, the lower the bending stiffness. This latter parameter ranges from 0.013 ± 0.006 N.m<sup>2</sup> in the top sample to 0.044 ± 0.020 N.m<sup>2</sup> in the basal sample. The apparent bending modulus sharply increases along the stem, from 8.7 ± 0.5 GPa for the basal segment to 12.9 ± 1.8 GPa for the apical segment, with a mean gradient of 6.6 GPa/m. These results reflect the gradient in mechanical properties along the stem.

In order to evaluate the influence of the fibers on the apparent bending modulus of the stem, the fiber contribution to inertia is computed for each sample as Equation V-7.

$$\text{Fiber contribution (\%)} = \frac{I_{\text{fibers}}}{I} \times 100 = \left( 1 - \left( 1 - \frac{2e}{D} \right)^4 \right) \times 100$$

**Equation V-7. Formula for the fiber contribution, where  $I$  is the second moment of area of the stem sample (previously defined),  $I_{\text{fibers}}$  is the second moment of area of the fibrous ring,  $D$  is the sample average diameter and  $e$  is the thickness of the fiber ring given by the average thickness of the fiber bundles (Table V-3).**

The relation between the fiber contribution and the apparent bending modulus of the stem is illustrated in Figure V-5.

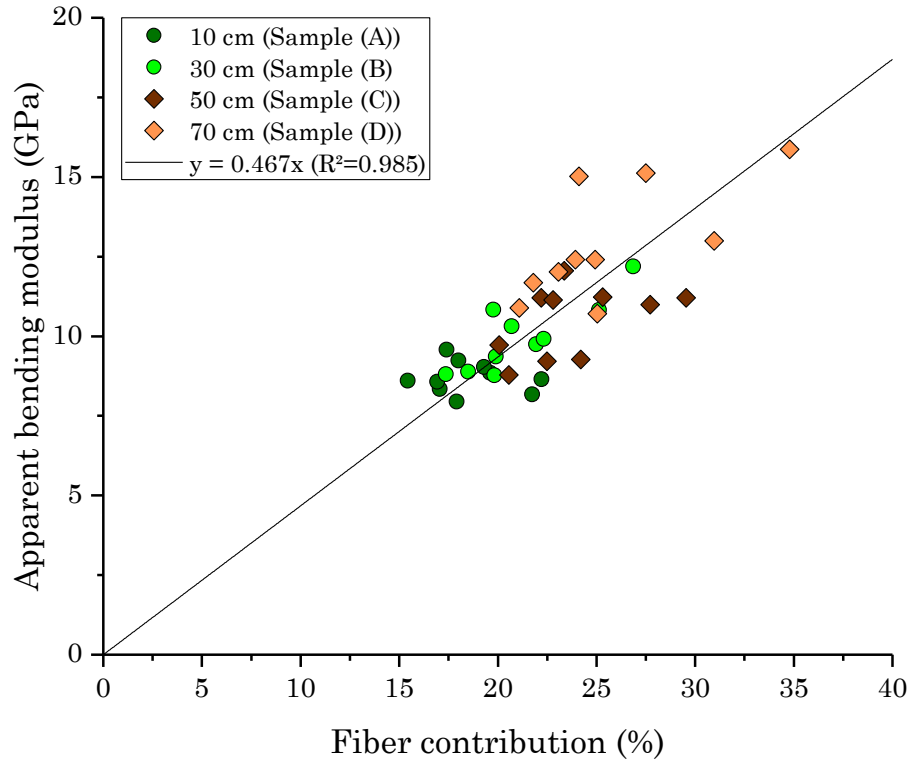


**Figure V-5. Apparent bending modulus of green flax stem samples plotted against the contribution of fibers to the second moment of inertia of the stem; a linear regression can be calculated with its intercept fixed at zero ( $R^2=0.985$ ;  $P<0.05$ ).**

This graph shows that the gradient in apparent bending modulus along the stem is mainly driven by the variation in fiber contribution. In fact, this gradient results from the distribution of fibers along the stem; the thickness of the fiber bundles is almost unchanged whereas the diameter decreases along the stem.

### 3.3. Safety against buckling of a living stem

Measurements carried out on living stems yield a total plant height of  $1.17 \pm 0.04$  m for an average diameter of  $3.24 \pm 0.37$  mm at the very base of the stems, and a total weight of  $5.76 \pm 1.65$  g, while the average apparent bending modulus of the samples is estimated at  $10.51 \pm 0.84$  GPa by bending tests. The safety factor against buckling ( $SF$ ) ranges between 1.30 and 1.60, with a mean value of 1.44. The fact that  $SF > 1$  for all plants implies that the flax plants are stable, in agreement with field observations showing their self-supporting habit. The taper coefficient ( $n$ ) is close to 0.5 ( $0.49 \pm 0.07$ ), indicating that the flax stems have a paraboloid shape. The load distribution parameter ( $m$ ) of  $1.08 \pm 0.05$ , *i.e.* close to unity, indicates that the center of mass of the plant is located near its mid-height. The load factor ( $L$ ) is estimated at  $1159 \pm 82$  kg/m<sup>3</sup>.

### 3.4. Effect of elastic modulus gradient on the stability of a flax stem

Figure V-6 shows the effect of an elastic modulus gradient on the stability of flax plants.

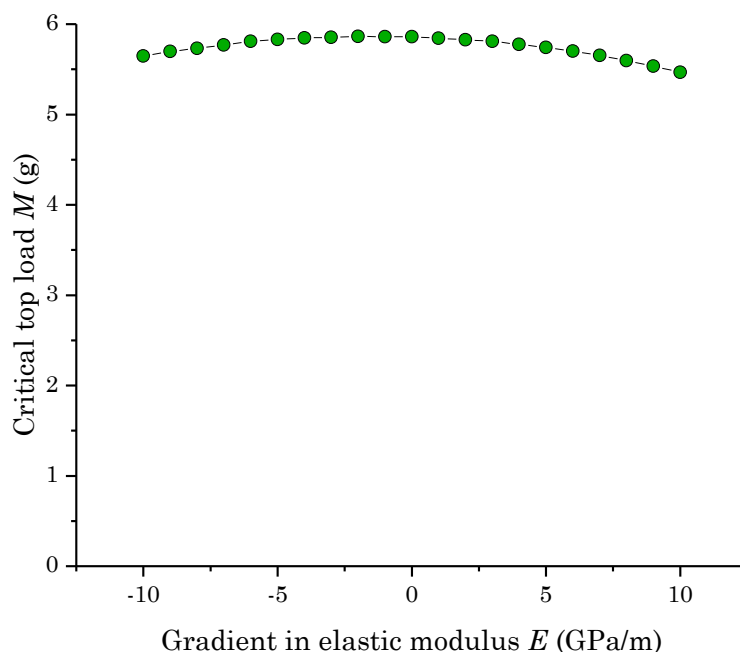


**Figure V-6. Effect of elastic modulus gradient on the stability of flax evaluated by changes in the critical load based on a numerical buckling model.**

From a qualitative viewpoint, the curve presents an optimum near -2 GPa/m, implying that the plant is more stable if the modulus of elasticity decreases slightly along the stem, so a strong positive gradient would mean that the situation of the flax stem is suboptimal. However, from a quantitative viewpoint, it appears that this effect is negligible. The strong positive gradient of +6.6 GPa/m observed in flax only reduces the critical load by approximately 3% compared to the optimal situation.

## 4. Discussion – Slenderness and stability of flax plants

The specific morphology of flax enables it to be much taller than other herbs of the same basal diameter, as illustrated in Figure V-1, while staying mechanically stable. The constraint of mechanical stability has implications in terms of how the height scales to the diameter. Substituting Equation V-5 into Equation V-6, it can be shown that, in order to ensure a given safety factor against buckling, plants of different size must scale such that  $H^3 \sim D^2$ , provided intensive parameters (form factor, load factor and modulus of elasticity) do not change with size. This scaling law corresponds to a straight line in Figure V-1, with a slope of  $2/3$ . The dotted line in Figure V-1 represents

the observed scaling relationship between diameter and height of trees, for which the slope is actually equal to  $2/3$ , suggesting that trees of different sizes have a constant safety factor against buckling. That most herbs do not align with this line can be ascribed to the fact that intensive parameters, such as the modulus of elasticity, are not actually the same as in trees. The modulus of elasticity of herbs is usually much lower than for trees [5,24,29,30]. This lower performance is reflected by the fact that all herbs studied by Niklas [5] lie below the line of trees. Flax, however, appears aligned with trees in Figure V-1, suggesting that it competes with trees in terms of performance of intensive parameters.

The taper coefficient ( $n$ ), close to 0.5, is slightly lower than the mean value of 0.66 observed by Jaouen et al. [11] on forest tree saplings. The load distribution parameter ( $m$ ) is close to unity, and lower than the average value of 1.62 obtained by Jaouen et al. [11], indicating that the relative position of the center of mass is higher in flax than in tree saplings. This is due to the concentration of loads near the top, caused by the terminal inflorescence, so the load distribution should have a negative effect on the stability of flax. The load factor ( $L$ ) is  $1159 \text{ kg/m}^3$ , which is slightly lower than the value of 1340 obtained by Jaouen et al. [11]. This low value is due to the low bulk stem apparent density (on average, about  $850 \text{ kg/m}^3$  for the technical stem) of flax compared to trees. This low load factor is beneficial for the stability of flax plants. The apparent bending modulus of flax stems (10.5 GPa in average) is much higher than other herbaceous plants [5,24,29,30] and closer to woody plants including self-supporting trees and shrubs [31]. For green wood, the bending modulus typically ranges between 5 and 20 GPa [32]. The values obtained on flax stems are thus comparable with the modulus of trees.

The bending modulus, exceptionally high for an herb, explains why flax is aligned with trees on Figure V-1; it is related to the specific architecture of flax stem, namely to the presence of an external ring of fibers with extraordinary mechanical properties. If the mechanical contribution of tissues other than phloem fibers is neglected, the relationship shown in Figure V-5 would yield an apparent modulus of 46.7 GPa for green fibers. This value is slightly lower than that given in the literature for dehydrated flax fibers, namely  $52.5 \pm 8.6 \text{ GPa}$ , [33], but consistent with the apparent tensile modulus obtained on green fibers, namely  $45.3 \pm 9.7 \text{ GPa}$  (Chapter III. 3.2.). This present result confirms that the high bending modulus of the flax plant can be attributed to the performance of its fibers. Moreover, the distribution of these fibers

within the section makes them a very efficient reinforcement. Indeed, the contribution of a fiber to the bending stiffness depends on its distance to the neutral line of the section, which is positioned at its center. Being located at the periphery of the section, phloem fibers are optimally positioned to provide the stem with high bending stiffness.

The observed gradient in bending modulus along flax stems is directly related to constraints of stem anatomy. The development of flax phloem fibers is such that they form a continuous ring of fixed thickness, irrespective of the diameter of the section (Table V-2). As a consequence, the relative contribution of fibers to inertia is larger for sections of smaller diameter (Figure V-5), located in apical parts of the stem. As fibers are the main contributor to bending stiffness, the bending modulus follows the same pattern and the gradient in bending modulus is a consequence of the constancy of the fiber ring thickness. The numerical analysis (Figure V-6) shows that this gradient has very low impact on the mechanical stability of the plants. Compared to a situation where the bending modulus would be constant (for example if the fiber ring thickness was proportional to the section diameter), the mechanical stability of flax is reduced by only a few percent. This shows that the distribution of fibers along the stem, contrary to their distribution within the section, is mostly neutral in terms of plant stability. Concentrating fibers in basal or apical parts does not impact the mechanical stability. This is because all parts of the plant, basal and apical, actually contribute equally to the bending of the plant. Indeed, basal parts are submitted to larger loads, but also have a larger inertia because of their larger diameter. Apical parts are less loaded but also have a lower inertia. Reinforcing a part at the expense of another results in compensation for the contributions of these two parts, and does not affect the overall stability of the plant.

The key to the mechanical performance of flax stems lies in the performance of its fibers, and in their optimal distribution within the section. It can be easily shown that, for a given amount of fibers, the specific core-rind structure set during flax growth enables maximizing the bending stiffness. This is a well-known fact in engineering sciences: for a given amount of material, a tubular structure is more efficient than a cylindrical structure. This strategy has, however, some drawbacks as in a tubular structure, the risk of stem ovalization and local buckling appears (Chapter IV). In the case of flax, this risk is prevented by the presence of an inner layer of xylem. Data from Figure V-4 and Table V-2 show that the xylem area is maximal in the basal parts of the stem. This is efficiently preventing the problem of local buckling in the basal

part of the stem, where the risk is the highest because of the lowest relative thickness of the fiber ring at that level.

## 5. Results – Conventional versus greenhouse cultivation

### 5.1. Architectural study of the stems grown outdoor or in greenhouse

Different parameters (Table V-4) were studied to evaluate the effects of seismomorphogenesis on flax stems. The greenhouse plants are significantly higher than plants cultivated in the field, with an increase of 44% in total stem height and 40% in technical stem height ( $P$ -values lower than 0.05) (Figure I-16). As a result, the length of the inflorescence is increased under greenhouse conditions. However, the diameters (either measured at the base of the stem or at mid-height) are smaller in greenhouse plants, but the difference is not statistically significant.

**Table V-4. External characteristics of flax stems; means and standard deviation (SD) are calculated on 15 tested plants. Means marked with \* are statistically different ( $P < 0.05$ ).**

	Plants from field		Plants from greenhouse	
	Mean	SD	Mean	SD
Total stem height (cm)	85.4*	5.7	123.2*	7.0
Technical stem height (cm)	64.3*	6.1	89.8*	3.9
Technical height ratio (%)	75.3	5.4	73.0	3.7
Basal diameter (mm)	2.58	0.31	2.42	0.35
Technical diameter (mm)	2.34	0.27	2.25	0.26
Total height-to-basal diameter ratio	334.6*	35.1	515.4*	58.2
Technical height-to-diameter ratio	278.7*	44.0	403.7*	40.3
Total stem weight (g)	2.05	0.61	2.48	0.74
Technical stem weight (g)	1.22*	0.29	1.49*	0.41
Technical weight ratio (%)	61.01	10.74	60.69	3.78
Total linear weight (g/m)	2.40	0.70	1.99	0.49
Technical linear weight (g/m)	1.91	0.49	1.66	0.42

The slenderness of greenhouse plants is significantly higher than in plants cultivated under conventional conditions, not only at the scale of the overall stem (with a total height-to-basal diameter ratio increased by 54%), but also as regards the technical ratio (45% improvement in the technical height-to-diameter ratio). In addition, no statistically significant difference is found in total stem weight, even though a slightly higher value is obtained from plants grown in the greenhouse. However, the increase is statistically significant when the technical stems are considered, with an average improvement of 22% for indoor plants, and this can be attributed to the height difference. It is important to note that the technical height ratio (around 75%) as well as the technical weight ratio (around 61%) are very similar under both types of growing conditions. Moreover, the total and technical linear weights are not statistically different. Finally, the structural distribution (*i.e.* the characteristics in terms of length and weight) of the technical stem and the inflorescence is maintained by flax plants regardless of the growth conditions. This structural analysis shows that changes in height and weight of the technical flax stems, and thus their slenderness as well, are the main characteristics influenced by wind action. Thus, seismomorphogenesis could influence the biomass yield per plant, and this aspect requires further investigation of the anatomy of the plants.

## 5.2. Anatomy of the stems grown outdoor and in greenhouse

Figure V-7 presents an example of transverse sections sampled at mid-height of the technical stems. A preliminary observation shows that, despite changes in slenderness, the internal arrangement of biological tissues is maintained by the plant. In addition, Table V-5 reports the average values of anatomical parameters resulting from the image analysis of transverse sections of flax stems. As previously shown by the architectural analysis, stems from the field are slightly larger than stems from the greenhouse. However, the tissue content and the fiber content are very similar between greenhouse and field cultivated plants when expressed in percentage area, with a slightly higher fiber content for field plants (Table V-5). In addition, the fiber diameter remains unchanged and the fiber bundles have very similar thickness between plants whatever their origin. Finally, the main difference regards the number of fibers observed on the stem sections, reaching a mean value of 1267 fibers per section for outdoor plants and 934 fibers for indoor plants.

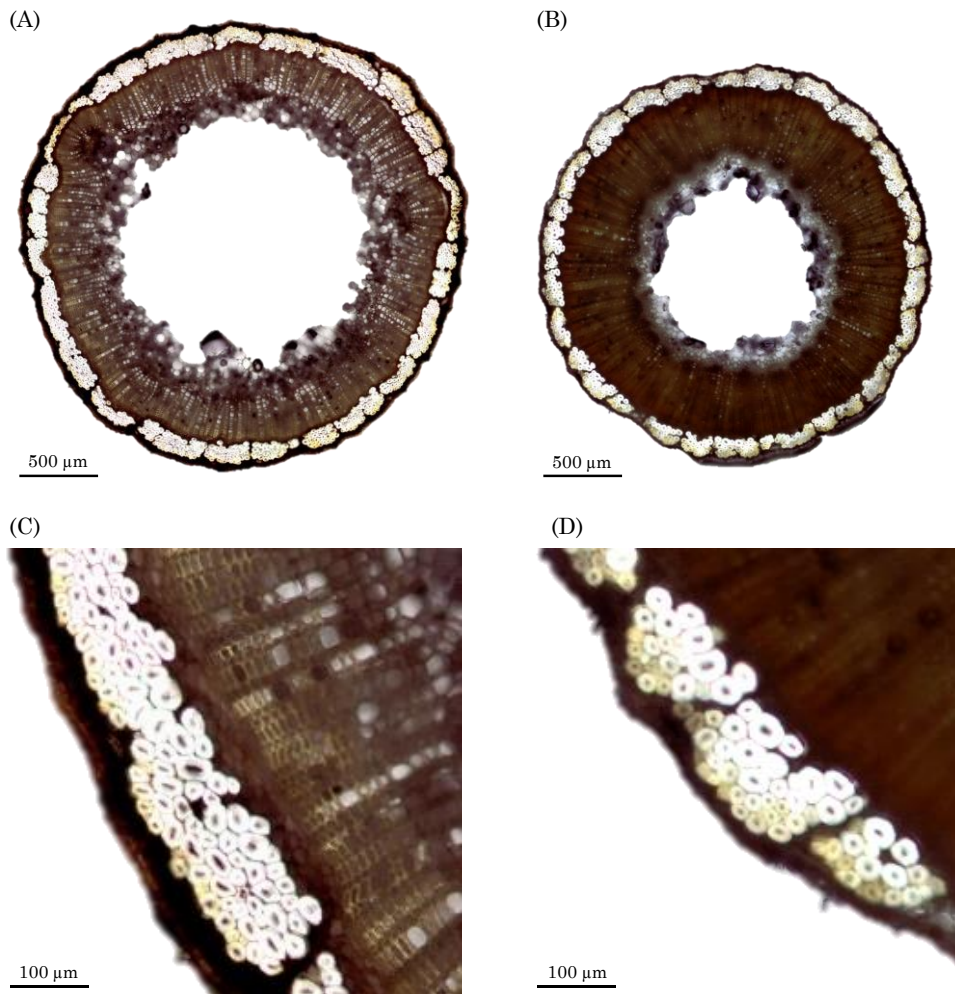


**Figure V-7.** Flax cross-sections at the middle of the technical stems for plants grown (A) in the field and (B) in a greenhouse. Fiber bundles at higher magnification for cross-sections of plants grown (C) in the field and (D) in a greenhouse.

**Table V-5.** Anatomical parameters of transverse sections sampled at mid-height of technical stems determined by image analysis. Means and standard deviations (SD) are calculated on sections obtained from two different plants per batch.

	Plants from field		Plants from greenhouse	
	Mean	SD	Mean	SD
Technical stem diameter (mm)	2.66	0.19	2.44	0.08
Tissue content (% of stem area)	74.4	1.1	77.7	4.0
Fiber content (% of tissue area)	15.8	2.3	14.0	1.1
Fiber content (mm <sup>2</sup> )	0.651	0.024	0.513	0.036
Fiber bundle thickness (μm)	102	18	95	16
Fibers per section	1267	63	934	8
Fiber diameter (μm)	24.0	8.1	25.1	8.3

To some extent, this difference could be due to changes in stem diameter [7], with indoor plants actually leading to a lower fiber yield in relation to stem cross-section. If such a relation is confirmed, it could be explained by the fact that indoor plants would require less support due to lower wind stress under greenhouse conditions. Prior to confirmation, the length of the elementary fibers needs to be investigated. In fact, fibers become more elongated by intrusive growth, for which the cell elongation rate exceeds that of neighboring cells, forcing the intrusive cell to penetrate between adjacent cells [34]. The intrusive growth increases the number of fibers in stem cross-sections [35] but not necessarily the number of fibers per stem.

### 5.3. Impact of the type of cultivation on the length of elementary fibers

To estimate the number of fibers per plant, the fiber length needs to be evaluated. However, the fiber content per plant can only be an estimation and a detailed analysis is not reasonably possible, as plants are known to contain thousands of fibers [36]. Hence, the present study gives only a general idea of the fiber content per plant. In this way, the fiber length was estimated for fibers extracted at mid-height of the technical stems. In this case, the fibers from plants cultivated in the field have a length of  $26.1 \pm 7.6$  mm (with 60% of the fibers belonging to this interval) whereas plants cultivated in greenhouses provide fibers with a length of  $26.4 \pm 6.2$  mm (63% of the fibers have a length in this interval). These results are similar to the average values given in the literature [36,37]. However, the fiber lengths are not statistically different ( $P=0.86$ ) between indoor and field plants. Finally, even though greenhouse plants are much higher than conventional plants, they do not provide longer fibers; the length of flax fibers is not influenced by the mechanically-induced stress in the present case.

We previously demonstrated that the shape of flax stems is not cylindrical, the number of fibers varies along the stem and intrusion actually appears within bundles. As a consequence, only a rough estimation of the number of fibers per stem is calculated in the present work. To perform this estimation, the volume of fibers per stem is calculated as the product of the mean value of the technical stem height and the fiber content (Table V-6).

**Table V-6. Average values used for estimation of the number of fibers per plant.**

	Plants from field	Plants from greenhouse
	Mean	Mean
Technical stem height (mm)	643	898
Fiber content in section (mm <sup>2</sup> )	0.651	0.513
Fiber content in volume (mm <sup>3</sup> )	419	460
Fiber diameter (mm)	0.0240	0.0251
Fiber length (mm)	26.1	26.4
Fibers per plant	$35.5 \times 10^3$	$35.2 \times 10^3$

Finally, it is possible to estimate the number of fibers  $n$  using Equation V-8.

$$n = \frac{4 \times V}{\pi \times D^2 \times L}$$

**Equation V-8. Estimation of the number of fibers  $n$  per plant, where  $V$  is the total fiber volume in the stem (mm<sup>3</sup>),  $D$  is the fiber diameter (mm) and  $L$  is the fiber length (mm).**

This leads to values of about  $35.5 \times 10^3$  fibers per plant grown in the field and  $35.2 \times 10^3$  fibers per plant cultivated in the greenhouse, *i.e.* a similar number of fibers per plant. These values are higher than the values given in the literature (10,000 to 20,000 fibers per plants)[36,38], probably because of the assumptions made for the calculations (for example, the intrusive elongation is not taken into account, which overestimates the number of fibers), but also due to the flax variety used here (Bolchoï is a recent variety selected for its high fiber yield). In conclusion, seismomorphogenesis does not influence either the morphology of the fibers or their number within the plant; only their distribution along the stem is modified.

#### 5.4. Bending properties of the stems

Since different fiber distributions are observed, the impact of seismomorphogenesis on the bending properties of the plants is investigated. Two parts of the stem are of interest here: the middle of the technical stem, as previously studied by anatomical analysis, and the basal part of the plant (which supports the overall plant weight and height). Figure V-8 presents the bending stiffness of each sample as a function of diameter.

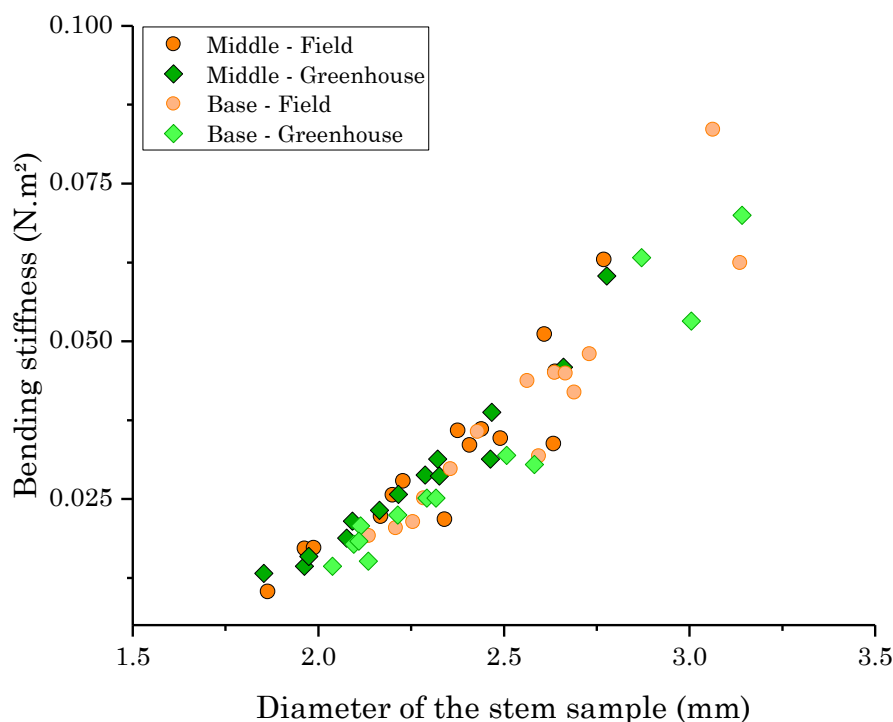


**Figure V-8. Bending stiffness of flax stems according to the diameter of the sample; plants from field and from greenhouse cultivation are compared based on the middle and basal parts of the stem.**

For a given diameter and location along the stem, the bending stiffness of the sample is very similar whether the plants were grown in the field or in the greenhouse. Thus, this property depends on the sample diameter, rather than the type of plant cultivation or sample location along the stem. The average bending stiffness of the middle parts of the stems reaches  $0.032 \pm 0.014$  N.m<sup>2</sup> for outdoor plants and  $0.028 \pm 0.013$  N.m<sup>2</sup> for greenhouse plants, the difference being not statistically different ( $P > 0.05$ ); the base of the stems yields values of  $0.040 \pm 0.018$  N.m<sup>2</sup> for outdoor plants and  $0.031 \pm 0.019$  N.m<sup>2</sup> for plants cultivated indoors, with a non-significant difference ( $P > 0.05$ ). Despite differences in plant height and weight, the wind exposure of plants does not impact their bending stiffness. We assume that bending stiffness is mostly dependent on the stem diameter. Since there is no significant difference in average stem diameter between outdoor and indoor plants, the bending stiffness is not statistically different between either.

In addition, knowing the geometry of the samples and their respective bending stiffness, it is possible to estimate the apparent modulus of the stems (Figure V-9)(method given in Chapter IV).

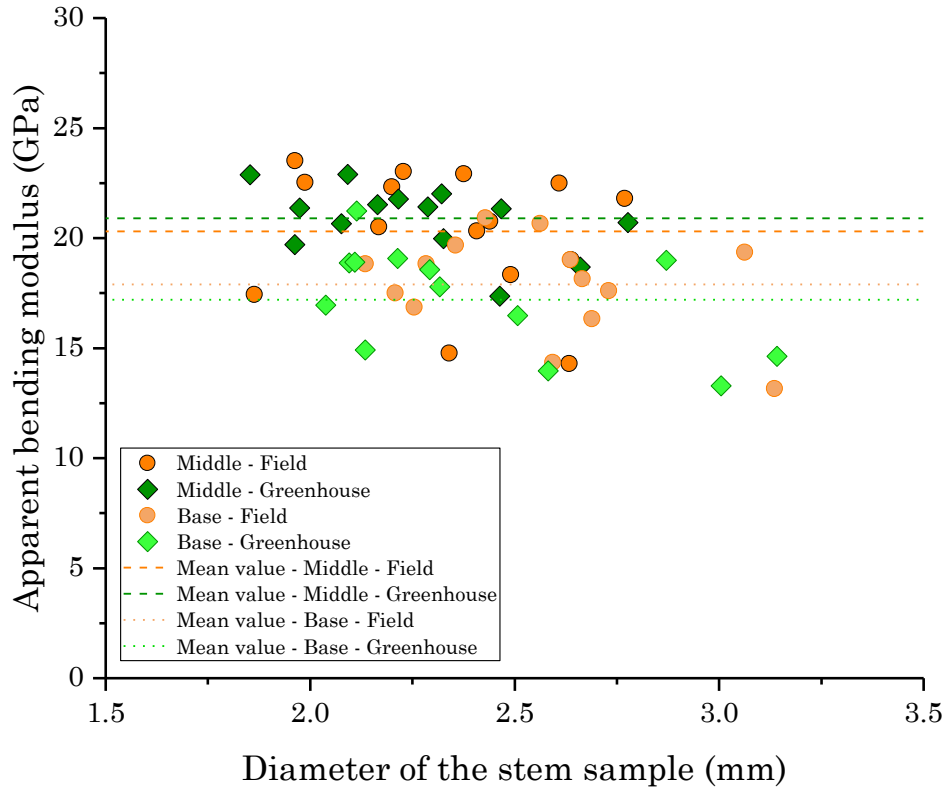


**Figure V-9. Apparent bending modulus of flax stems according to the diameter of the sample; plants from field and from greenhouse cultivation are compared based on the middle and basal parts of the stem. Mean moduli are given for each batch.**

Average apparent moduli of  $20.3 \pm 2.9$  GPa and  $20.9 \pm 1.5$  GPa are estimated for the middle parts of outdoor and indoor plant stems, respectively. These values are both very similar to measurements at mid-height for conventionally grown flax plants given in Chapter IV, and also very little dispersed despite scattered stem diameters for both batches. Interestingly, there is no statistical difference between the apparent bending moduli of plants from the field or greenhouse and the mechanical properties of plants are considered as similar irrespective of their origin. This result is also confirmed for samples from the basal part of the plants, with apparent moduli of  $17.9 \pm 2.2$  GPa and  $17.2 \pm 2.4$  GPa ( $P > 0.05$ ) for outdoor and indoor plants, respectively. In other words, the fact that plants are grown in the field or indoors does not change the mechanical properties of the plants at the stem scale.

### 5.5. Influence of the type of cultivation on fiber mechanical properties

Despite similar mechanical properties at the stem scale, the distribution of the fibers within the plants is found to be different. To assess the impact of fiber distribution on mechanical performances at the fiber scale, tensile tests were performed on elementary fibers. Fiber mechanical properties of indoor plants are as high as those

obtained on fibers from conventional cultivation (Table V-7). Moreover, both batches have properties that are comparable to the average values measured in Chapter II. 3.2. and from literature for fibers extracted from conventionally cultivated plants [33].

**Table V-7. Results of tensile tests performed on elementary fibers extracted from the middle of retted stems.**

	Plants from field		Plants from greenhouse	
	Mean	SD	Mean	SD
Fiber diameter ( $\mu\text{m}$ )	23.5	3.3	22.2	4.1
Tangent modulus (GPa)	54.7	13.2	56.3	15.1
Strength at break (MPa)	1017	281	1040	391
Strain at break (%)	2.09	0.62	1.99	0.65

Each of the mechanical criteria are tested statistically for differences between fiber batches; none of the mechanical properties are found to be statistically different between the two fiber batches ( $P > 0.05$ ). Finally, flax fibers have the same morphological and mechanical characteristics regardless of the influence of seismomorphogenesis.

## 6. Discussion – Conventional versus greenhouse cultivation

Changes in total plant height and technical stem height were highlighted and affect the slenderness of flax plants. These changes are the main characteristics that differentiate greenhouse plants from conventional ones. The considerable increase in plant height and slenderness is made possible because the risk of lodging, induced by the action of wind and rain [39], is greatly reduced when plants are cultivated indoors, despite the identical average bending properties of the plants. Moreover, even though the height and slenderness of plants are modified, flax fibers maintain their mechanical performances and morphological characteristics.

Seismomorphogenesis is assumed to be the only phenomenon inducing differences between the two sets of plants. Conversely, plants grown in fields are actually more exposed to other factors that could also partly influence changes, such as rainfalls or greater temperature fluctuations, factors that could potentially be extended to insects or diseases for example during coming cultivations. Thus, the cultivation of flax in greenhouses could be of interest to prevent yield losses caused by lodging, severe meteorological events or other undesired factors while preserving the fiber properties.

The growth conditions (principally ambient temperature and watering) can be controlled in greenhouse cultivation, which is evidently not the case in fields. This control is important because it could allow several crop harvests per year, thus increasing the availability of flax fibers for the industry while providing fibers with similar favorable performances.

However, the growth of flax in greenhouses at an industrial scale raises numerous additional issues, even though this type of cultivation preserves the fiber yield and quality. In fact, industrial applications would require substantial changes to the cultivation system, making it extremely difficult to be developed. For instance, an extended crop rotation is required to preserve soil fertility and soil self-cleaning [40], preventing successive cultivations of flax in the same greenhouse. Another issue would be the feasibility of retting. This latter process ensures an efficient technical fiber extraction and division as well as suitable fiber mechanical properties [41]. Even if it is possible to reproduce in the greenhouse, the weather conditions required for the development of microorganisms that ensure retting, another difficulty would be the use of agricultural machinery designed to uproot, drop off, return and harvest the plants prior to as well as after retting. An additional problem would be the scaling of scutching machines, which are at present only sized for flax plants that do not exceed 1 m in height. To address these problems, the processing of flax needs to be entirely redesigned. Another possibility would be the development of flax varieties dedicated to indoor cultivation; this would necessitate long research and development works to catch up with decades of varietal selection of conventional varieties.

## 7. Results and discussion – Plant gravitropic response

Hereafter, a color code is used to link the results in Table V-8 to the corresponding discussion. Table V-8 presents the characteristics of fibers the three stages of plant development, comparing the **control (C)** and both sides of tilted plants for each stage from tensile tests. If tilting takes place during the **vegetative stage (VS)** or **fast growth (FG)**, plants restore their vertical position with the remaining curvature in the basal part of the stem (Figure V-2). However, this recovery does not happen at **plant maturity (M)**, but a general curvature is noticeable. Thus, the basal part of these plants are sampled for comparison.

**Table V-8. Characteristics of elementary flax fibers according to the type of inclination (control (C) or curvature side (opposite side (OS) or pulling side (PS)), plant development stage at inclination (vegetative stage (VS), fast growth (FG) or maturity (M)) and age at sampling. Cell wall properties are obtained considering the fiber mean filling rate. The superscript letters indicate that the difference of the means is statistically significant at the 0.05 level.**

Stage	Batch	Age at tilting (days)	Age at sampling (days)	Fiber diameter (µm)	Mean filling rate (%)	Fiber mechanical properties			Cell wall mechanical properties	
						Tangent modulus (GPa)	Strength at break (MPa)	Strain at break (%)	Tangent modulus (GPa)	Strength at break (MPa)
VS	C	No tilting	33	18.1 ± 3.4	77.5	32.7 ± 11.9	837 ± 261 <sup>g</sup>	2.65 ± 0.68	42.2 ± 15.3 <sup>i</sup>	1080 ± 337 <sup>l</sup>
	OS	29	33	17.7 ± 3.9	58.5	31.0 ± 9.0	680 ± 232	2.25 ± 0.56	53.1 ± 15.4 <sup>i</sup>	1164 ± 397 <sup>m</sup>
	PS	29	33	17.1 ± 3.0	35.5	26.9 ± 8.5	614 ± 247 <sup>g</sup>	2.41 ± 0.49	75.6 ± 23.8 <sup>i</sup>	1727 ± 694 <sup>l,m</sup>
FG	C	No tilting	44	21.8 ± 3.6	88.7	36.6 ± 11.4	946 ± 393 <sup>h</sup>	2.79 ± 0.89	41.3 ± 12.8 <sup>j</sup>	1067 ± 443
	OS	40	44	20.2 ± 4.0	90.0	38.8 ± 11.6	922 ± 341	2.55 ± 0.91	43.1 ± 12.9 <sup>k</sup>	1024 ± 379
	PS	40	44	23.2 ± 4.1	51.6	29.9 ± 9.7	689 ± 228 <sup>h</sup>	2.46 ± 0.58	58.0 ± 18.8 <sup>j,k</sup>	1336 ± 444
M	C	No tilting	81	21.9 ± 3.9	98.5	52.9 ± 9.5 <sup>a,b</sup>	1028 ± 316	2.01 ± 0.46	53.7 ± 9.6	1044 ± 321 <sup>n</sup>
	OS	29	81	23.5 ± 4.2	91.9	45.7 ± 9.7	873 ± 233	1.99 ± 0.51	49.8 ± 10.6	950 ± 254 <sup>o</sup>
	PS	29	81	22.5 ± 3.7	70.2	42.9 ± 8.3 <sup>a</sup>	990 ± 264	2.35 ± 0.52	61.1 ± 11.8	1409 ± 376 <sup>n,o</sup>
	OS	40	81	22.4 ± 2.8	90.3	48.1 ± 9.4	884 ± 238	1.85 ± 0.41	53.2 ± 10.4	978 ± 263
	PS	40	81	22.8 ± 4.3	84.7	41.1 ± 10.4 <sup>b</sup>	815 ± 250	2.10 ± 0.42	48.5 ± 12.3	961 ± 295
	OS	77	81	23.6 ± 3.2	86.2	54.7 ± 8.9	1076 ± 294	2.04 ± 0.50	63.6 ± 10.3	1249 ± 341
	PS	77	81	23.9 ± 3.5	77.4	49.3 ± 11.9	1023 ± 301	2.11 ± 0.44	63.7 ± 15.4	1322 ± 389

No significant difference is observed between batches neither in terms of average fiber diameter nor strain at break. However, the fiber strength at break from the pulling side (PS) of developing fibers (*i.e.* during the vegetative stage and fast growth of the plants) is significantly decreased immediately after the restoration of the vertical position. This difference is not visible at maturity, as none of fiber batches exhibits a statistically difference anymore. Moreover, if no difference is observed in terms of fiber tangent modulus 4 days after inclination whatever the stage of development, the process of fiber thickening is nevertheless influenced if yet not finalized at the time of tilting. Indeed, mature fibers from the pulling side (PS) of plants tilted before maturity exhibit a statistically lower modulus (-22.4% and -18.9% for plants tilted at fast growth and vegetative stage, respectively) compared to other batches. Finally, if the tangent moduli are decreased for fibers of plants tilted during their growth, the resulting performances remain suitable for composite applications, as within the same range of most moduli given for several textile flax varieties (Chapter II-3.2.). Additionally, to determine the impact of a gravitropic response of the plant on the fiber cell wall, the mean filling rate of fibers from each batch was estimated and used to evaluate the mean tensile properties of the cell wall. During the vegetative stage, when control fibers (C) exhibit the lowest filling rate, the gravitropic response greatly impact the mechanical properties of the cell wall. Namely, after restoring its vertical position, the plant exhibits fibers with a much higher cell wall tangent modulus on both sides of the remaining curvature, even more pronounced on the pulling side (PS)(about +80%). Similarly, the cell wall strength at break is great increased on the pulling side (about +60%). If the gravitropic response occurs during fast growth, when thickening is still happening, the cell wall tangent modulus of the pulling side is again greater, but at that time to a lesser extent (+40% compared to the control). However, if the fiber strength at break seems increased on the pulling side at that stage, the increase is not significant. Finally, these results highlight the mechanical role of flax fibers in the support of the plant during its development; the fibers show decreased filling rates but increased fiber cell wall performances to help the stem to restore its position and get strengthened in the curvature zone. Interestingly, at maturity, when cell wall thickening is finalized, differences in mechanical properties of cell walls are not statistically significant despite changes in filling rates (with lowest values on the pulling sides). A unique significant difference remains in terms of cell wall strength at break regarding the pulling side of plants tilted during the vegetative stage, which exhibits the greatest performances.

## 8. Conclusions

Compared to other plants and trees, the flax plant is a remarkable structure through a considerable slenderness and it nevertheless is mechanically stable. The stability of the flax plant could be explained by the high apparent bending modulus of the stem (maximum values of  $12.9 \pm 1.8$  GPa for the apical part of the technical stem), which is much higher than observed in other herbaceous plants. The difference in modulus could be related to the fibrous external ring formed by the fiber bundles within the flax stem. This ring accounts for a bending modulus reaching values comparable with trees. In addition, even though to a lesser extent, other parameters are favorable to the stability of flax; namely, the paraboloid shape (reflected by the taper coefficient of 0.5) and a rather low load factor of  $1159 \text{ kg/m}^3$  compared with trees. Moreover, the unusually high center of mass reduces the stability of the plant only to a small extent. Finally, the varietal selection of flax over many years as well as cultural practices (such as the number of plants per meter square) have led to the increase of fiber yield and lodging resistance, thus giving rise nowadays to its extremely slender but mechanically stable structure.

In response to mechanically-induced stresses such as those due to the wind, the architectural and mechanical parameters of plants and trees can be greatly impacted. In the case of flax, plants grown in greenhouses show certain architectural parameters that differ significantly from conventionally grown plants (*i.e.* cultivated in fields). Indeed, the height of both the whole plant and the technical stems is greatly increased (by up to +44% of the total height) when flax is submitted to a much gentler mechanically-induced stress. However, the average diameter of the plant is not significantly affected; this phenomenon results in greenhouse plants displaying much greater slenderness than conventional flax plants. Owing to these architectural modifications, the fibers are distributed differently along the stems. We highlight here an interesting plant adjustment, whereby fiber properties (morphological as well as mechanical) are unaffected despite architectural changes at the stem scale. Thus, fibers, which are known as ‘plant muscles’, are actually not reinforced either by wind action or optimal growing conditions. This means that the number of fibers per plant and the stem mechanical properties remain closely similar even though the plant appearance is highly modified. Finally, the cultivation of flax indoors has no influence at the fiber scale, and its industrial development needs to be discussed.

Interestingly, flax plants have the ability to restore their vertical position through a gravitropic response, *i.e.* flax can recover from lodging depending on the time of inclination. This plant reaction provides fibers with decreased moduli when originating from the pulling side of the stem, if the plant inclination happens during the vegetative stage of fast growth period. However, the fibers properties remain satisfying for composite reinforcement, even though more scattered than usual induced by the two sides of the curvature. Additionally, for this latter reason, the filling rate changes depending on the side of the curvature. Finally, the gravitropic reaction of flax is linked with fibers exhibiting extraordinary cell wall mechanical properties; the flax cell wall characteristics are adjustable over fiber development, providing the plant with stability, response to lodging and mechanical support.

## 9. References

1. Jankauskiene, Z. Results of 90 years of flax breeding in Lithuania. *Proc. Latv. Acad. Sci. Sect. B Nat. Exact, Appl. Sci.* **2014**, *68*, 184–192, doi:10.2478/prolas-2014-0022.
2. Fischer, R. A.; Stapper, M. Lodging effects on high-yielding crops of irrigated semidwarf wheat. *F. Crop. Res.* **1987**, *17*, 245–258, doi:10.1016/0378-4290(87)90038-4.
3. Vera, C. L.; Duguid, S. D.; Fox, S. L.; Rashid, K. Y.; Dribnenki, J. C. P.; Clarke, F. R. Short Communication: Comparative effect of lodging on seed yield of flax and wheat. *Can. J. Plant Sci.* **2012**, *92*, 39–43, doi:10.4141/cjps2011-031.
4. Berry, P. M.; Spink, J. Predicting yield losses caused by lodging in wheat. *F. Crop. Res.* **2012**, *137*, 19–26, doi:10.1016/j.fcr.2012.07.019.
5. Niklas, K. J. Plant height and the properties of some herbaceous stems. *Ann. Bot.* **1995**, *75*, 133–142.
6. Niklas, K. J.; Spatz, H.-C. Growth and hydraulic (not mechanical) constraints govern the scaling of tree height and mass. *Proc. Natl. Acad. Sci. U. S. A.* **2004**, *101*, 15661–15663, doi:10.1073/pnas.0405857101.
7. Bourmaud, A.; Gibaud, M.; Baley, C. Impact of the seeding rate on flax stem stability and the mechanical properties of elementary fibres. *Ind. Crops Prod.* **2016**, *80*, 17–25, doi:10.1016/j.indcrop.2015.10.053.
8. McMahon, T. Size and shape in biology. Elastic criteria impose limits on biological proportions, and consequently on metabolic rates. *Science (80)*. **1973**, *179*, 1201–1204, doi:10.1017/CBO9781107415324.004.
9. Niklas, K. J. Interspecific allometries of critical buckling height and actual plant height. *Am. J. Bot.* **1994**, *81*, 1275–1279, doi:10.2307/2445403.
10. Greenhill, A. G. Determination of the greatest height consistent with stability that a vertical pole or mast can be made, and the greatest height to which a tree of given proportions can grow. *Proc. Camb. Philol. Soc.* **1881**, *4*, 65–73.
11. Jaouen, G.; Alméras, T.; Coutand, C.; Fournier, M. How to determine sapling buckling risk with only few measurements. *Am. J. Bot.* **2007**, *94*, 1583–1593.
12. Biddington, N. L. The effects of mechanically-induced stress in plants - a review. *Plant Growth Regul.* **1986**, *4*, 103–123, doi:10.1007/BF00025193.

13. Jaffe, M. J. Thigmomorphogenesis : The response of plant growth and development to mechanical stimulation. *Planta* **1973**, *114*, 143–157, doi:10.1007/BF00387472.
14. Mitchell, C. Seismomorphogenic regulation of plant growth. *J. Am. Soc. Hortic. Sci.* **1975**, *100*, 161–165.
15. Brüchert, F.; Gardiner, B. The effect of wind exposure on the tree aerial architecture and biomechanics of Sitka spruce (*Picea sitchensis*, Pinaceae). *Am. J. Bot.* **2006**, *93*, 1512–1521, doi:10.3732/ajb.93.10.1512.
16. Crook, M.; Ennos, R. Mechanical differences between free-standing and supported wheat plants, *Triticum aestivum* L. *Ann. Bot.* **1996**, *77*, 197–202, doi:10.1006/anbo.1996.0023.
17. Grace, J.; Russell, G. The effect of wind on grasses. *J. Exp. Bot.* **1977**, *28*, 268–278, doi:http://dx.doi.org/10.1016/0378-7788(77)90014-7.
18. Berry, P. M.; Sterling, M.; Spink, J. H.; Baker, C. J.; Sylvester-Bradley, R.; Mooney, S. J.; Tams, A. R.; Ennos, A. R. Understanding and reducing lodging in cereals. *Adv. Agron.* **2004**, *84*, 217–271, doi:10.1016/S0065-2113(04)84005-7.
19. Ibragimova, N. N.; Ageeva, M. V.; Gorshkova, T. A. Development of gravitropic response: unusual behavior of flax phloem G-fibers. *Protoplasma* **2017**, *254*, 749–762, doi:10.1007/s00709-016-0985-8.
20. Coutand, C. Mechanosensing and thigmomorphogenesis, a physiological and biomechanical point of view. *Plant Sci.* **2010**, *179*, 168–182, doi:10.1016/j.plantsci.2010.05.001.
21. Mellerowicz, E. J.; Gorshkova, T. A. Tensional stress generation in gelatinous fibres: a review and possible mechanism based on cell-wall structure and composition. *J. Exp. Bot.* **2012**, *63*, 551–565, doi:10.1093/jxb/err339.
22. Lefeuvre, A.; Bourmaud, A.; Lebrun, L.; Morvan, C.; Baley, C. A study of the yearly reproducibility of flax fiber tensile properties. *Ind. Crops Prod.* **2013**, *50*, 400–407.
23. Tiver, N. S. Studies of the flax plant 1. Physiology of growth, stem anatomy and fibre development in fibre flax. *Aust. J. Exp. Biol. Med. Sci.* **1942**, *20*, 149–160.
24. Leblicq, T.; Vanmaercke, S.; Ramon, H.; Saeys, W. Mechanical analysis of the bending behaviour of plant stems. *Biosyst. Eng.* **2015**, *129*, 87–99, doi:10.1016/j.biosystemseng.2014.09.016.
25. Timoshenko, S. P. *Strength of materials - Part 2 - Advanced theory and problems*; Van, N., Ed.; van, Nostrand, 1930;
26. Alméras, T.; Derycke, M.; Jaouen, G.; Beauchêne, J.; Fournier, M. Functional diversity in gravitropic reaction among tropical seedlings in relation to ecological and developmental traits. *J. Exp. Bot.* **2009**, *60*, 4397–4410, doi:10.1093/jxb/erp276.
27. Alméras, T.; Gril, J.; Costes, E. Bending of apricot tree branches under the weight of axillary growth: Test of a mechanical model with experimental data. *Trees - Struct. Funct.* **2002**, *16*, 5–15, doi:10.1007/s00468-001-0139-1.
28. Robinson, B. The time to harvest fiber flax. *Tech. Bull. 236. United States Dep. Agric.* **1931**, *22*.
29. Herrel, A.; Speck, T.; Rowe, N. P. *A mechanical approach to the ecology of animals and plants*; Herrel, A., Speck, T., Rowe, N. P., Eds.; Taylor & Francis, 2006; ISBN 9780849332098.
30. O'Dogherty, M. J.; Huber, J. A.; Dyson, J.; Marshall, C. J. A study of the physical and mechanical properties of wheat straw. *J. Agric. Eng. Res.* **1995**, *62*, 133–142.
31. Speck, T.; Burgert, I. Plant stems: functional design and mechanics. *Annu. Rev. Mater. Res* **2011**, *41*, 169–193, doi:10.1146/annurev-matsci-062910-100425.
32. Kretschmann, D. E. Chapter 5 - Mechanical properties of wood. In *Wood Handbook - Wood as an engineering material . General Technical Report FPL-GTR-190. US Department of Agriculture, Washington*; 2010; pp. 1–46.

33. Baley, C.; Bourmaud, A. Average tensile properties of French elementary flax fibers. *Mater. Lett.* **2014**, *122*, 159–161, doi:10.1016/j.matlet.2014.02.030.
34. Snegireva, A. V.; Ageeva, M. V.; Amenitskii, S. I.; Chernova, T. E.; Ebskamp, M.; Gorshkova, T. A. Intrusive growth of sclerenchyma fibers. *Russ. J. Plant Physiol.* **2010**, *57*, 342–355, doi:10.1134/S1021443710030052.
35. Gorshkova, T. A.; Sal'nikov, V. V.; Chemikosova, S. B.; Ageeva, M. V.; Pavlencheva, N. V.; Van Dam, J. E. G. The snap point: A transition point in *Linum usitatissimum* bast fiber development. *Ind. Crops Prod.* **2003**, *18*, 213–221, doi:10.1016/S0926-6690(03)00043-8.
36. van Dam, J. E. G.; Gorshkova, T. A. Cell walls and Fibers / Fiber formation. In *Encyclopedia of Applied Plant Sciences*; Elsevier Ltd, 2003; pp. 87–96.
37. Koch, P. A. *Microscopic and chemical testing of textiles*; Chapman and Hall, London, 1963;
38. Gorshkova, T. A.; Ageeva, M. V.; Salnikov, V. V.; Pavlencheva, N. V.; Snegireva, A. V.; Chernova, T. E.; Chemikosova, S. B. стадии формирования лубяных волокон *Linum usitatissimum* (Linaceae). *Bot. J.* **2003**, *88*, 1–11.
39. Brulé, V.; Rafsanjani, A.; Pasini, D.; Western, T. L. Hierarchies of plant stiffness. *Plant Sci.* **2016**, *250*, 79–96, doi:10.1016/j.plantsci.2016.06.002.
40. Heller, K.; Sheng, Q. C.; Guan, F.; Alexopoulou, E.; Hua, L. S.; Wu, G. W.; Jankauskienė, Z.; Fu, W. Y. A comparative study between Europe and China in crop management of two types of flax: linseed and fibre flax. *Ind. Crops Prod.* **2015**, *68*, 24–31, doi:10.1016/j.indcrop.2014.07.010.
41. Martin, N.; Mouret, N.; Davies, P.; Baley, C. Influence of the degree of retting of flax fibers on the tensile properties of single fibers and short fiber/polypropylene composites. *Ind. Crops Prod.* **2013**, *49*, 755–767, doi:10.1016/j.indcrop.2013.06.012.



## GENERAL CONCLUSION

---

### Conclusions

Flax fibers, owing their plant-based nature and high specific mechanical properties, are valuable reinforcements for more ecologically friendly and performant composite materials. The present thesis proposes a multi-scale mechanical study of flax, from the stem to the fiber cell wall. This approach intends to improve our knowledge of flax plant biomechanics, our understanding of the origin of fiber performances and our expertise in the development of fibers and associated composites gifted with optimized reproducibility of their mechanical properties.

*Chapter I*, as a literature review, gives an overview of the general acquaintance with flax. First of all, a state of the art of the development of the plant, including its growth stages, internal organization, and fiber development is given. This first part offers thoughtful reflections on the uncommon characteristics of flax fibers and sets up notions and vocabulary for the following sections and chapters. Then, the varietal selection of several main industrial crops is reviewed, together with a state of the art regarding the lodging phenomenon. This latter is expected to be linked to the plant development itself, and we highlight that fiber mechanical properties could be a relevant parameter to consider in order to improve the lodging resistance through the varietal selection. Moreover, the effect of cultural conditions as well as the impact of main tropisms are reviewed. This highlights the possibility that modifications in cultural conditions and use of external stimuli are possible experimental approaches toward the understanding of flax overall biomechanics, through the study of plant reaction and reinforcement mechanisms under specific conditions.

*Chapter II* demonstrates that, through the varietal selection, it is possible to increase the fiber yields while preserving the excellent specific mechanical properties of flax fibers. Thus, the breeders' work is an indispensable expertise for developing the industrial use of flax fibers, both in future composite materials and for wider applications. Recent flax varieties show a special architecture, resulting from the varietal selection performed over many years aiming at increasing fiber yields while decreasing the risk of lodging. Nevertheless, whatever the variety, the flax stem can be assimilated to a composite structure with an outer protection (the epidermis), a unidirectional ply on the periphery (the fiber bundles) and a porous core (the xylem)

assembled as a hollow circular structure. More particularly, the significant role of flax fibers in the plant mechanical support is underlined, while their local organization is linked with the intrusive growth. Finally, *Chapter II* proposes a biomimetic approach, based on experimental data sets and literature, in order to suggest the flax stem as a source of inspiration for future composite materials.

*Chapter III* evidences changes in fiber performances taking place plant development and retting. The presented results reveal increases in the cell wall modulus with the cell wall thickening and with the retting level. We suggest that, for the fiber cell wall, the cellulose contribution rises with fiber maturity, leading to a greater cell wall modulus of flax fibers. In addition, an increase in crystallinity with retting, mainly due to the disappearance of amorphous polymers, accompanied by a compaction of inaccessible cell wall polymers, provides a structural explanation for the improvement in mechanical performances of the fiber cell wall during retting.

*Chapter IV* reveals the fiber contribution to the stem bending stiffness of flax, by comparing entire stems with stems devoid of fibers. This chapter also highlights that it is possible to estimate the mean apparent modulus of flax fibers through a simple bending test on stems. Additionally, the compression behavior of flax fiber bundles and their buckling mechanisms within a stem are investigated. This study makes possible to estimate the stress causing bundles instability within a flax stem by theoretical and experimental approaches. Thus, despite an optimal fiber arrangement within the stems and despite their strong cohesion through the middle lamellae, the limited compression strength of flax fibers is illustrated; actually, the compressive strength of the stem is ensured by the xylem core, as it is the case in man-made sandwich structures.

*Chapter V* investigates, in the first section, the mechanical stability of flax under conventional cultural conditions. Indeed, the varietal selection of flax has led to impressively slender structures compared to other herbaceous plants, without penalizing their mechanical stability. Their stability is actually ensured by the great stem bending modulus originating from the external ring of high-performance fiber bundles, associated with an inner thick porous xylem providing the high resistance to local buckling. In the second section, the differences between greenhouse and field cultivation in plant architecture and anatomy as well as the fiber yield and mechanical performances of flax fibers are investigated. Despite the greatly increased plant height under greenhouse conditions, similar fiber length and number of fibers per plant are

obtained under both types of cultivation. Hence, *Chapter V* shows that the greenhouse cultivation of flax does not appear to favor higher fiber yields or quality, but these essential criteria are preserved. In the final section, the gravitropic response of flax is studied to simulate lodging and recovery and explore their influence on the mechanical performances of flax fibers. Depending on the time of lodging, greater changes in fiber mechanical properties are highlighted in the earliest stage of the experiment. Moreover, these changes also depend on the studied side of the stem curvature, being larger on the pulling of the stems. Thus, *Chapter V* confirms that flax fibers are involved in the plant gravitropic reaction. Nonetheless, fibers maintain their efficient mechanical characteristic which allow their use as reinforcements for composite materials in case of plant lodging.

### **On-going works and Perspectives**

This thesis work has provided important insights into the structure and mechanical performances of flax fibers and stems. They help to explain and better understand why and how these unusual plants and fibers achieve such a high level of performance. An exceptional architecture, improved by man's hand thanks to varietal selection, makes this plant a unique model of stability and a potential source of inspiration for the materials of tomorrow. Nevertheless, flax has not yet delivered all its mysteries.

With a view to a successful understanding, investigations remain to be done to better understand the relationship between the structure and properties of flax cell walls. At the end of this PhD, we undertook works to explore the performances of the cell walls at the SOLEIL Synchrotron; these biochemical investigations reveal a highly complex parietal structure, requiring extensive work of understanding and interpretation. However, the first conclusions highlight structural modifications related to gravitropic reactions of plants and to the level of retting; the investigations must be continued to better understand the changes in the biochemical structure caused by these phenomena. The study of the impact of retting on the walls was also carried out by NMR and Raman Spectroscopy thanks to exploratory works. Elements of understanding have been obtained by NMR results on the evolution of the structure and architecture of the walls during the retting phase, but they need to be deepened and enriched; the path of mechanical and physicochemical coupling at the scale of the wall is a promising prospect that may soon be explored by combining AFM-Peak Force and AFM-Raman technologies.

A more detailed analysis of living plants is required, more specifically regarding plant biomechanical performances during growth and at maturity. This would include the evaluation of growth stresses as well as the role of turgor pressure in the mechanical stability of flax stems and of their bending strength. This work also opened the way to understanding the phenomena governing plant straightening and the influence of external stresses on the structure and performances of flax stems and fibers. The conducted greenhouse trials did not show major differences with field crops. This work could be continued by choosing fully comparable cultivation parameters between the two cultivation modes; it should also be reproduced on different varieties in order to obtain generalizable conclusions. As far as the study of plant recovery is concerned, we have obtained interesting conclusions on fiber performances, but the phenomena involved still need to be explored, whether at the scale of the cell wall or of fiber development; in-situ explorations during a recovery phenomenon could allow us to go further, but this work on living plants is complex. The movements induced by growth and the possible alteration of green materials by analysis techniques are experimental limits, all the more so as these analyses require the use of highly resolving instruments that are very sensitive to potential external disturbances. Nevertheless, this possibility could be explored in future works through tomography trials on living plants, for example.

Finally, varietal selection has shown us how its progress can transform the architecture and structure of flax stems. We are probably not at the limits of its advancements; new varieties, even richer in fibers, are under development. The question of limits in terms of fiber yield may arise. How will the plant structure evolve and what will be the allocate of xylem in future varieties? The mechanical role of the xylem part is proven in the stability of plants and its conduction function is unavoidable, so a compromise will naturally have to be found. Future varieties open up new perspectives in terms of fiber yield but also in terms of stability. This plant which already beats all records in terms of slenderness will probably continue to surprise and fascinate us for a long time.



**Titre :** Caractérisation multi-échelle des tiges et fibres de lin: structure et performances mécaniques

**Mots clés :** Biocomposites ; Caractérisation multi-échelle ; Fibres de lin ; Paroi végétale ; Propriétés mécaniques ; Structure de tige.

**Résumé :** Le lin (*Linum usitatissimum* L.) est une plante aux intérêts multiples. Sa tige est source de fibres, depuis longtemps utilisées dans le domaine du textile. Ce potentiel économique justifie la sélection variétale du lin en vue de développer des variétés plus riches en fibres et offrant une meilleure résistance aux maladies et la verse. Plus récemment, les fibres de lin ont vu leur utilisation s'étendre au renfort de matériaux composites grâce à leurs étonnantes propriétés mécaniques et morphologiques. Ces propriétés singulières s'expliquent grâce à leur développement et à leurs fonctions dans la tige. Ainsi, ce travail de thèse propose une caractérisation multi-échelle du lin, de la tige jusqu'à la paroi cellulaire de la fibre, afin de comprendre le lien entre les paramètres de croissance de la plante, le développement des fibres et leurs propriétés.

L'architecture générale d'une tige de lin est explorée, ainsi que les conséquences de la sélection variétale sur cette structure et sur les propriétés des fibres. De plus, l'évolution des propriétés mécaniques des parois de fibres au cours de la croissance de la plante et de la phase de rouissage est caractérisée. En complément, la contribution des fibres à la rigidité en flexion d'une tige est mise en évidence, de même que leur rôle dans la résistance des tiges au flambage. Enfin, l'influence des conditions de culture sur les architectures des tiges et propriétés des fibres est étudiée par le biais de cultures en serre ou encore en simulant un phénomène de verse. Cette approche originale met en valeur les caractéristiques remarquables du lin qui en font un modèle de bioinspiration pour les matériaux composites de demain.

**Title :** Multi-scale characterization of flax stems and fibers: structure and mechanical performances

**Keywords :** Biocomposites; Flax fibers; Mechanical properties; Multi-scale characterization; Plant cell wall; Stem architecture.

**Abstract :** Flax (*Linum usitatissimum* L.) is a plant with multiple interests. Its stem provides fibers, which have long been used in the textile industry. The economic potential of flax explains its varietal selection, aiming at developing varieties exhibiting higher fiber yields as well as greater resistance toward diseases and lodging. More recently, flax fibers have been dedicated to the reinforcement of composite materials due to their outstanding mechanical and morphological properties. These singular characteristics are related to fiber development and functions within the stem. Thus, the present work offers a multi-scale characterization of flax, from the stem to the fiber cell wall, in order to understand the link between plant growth parameters, the development of its fibers and their properties.

The general architecture of a flax stem is investigated, as well as the impact of the varietal selection on this structure and on fiber performances. Moreover, changes in mechanical properties of fiber cell walls over plant growth and retting process are characterized. In addition, the fiber contribution to the stem stiffness is highlighted, as well as the fiber role in the resistance of the stem to buckling. The influence of culture conditions on stem architecture and fiber features is also studied through cultivations in greenhouse and by simulating a lodging event. This original approach emphasizes the uncommon characteristics of flax, which make this plant an instructive model toward future bioinspired composite materials.